WATER FLOW MEASUREMENTS IN A 180 DEGREE TURN-AROUND DUCT

by
V. A. Sandborn and J. C. Shin
Colorado State University
Fort Collins, Colorado

Prepared Under Contract No. NAS8-36354

For George C. Marshall Space Flight Center

NATIONAL AERONAUTICS AND SPACE ADMINSTRATION

June, 1989

CR-183993

FINAL REPORT

Contract No. NAS8-36354

MEASUREMENT OF TERMS AND PARAMETERS IN TURBULENT MODELS

Virgil A. Sandborn
Colorado State University

SUMMARY

Experimental measurements of the mean and turbulent velocity field in a water flow, turn-around-duct was documented. Detailes of the measurements and data obtained was submitted to NASA-Marshall Space Flight Center in a report entitled "Water Flow Measurements in a 180 Degree Turn-Around-Duct" by V. A. Sandborn and J. C. Shin. A copy of this report is included as part of the final report. Further evaluation of the data obtained was employed by Dr. Shin in a PhD Dissertation entitled "Experiments on Turbulent Shear Flow in a Turn-Around Duct". A copy of this Dissertation is also included as part of the final report. These two reports cover all results obtained during the contract peroid.

The small radius of curvature duct experiments were made over a range of Reynolds numbers (based on a duct height of 10cm) from 70,000 to 500,000. For this particular channel the flow is dominated by the inertia forces. Details of the inertia dominated curved duct flow are covered by Dr. Shin in the enclosed Dissertation. Use of the local bulk velocity to non-dimensionalize the local velocity was found to limit Reynolds number effects to the regions very close to the wall. Only secondary effects on the flow field were observed when the inlet or exit boundary conditions were altered. The flow over the central two-thirds of the channel was two dimensional.

Mean tangental and radial velocities, streamlines, pressure distributions, surface shear stress; tangental, radial and lateral turbulent velocities and the Reynolds turbulent shear values are tabulated in the two reports. The flow along the inner surface of the turn was found to relaminarize due to the large acceleration of the flow in this region. Near the exit of the turn on the inner surface a separation bubble occurs. At low Reynolds numbers the separation bubble size varies, however, above a Reynolds number of 300,000 the bubble mean flow was insensitive to Reynolds number. It appears that the separation is also controled by the inertia forces. The flow along the outer surface developes very large turbulent velocities in all three directions. While low speed flow visualization suggests the development of longitudinal vortices along the outer wall, it was

not possible to identify the motion from the measurements. The vortices were highly time dependent, thus the time averaged measurements do not indicate any lateral aray of velocity variations.

It is evident from the experimental study that a complex numerical modeling technique must be developed to predict the flow in the turn-around-duct. The model must be able to predict relaminarization along the inner-convex-wall. It must also allow for the major increase in turbulence produced by the outer-concave-wall. It appears that the existing numerical models can not predict the occurance of separation along the inner wall at the exit of the turn. The separation occurs well downstream of the point where it appears on a circular cylinder. Obviously, the inertia forces in the curved duct restrict the separation from occuring until near the exit. It was originaly assumed that the flow along the convex wall had returned to a turbulent boundary layer to delay the onset of separation. However, it may not be necessary for the surface layer to return to a turbulent state to delay the separation in the inertia dominated turn-around-duct.

NOMENCLATURE

c_p	static pressure coefficient, eq. (1)
f	frequency, hz
F	Froude number, $U/\sqrt{\ell g}$
g	acceleration of gravity
H	duct height
ℓ	characteristic length
p	static pressure
p_{ref}	static pressure at duct inlet
R	duct radius of curvature, 10cm
Re	Reynolds number, $U_m H/\nu$
s	curvilinear distance in streamwise direction
t	time
T	temperature
u	tangential turbulent velocity
U	local tangential mean velocity
U_m	integral mean or bulk velocity (usually specified at upstream)
U	surface shear velocity, $\sqrt{\tau_w/\rho}$
v	radial turbulent velocity
V	local radial mean velocity
w	spanwise turbulent velocity
x	distance in streamwise direction (along inner or outer surface)
y	distance normal to the duct surface
z	spanwise distance parallel to the duct surface
Δ	vertical distances of the static pressure taps
ϵ	static pressure tap error
ϕ	hot film yaw angle to the tangential flow
ρ	fluid density
ν	fluid kinematic viscosity
τ_w	surface shear stress

WATER FLOW MEASUREMENTS IN A 180 DEGREE TURN-AROUND RECTANGULAR DUCT

by
V. A. Sandborn and J. C. Shin

ABSTRACT

The mean and turbulent velocity field in a water flow, turn-around duct has been documented. Affects of Reynolds number, inlet conditions, and exit screens were evaluated. The small radius of curvature duct was operated over a range of Reynolds numbers from 70,000 to 500,000.

The mean flow in the turn-around duct is dominated by the inertia forces. The use of the local bulk velocity to non-dimensionalize the velocities greatly reduces the Reynolds number variations. Only secondary affects were observed when the inlet or exit boundary conditions were altered. The inlet conditions were varied from a smooth surface to roughness on the inner surface inlet, and also trip wires on both the upper and lower inlet surfaces. Mean tangential velocities, flow direction, tangential and radial turbulent velocities, and the Reynolds turbulent shear values are tabulated.

The flow along the inner surface of the bend is first relaminarized by the large acceleration of the flow. Near the exit of the turn on the inner surface a separation bubble occurs. The separation bubble varies with Reynolds number, however above a Reynolds number of 300,000 the separation bubble mean flow is insensitive to Reynolds number. The flow along the outer surface develops very large tangential and radial turbulent velocities. Near the exit of the turn the radial turbulent velocity component is approximately twice the magnitude of the tangential turbulent velocity.

INTRODUCTION

Extension of fluid turbulent modeling to complex shear flows requires experimental measurements both for checking predictions and for modeling improvements. The flow in a 180 degree, small radius of curvature, turn-around duct is a case where a number of flow phenomena occur. The outer concave region contains a very large magnitude turbulent flow. The inner convex region initially contains large flow acceleration which produced relaminarization. The flow transitions back to turbulent and then separates on the inner surface at the exit of the turn. Coupled with the numerous phenomena is the observation that the flow is dominated, particularly at the high Reynolds numbers, by the inertia terms. The present report is a summary of measurements made as a directed effort to improve documentation of the flow in the 180 degree, turn-around duct.

EXPERIMENTAL STUDY

TABULATED MEASUREMENTS - Detailed measurements of the surface static pressure, mean velocities, flow angles, tangential and radial turbulent velocities, and the turbulent Reynolds stress were made for a number of stations around the duct and over a range of Reynolds numbers. Tabulated data obtained are given in Appendices A, B and C. Appendix A contains a set of data obtained with trip wires placed in the duct inlet. Appendix B contains data obtained for the case of roughness on the lower surface of the inlet. Appendix C contains data obtained in the original evaluation of the flow facility with smooth inlet conditions. Both Appendix A and B also contain information on the flow when different exit screens were in place. The major part of the data in Appendix A was recorded for an upstream mean or bulk velocity of 2.83 m/sec or a nominal Reynolds number of 200,000. The data were focused on the approach flow and the area of relaminarization, although detailed measurements were taken completely around the duct. The data of Appendix B were directed toward the evaluation of Reynolds number variations and detailed measurements in the separation bubble region. Although the upstream inlet conditions are different for the data of the three Appendices, the mean velocity profiles in the turn are nearly the same. The mean and turbulent velocity data reported in Appendices A and B were obtained using a laser velocimeter-counter system which proved to be more accurate than the laser-tracker system employed for the measurements tabulated in Appendix C.

FLOW FACILITY - A special two-dimensional channel, shown in figure 1, was constructed for the evaluation of the flows in a turn-around duct. The channel is 10 cm high and 100 cm wide, with a 10 cm centerline radius of curvature. The working fluid was water which was supplied through a 61 cm diameter pipe. The water was taken directly from a large reservoir that produces a constant head of approximately 75 meters. The water flow was controlled by a 61 cm diameter valve, 104 meters upstream of the channel inlet. A section 145 cm long is used to transition from the circular pipe to the rectangular duct. For the studies reported herein no screens or flow straighteners were employed in the inlet section. A rectangular entrance region 127cm long is included ahead of the turn section. The exit of the turn is also a straight rectangular section 43.2 cm long. The outlet of the channel could be restricted by screens. The screens were employed to increase the flow exit resistance so that the water completely filled the channel at low flow rates. By increasing or decreasing the outlet resistance it was possible to operate the facility over a wide range of flow velocities. For Reynolds numbers greater than approximately 500,000 the exit screen will be removed. With the dense screens in place the facility operated at a Reynolds number of the order of 80,000 with slightly greater than one atmosphere of pressure in the test section. With the large reservoir water head available very high flow rates are possible. The major limitations on the flow is the strength of the test section. The

large reservoir also insures constant temperature of the water during a run, which is of the order of 7°to 10°Celsius - depending on the time of the year. The facility was built of clear lucite for ease of access of the optical laser velocimeter. The lucite was re-enforced with steel to strengthen the structure. The outer turn was made from a solid block of lucite. Provisions for static taps and the mounting of probes and surface transducers are included around the complete test section.

PRESSURE MEASUREMENTS - Details of the static pressure instrumentation locations are given in Appendix A. Thirty taps along the centerline of the duct were used to measure the surface static pressures. The taps were 0.81 mm in diameter. For this diameter of static tap and a maximum surface shear velocity, $U_\tau = (\tau_w/\rho)^{1/2}$, of 0.3 m/sec, the measured static pressure error determined from the data of Franklin and Wallace (1970) is $\epsilon/\tau_w = 0.56$, or $\epsilon = 52\ N/m^2$. This error is related to the maximum uncertainty in the pressure measurements. For a pressure of one atmosphere (86,200 N/m^2 for the test conditions) the measured pressure error is 0.06 percent. The use of a differential pressure, $p - p_{ref}$, would cancel the error if U_τ was the same for the two pressure taps. Oil and water manometers and also diaphragm pressure transducers were employed in the measure of the static pressures. In all measurements the first pressure tap, 109.2 cm upstream of the start of the turn, was used as the reference pressure, figure A-2. Both, surveys around the facility, and individual pressure differences as a function of Reynolds number were measured during the study. Table A-Ia, B-Ia and b, and C-I list the measured pressure coefficients as a function of Reynolds number. In all cases the reference plane of the manometers or pressure transducers was located below the lowest point of the facility, figure A-2 (insert), so the static head from location to location does not enter the measurements. The actual static heights for each tap around the turn are noted on figure A-2. When the diaphragm pressure transducers were employed an averaging time of the order of 30 seconds was used for each individual pressure difference measurement. In all cases the pressure coefficient c_p were tabulated.

$$c_p = \frac{p - p_{ref}}{(1/2)\rho U_m^2} \qquad (1)$$

Table A-Ic lists the magnitude of the reference pressure (above atmospheric pressure) as a function of the Reynolds number and for different exit screens.

VELOCITY MEASUREMENTS - A forward scattering, single component, laser velocimeter was employed to measure the mean and turbulent velocity distributions in the duct. A 19 milliwatt, He-Ne laser was used as the light source. The effective beam diameter was of the order of 0.5mm. The forward scattered signals were sensed by a photodiode. An optical frequency shifter (Bragg cell) was used in the separated flow regions. A tracker system was employed in the preliminary measurements, Appendix C, and a counter system was used in the later evaluations, Appendix A and B. A 580

mm focal length lens was employed for the present measurements. Coupled with the refraction effects of the water this focal length was sufficient to allow measurements to be made over most of the width of the channel. The lens-laser system produced an interference fringe spacing of 7.360×10^{-6} meters in air. The refractive effects of water alters the beam angles and the light wave length such that the fringe spacing remains the same as in air. The mean velocity was determined by measuring the average frequency of the doppler bursts and then multiplying the frequency by the fringe spacing. The turbulent velocities were evaluated from the measured root mean square of the frequencies and then multiplying this rms by the fringe spacing. Frequency sample rates were high enough, so that accurate values were obtained with no need for corrections. The laser crossed beams were set at two or more different angles to determine the local flow direction, (from which the magnitude of the radial mean velocity component was evaluated). The radial, and Reynolds shear stress, turbulent components were also obtained from the rotated beam data. Near the surfaces beam rotation was impossible, so the flow angle, radial turbulent component and turbulent shear stress could not be obtained. Angles from 20 to 45 were employed to evaluate the radial information. For all of the velocity distributions the measurements were taken along radial distances (perpendicular to the walls). For most of the measurements data rates in the range from 2000 to 10,000 per second were indicated. The lowest data rates were encountered near the surface and in the separation region. The laser system was mounted on a rotary milling table, in order to move the beams across the test section in the radial direction. The movement was determined by dial indicators, which could be read to 0.030 mm. The initial location of the measurements with respect to the channel surface was limited to ± 0.25 mm. Evaluation of the flow angles from the rotated beams varied by approximately ± 1 degree. The output of the laser counter or tracker was time averaged over 20 to 90 seconds depending on the sample rate. Repeatability of the mean velocities was found to be approximately ± 0.005 m/sec in the steady flow regions. The turbulent velocities were also determined by time averaging the fluctuating velocities over the 20 to 90 seconds. A constant temperature, hot film anemometer was also used in the preliminary measurements. A direct comparison of the tangential turbulent intensities measured with the laser velocimeter and with a hot film probe is shown on Figure 2a). Figure 2b) is a comparison of the tangential turbulent anemometer and the laser velocimeter. The laser velocimeter data agree with the anemometer results up to a frequency of 100 hz. The deviation above 100 hz is due mainly to the failure of the scattering particles in the flow to follow the high frequency fluctuations. The deviation of the laser measurements at the high frequencies did not affect the evaluation of the rms turbulent values, since the major contributions to the rms signals come from frequencies below 100 hz (i.e. at 100 hz the energy is roughly 1.7 times less than that at 2hz).

Due to the high particle content of the flow it proved difficult to maintain accurate calibration of the hot films. Thus,

the laser velocimeter was extensively employed for the measurements.

SURFACE SHEAR STRESS - The surface shear stress was not directly measured. Empirical relations which included fitting of the mean velocity measurements to the law of the wall, Clauser (1956), were used to evaluate the surface shear, Figure 3. A Stanton tube probe was calibrated at a location -1.7H upstream of the start of the turn. The probe consisted of two static holes (0.6 mm in diameter) placed side by side. Over one of the static holes a thin razor blade was mounted. The lip of the razor blade was less than 0.1 mm above the surface. The Stanton tube senses the mean flow velocity very near the surface. Ideally, it is desirable to measure the velocity in the "linear" viscous sublayer. For the present flow the linear sublayer thickness ($yU_\tau/\nu = 5$) is of the order of 0.09 mm (for Re = 140,000) to 0.02 mm (for Re = 450,000). Figure 4 shows a typical calibration curve for the Stanton tube. The difference in pressure is measured directly with a capacitance, diaphragm type pressure transducer. For the particular diaphragm used, shear velocities from 0.06 to 0.80 m/sec can be measured. A surface-heat transfer, thin film gage, 0.15x1.2 mm, was also used to evaluate the fluctuating surface shear. The analogy between surface heat transfer and surface shear requires that the streamwise length of the gage be no greater than the linear viscous sublayer thickness.

FLUID PROPERTIES - The density and viscosity of the supply water were periodically checked with a hydrometer and an Ostwald type capillary viscometer. Within the three place readability of these instruments the water properties agree with tabulated values for pure water.

FACILITY FLOW EVALUATION - The large aspect ratio, 10:1, duct was employed to develop a quasi-two-dimensional, flow. Initial evaluation of the flow with a smooth inlet, Sandborn (1988) indicated a slight variation of the velocity distribution in the lateral direction across the inlet. The addition of first roughness and more recently trip wires on the inlet improved the flow in the rectangular entrance, and produced a near symmetric approach flow at the higher Reynolds numbers. The initial velocity distributions, Appendix C, of the approach flow indicated thicker boundary layers on the outer surface than on the inner wall. Figure 5a) shows velocity distributions at x = -2.54H upstream of the start of the turn for a number of Reynolds numbers for the trip wires on the inlet. The flow is approaching fully developed channel flow with the inner surface layer being just slightly thicker than the outer layer. The use of an exit screen does not appear to alter the upstream flow in the duct. Figure 6 shows measured velocity distributions at the 2.54H location for the case of no exit screen compared with a dense exit screen. Figure 7 shows typical centerline tangential and radial turbulent intensity variations as a function of Reynolds number measured in the rectangular entrance duct. The variation of the intensities with Reynolds number is similar to results obtained for fully developed

pipe and channel flow, Sandborn (1972). The magnitude of the tangential turbulent component is slightly less at the inlet than values obtained at the centerline of fully developed pipe flow. The slight increase in the magnitude of the turbulent intensity with distance along the duct indicates the centerline fully developed conditions are being approached. The larger magnitude of the radial velocity component suggests the inlet contraction damped the tangential component more than the radial component, which would be predicted theoretically. A detailed evaluation of the lateral or spanwise variation of the mean and turbulent velocities in the turn was made. Figure 8a) shows the spanwise variation of the mean velocities near the duct center at a number of locations around the turn. The data of Figure 8a) is for the case with roughness on the inlet. Although small variations in the velocity are observed, the flow was nearly two-dimensional. Some of the variation is due in part to the measuring technique. The present actuator system can span approximately 20 cm. The focal lens must then be remounted or replaced by a shorter focal length lens for each 20 cm segment. Slight inaccuracies in the lens alignment can result in small shifts in the measured velocities. Figure 8b) shows the variation in the measured tangential turbulent velocities. The actual variation of the turbulent velocity across the span is small over the central region of the duct. Only near the side walls are large variations observed. Appendix D gives a more detailed set of information on the spanwise variations measured around the duct. It was found that the most pronounced variations in spanwise mean velocity and turbulence occurred in and near the separation bubble. Some of the variation in the separation bubble and in the exit duct appeared to be related to the uniformity of the exit screen. Removal of the exit screen improved the two-dimensional aspect of the flow in the downstream region. An attempt was made to identify the existence of cell like structures which would relate to possible Taylor-Gortler vortex motion in the outer concave region of the flow. Figure D-5 shows a set of data taken at the 90 degree location. No identifiable spanwise periodic variation in either the tangential or radial mean flow was observed. Figure D-5d) shows an apparent spanwise periodic character in the radial turbulent velocity variation, but the magnitude of the variation is extremely small (of the order of 1 percent). The spanwise surveys would appear to justify treating the present turn-around duct flow as quasi-two-dimensional. Only in the separation region are deviations from two-dimensional flow of sufficient magnitude to be of importance.

TURN-AROUND DUCT FLOW EVALUATION - Figure 9 summarizes the main global flow characteristics observed for the small radius of curvature, turn-around, two dimensional duct. The very rapid turning of the flow at the start of the curve has the effect of wiping the turbulent boundary layer off the inside surface. The boundary layer was so thin that it was nearly impossible to detect a decrease in velocity with the laser velocimeter as the inner wall was approached. The large acceleration of the inner region flow is present around to 90 degrees. The flow at the start of the bend effectively turns away from the outer surface, which produces an

adverse pressure gradient on the outer surface. Measurements at low Reynolds number (Re = 70,000) indicated that the start of "incipient detachment" of the turbulent boundary layer (greater than 1 percent flow reversal) was present along the outer surface for approximately 15 degrees around the turn. For higher Reynolds numbers no evidence of flow reversal was found. At approximately 15 degrees around the turn the radial turbulent velocity component in the outer region starts to increase rapidly. The radial component growth continues around the turn and it reaches values twice the magnitude of the tangential velocity component. The tangential velocity component also grows in magnitude along the outer portion of the turn around to about 30 degrees. It then decreased in magnitude and becomes more uniform over the outer half of the turn. For high Reynolds numbers a separation bubble appears on the inside surface at approximately 150 degrees around the turn. The character of the bubble changed for Reynolds numbers below approximately 300,000. The bubble extends around the exit of the turn to approximately one duct height downstream of the turn. The maximum radial extent of the separation bubble is roughly 0.2 of the duct width.

The boundary layer on the outer surface downstream of the turn appears to be very thin. Apparently the combination of the flow turning back into the straight duct and the large radial turbulent velocities act to reduce the velocity gradient over the outer flow region.

STATIC PRESSURE DISTRIBUTION - Typical static pressure variations around the facility are plotted on Figure 10. The data shown on Figure 10 are for the rough inlet case, Table B-Ib. The pressure decreases along the entrance region indicating the flow is developing toward the fully developed conditions. Over the outer surface the pressure initially rises and then becomes nearly constant from 50 degrees around to 130 degrees. There is a moderate favorable pressure gradient on the outer surface at the exit of the turn. Downstream of the turn the pressure becomes nearly constant. On the inside surface of the turn the flow accelerates and a large favorable pressure gradient develops. The acceleration starts a short distance upstream of the turn and reaches a maximum between 10 and 20 degrees around the turn. As noted the favorable pressure gradient is sufficient to relaminarize the approach turbulent boundary layer. The minimum pressure occurs just before the 90 degree location, and a strong adverse pressure gradient exists downstream of the 90 degree station. A small perturbation in the pressure is observed between 150 and 170 degrees on the inner surface. The inner surface separation bubble starts to develop at the 150 degree location. By approximately 2 channel widths downstream of the turn the outer and inner pressure values are the same. Figure 11 compares the pressure distributions measured with and without an exit screen. These measurements are for the case of trip wires on the inlet. The effect of the exit screen on the pressure distribution was small. Figure 12 is a replot of the data of Figure 11 compared with potential flow calculations. The pressure along the outer surface is similar to

the potential flow variation. Along the inner wall the potential flow calculations indicate a larger favorable pressure gradient at the start of the turn and a more gradual transition to the adverse gradient in the downstream part of the turn. Obviously the potential calculations fail to account for the dissipation in the duct, so the downstream pressure does not agree with the measurements. Figure 13 compares the static pressure measurements with data reported by Monson and Seegmiller (1989). The measurements of Monson and Seegmiller were made in a turn-around duct in high pressure air. This duct is 3.8 cm high and 38 cm wide, with a centerline radius of curvature of 3.8 cm. The high Reynolds number, Re = 1,000,000, data agrees with the present outer wall results, while the low Reynolds number, Re = 100,000 measurements agree with the pressures measured along the inner surface. The present water flow duct measurements show only secondary differences with Reynolds number. The water flow facility operation at low Reynolds numbers may be different from the air facility, since the Froude number of the water duct approaches 1. [Froude number, F $(=U/\sqrt{\ell g})$, is the ratio of inertia to gravitational force. The facility was setup in the horizontal plane for convenience of the laser velocimeter operation, so the water flows down around the turn. In metric units $(\ell g)^{1/2}$ is of the order of 1 if the characteristic length, ℓ, is taken as the radius of curvature or duct width. For a Reynolds number of 70,000 the mean flow velocity is also approximately 1 m/sec.] The original measurements, Appendix C, showed the pressure distribution around the duct was nearly the same for Reynolds numbers from 77,000 to 207,000, Sandborn (1988). Thus, it was assumed that the Froude number was not a factor.

MEAN VELOCITY DISTRIBUTION - Figure 14 shows typical velocity profiles at select locations around the duct. The measured velocities are non-dimensionalized by the local mean or bulk velocity, U_m, for the flow. Since the flow is closely two-dimensional the mean velocity was obtained by integrating over the centerline velocity distribution only, the Reynolds number, Re $(=U_m H/\nu)$, is defined using the mean velocity and the channel width, H. In water flow it is common to employ a hydraulic diameter, which is approximately 2H for a rectangular channel, however, since the present flow is nearly two-dimensional the channel width was taken as the characteristic length. As may be seen on Figure 14, the velocity distributions at each specific location are nearly identical independent of the Reynolds number. The data shown on Figure 14 were obtained from cross plots of measurements made at fixed radial points, while the mean flow velocity was varied. Figure 15 shows a typical set of measurements of the velocity variation at 90 degrees around the turn for fixed radial distances. These data demonstrate that the effect of Reynolds number on the non-dimensional velocity ratio is small. Only in the region of the separation bubble was a pronounced Reynolds number effect observed.

Figure 16 compares the mean velocity distributions at the 90 degree location for the three inlet conditions; smooth, roughness and trip wires. Figure 17 is a comparison of the mean velocity distributions at the 90 degree location with or without an exit

screen. The effect of either the upstream inlet or downstream exit conditions on the flow in the turn is quite small. The large inertia changes in the turn dominate effects related to the entrance and exit boundary conditions. At the start of the turn, Figure 14b), and around to 90 degrees it was not possible to obtain laser velocimeter data close to the inside wall to record a decrease in the local velocity. As the outer wall is approached the surface curvature blocks the laser beams at the side of the facility, so measurements close to the outer wall are limited. Figure 14e) shows the velocity distribution 3.03H downstream of the turn exit. The boundary layer along the outer surface at the turn exit undergoes an acceleration similar to the flow along the inner surface at the start of the turn. The outer surface boundary layer is quite thin at the exit of the turn. Figure 18 is a comparison of the water channel velocity distributions with the profiles of Monson and Seegmiller. The air tunnel data at the start of the turn, Figure 18a, has a thicker inner wall boundary layer than observed in the water channel. The agreement of the two turn-around duct flows at the 90 degree location, Figure 18b), is very close over the center portion of the flow. The air tunnel reference velocity used for the flows appears to be different from the local mean velocity, since the area under the two Reynolds number curves are not equal. If the air data were normalized by the local mean velocity the Reynolds number variation would be quite small and the agreement with the water channel data would be even closer.

SEPARATION BUBBLE - Detailed sets of measurements in the separation bubble were made for both the cases of inlet roughness and trip wires, Tables A-IIa and B-IIc. Figure 19 is a plot of the velocity and percentage time the flow was reversed near the inner wall in this separation region for the rough inlet case. The photo is a visualization of the separation bubble. Air bubbles were injected through the 90 degree location static tap. The breakup of the bubble stream at roughly 170 degrees corresponds to the start (transitory detachment) of the separation bubble. At 150 degrees around the turn, Figure 19a), the flow was reversed 10 percent of the time at a distance of 0.005H from the inner surface. By 160 degrees, Figure 19b), the higher Reynolds number flows, Re > 300,000, are reversed approximately 25 percent of the time. The measurements at 170 degrees, Figure 19c), indicate the point of zero mean surface shear has been reached for the complete range of Reynolds numbers. The lower Reynolds number flow, Re = 200,000, did not develope as large a separation bubble as that of the higher flow rates. However, the most recent measurements at Re = 206,000 with the trip wires on the inlet and a dense exit screen, shown on figure 19d), indicate a more pronounced separation than obtained for the rough inlet case. Figure 20 shows the velocity variation with Reynolds number at fixed heights from the inner surface at the turn exit. The character of the separation bubble changes at a Reynolds number of 300,000. Beyond Re = 300,000 the flow is not altered by increasing velocity. Figure 21 compares measurements made at the exit of the turn with and without an exit screen. The coarse exit screen did not have an apparent effect on the velocity

distribution in the separation bubble region for the rough inlet case. Also shown on figure 21 are faired curves of the measurements of Monson and Seegmiller (1989) at the turn exit. The separation bubble in the air facility is more pronounced than obtained in the water channel. Dimensionwise the air and water bubbles are nearly the same physical heights even though the channel width is 3.81 cm for the air and 10 cm for the water facility. An estimate of scales related to the radial distances gives:

CSU Water Facility	Nasa Air Facility
Radius R = 10cm	R = 3.82cm
$\nu = 1.57 \times 10^{-6}$ m^2/s	$\nu = 1.25 \times 10^{-6}$ m^2/s

Assume a viscous length = $(\nu t)^{1/2}$, where the time t = transient time, t = s/U

Est.	U = 7.13 m/s	U = 32.9 m/s
	s = 0.314/m	s = 0.120/m
	t = 0.0440 sec	t = 0.00365 sec
	$(\nu t)^{1/2} = 2.63 \times 10^{-4}$ m	$(\nu t)^{1/2} = 6.75 \times 10^{-5}$ m
	$(\nu t)^{1/2}/R = 2.63 \times 10^{-3}$	$(\nu t)^{1/2}/R = 1.77 \times 10^{-3}$

The transient time of a fluid element in the water duct is an order of magnitude greater than in the air duct. The nondimensional viscous transport scale is 50 percent greater for the water channel, which may effect the size of the separation bubble.

TURBULENT VELOCITY DISTRIBUTIONS - Figure 22 shows faired curves of the tangential turbulent velocity component variation around the turn. A pronounced reduction in the magnitude of $\sqrt{u^2}$ occurs near the inside convex surface as the flow enters the turn. The values of $\sqrt{u^2}$ remain small along the inner wall around to nearly 90 degrees. From 90 degrees on downstream the tangential component grows to extremely large values once separation occurs. The tangential turbulent velocity increases in magnitude along the outer surface boundary layer as the flow enters the turn. The increase is typical of turbulence growth observed in adverse pressure gradients. At approximately 30 degrees around the turn the distribution changes. The large magnitude fluctuations tend to spread out over a large portion of the outer flow region. As the flow proceeds around the turn beyond 30 degrees the magnitude of the tangential turbulence decreases and becomes more uniform over the outer half of the duct. By 120 degrees the values of $\sqrt{u^2}$ are nearly constant across two thirds of the outer flow. Preliminary measurements, Appendix C, at low Reynolds numbers indicated $\sqrt{u^2}$ varied greatly with Reynolds number, Sandborn (1988). However, the higher Reynolds number measurements with the roughness on the inlet indicate smaller variations with Reynolds number, Figure 23. Reynolds number effects on $\sqrt{u^2}$ in the separation bubble are shown on Figure 24.

The appearance of large magnitude fluctuations across the outer half of the concave flow in the turn would be consistent with a Taylor-Gortler vortex instability. Flow visualization using milk and also air bubbles as tracers suggest that large scale, "highly time dependent" vortex like structures exist in the concave flow.

These motions shift rapidly from side to side with time, so that no stationary vortex array can be identified. Figure 25 show faired curves of the radial turbulent velocity component $\sqrt{v^2}$, variation around the turn. The radial component does not change along the inside region for the initial part of the turn. Unfortunately, the measurements are limited to some distance away from the surface. As in the case of a contraction the tangential component of the turbulence is damped more by the acceleration than the radial component. The magnitude of the radial component increases as the separation bubble is approached. No measurements of $\sqrt{v^2}$ were made in the separation region. Along the outer concave surface the magnitude of the radial component increases rapidly from 15 degrees around to the exit of the turn. It is nearly twice as large as the tangential component, which appears to further reinforce the existence of a highly time dependent vortex like motion.

Large variations of $\sqrt{v^2}$ with Reynolds number were observed at all locations around the turn. Figure 26 shows measurements of $\sqrt{v^2}/U_m$ made at the 90 degree location with and without an exit screen. The radial turbulent component is sensitive to both Reynolds number and boundary condition changes. These large variations in $\sqrt{v^2}$ with only secondary effects being observed for the mean velocity distributions, lead to the conclusion that the turbulent fluctuations are not directly coupled with the mean flow.

The turbulent shear stress $\overline{uv}/U_m^2$ variation around the turn is shown on Figure 27. The sign convention is that v is positive away from the inner surface. Thus, negative values of $\overline{uv}$, usually obtained for turbulent boundary layers, would occur along the inside wall. Following this convention the values of $\overline{uv}$ along the outer surface have a positive sign. The magnitude of $\overline{uv}$ approaches zero at 15 degrees around the turn and is slightly positive along the inside convex part of the flow around to 90 degrees. In the separation bubble region very large positive values of $\overline{uv}$ were encountered. Large values of $\overline{uv}$ occur in the outer flow around to greater than 120 degrees. Downstream of the turn ($x > 1.5H$) large negative values of $\overline{uv}$ occur along the inner part of the flow. The outer flow values of uv decrease once the turn exit is reached.

SURFACE SHEAR STRESS - Figure 28a) shows the variation with Reynolds number of $U_\tau/U_m (= c_f/2)$ obtained for a number of locations on the out-side surface of the turn. These values were obtained with the Stanton tube. The measurements were taken with trip wires on the inlet. Figure 28b) compares the Stanton tube and heat transfer gage evaluations of surface shear at 90 degrees around the turn. The heat transfer gage indicates too high a value of U_s for the high Reynolds numbers. The deviation of the heat transfer data is consistent with the effect of too large a streamwise width of the thin film gage. The Stanton tube evaluation employed the direct calibration, figure 4, obtained at the -1.7H upstream station. An uncertainty exists due to the pressure gradient at each location around the turn. The equation of motion very near the surface may be approximated as

$$\frac{1}{\rho}\frac{\partial p}{\partial s} = \nu\frac{\partial^2 U}{\partial y^2} \qquad (2)$$

Integration of equation (2) assuming the pressure gradient is not a function of y, indicates the velocity varies as

$$U = \frac{yU_\tau}{\nu} + \frac{y^2}{\nu}\frac{1}{\rho}\frac{\partial p}{\partial s} \qquad (3)$$

No corrections for the second order pressure gradient effect was made for the evaluations shown on figure 28. The effective y-distance for the Stanton tube was not known. At 10 degrees around the turn the surface shear is small due to the near separation of the boundary layer. The ratio U_τ/U_m is approximately constant at the 10 degree location for Reynolds numbers greater than 300,000. The surface shear remains nearly constant along the outer surface from 70 to 110 degrees. In the downstream portion of the turn the surface shear increases rapidly. Figure 29 shows estimated values at 90 degrees around the turn of the fluctuating surface shear intensity obtained from the surface thin film sensor. At the lower Reynolds numbers, where the thin film and Stanton tube results of the mean shear are approximately equal, the fluctuation, τ_w' (estimate of the rms surface shear), is of the same order of magnitude as the mean surface shear.

CONCLUSION

Measurement of the mean and turbulent velocities in a 180 degree, turn-around duct are reported. A high Reynolds number, water channel was employed to evaluate the flow quantities in a small radius of curvature (ratio of channel width to centerline radius of one) duct. Measurements for a range of Reynolds numbers from 70,000 to 500,000 are reported.

The flow in the turn is dominated by the inertia forces. Variation of either the upstream inlet or downstream exit conditions have only secondary effects on the flow in the turn. The local velocity distributions at each individual location around the turn were nearly similar when non-dimensionalized by the local bulk velocity of the flow. The large aspect ratio, 10:1, of the duct produced a quasi-two-dimensional flow. At the turn entrance, the flow along the outer concave surface experiences an adverse pressure gradient, which produced a near separation condition for the lowest Reynolds number flow. However, at the higher Reynolds numbers no separation was observed. By approximately 15 degrees around the turn large radial turbulent velocity components are measured in the outer concave part of the turn. The large radial velocity components of turbulence suggest a Taylor-Gortler type vortex motion exists in the concave outer region of the turn; however, no vortex cell like characteristics could be identified in the measurements. The large radial turbulent velocities persist around the complete turn. Very large accelerations of the flow occur near the inner convex surface at the start of the turn. The tangential turbulent velocities and the Reynolds shear stress along the inner wall were damped. Relaminarization of the boundary layer occurs along the inner wall. A separation bubble occurs on the

inner convex surface at approximately 150 degrees around the turn. The separation bubble persists for some distance downstream of the turn exit. The separation bubble is Reynolds number dependent at the lower Reynolds numbers. For Reynolds numbers greater than 300,000 the velocity variations in the separation bubble are similar when non-dimensionalized by the bulk velocity. the separation velocity distribution was altered when a dense screen was placed at the duct exit.

The measured turbulent velocity components were more sensitive to Reynolds number than the mean velocities. It appears that the variation of the turbulent velocities are relatively independent of the mean flow. Beyond the turn exit the large turbulent mixing and the mean flow turning appear to reduce the thickness of the outer wall boundary layer.

REFERENCES

Clauser, F. H. (1956) The turbulent boundary layer. ADVANCES IN APPLIED MECHANICS, vol. 4, p 1, Academic Press, New York.

Franklin, R. E. and Wallace J. M. (1970) Absolute measurements of static-hole error using flush transducers. Journal of Fluid Mechanics, vol. 42, pp. 33-44.

Monson, D. and Seegmiller, H. L. (1988) Comparison of LDV measurements and Navier-Stokes solutions in a two-dimensional 180 degree turn-around duct. AIAA Paper AIAA 89-0275. (Paul K. McConnaughey co-author on calculations.)

Sandborn, V. A. (1972) RESISTANCE TEMPERATURE TRANSDUCERS. Metrology Press, Fort Collins, Colo. (figure 7.9).

Sandborn, V. A. (1988) Measurements of turbulent flow quantities in a rectangular duct with a 180 degree bend. NASA Conference Pub. 3012, Advanced Earth to Orbit Propulsion Technology 1988, vol II. May 10-12,1988, NASA George C. Marshall Flight Center, Huntsville, ALA.

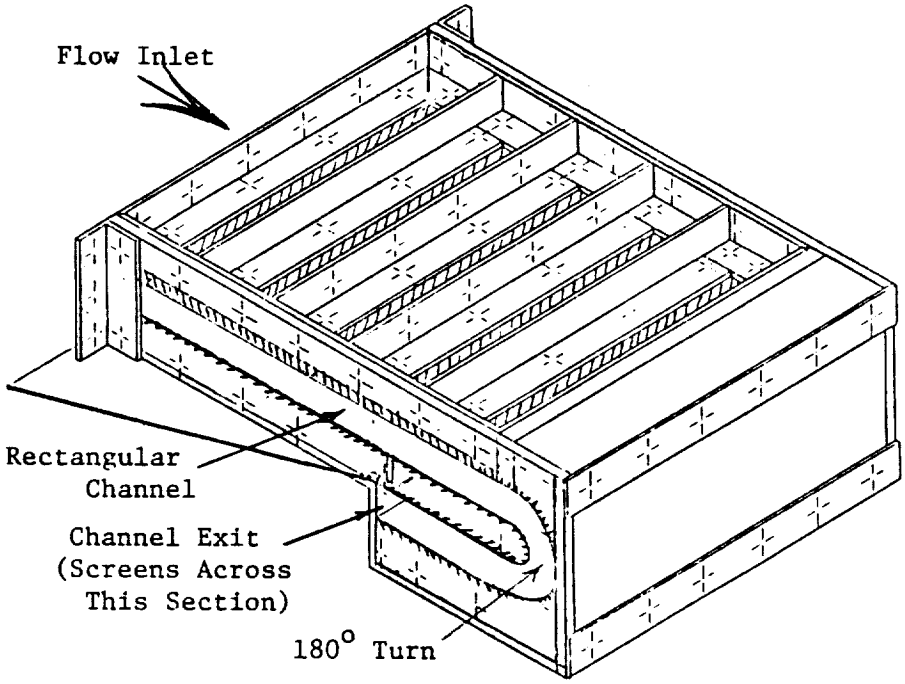

a) Schematic Sketch of the 180° Turn Facility

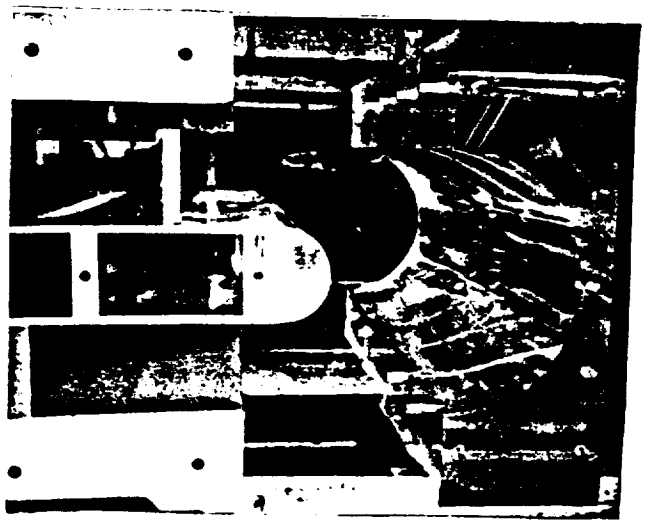

b) Detail of the Construction of the 180° Turn

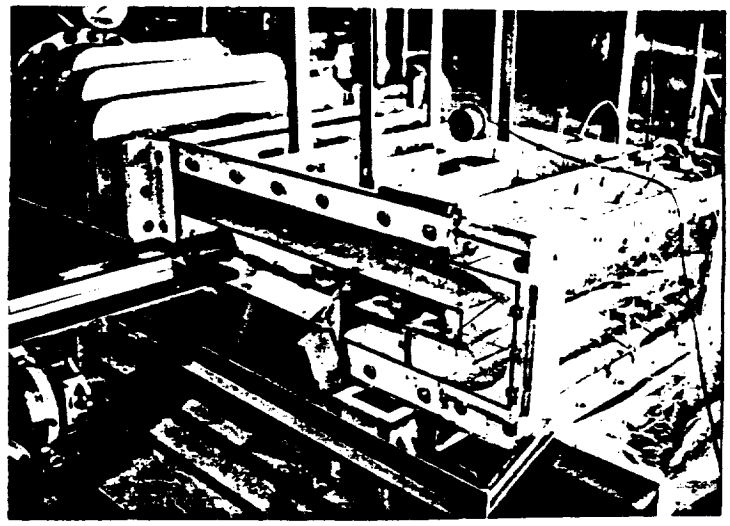

c) Operating 180° Turn Facility

Figure 1. The 180° Turn Water Flow Facility

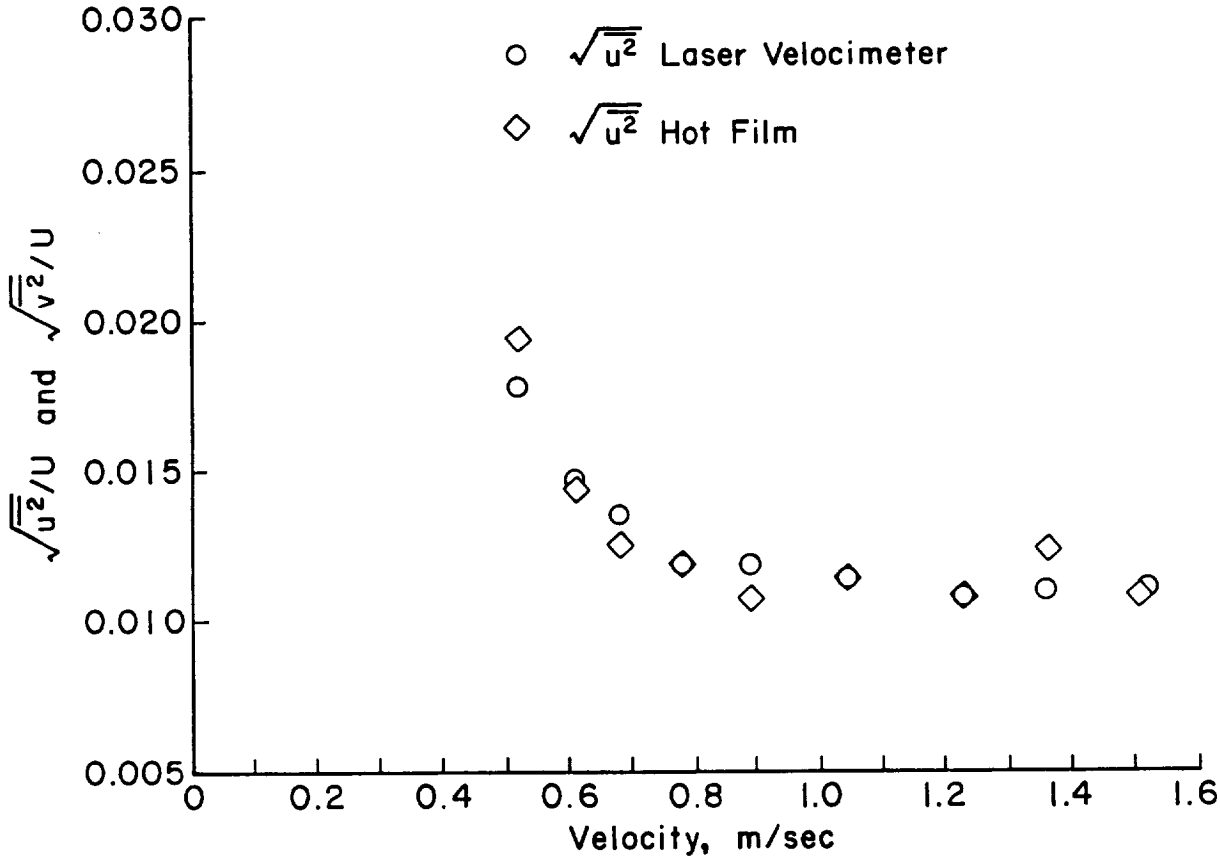

a) Turbulent Intensity

Figure 2. Comparison of Laser Velocimeter and Hot Film Anemometer Measurements in the Water Duct.

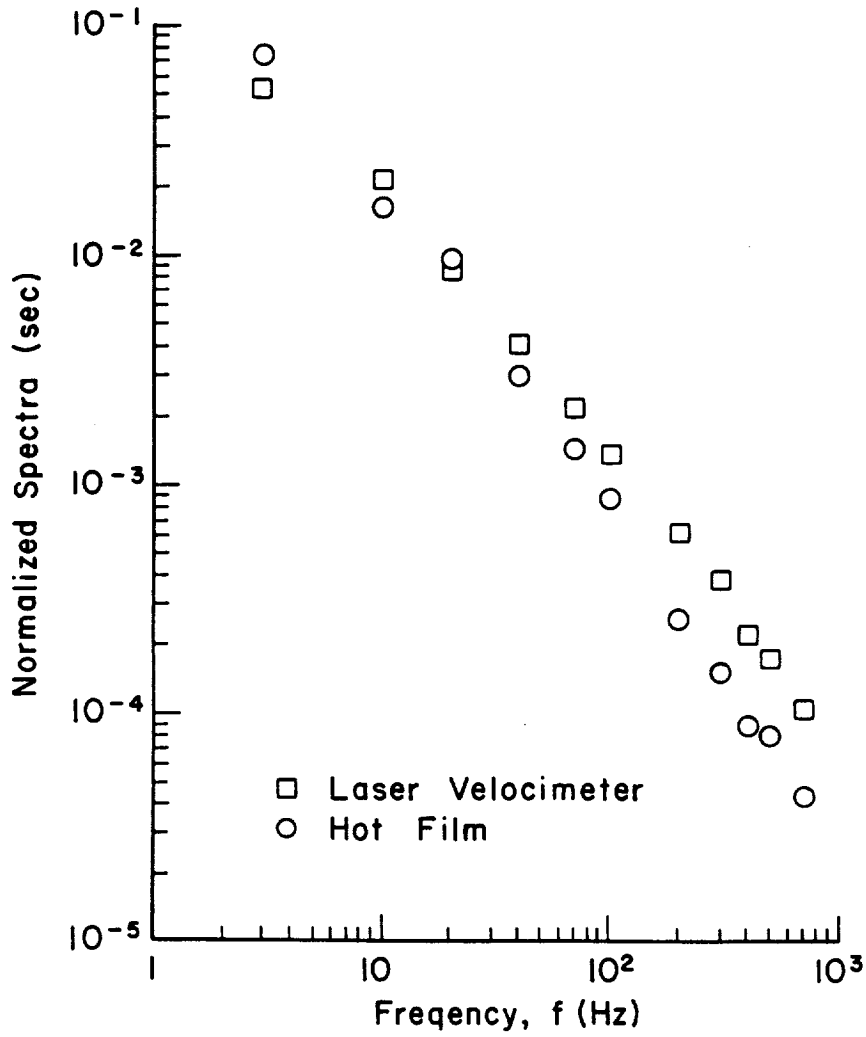

b) Tangential Turbulent Spectra

Figure 2. (Concluded) Comparison of Laser Velocimeter and Hot Film Anemometer Measurements in the Water Duct.

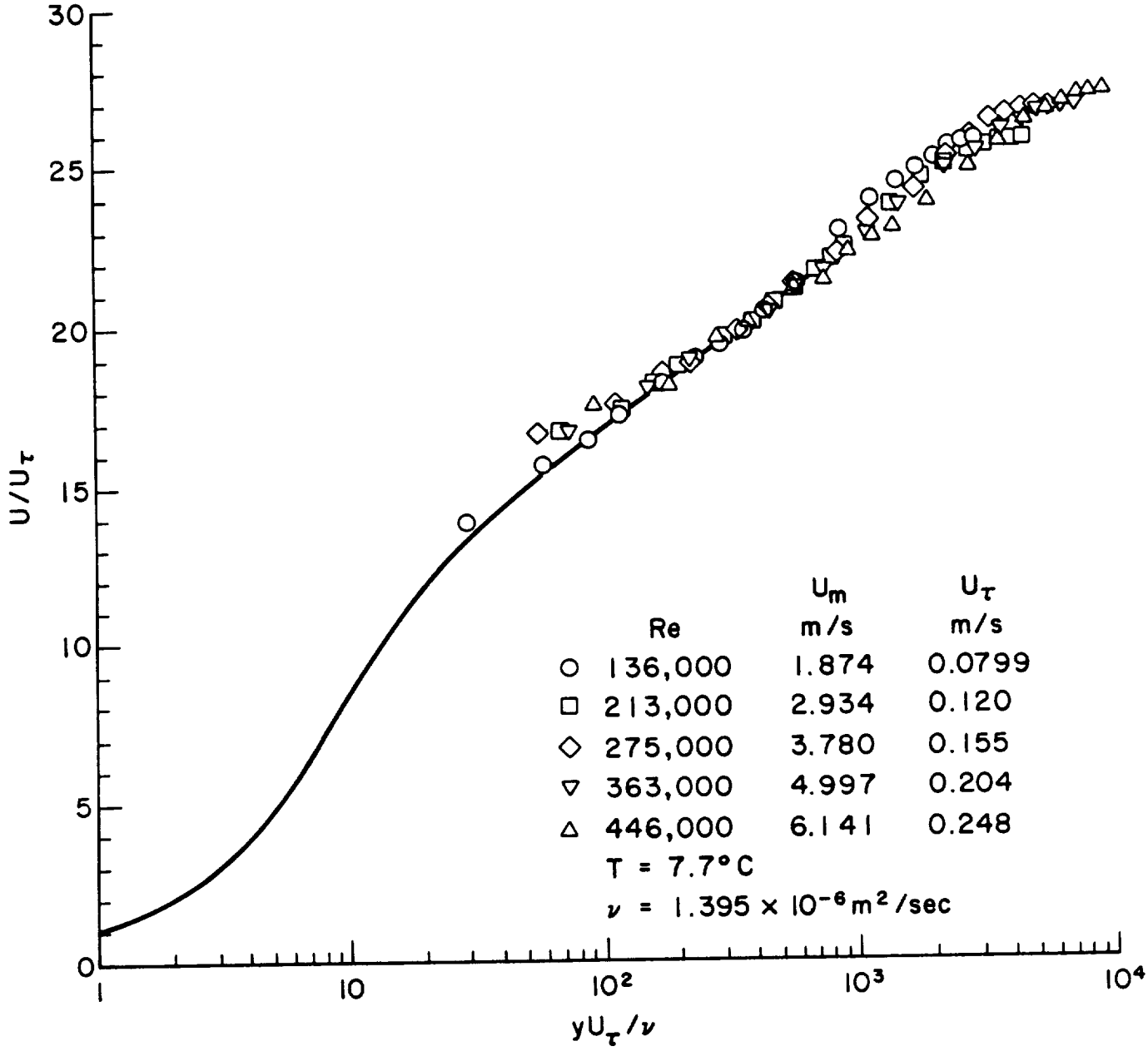

Figure 3. Log Law Plot of the Outer Surface Boundary Layer at -1.7H Upstream of the Start of the Turn.

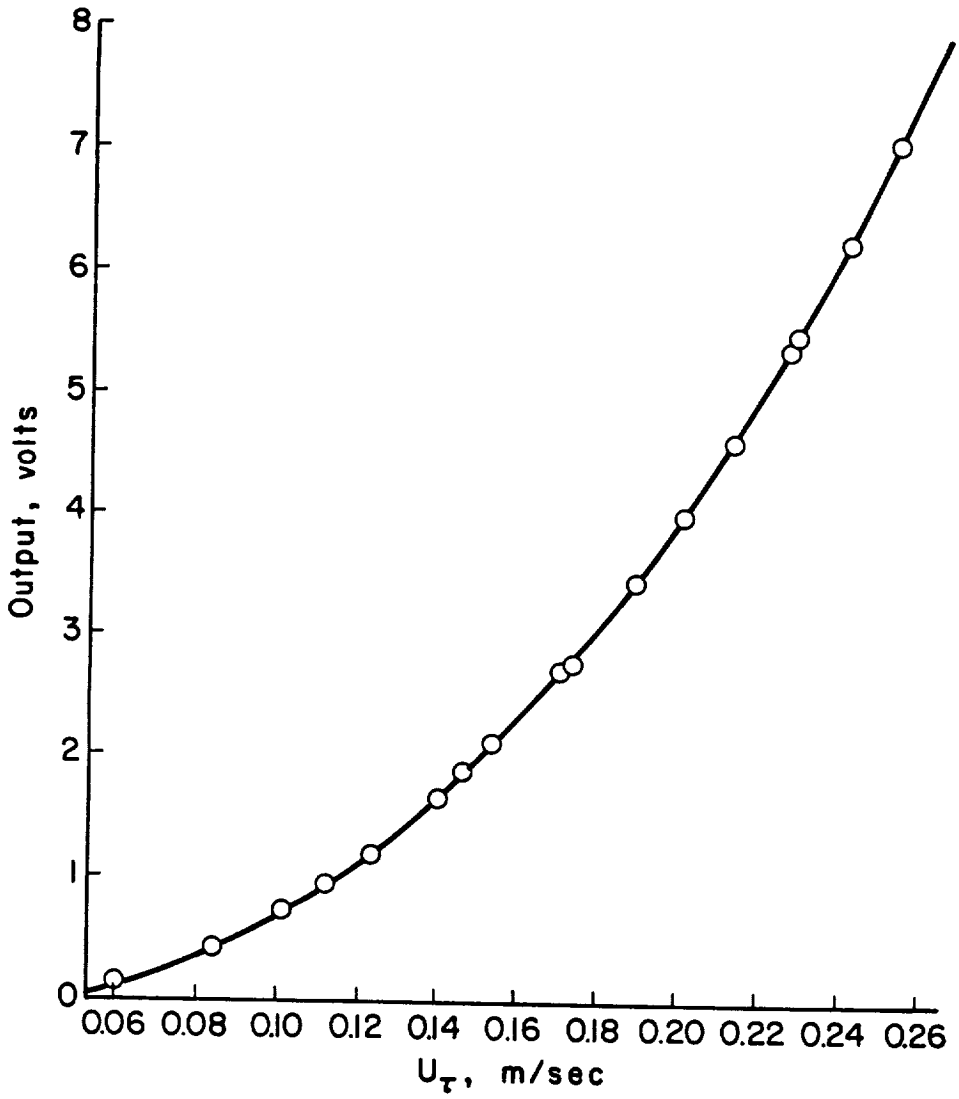

Figure 4. Calibration of the Stanton Tube for Surface Shear Evaluation.

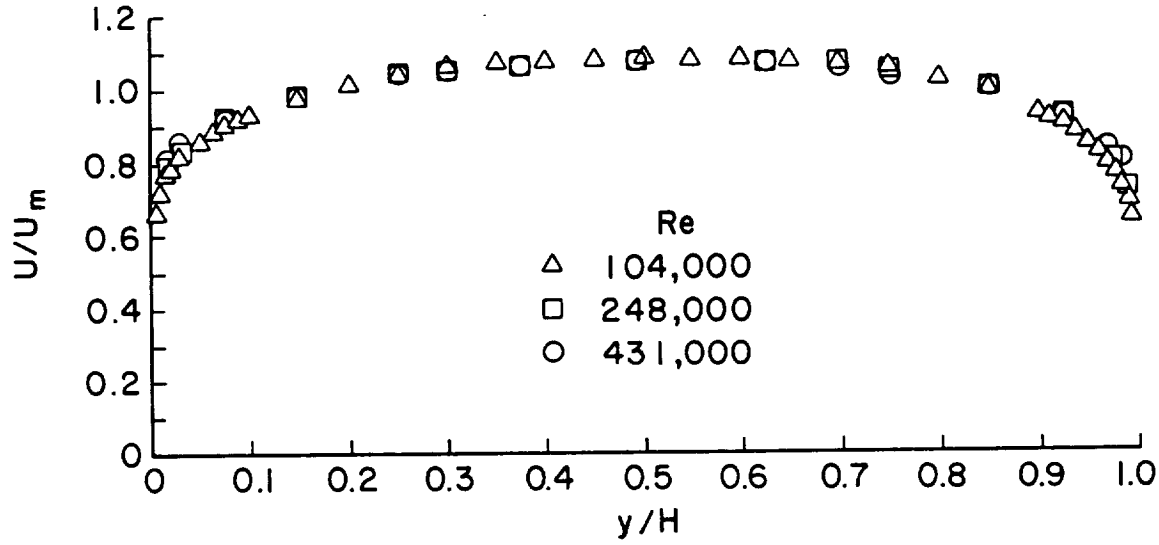

a) Mean Velocity Distribution

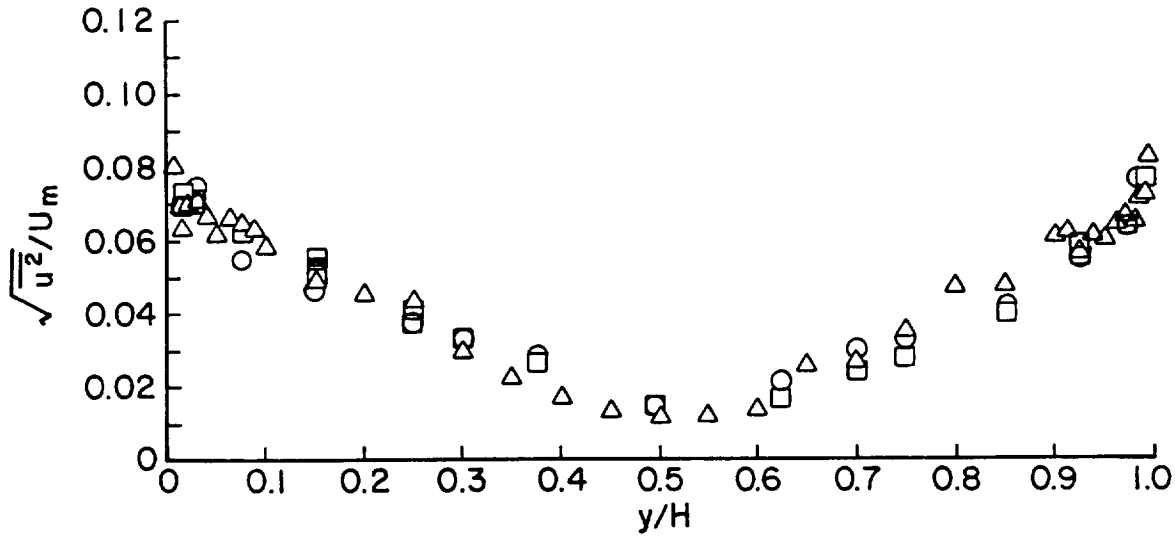

b) Tangential Turbulent Velocity Distribution

Figure 5. Velocity Distributions in the Inlet Duct of the Water Facility. -2.54H, Trip Wires on the Inlet.

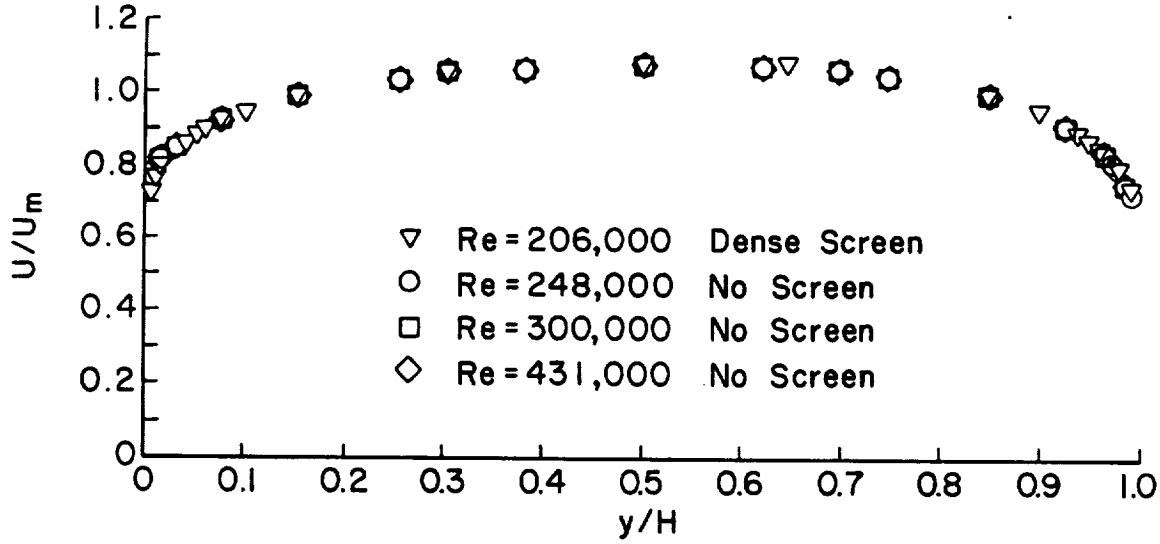

a) Mean Velocity Distribution

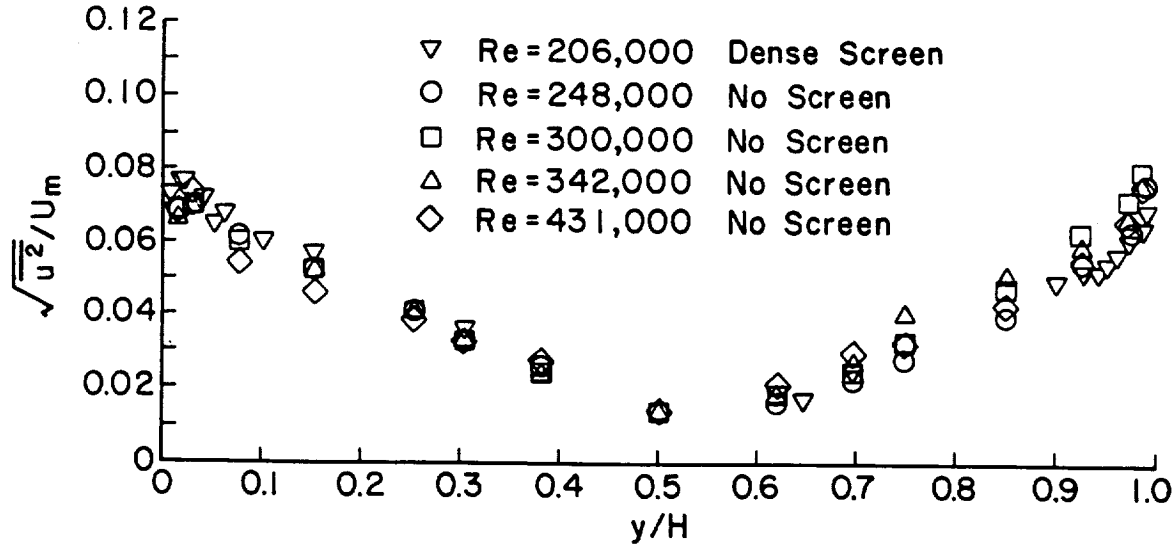

b) Tangential Turbulent Velocity Distribution

Figure 6. Comparison of Flow in the Duct With and Without Exit Screens, -2.54H, Trip Wires on the Inlet.

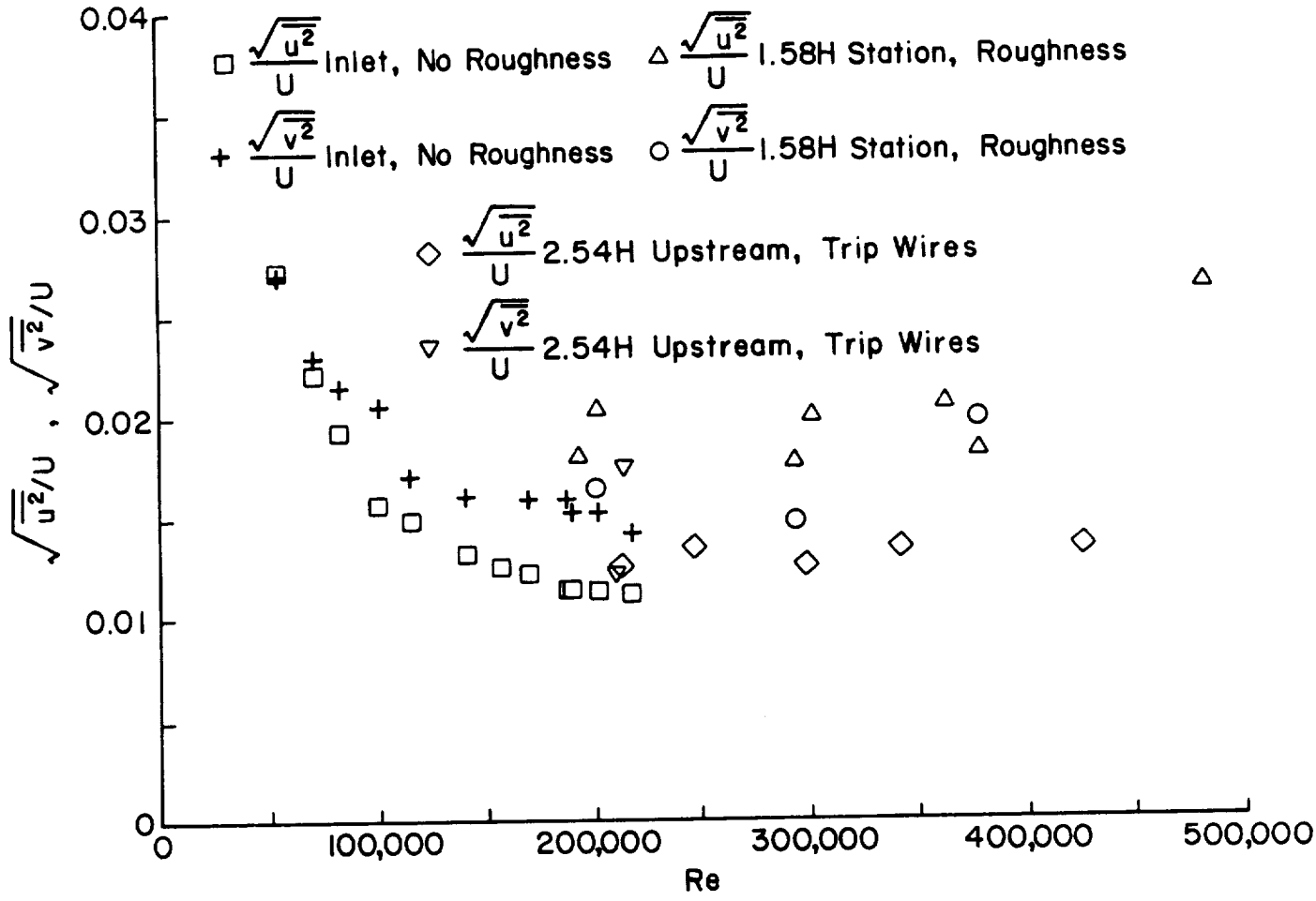

Figure 7. Turbulent Intensity Variation Upstream of the Turn.

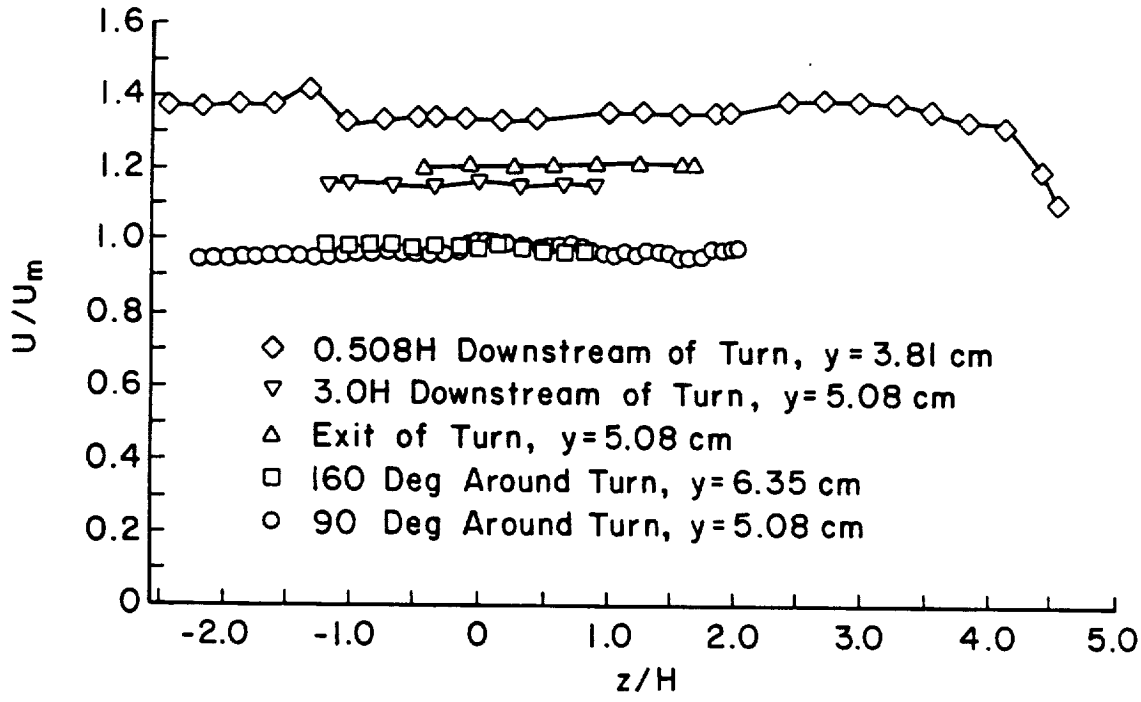

a) Mean Velocity Variation

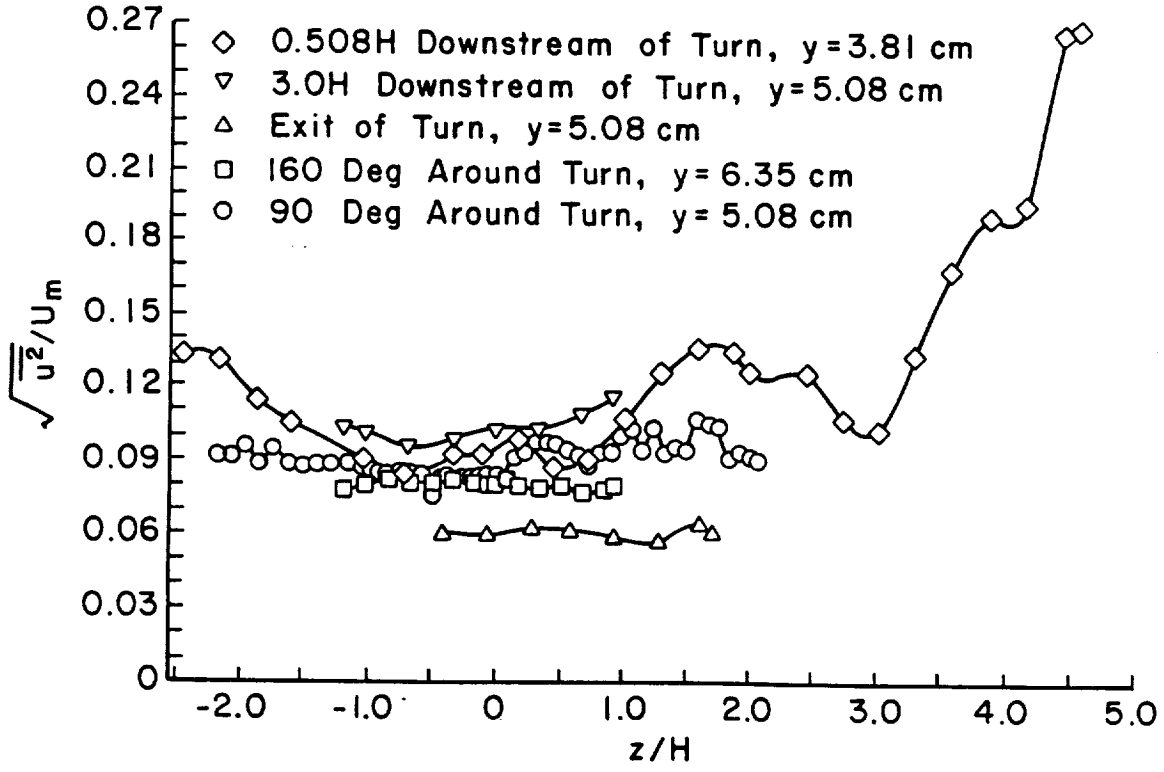

b) Tangential Turbulent Velocity Variation

Figure 8. Spanwise Variation of the Mean and Turbulent Velocities at the Centerline of the Duct. Roughness on the Inlet.

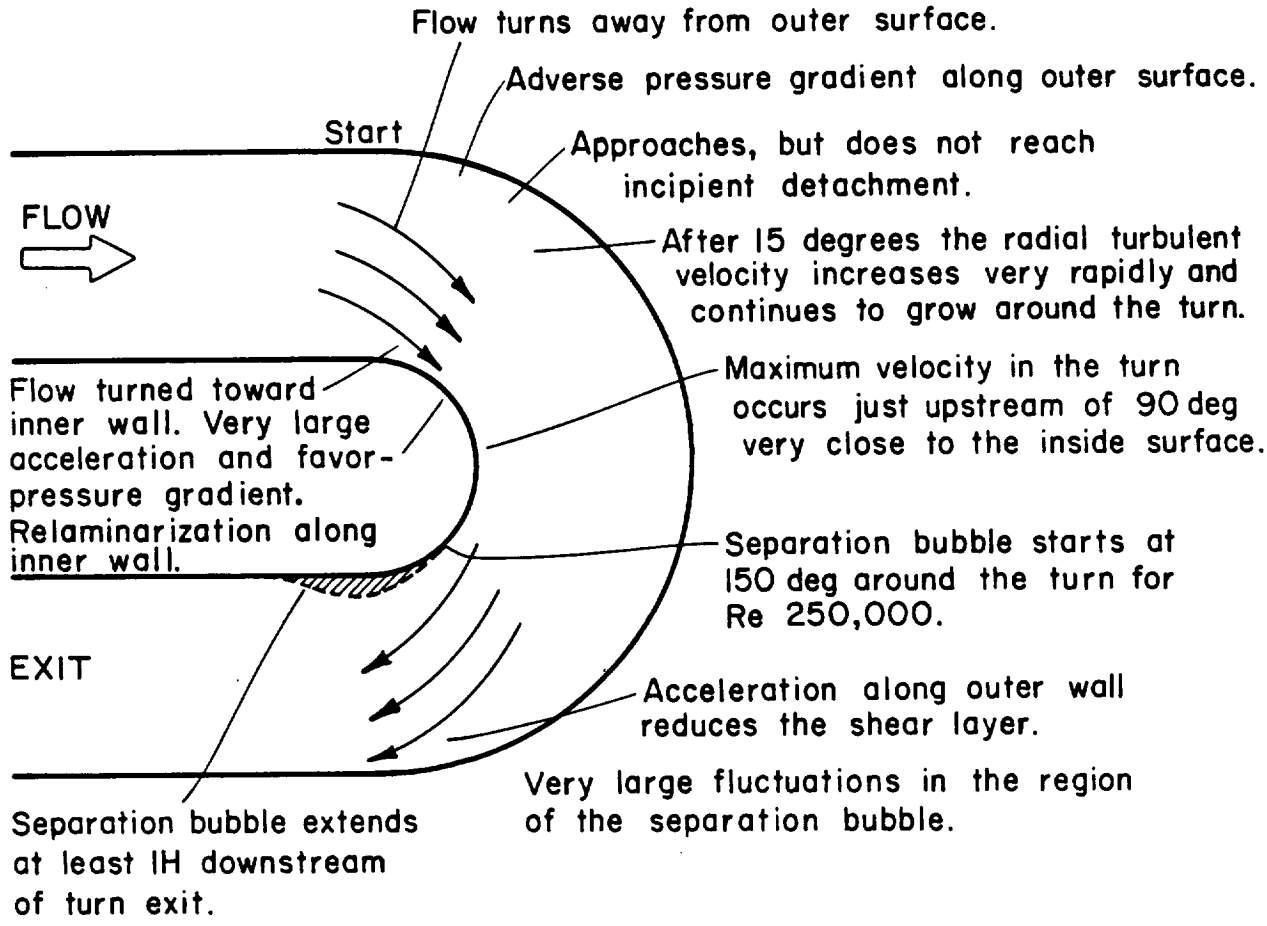

Figure 9. Global Characteristics Observed in the Turn-Around Duct.

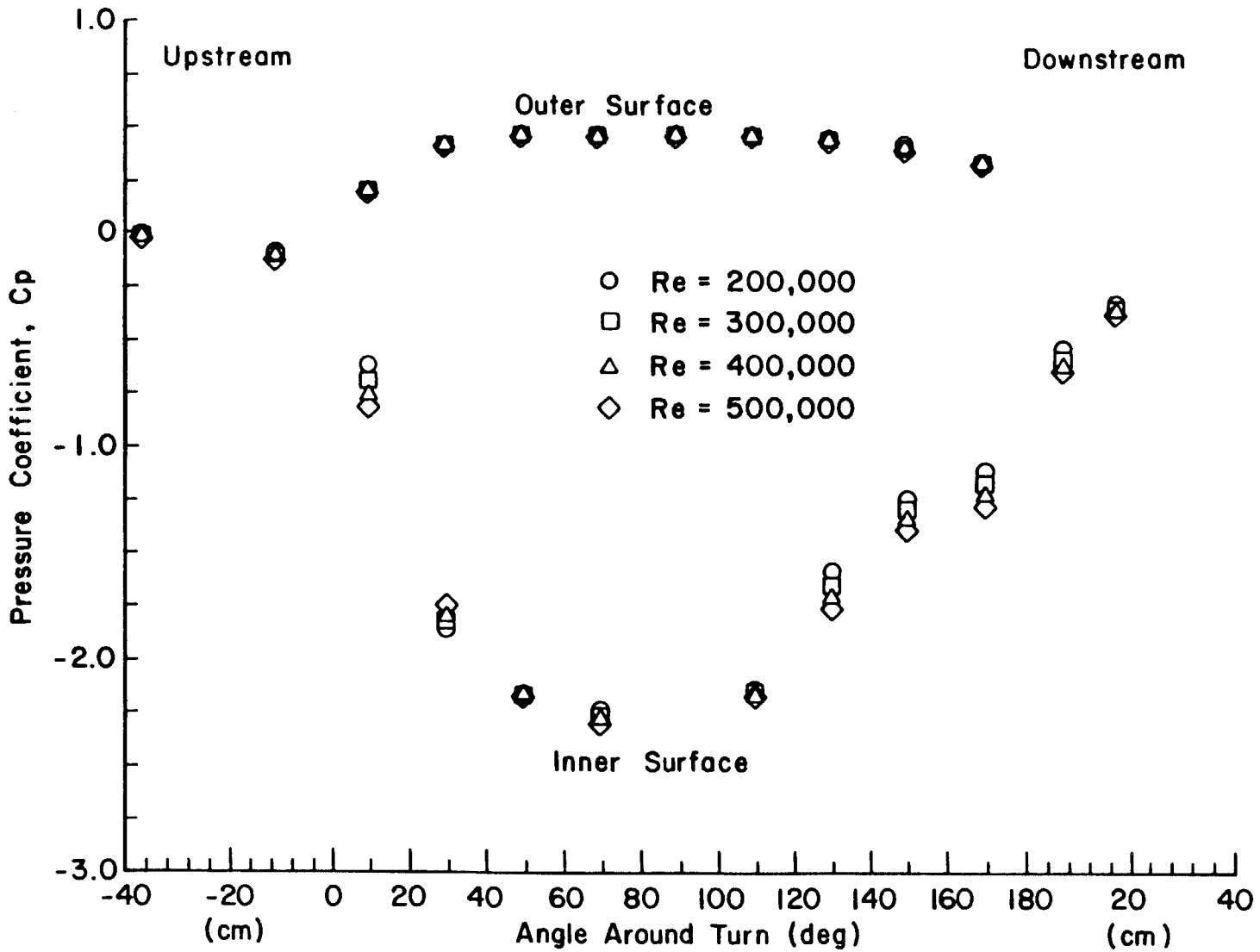

Figure 10. Static Pressure Variation with Reynolds Number Around the Duct. Roughness on the Inlet.

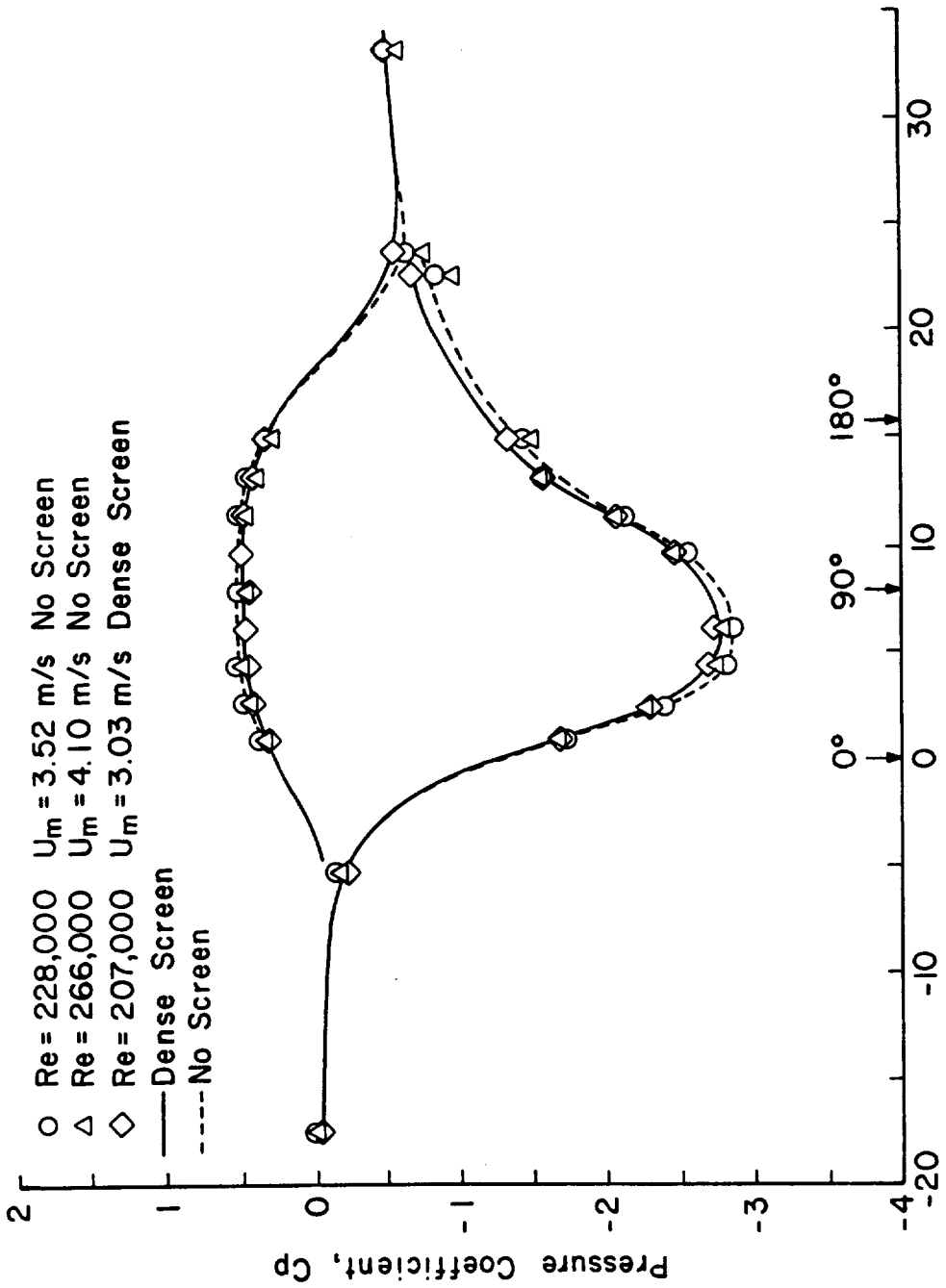

Figure 11. Effect of Exit Screen on the Static Pressure Distribution in the Duct.

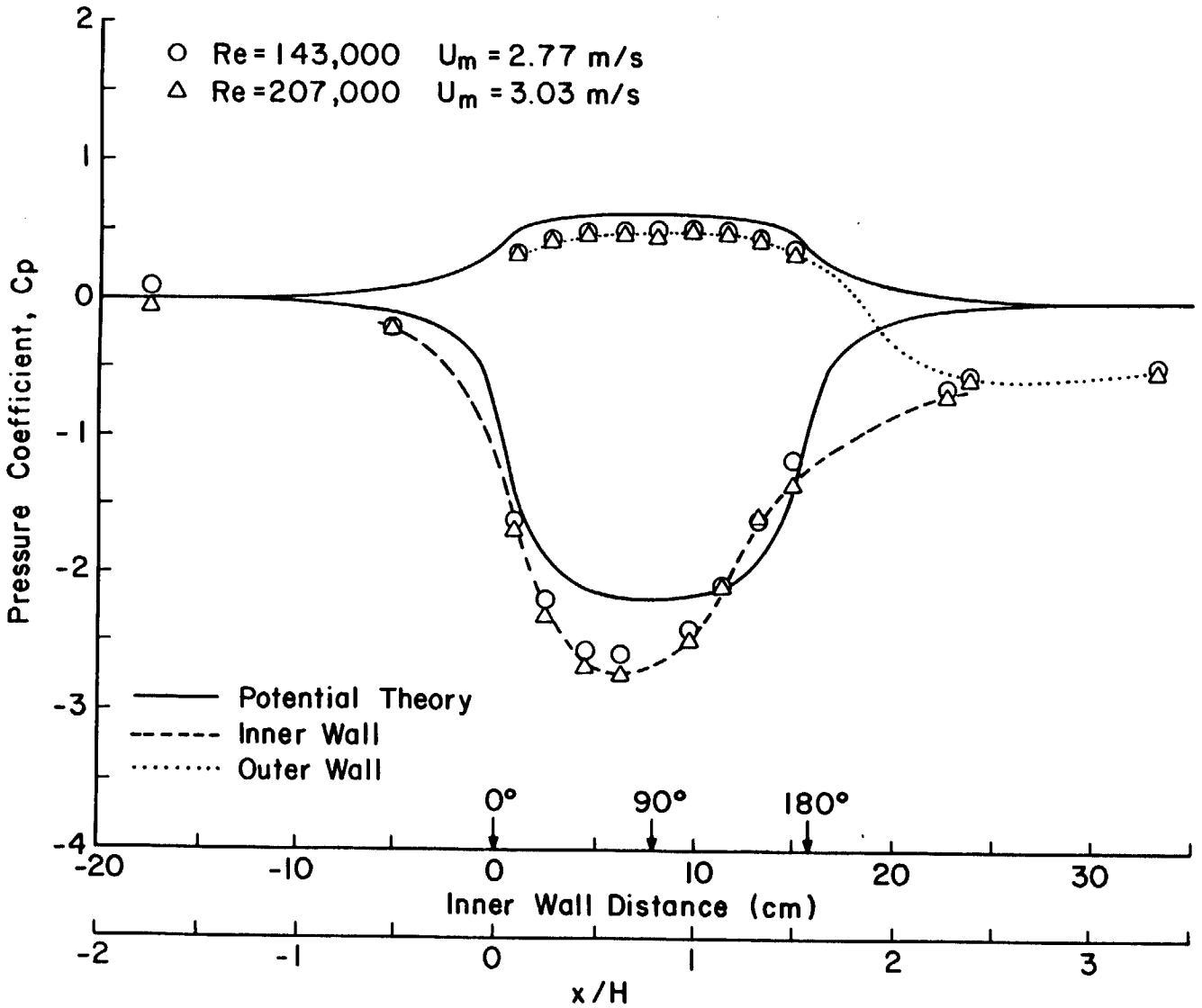

Figure 12. Comparison of Static Pressure Measurements in the Water Duct with Potential Flow Calculations

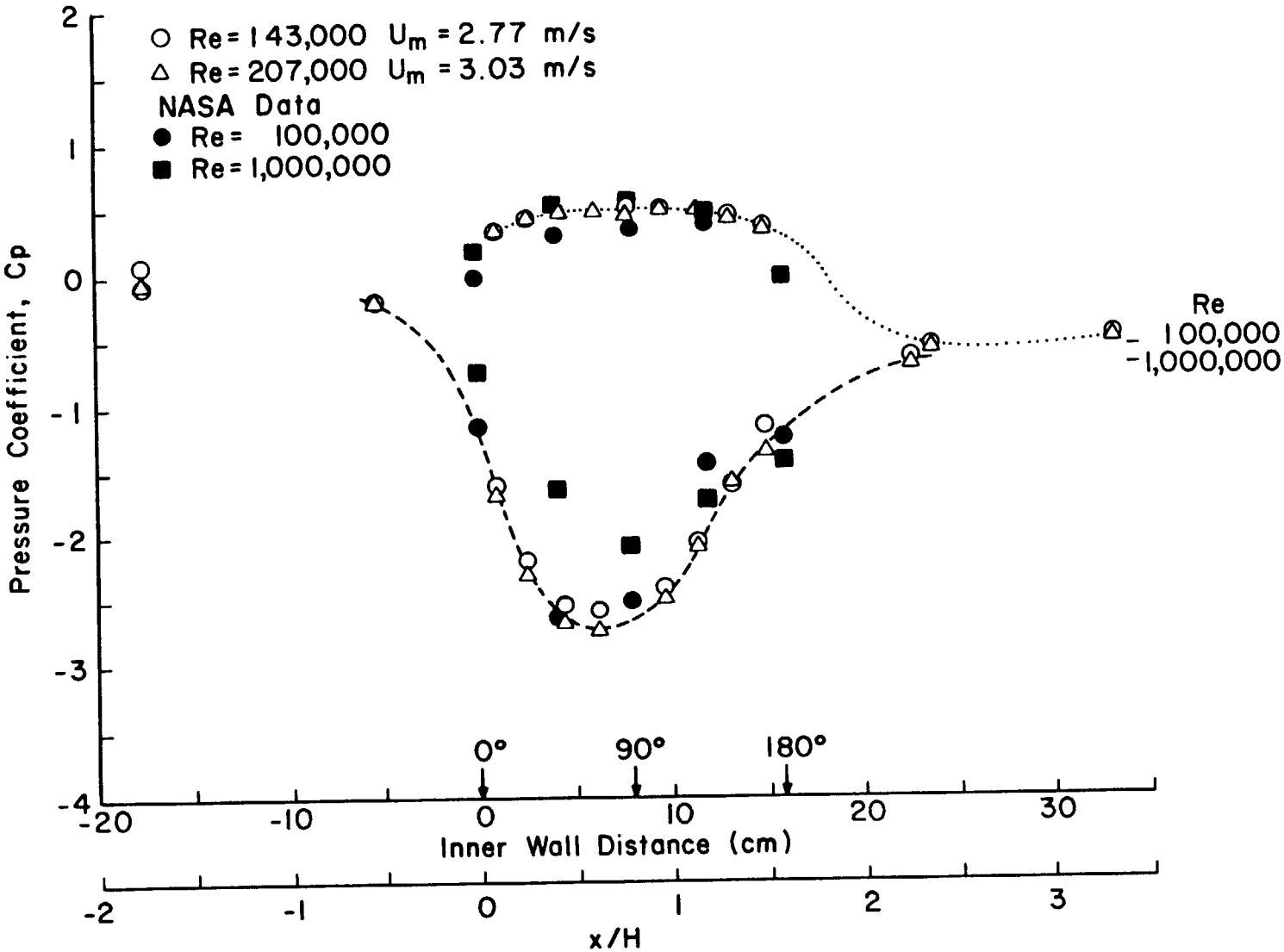

Figure 13. Comparison of the Water Duct Static Pressure Distribution with the Air Flow Measurements of Monson and Seegmiller (1989).

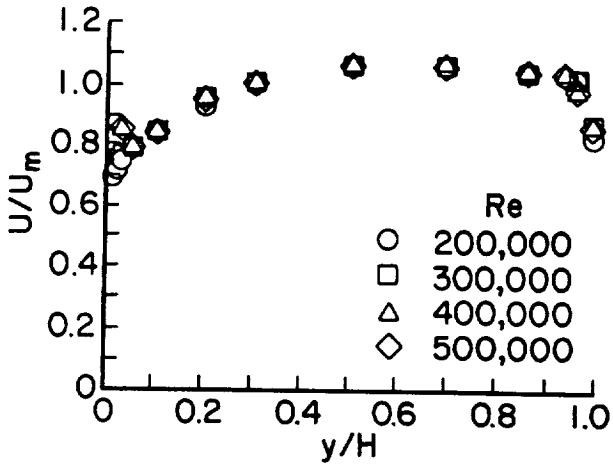

a) 10H Upstream of the Turn

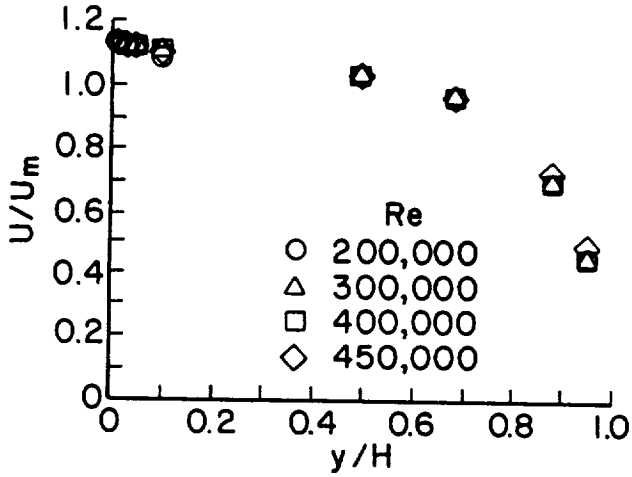

b) Start of the Turn

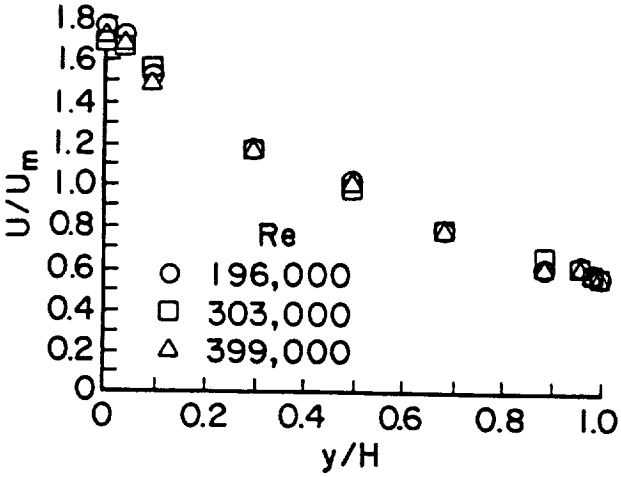

c) 90 Degrees Around the Turn

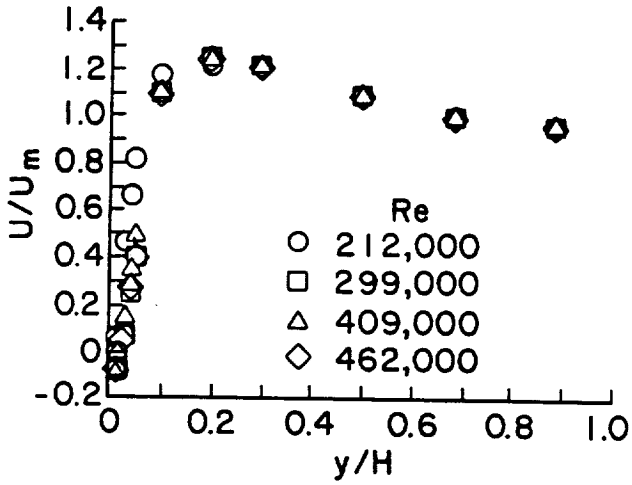

d) Exit of the Turn

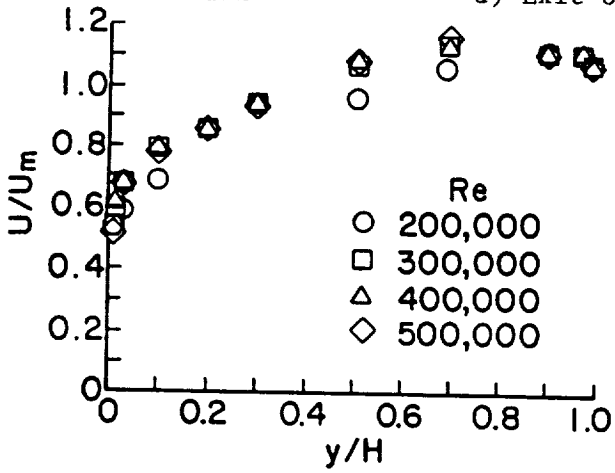

e) 3.03H Downstream of the Turn

Figure 14. Mean Velocity Distributions Around the Duct. Roughness on the Inlet.

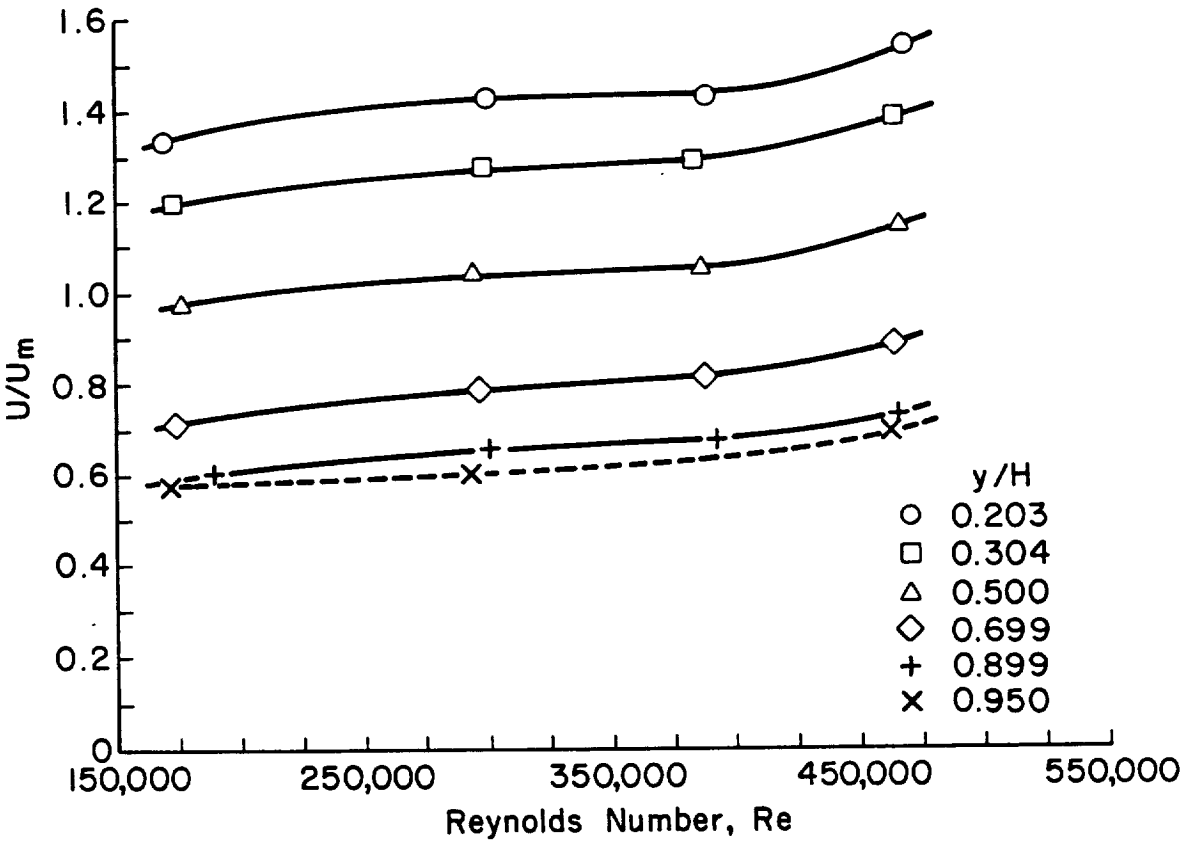

a) Outer Region

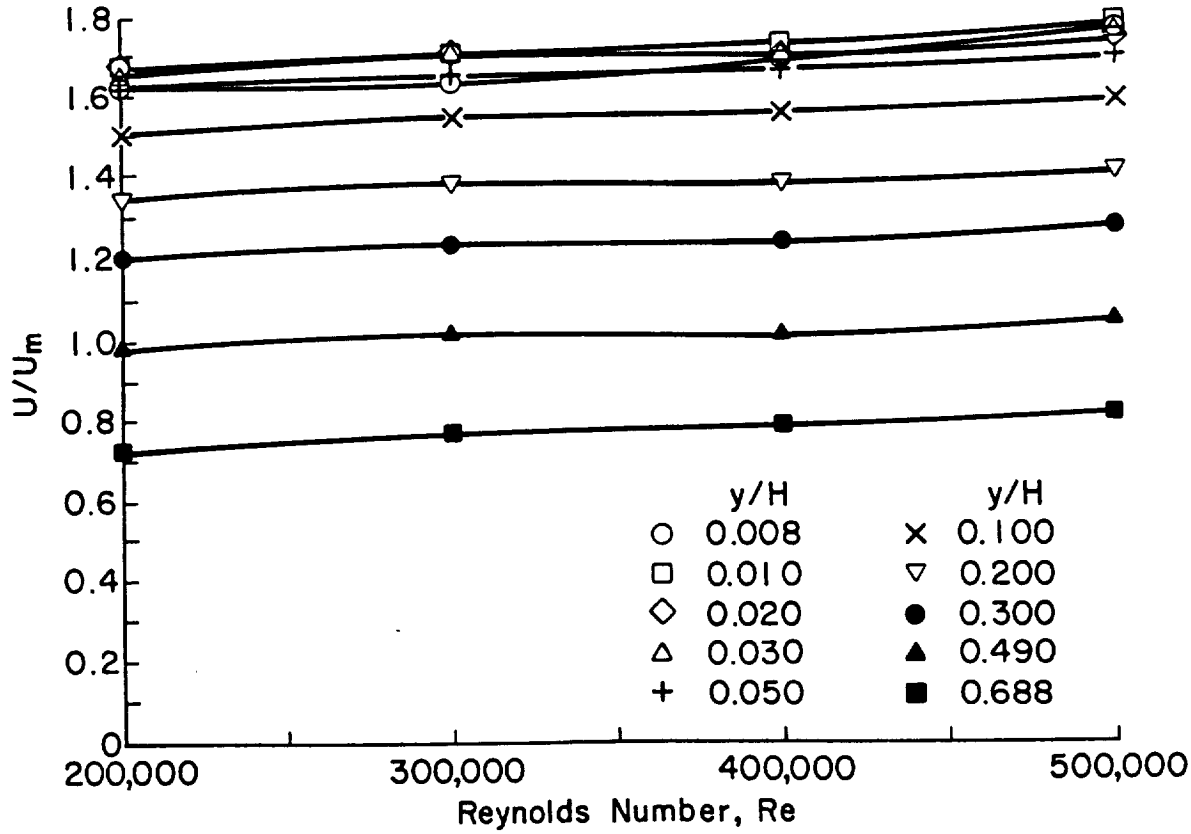

b) Inner Region

Figure 15. Mean Velocity Variation with Reynolds Number at the 90 Degree Location. Roughness on the Inlet.

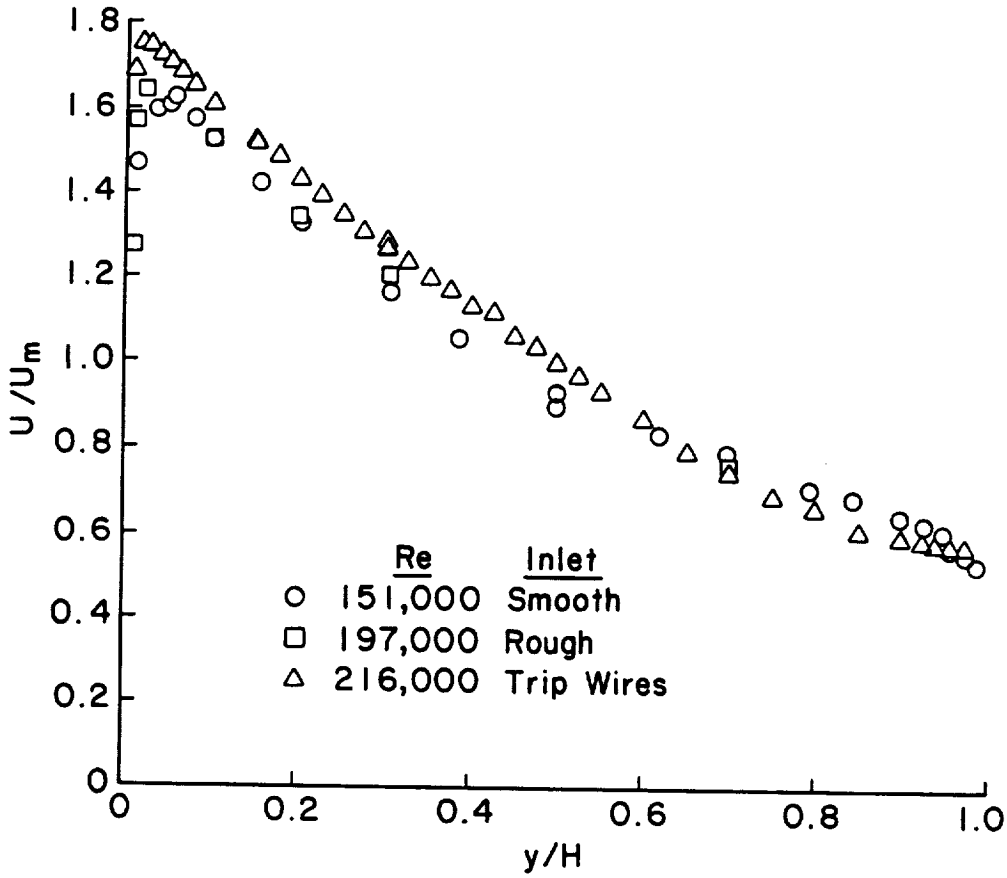

Figure 16. Mean Velocity Distributions at 90 Degrees Around the Turn for the Three Inlet Conditions.

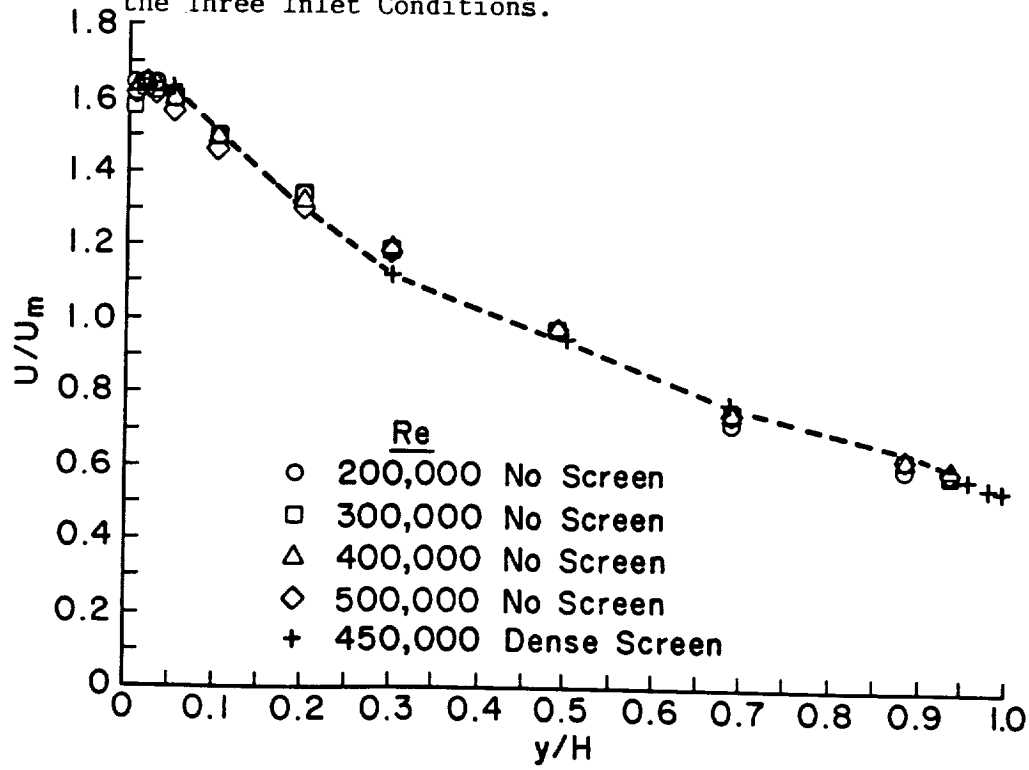

Figure 17. Mean Velocity Distributions at 90 Degrees Around the Turn for Different Exit Screens.

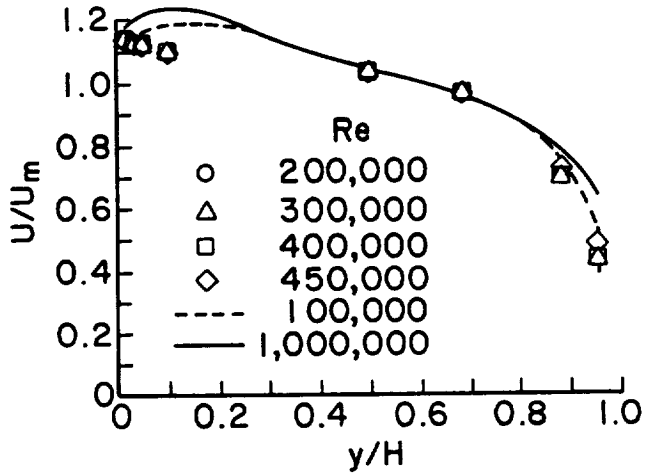

a) Start of the Turn

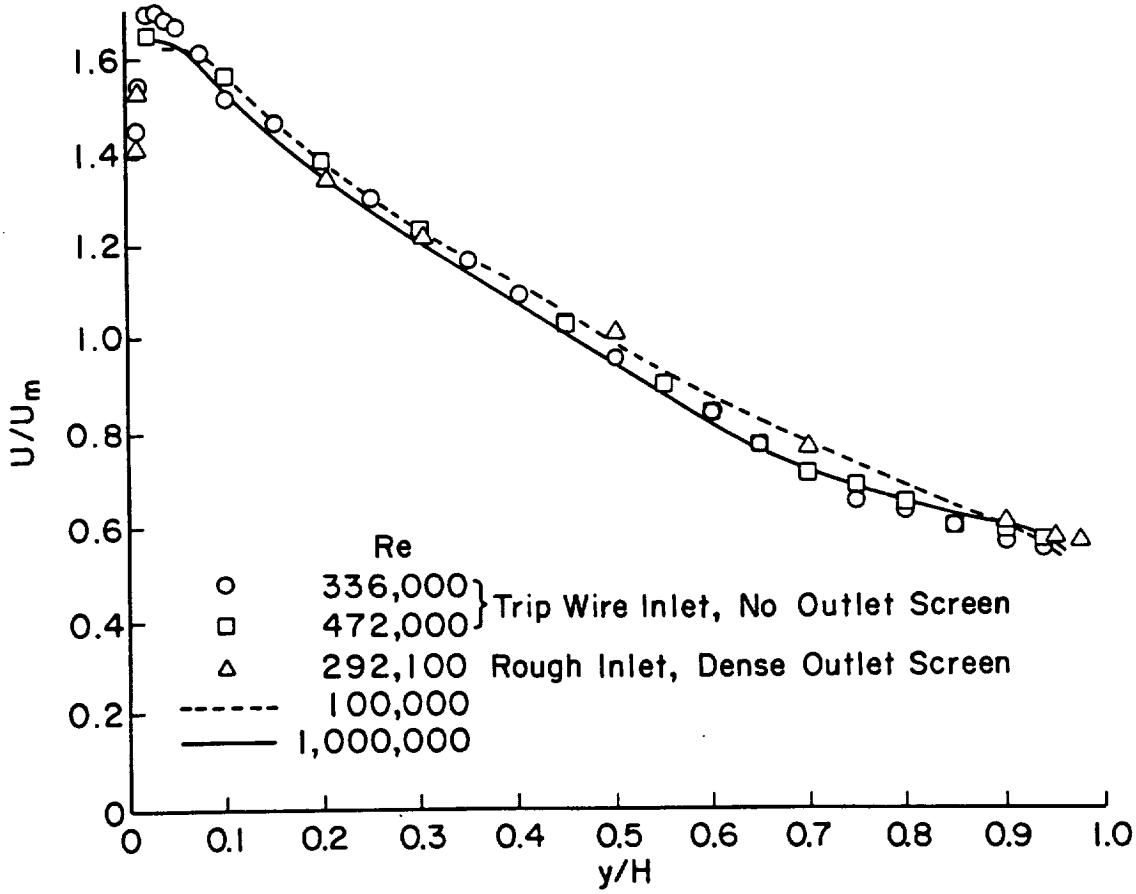

b) 90 Degrees Around the Turn

Figure 18. Comparison of the Mean Velocity Distributions with Measurements of Monson and Seegmiller (1989).

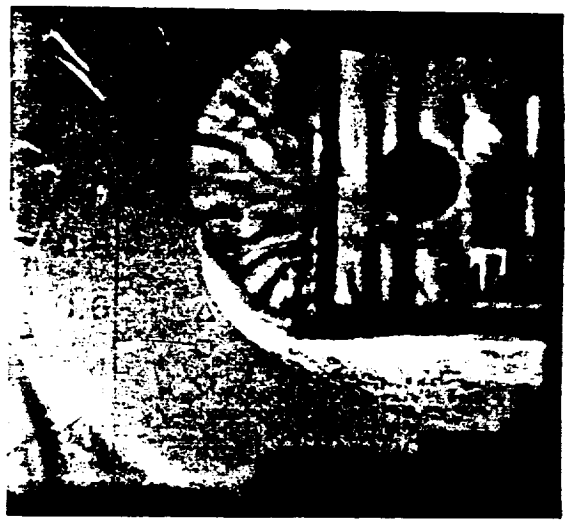

ORIGINAL PAGE IS
OF POOR QUALITY

a) Air Bubble Visualization of the Separation at the Turn Exit

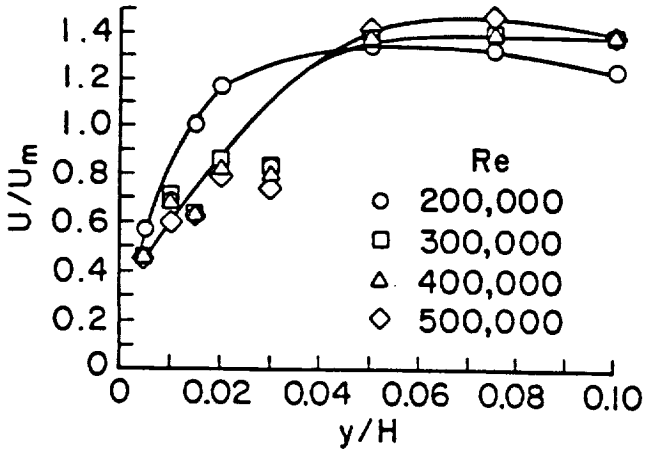

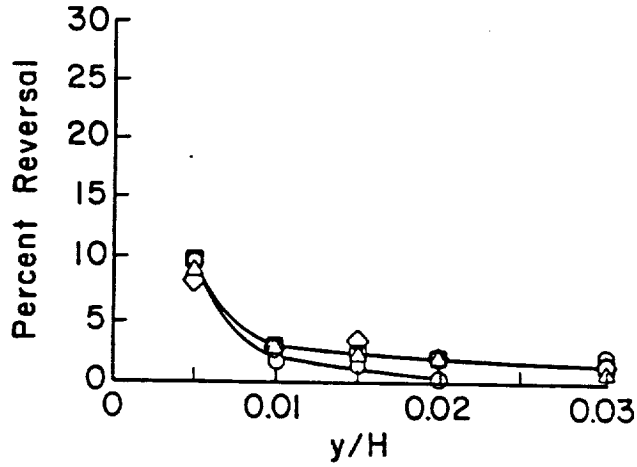

b) 150 Degrees Around the Turn

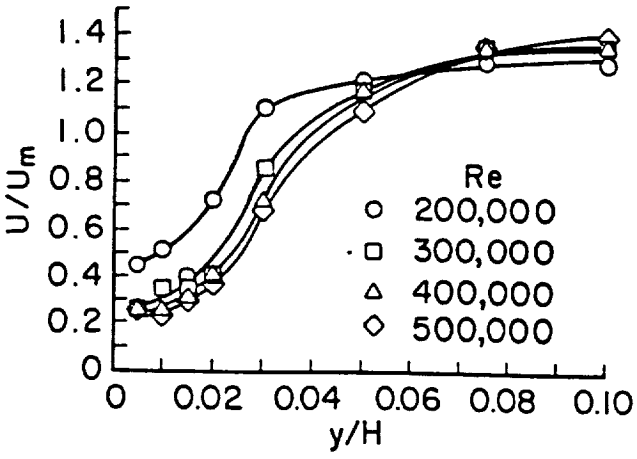

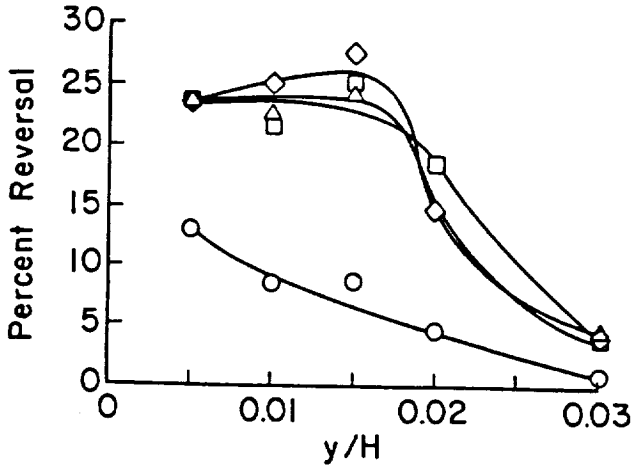

c) 160 Degrees Around the Turn

Figure 19. Velocity Distributions and Flow Reversal in the Separation Bubble. Roughness on the Inlet.

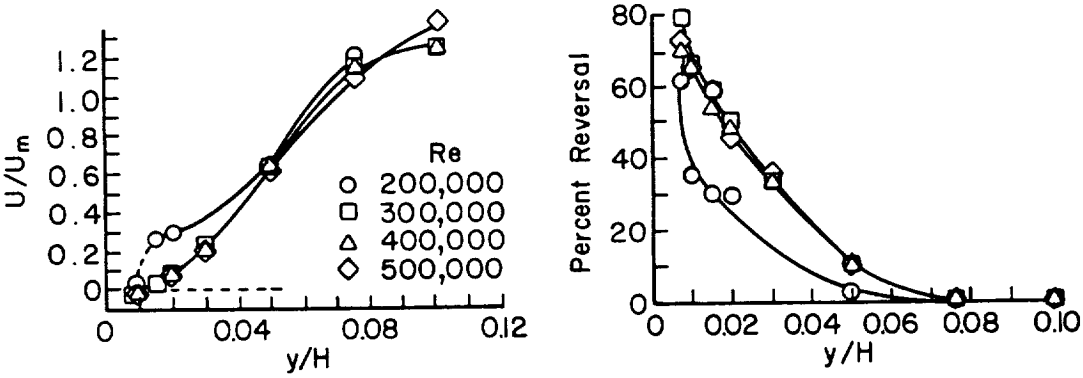

d) 170 Degrees Around the Turn

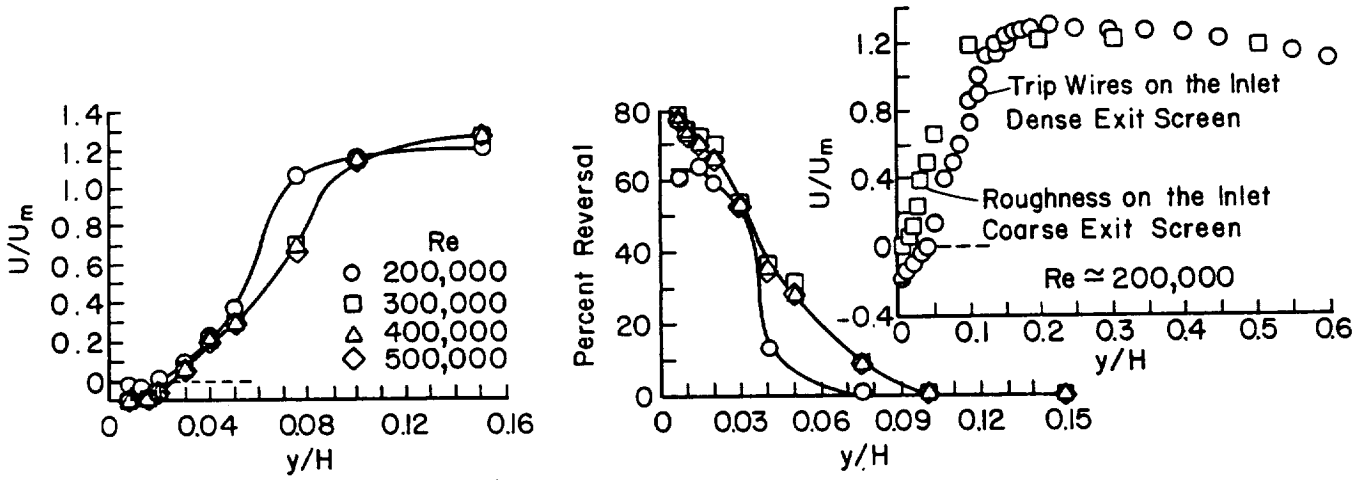

e) Exit of the Turn

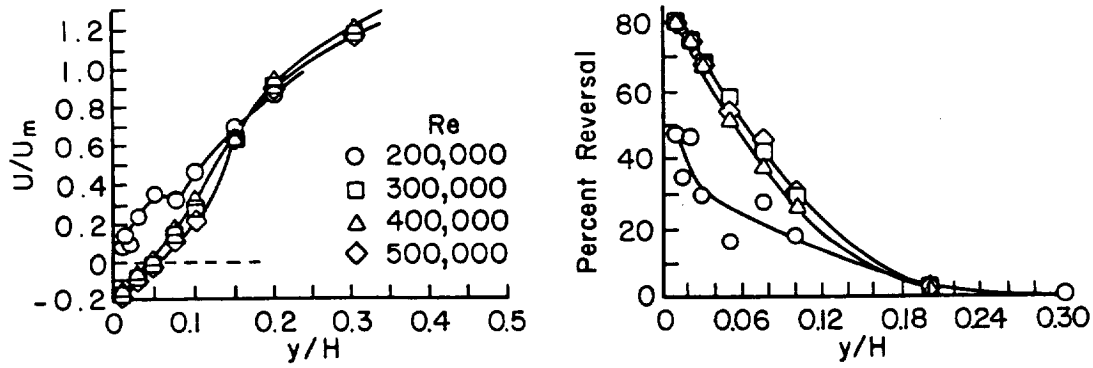

f) .505H Downstream of the Turn

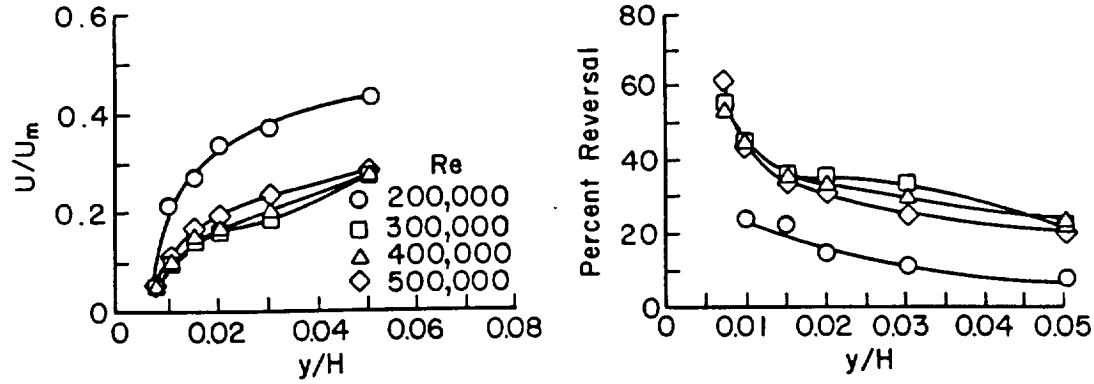

g) .758H Downstream of the Turn

Figure 19. (Concluded) Velocity Distributions and Flow Reversal in the Separation Bubble. Roughness on the Inlet

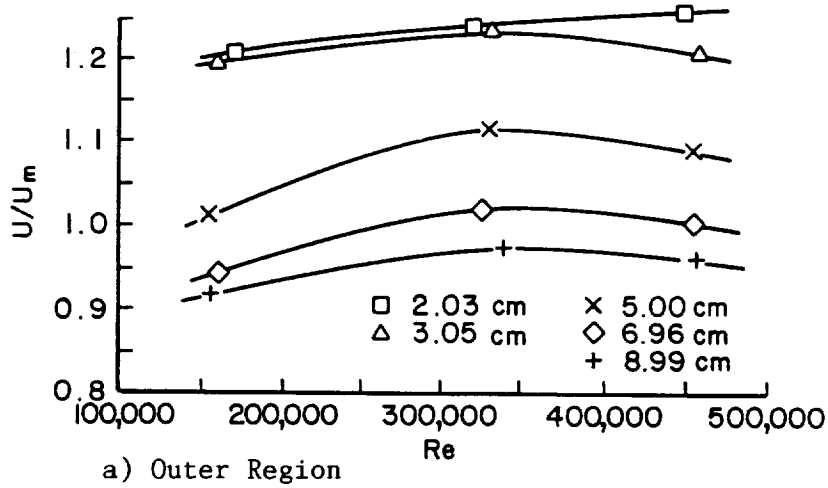

a) Outer Region

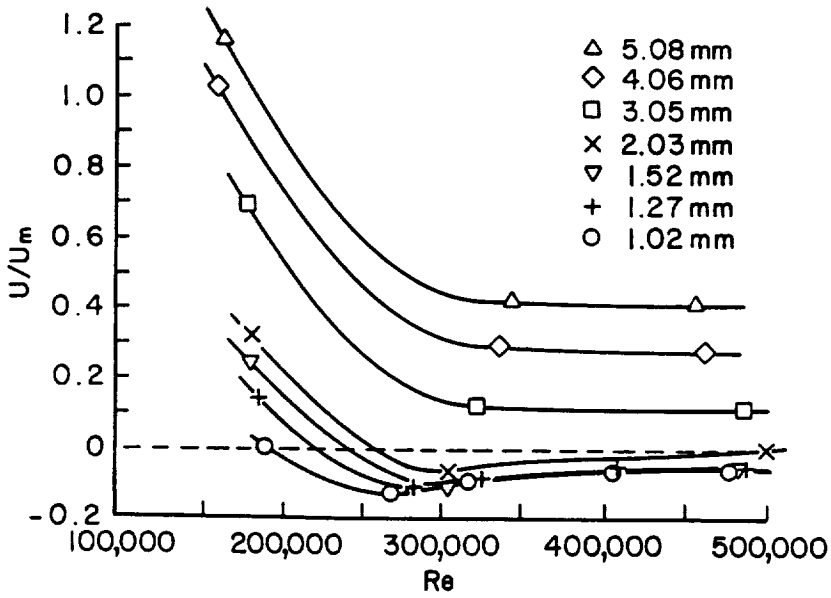

b) Inner Region

Figure 20. Mean Velocity Variation with Reynolds Number at the Turn Exit. Roughness on the Inlet.

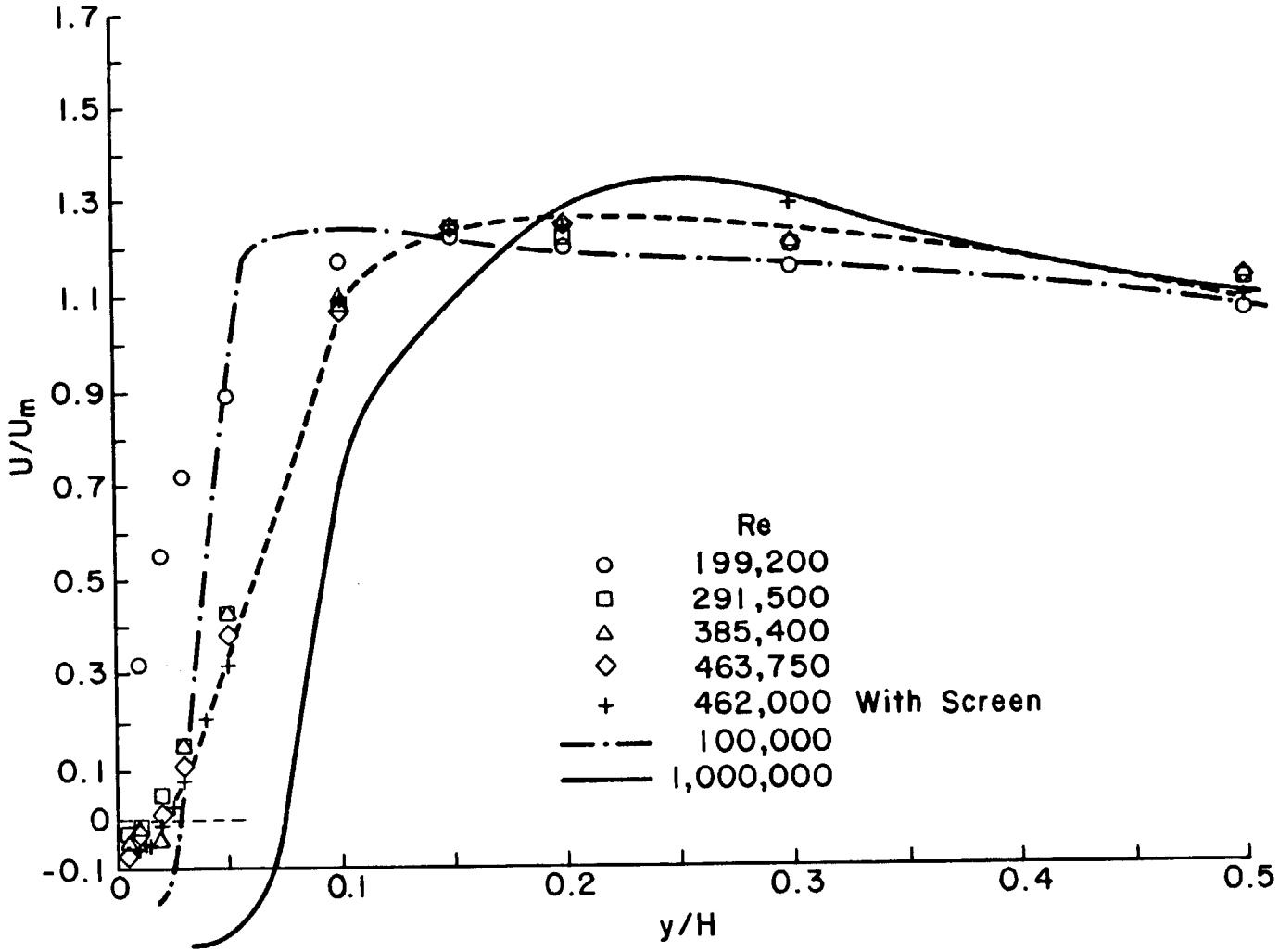

Figure 21. Velocity Variation at the Exit of the Turn with and without an Exit Screen Compared with Measurements of Monson and Seegmiller (1989).

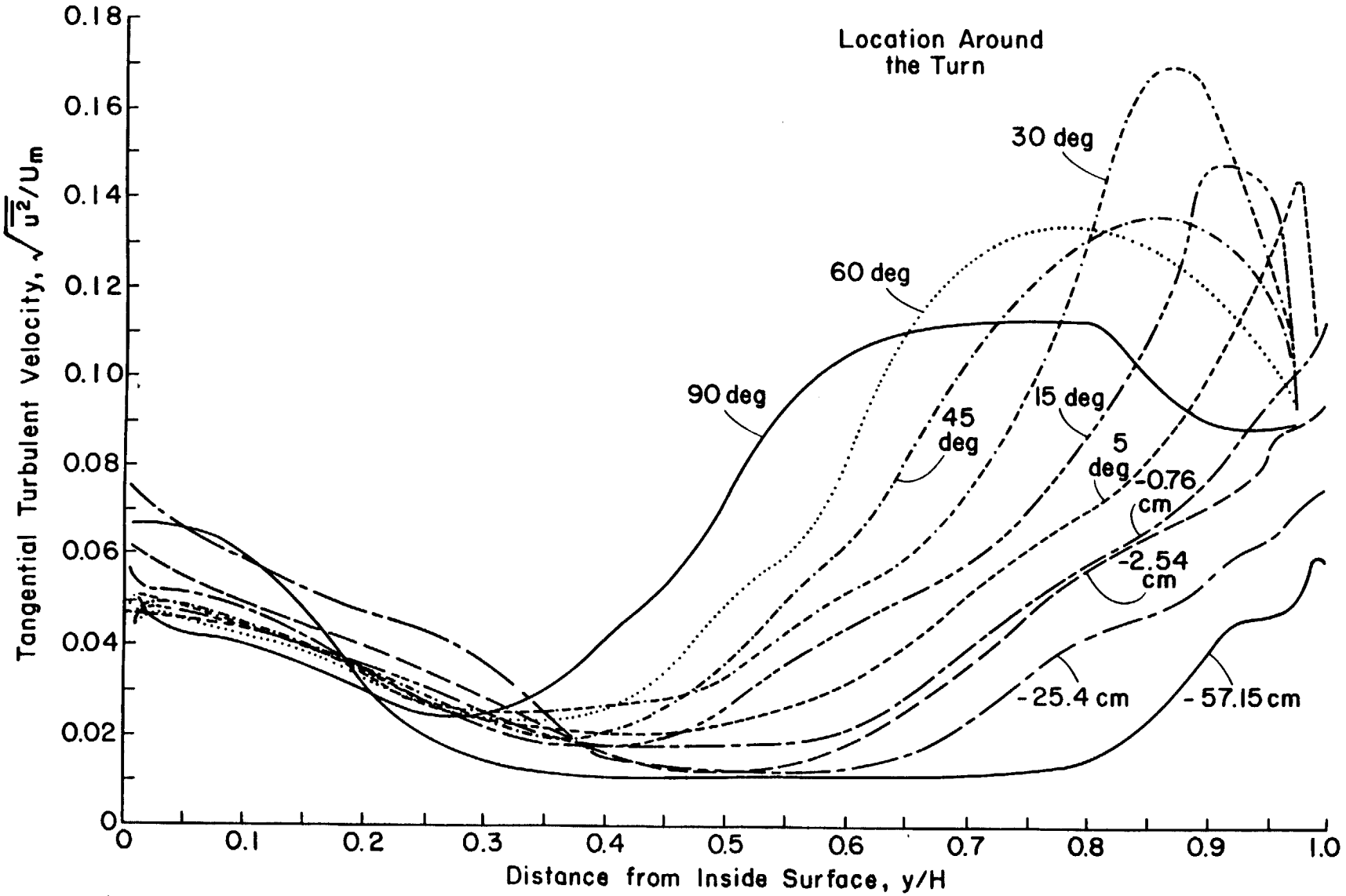

a) Around the Turn to 90 Degrees

Figure 22. Tangential Turbulent Velocity Variations Around the Duct.

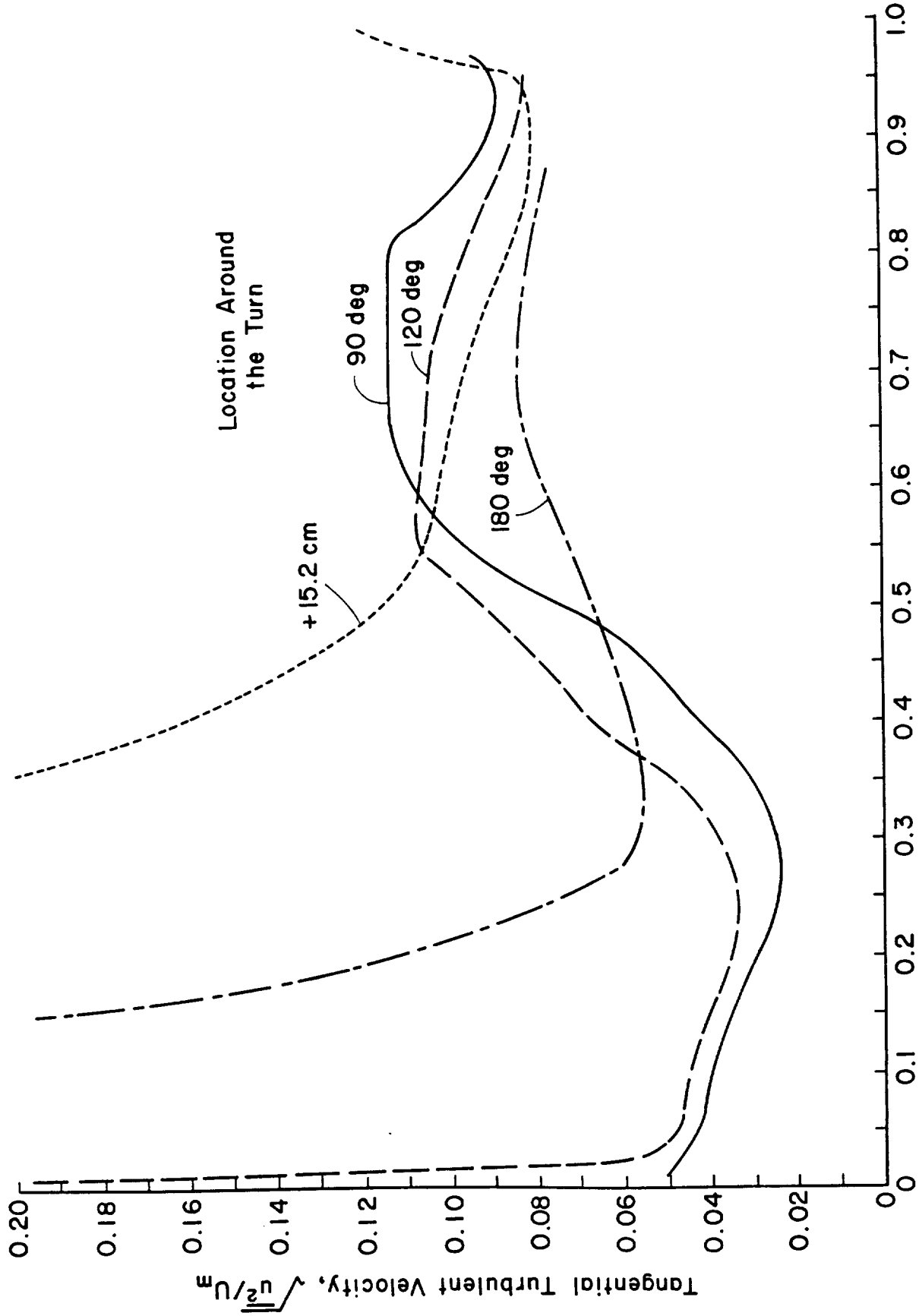

b) Downstream of 90 Degrees

Figure 22. (Concluded) Tangential Turbulent Velocity Variation Around the Duct.

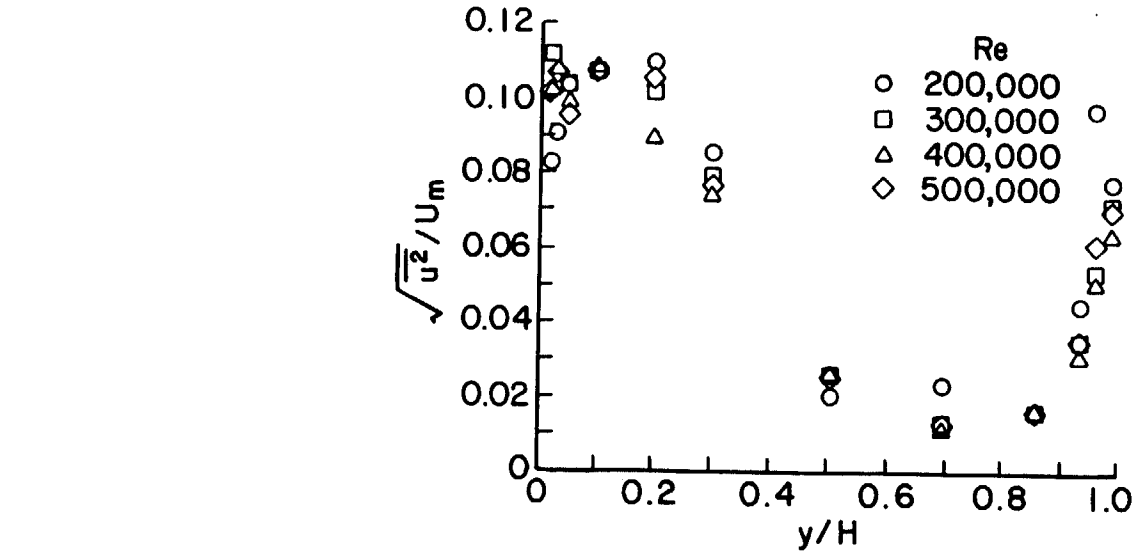

a) 10H Upstream of the Turn

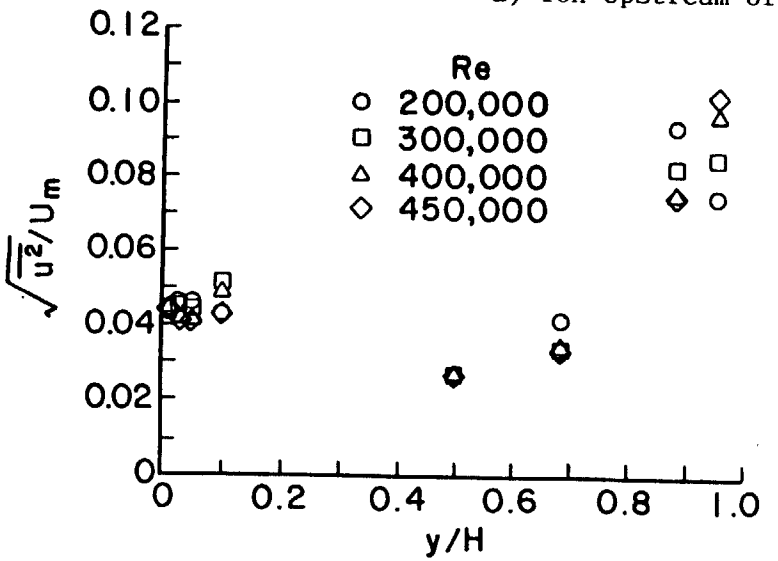

b) Start of the Turn

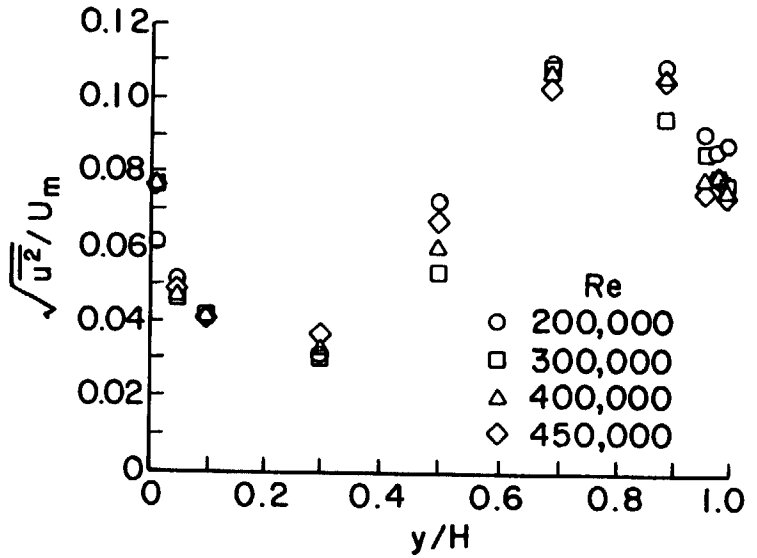

c) 90 Degrees Around the Turn

Figure 23. Tangential Turbulent Velocity Variation Around the Duct. Roughness on the Inlet.

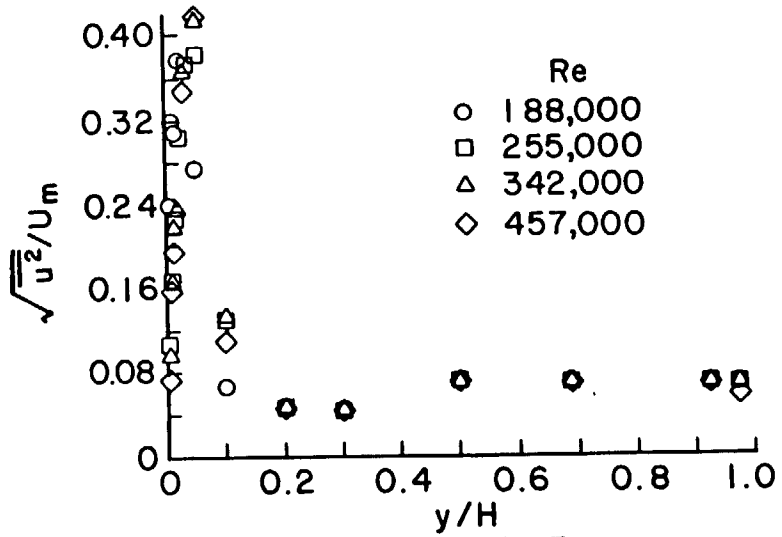

d) 170 Degrees Around the Turn

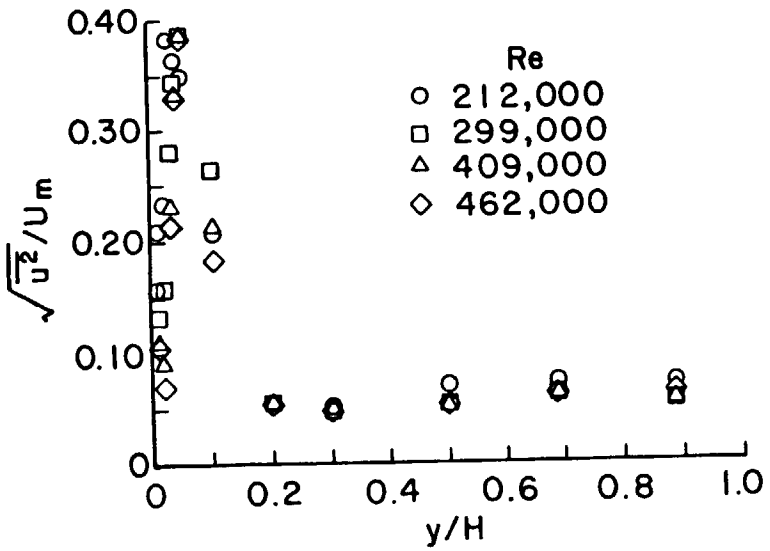

e) Exit of the Turn

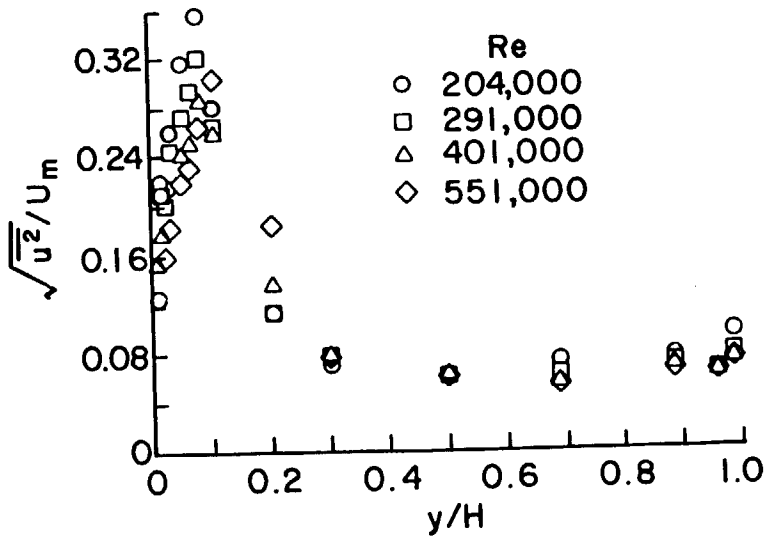

f) .508H Downstream of the Turn

Figure 23. (Concluded) Tangential Turbulent Velocity Variation Around the Duct. Roughness on the Inlet.

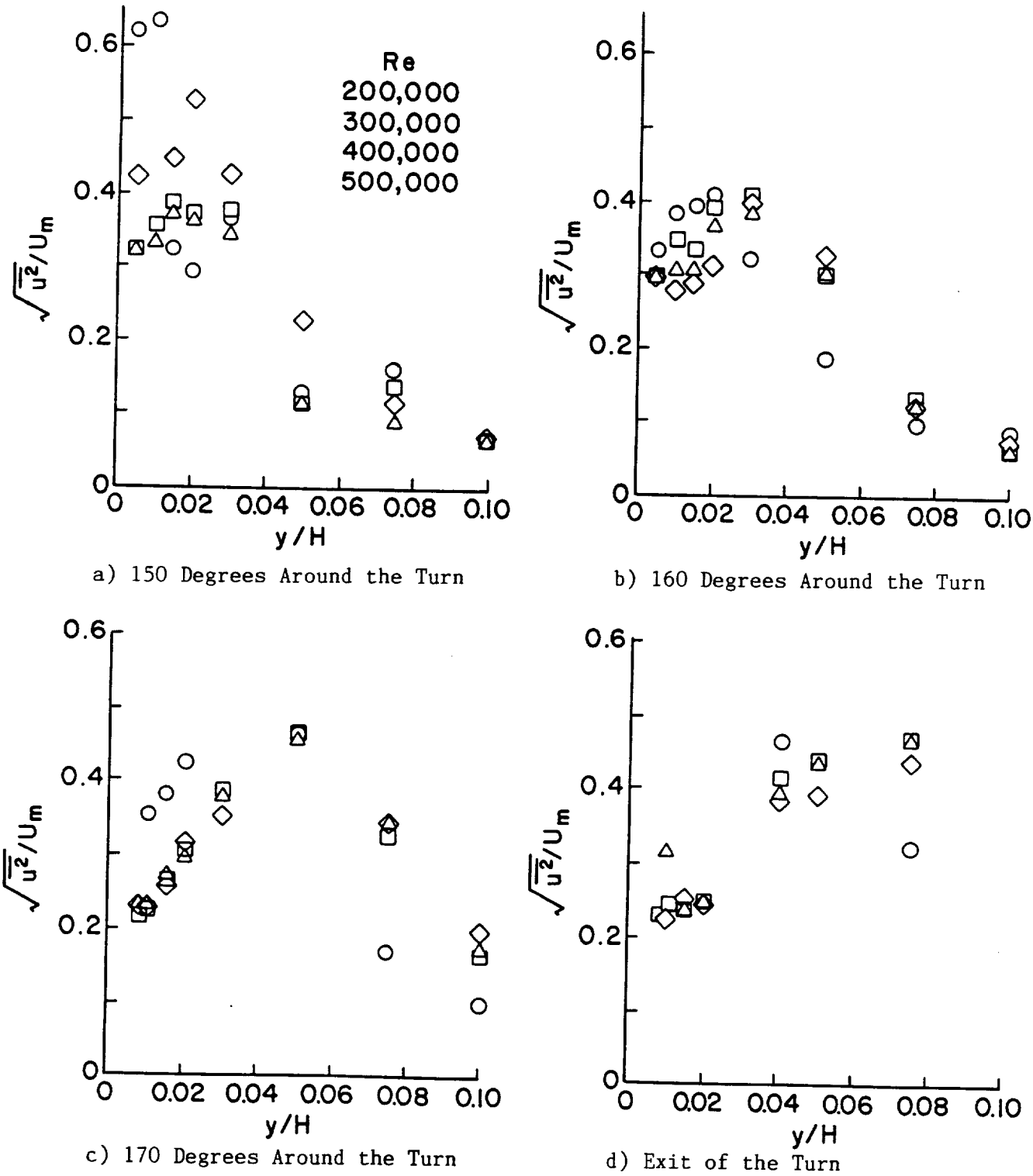

a) 150 Degrees Around the Turn

b) 160 Degrees Around the Turn

c) 170 Degrees Around the Turn

d) Exit of the Turn

Figure 24. Tangential Turbulent Velocity Variation in the Separation Region. Roughness on the Inlet.

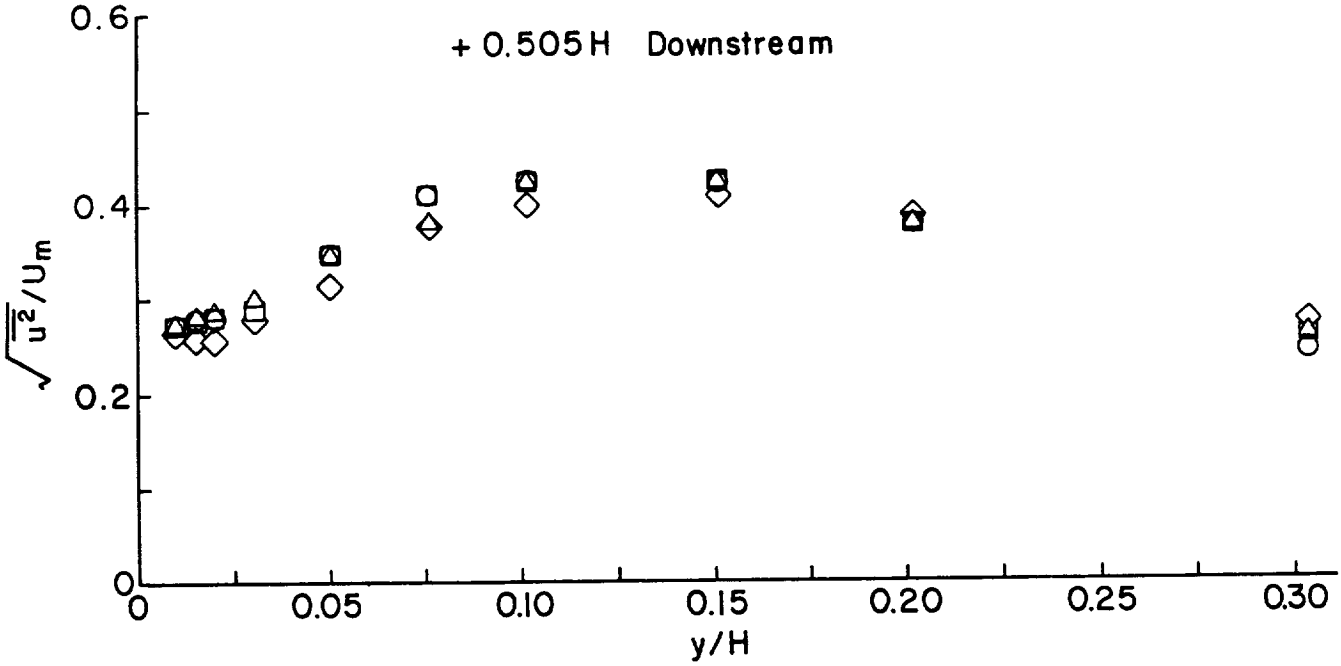

e) .505H Downstream of the Turn

Figure 24. (Concluded) Tangential Turbulent Velocity Variation in the Separation Region. Roughness on the Inlet.

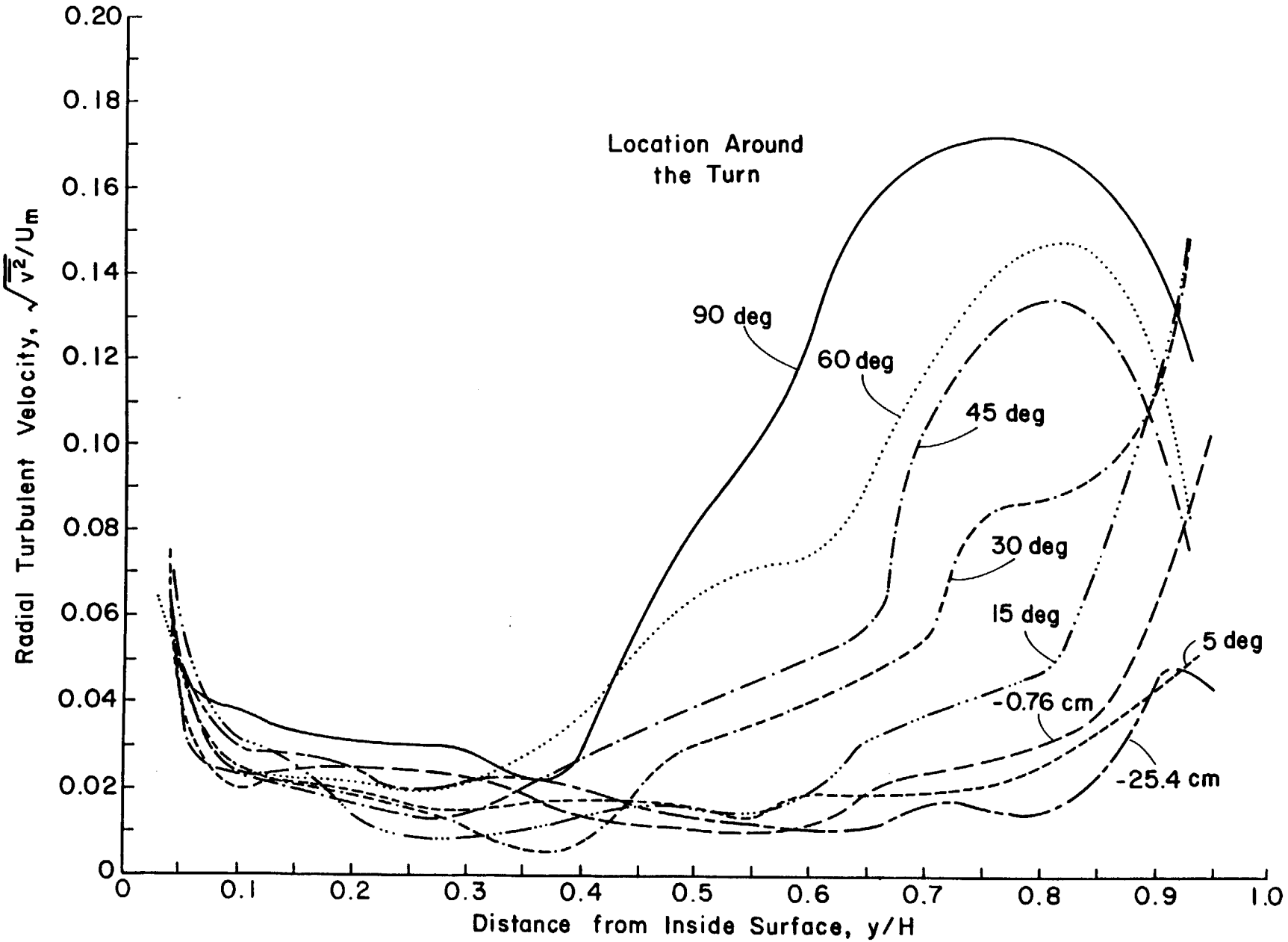

a) Around the Turn to 90 Degrees

Figure 25. Radial Turbulent Velocity Variation Around the Duct.

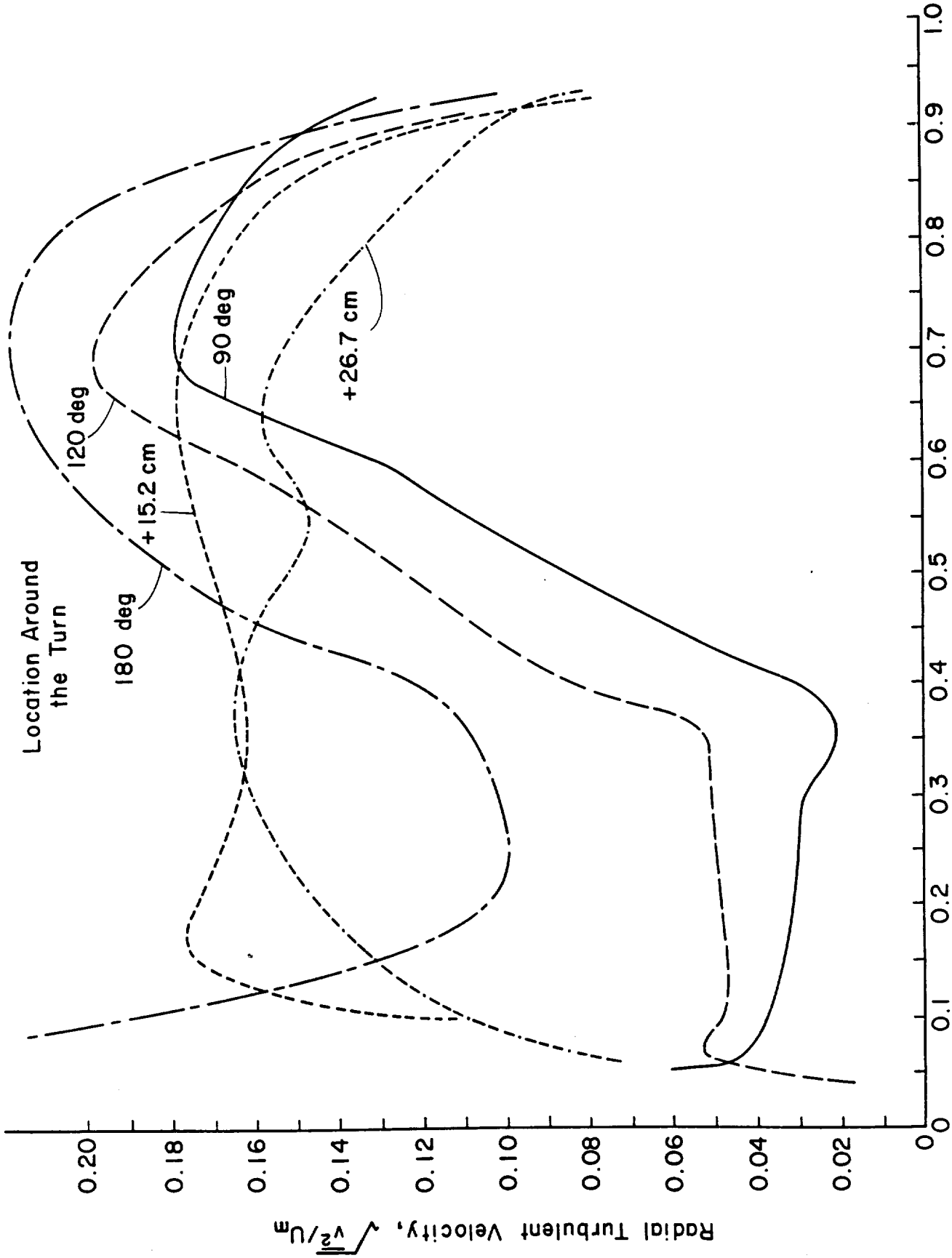

b) Downstream of 90 Degrees

Figure 25. (Concluded) Radial Turbulent Velocity Variation Around the Duct.

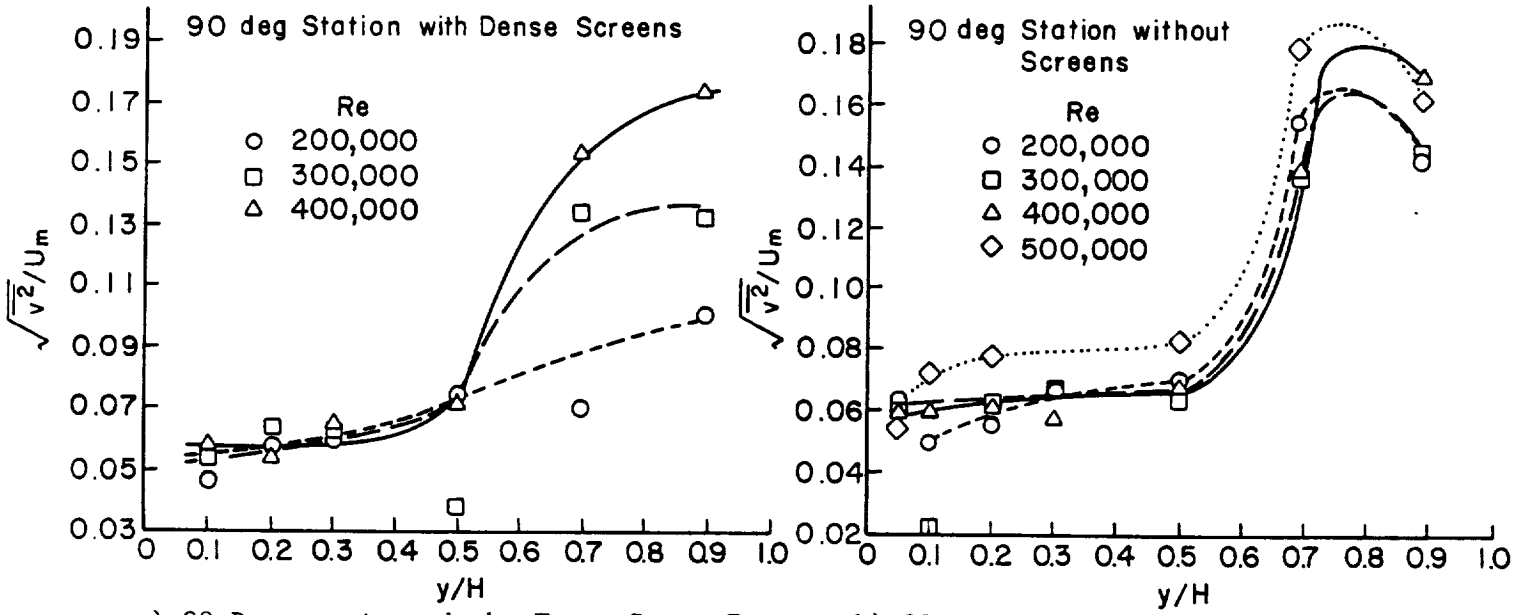

a) 90 Degrees Around the Turn, Dense Exit Screen

b) 90 Degrees Around the Turn, No Exit Scree

Figure 26. Radial Turbulent Velocity Variation with Reynolds Number and Exit Screen. Roughness on the Inlet.

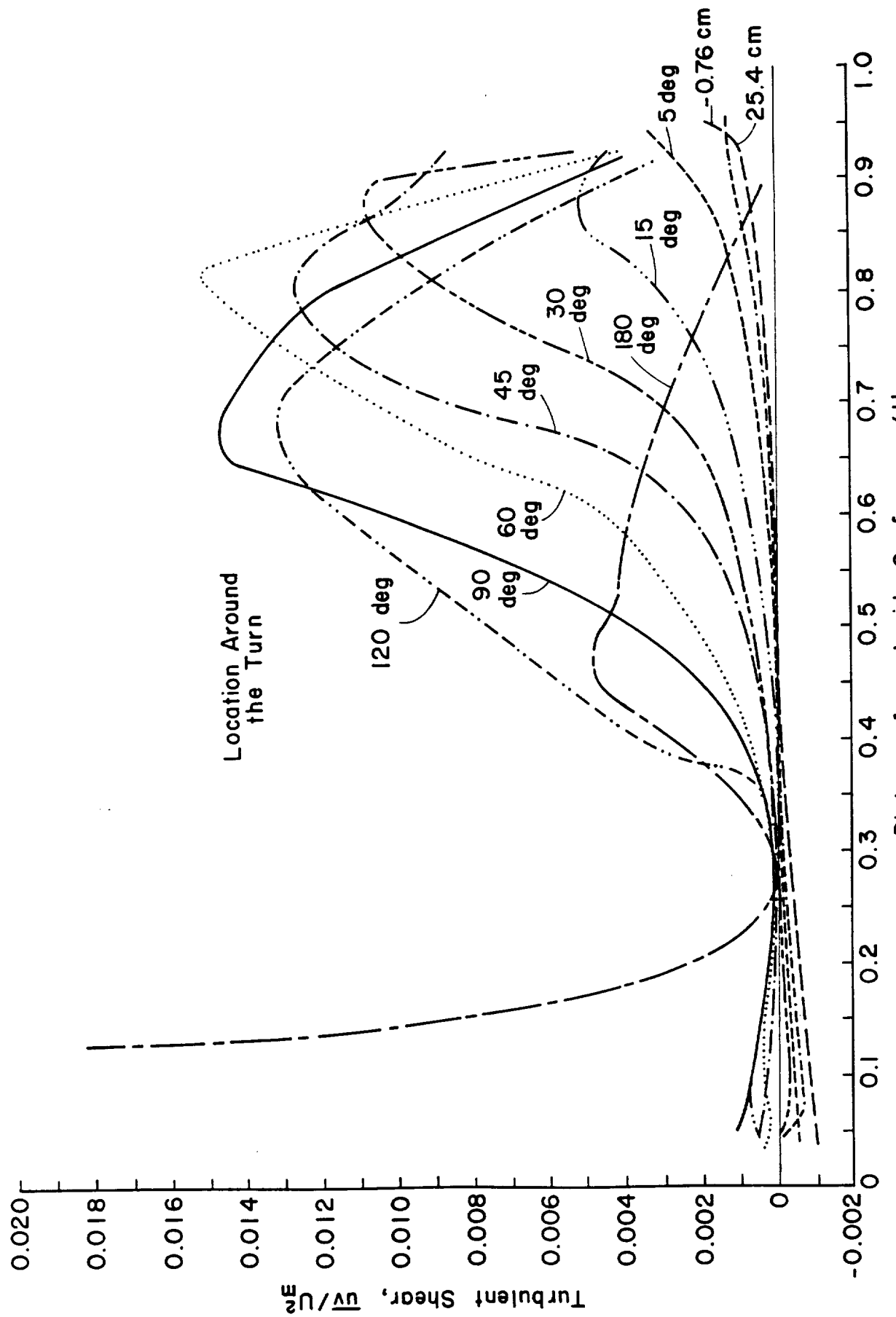

Figure 27. Turbulent Shear Stress Variation Around the Duct.

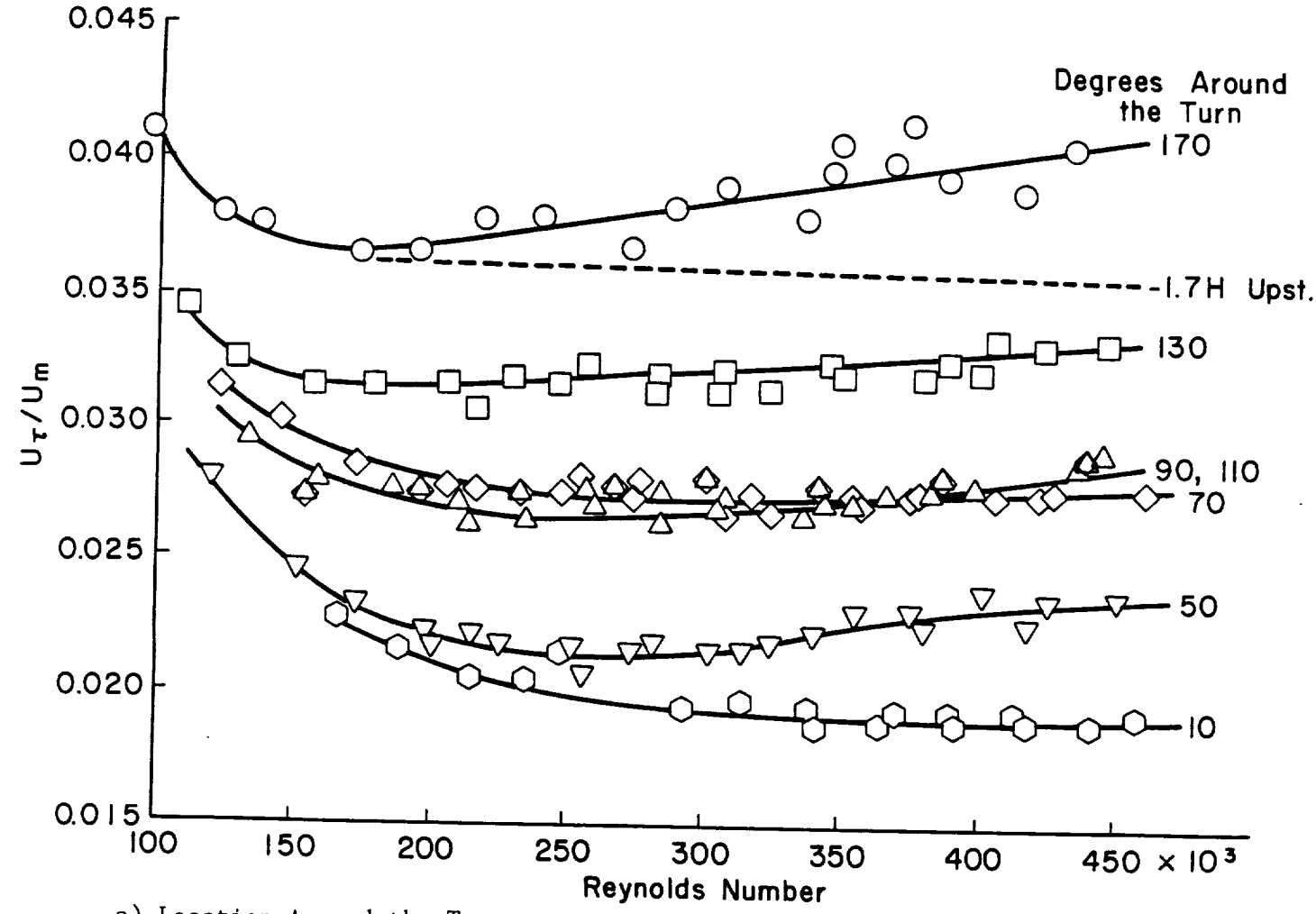

a) Location Around the Turn

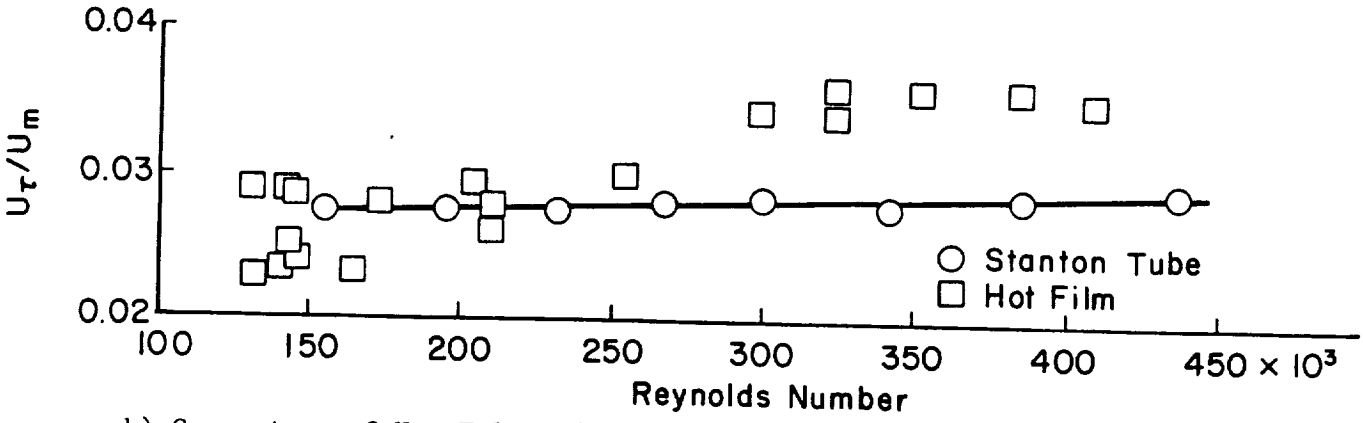

b) Comparison of Hot Film and Stanton Tube at 90 Degrees Around the Turn

Figure 28. Surface Shear Stress Variation with Reynolds Number. Trip Wires on the Inlet, Dense Screen at the Exit.

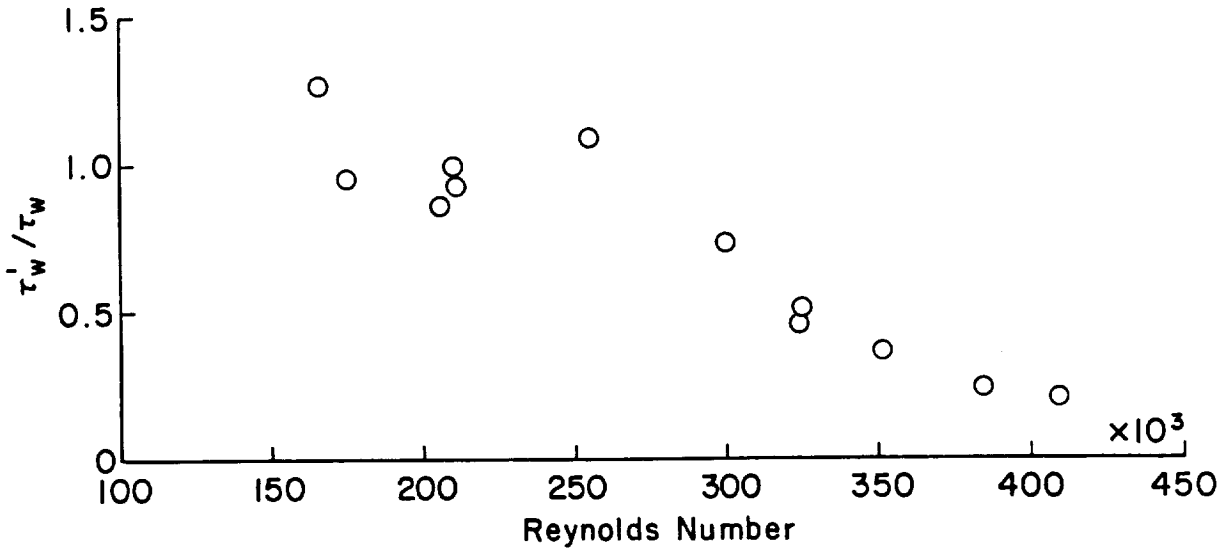

Figure 29. Surface Shear Turbulent Intensity at 90 Degrees Around the Turn.

APPENDIX A

TABULATED DATA FOR FLOW WITH TRIP WIRES ON THE UPPER AND LOWER SURFACE OF THE DUCT INLET

A set of mean and turbulent velocity distributions were obtained for the case where trip wires were placed on both the upper and lower surfaces of the duct inlet, Figure A-1. The trip wires, 1.3 mm in diameter, were coated with epoxy paint which served to bond them to the inlet.

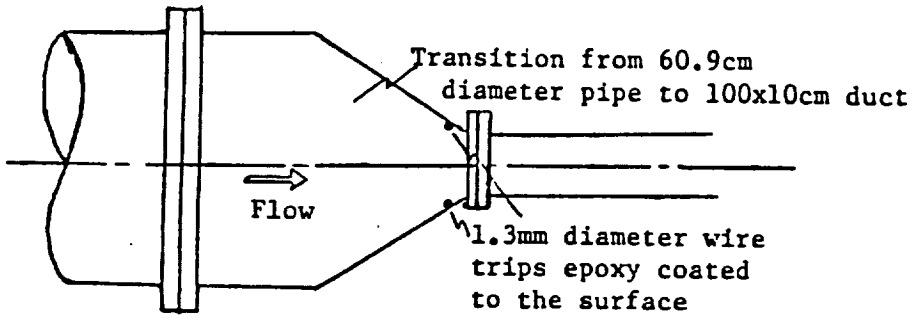

Figure A-1. Trip Wire Inlet Condition

The static pressure distributions around the duct were measured from the static taps shown on Figure A-2. Tap number 1 was used as the reference pressure in computing the pressure coefficient.

$$c_p = \frac{p - p_{ref}}{(1/2)\rho U_m^2} \qquad (A\text{-}1)$$

where U_m is the mean or bulk velocity of the flow. The measurements were made with the transducer located below the plane of the facility, so that the static head from location to location does not enter into the measurements, see insert on Figure A-2. Values of the static head heights for each location around the turn are noted on Figure A-2; where

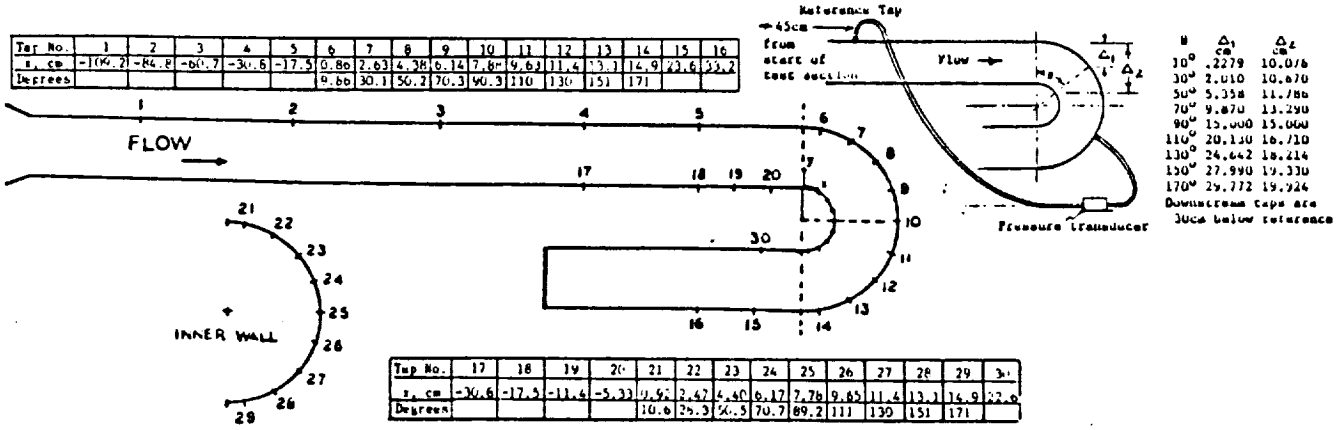

Tap No.	1	2	3	4	5	6	7	8	9	10	11	12	13	14	15	16
x, cm	-106.2	-84.8	-60.7	-30.6	-17.5	0.86	2.63	4.38	6.14	7.89	9.63	11.4	13.1	14.9	23.6	33.2
Degrees						9.86	30.1	50.2	70.3	90.3	110	130	151	171		

Tap No.	17	18	19	20	21	22	23	24	25	26	27	28	29	30
x, cm	-30.6	-17.5	-11.4	-5.33	0.92	3.47	4.40	6.17	7.76	9.65	11.4	13.1	16.9	22.9
Degrees					10.6	29.3	50.5	70.7	89.2	111	130	151	171	

θ	Δ_1 cm	Δ_2 cm
10°	.2279	10.076
30°	2.010	10.670
50°	5.358	11.786
70°	9.870	13.290
90°	15.000	15.060
110°	20.130	16.710
130°	24.642	18.214
150°	27.990	19.330
170°	29.772	19.926

Figure A-2. Location of Static Pressure Taps Around the Facility.

Δ_1, corresponds to the outside surface taps and Δ_2 to the inside surface taps. Time averaging up to 35 seconds were used for the individual pressure measurements.

Table A-Ia lists the static pressure coefficients measured around the duct for the trip wire inlet. For the data of Table A-Ia a "dense" screen was employed at the duct outlet. Table A-Ib lists the static pressure coefficient variation with Reynolds number for the cases of a dense screen and no screen at the duct outlet.

Table A-IIa lists the mean and turbulent velocity measurements in the upstream part of the duct around to the 120 degree location for a bulk Reynolds number of 218,000. The flow in the duct was set to the desired Reynolds number and the complete velocity profile was measured at a particular location. This set of data is the most detailed of the measurement reported.

Table A-11b lists the mean and turbulent velocity measurements made at a location 25.4 cm upstream of the start of the turn for several Reynolds numbers and for the cases of a dense screen and no screen at the outlet. Also tabulated are data at the 90 degree location for two Reynolds numbers and no exit screen. The mean velocity, U_m =2.819 m/sec, listed on Table A-IIa corresponds to the value at the entrance to the duct. The local mean velocity varies slightly along the duct, thus the tabulated values of U/U_m versus y/H are slightly different from the values obtained when the local mean velocity is employed.

Table A-III lists values of U/U_m obtained with the Stanton tube at a number of locations around the turn. Mounting the sensor flush with the surface was done by observing the light scattering from the tube. Comparison of repeat mountings at the calibration station indicated an uncertainty of ± 5 percent in the resulting calibration curve. Mounting in the curved wall is subject to further uncertainty. The variation of U/U_m for locations 70, 90, 110 degrees, figure 28a), at specific Reynolds numbers appears to be an indication of the uncertainty expected in the curved region.

A hot film anemometer was employed to measure the spanwise turbulent velocity component, $\sqrt{\overline{w^2}}$. The measured values at 90 degrees around the turn are listed in Table A-IVa. Table A-IVb lists the faired values of the spanwise turbulent velocity for specific Reynolds numbers. The data of Table A-IVb are plotted on figure A-3 and compared with faired values of the radial turbulent velocity components (listed in Tables A-IIa and b). A faired curve of the tangential turbulent velocity component obtained when $\sqrt{\overline{w^2}}$ was measured is also shown on figure A-3. The spanwise and radial turbulent velocities are nearly the same over the middle region of the outer flow (outer half of the duct along the concave surface).

The spanwise turbulent velocity is larger than the radial component both near the surface and in the center of the duct. These large spanwise fluctuations appear to be consistent with the concept that the flow in the concave region contains highly time dependent vortex type motion.

For the spanwise velocity measurements the hot film was operated in conjunction with the laser velocimeter. The hot film sensor calibration varied with time due to contamination in the water. The laser velocimeter was employed to evaluate the mean and turbulent tangential velocities for each measured point. While the hot film varied with time, it has been documented, Sandborn (1973), (pp.368-71), that the sensor sensitivities are only slightly affected by the contamination. The hot film sensitivities to velocity and flow angle were determined graphically for the sensor output and the laser velocity data. The values of $\sqrt{w^2}$ were obtained from a "local linearized" relation, Sandborn (1973), [pp.290-91 and eq. (7.28)]. It was assumed that no correlation exists between u and w in the present quasi-two-dimensional flow.

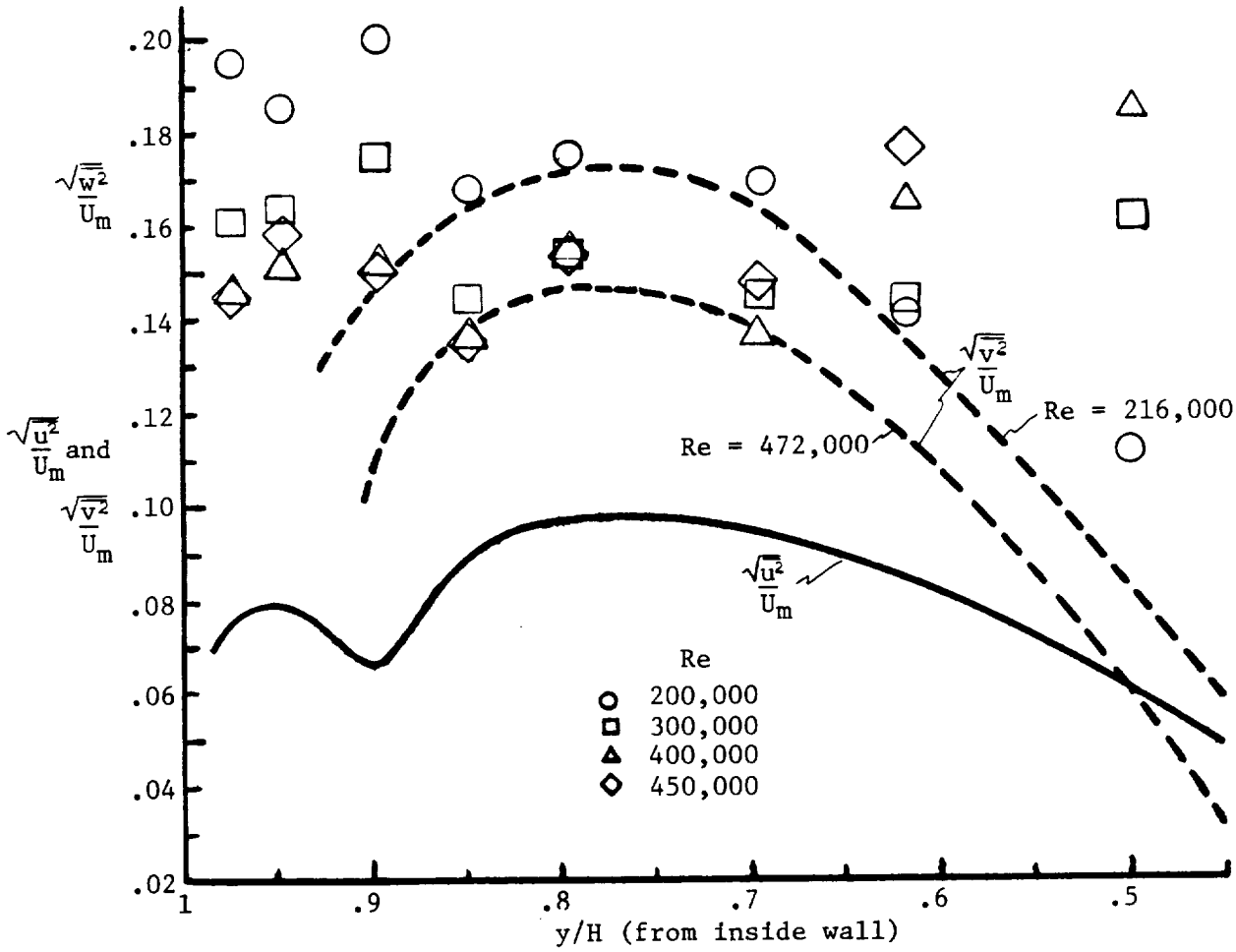

Figure A-3. Spanwise Turbulent Velocity Variation at 90 Degrees Around the Turn.

TABLE A-Ia. Static Pressure Coefficient Distributions. Trip Wires on Inlet; Dense Screen at Exit.

Tap No.	x(cm)	Cp Re=143,000 Um=2.77m/s	Cp Re=207,000 Um=3.03m/s	Cp Re=228,000 Um=3.52m/s	Cp Re=266,000 Um=4.10m/s	C_p Re=296,000 U_m=4.56m/s
	Outer wall					
2	-84.840	0.0560	0.0526			
3	-60.710	0.0468	0.0398			
4	-36.830	0.0243	-0.0211	0.0270	0.0140	
5	-17.530	0.0746	-0.0507	0.0030	-0.0100	
6	0.860 (9.86°)	0.3250	0.3340	0.3830	0.3520	
7	2.627 (30.10°)	0.4260	0.4240	0.4770	0.4500	0.379
8	4.383 (50.22°)	0.4750	0.4780	0.5360	0.5020	0.455
9	6.137 (70.33°)	0.4770	0.4740			0.417
10	7.880 (90.30°)	0.5030	0.4600	0.5175	0.4776	
11	9.634 (110.4°)	0.4980	0.5020			
12	11.390 (130.5°)	0.4850	0.4860	0.5300	0.4810	0.417
13	13.140 (150.6°)	0.4490	0.4370	0.4680	0.4170	0.360
14	14.910 (170.8°)	0.3670	0.3450	0.3590	0.2980	0.303
15	23.650 (7.94cm downstream)	-0.5330	-0.5500	-0.6220	-0.7270	-0.682
16	33.170 (17.46cm downstream)	-0.4650	-0.4820	-0.5000	-0.5630	-0.568
	Inner wall					
17	-36.830	-0.0605	-0.0320	0.0430	0.0190	
18	-17.530	-0.0807	-0.0560	0.0160	-0.0050	
19	-11.430					
20	-5.334	-0.2030	-0.2060	-0.1340	-0.1580	-0.152
21	0.921 (10.56°)	-1.6050	-1.6800	-1.7260	-1.6690	-1.421
22	2.470 (28.30°)	-2.1850	-2.2950	-2.3890	-2.3150	-1.933
23	4.403 (50.46°)	-2.5560	-2.6760	-2.8080	-2.7230	-2.255
24	6.169 (70.69°)	-2.5830	-2.7370	-2.8500	-2.7660	-2.463
26	9.652 (110.6°)	-2.4040	-2.4790	-2.5430	-2.4570	-2.084
27	11.380 (130.4°)	-2.0730	-2.0780	-2.1230	-2.0510	-1.736
28	13.140 (150.6°)	-1.5970	-1.5700	-1.5480	-1.5340	-1.307
29	14.880 (170.5°)	-1.1580	-1.3360	-1.4390	-1.4660	-1.243
30	22.560 (6.85cm downstream)	-0.6260	-0.6800	-0.8280	-0.9390	-0.872

TABLE A-Ib. Static Pressure Coefficients for Two Exit Screen Conditions.

i) No Exit Screen

Tap No.	x(cm)	Cp Re=386,000 Um=5.96m/s	Cp Re=215,000 Um=3.31m/s	Cp Re=273,000 Um=4.22m/s
	Outer wall			
10	7.880 (90.30°)	0.5270	0.4431	0.4316
14	14.910 (170.8°)	0.2880	0.3129	0.2659
15	23.650 (7.94cm downstream)	-0.8470	-0.5332	-0.7048
16	33.170 (17.46cm downstream)	-0.6570	-0.5025	-0.6072
	Inner wall			
24	6.169 (70.69°)	-2.970		
29	14.880 (170.5°)	-1.722	-1.226	-1.3150
30	22.560 (6.85cm downstream)	-1.0950	-0.6938	-0.9446

ii) Dense Exit Screen

Tap No.	x(cm)	Cp Re=166 000 Um=2.56m/s	Cp Re=178,000 Um=2.74m/s	Cp Re=203,000 Um=3.12m/s	Cp Re=241,000 Um=3.72m/s	Cp Re=336,000 Um=5.18m/s
	Outer wall					
10	7.880 (90.30°)					0.2186
14	14.910 (170.8°)					-0.2370
15	23.650 (7.94cm downstream)					-0.9217
16	33.170 (17.46cm downstream)					-0.7773
	Inner wall					
24	6.169 (70.69°)	-2.611	-2.559	-2.598	-2.633	
29	14.880 (170.5°)					-1.4150
30	22.560 (6.85cm downstream)					-1.1100

Table A-Ic. Change of Static Pressure at the Reference Tap with Reynolds Number.

Coarse Screen		No Screen		Dense Screen	
Static press. kgf/cm^2	Re	Static press. kgf/cm^2	Re	Static press. kgf/cm^2	Re
0.4360	494,000	0.0338	359,000	0.5063	369,000
0.3129	423,500	0.0598	417,000	0.1266	191,000
0.2672	378,000	0.0809	445,000	0.5190	372,000
0.1899	320,000	0.1090	523,500	0.4557	354,000
0.1174	275,000	0.1273	534,000	0.4726	354,000
0.0738	222,000	0.0668	422,000	0.1336	191,000
0.0352	176,000	0.0345	345,000	0.6546	415,000
0.1231	277,000	0.0141	267,000	0.5211	369,000
0.2074	332,000			0.4290	319,000
0.2707	384,000			0.3130	277,000
0.3411	437,000			0.2145	228,000
0.4184	452,000			0.1477	194,000
0.4641	503,000				
0.5028	524,000				
0.5309	534,000				
0.0352	184,000				

$\nu = 1.32 \times 10^{-6}\ m^2/sec$

TABLE A-IIa. Mean and Turbulent Velocity Around the Duct. Trip Wires on Inlet; Dense Screen at Exit.

x = -94.0cm
Re= 210,000
U_m= 2.819m/sec
T = 9.1°C
ν = 1.341x10^{-6}m^2/sec

y/H	yc/H	U/Um	$\sqrt{\overline{u^2}}/U_m$
.0050	.9950	.7866	.06667
.0100	.9900	.8086	.07074
.0150	.9850	.8307	.06731
.0200	.9800	.8478	.06437
.0300	.9700	.8678	.06744
.0400	.9600	.8766	.06558
.0500	.9500	.8943	.06584
.0625	.9375	.9055	.06319
.0750	.9250	.9139	.06398
.0875	.9125	.9354	.06306
.1000	.9000	.9462	.05938
.1500	.8500	.9979	.04857
.2000	.8000	1.0249	.03110
.2500	.7500	1.0362	.01920
.3000	.7000	1.0419	.01401
.3500	.6500	1.0453	.01177
.4000	.6000	1.0442	.01030
.4500	.5500	1.0439	.01107
.5000	.5000	1.0463	.01050
.5500	.4500	1.0458	.01158
.6000	.4000	1.0459	.01203
.6500	.3500	1.0470	.01158
.7000	.3000	1.0479	.01146
.7500	.2500	1.0480	.01331
.8000	.2000	1.0428	.01517
.8500	.1500	1.0295	.02464
.9000	.1000	.9835	.04204
.9125	.0875	.9655	.04304
.9250	.0750	.9505	.04710
.9375	.0625	.9384	.04707
.9500	.0500	.9105	.04835
.9600	.0400	.8942	.04678
.9700	.0300	.8619	.05257
.9800	.0200	.8516	.05315
.9850	.0150	.8314	.05679
.9900	.0100	.8105	.06046
.9950	.0050	.7996	.05960

x = -57.2cm
Re= 211,000
U_m= 2.819m/sec
T = 9.2°C
ν = 1.339x10^{-6}m^2/sec

y/H	yc/H	U/Um	$\sqrt{\overline{u^2}}/U_m$
.0051	.9949	.7465	.06564
.0101	.9899	.7741	.06990
.0152	.9848	.7969	.06312
.0203	.9797	.8154	.06504
.0304	.9696	.8399	.05826
.0405	.9595	.8530	.06136
.0506	.9494	.8723	.05890
.0633	.9367	.8874	.05867
.0759	.9241	.9079	.05806
.0886	.9114	.9198	.05311
.1013	.8987	.9355	.05414
.1519	.8481	.9712	.05081
.2025	.7975	1.0004	.04384
.2532	.7468	1.0256	.03698
.3038	.6962	1.0378	.03052
.3544	.6456	1.0490	.01766
.4051	.5949	1.0533	.01542
.4557	.5443	1.0556	.01081
.5000	.5000	1.0566	.01037
.5443	.4557	1.0576	.01063
.5949	.4051	1.0576	.01158
.6456	.3544	1.0570	.01299
.6962	.3038	1.0573	.01395
.7468	.2532	1.0479	.02265
.7975	.2025	1.0342	.03244
.8481	.1519	1.0019	.04224
.8987	.1013	.9657	.04982
.9114	.0886	.9438	.05413
.9241	.0759	.9278	.05736
.9367	.0633	.9170	.05919
.9494	.0506	.8905	.05899
.9595	.0405	.8704	.06040
.9696	.0304	.8512	.06354
.9797	.0203	.8179	.06881
.9848	.0152	.8039	.06917
.9899	.0101	.7919	.06775
.9949	.0051	.7697	.07214

TABLE A-IIa. (Continued) Mean and Turbulent Velocity Around the Duct. Trip Wires on Inlet; Dense Screen at Exit.

x = -34.3cm
Re= 213,000
U_m= 2.819m/sec
T = 9.2°C
$\nu = 1.339 \times 10^{-6} m^2/sec$

y/H	yc/H	U/Um	$\sqrt{\overline{u^2}}/U_m$
.0075	.9925	.7874	.07147
.0100	.9900	.7982	.07076
.0150	.9850	.8114	.06881
.0175	.9825	.8123	.06837
.0226	.9774	.8398	.06453
.0301	.9699	.8505	.06785
.0401	.9599	.8699	.06475
.0501	.9499	.8849	.06350
.0627	.9373	.9076	.06063
.0752	.9248	.9262	.06015
.0877	.9123	.9305	.05806
.1003	.8997	.9458	.05903
.1504	.8496	.9856	.04941
.2005	.7995	1.0130	.04588
.2506	.7494	1.0372	.03711
.3008	.6992	1.0551	.03078
.3509	.6491	1.0627	.02374
.4010	.5990	1.0692	.01850
.4511	.5489	1.0733	.01625
.5013	.4987	1.0746	.01305
.5489	.4511	1.0744	.01235
.5990	.4010	1.0763	.01081
.6491	.3509	1.0737	.01651
.6992	.3008	1.0701	.01933
.7494	.2506	1.0604	.02803
.7995	.2005	1.0389	.03750
.8496	.1504	1.0137	.04312
.8997	.1003	.9598	.05631
.9123	.0877	.9395	.05903
.9248	.0752	.9243	.06097
.9373	.0627	.9062	.05867
.9499	.0501	.8867	.06187
.9599	.0401	.8657	.06350
.9699	.0301	.8421	.06788
.9799	.0201	.8150	.06702
.9850	.0150	.7972	.07229
.9900	.0100	.7743	.07268
.9950	.0050	.7459	.07358

x = -25.4cm
Re= 213,000
U_m= 2.819m/sec
T = 9.2°C
$\nu = 1.339 \times 10^{-6} m^2/sec$

y/H	yc/H	U/Um	$\sqrt{\overline{u^2}}/U_m$
.0050	.9950	.7622	.07454
.0100	.9900	.7879	.07255
.0150	.9850	.8151	.07316
.0201	.9799	.8284	.07051
.0301	.9699	.8576	.06840
.0401	.9599	.8706	.06840
.0501	.9499	.8947	.06507
.0627	.9373	.9098	.06350
.0752	.9248	.9280	.06190
.1003	.8997	.9532	.06174
.1504	.8496	.9942	.05196
.2005	.7995	1.0242	.04704
.2506	.7494	1.0402	.04338
.3008	.6992	1.0608	.03501
.3509	.6491	1.0739	.02515
.4010	.5990	1.0852	.01504
.4511	.5489	1.0851	.01370
.5013	.4987	1.0869	.01318
.5489	.4511	1.0867	.01248
.5990	.4010	1.0859	.01274
.6491	.3509	1.0830	.01926
.6992	.3008	1.0789	.02412
.7494	.2506	1.0613	.03378
.7995	.2005	1.0418	.04377
.8496	.1504	1.0078	.04831
.8997	.1003	.9646	.05490
.9123	.0877	.9426	.05886
.9248	.0752	.9270	.06139
.9373	.0627	.9061	.06443
.9499	.0501	.8831	.06533
.9599	.0401	.8626	.06488
.9699	.0301	.8376	.07316
.9799	.0201	.8059	.06907
.9850	.0150	.7761	.07562
.9900	.0100	.7449	.07358
.9950	.0050	.7192	.07642

TABLE A-IIa. (Continued) Mean and Turbulent Velocity Around the Duct. Trip Wires on Inlet; Dense Screen at Exit.

x = -17.27
Re= 213,000
U_m= 2.819m/sec
T = 9.2°C
ν = $1.339 \times 10^{-6} m^2/sec$

y/H	yc/H	U/Um	$\sqrt{\overline{u^2}}/U_m$	Angle (deg)	$\sqrt{\overline{v^2}}/U_m$	$\overline{uv}/U_m^2$
.0050	.9950	.7702	.07351			
.0100	.9900	.8023	.07425			
.0150	.9850	.8241	.07108			
.0201	.9799	.8440	.06628			
.0301	.9699	.8604	.06901			
.0401	.9599	.8863	.06859			
.0501	.9499	.9084	.06662			
.0627	.9373	.9149	.06654	.774	.06281	-.001398
.0752	.9248	.9341	.06162	.011	.03836	-.000864
.0877	.9123	.9444	.06043	-.361	.03360	-.000967
.1003	.8997	.9677	.05816	.090	.03310	-.000997
.1504	.8496	1.0018	.05331	-.216	.02978	-.000663
.2005	.7995	1.0384	.04409	.334	.02645	-.000545
.2506	.7494	1.0569	.03955	.390	.02948	-.000479
.2632	.7368	1.0571	.03742			
.2757	.7243	1.0615	.03523			
.3008	.6992	1.0663	.03135	.183	.02743	-.000422
.3509	.6491	1.0826	.02655	.245	.02309	-.000275
.4010	.5990	1.0892	.02118	.328	.00958	-.000057
.4511	.5489	1.0944	.01542	.329	.01715	-.000026
.5013	.4987	1.0943	.01555	-.024	.01160	.000022
.5464	.4536	1.0928	.01133	-.052	.01520	-.000001
.5965	.4035	1.0930	.01459	.539	.01279	-.000032
.6466	.3534	1.0851	.02074	.000	.00822	.000022
.6967	.3033	1.0789	.02547	.258	.00863	.000044
.7469	.2531	1.0657	.03385	.740	.01884	.000172
.7970	.2030	1.0432	.04005	.711	.02914	.000409
.8471	.1529	1.0078	.05295	.681	.02785	.000619
.8972	.1028	.9546	.05769	.603	.03648	.000757
.9098	.0902	.9366	.05852	.968	.04761	.000886
.9223	.0777	.9216	.06366	.704	.04640	.001176
.9348	.0652	.8986	.06657	-.029	.04523	.001099
.9474	.0526	.8811	.06459	.369	.08632	.001267
.9574	.0426	.8528	.07092			
.9674	.0326	.8333	.06974			
.9774	.0226	.7972	.07102			
.9825	.0175	.7728	.07681			
.9875	.0125	.7403	.07645			
.9925	.0075	.7137	.08039			

TABLE A-IIa. (Continued) Mean and Trubulent Velocity Around the Duct. Trip Wires on Inlet; Dense Screen at Exit.

x = -12.70cm
Re= 216,000
U_m= 2.819m/sec
T = 9.5°C
$\nu = 1.324 \times 10^{-6} m^2/sec$

y/H	yc/H	U/Um	$\sqrt{\overline{u^2}}/U_m$	Angle (deg)	$\sqrt{\overline{v^2}}/U_m$	$\overline{uv}/U_m^2$
.0050	.9950	.7717	.07585			
.0100	.9900	.8136	.06898			
.0150	.9850	.8318	.07150			
.0201	.9799	.8499	.06773			
.0301	.9699	.8798	.06943			
.0401	.9599	.8969	.06578			
.0501	.9499	.9090	.06526	-.810	.04238	-.001213
.0627	.9373	.9338	.06169	.257	.06893	-.000840
.0627	.9373	.9254	.06188	-.304	.05187	-.000783
.0752	.9248	.9465	.06316	.002	.04170	-.000886
.0752	.9248	.9485	.06226	-.454	.03755	-.001034
.1003	.8997	.9731	.05631	-1.131	.02840	-.000736
.1003	.8997	.9719	.05899	-.100	.03173	-.000881
.1253	.8747	.9932	.05651	.659	.03179	-.000867
.1504	.8496	1.0137	.05292	-.385	.02735	-.000603
.1504	.8496	1.0166	.04952	.582	.03261	-.000647
.2005	.7995	1.0463	.04377	-.150	.03244	-.000604
.2506	.7494	1.0636	.03775	-.196	.02354	-.000358
.3008	.6992	1.0865	.02988	-.367	.02811	-.000266
.3509	.6491	1.0918	.02790	-.286	.01979	-.000140
.3509	.6491	1.0882	.02937	.034	.01317	-.000104
.4010	.5990	1.0981	.01600	-.085	.01777	-.000042
.4511	.5489	1.0981	.01517	.364	.01416	-.000036
.5013	.4987	1.0994	.01190	.153	.01703	-.000011
.5489	.4511	1.0979	.01286	-.340	.01381	-.000005
.5990	.4010	1.0941	.01600	-.021	.00912	-.000002
.6491	.3509	1.0912	.01702	-.116	.02022	-.000012
.6992	.3008	1.0774	.03014	-1.621	.01682	.000200
.7494	.2506	1.0623	.03648	-.188	.02280	.000196
.7995	.2005	1.0363	.04755	-.661	.02132	.000553
.8496	.1504	.9979	.05241	.000	.03345	.000676
.8997	.1003	.9417	.05989	-.158	.03606	.000870
.9248	.0752	.9102	.06274	.048	.04853	.001106
.9373	.0627	.8922	.06092	-.490	.06256	.000127
.9499	.0501	.8748	.06745	-.162	.05964	.001180
.9599	.0401	.8383	.06884			
.9699	.0301	.8128	.07543			
.9799	.0201	.7849	.07405			
.9850	.0150	.7634	.07281			
.9900	.0100	.7318	.07779			
.9950	.0050	.6951	.07770			

TABLE A-IIa. (Continued) Mean and Turbulent Velocity Around the Duct. Trip Wires on Inlet; Dense Screen at Exit.

x = -7.62cm
Re= 215,000
U_m= 2.819m/sec
T = 9.4°C
ν = $1.329 \times 10^{-6} m^2/sec$

y/H	yc/H	U/Um	$\sqrt{\overline{u^2}}/U_m$	Angle (deg)	$\sqrt{\overline{v^2}}/U_m$	$\overline{uv}/U_m^2$
.0050	.9950	.7983	.07070			
.0075	.9925	.8106	.06942			
.0100	.9900	.8068	.07156			
.0125	.9875	.8528	.06728			
.0150	.9850	.8615	.06891			
.0175	.9825	.8637	.06744			
.0201	.9799	.8737	.06718			
.0251	.9749	.8929	.06809			
.0301	.9699	.9062	.06515			
.0401	.9599	.9284	.06412			
.0501	.9499	.9406	.06476			
.0627	.9373	.9608	.05932	-.414	.05619	-.000967
.0752	.9248	.9819	.05958	-.288	.04411	-.000928
.1003	.8997	1.0004	.05759	-.713	.02765	-.000708
.1504	.8496	1.0402	.05183	-1.017	.02724	-.000611
.2005	.7995	1.0735	.04562	-1.503	.02248	-.000480
.2506	.7494	1.0919	.03782	-1.037	.02452	-.000324
.3008	.6992	1.1065	.03264	-1.263	.02751	-.000458
.3509	.6491	1.1106	.02464	-1.358	.02155	-.000139
.4010	.5990	1.1146	.01824	-1.718	.01948	-.000106
.4511	.5489	1.1135	.01747	-1.604	.00835	-.000023
.5013	.4987	1.1101	.01484	-1.564	.01346	-.000026
.5489	.4511	1.1084	.01357	-1.193	.01521	.000016
.5990	.4010	1.1027	.01951	-1.333	.00883	.000020
.6491	.3509	1.0950	.02240	-1.295	.01309	.000091
.6992	.3008	1.0882	.02572	-1.657	.01990	.000148
.7494	.2506	1.0649	.03584	-1.587	.02775	.000262
.7995	.2005	1.0335	.04575	-1.901	.02653	.000457
.8496	.1504	.9951	.05331	-1.505	.03506	.000694
.8997	.1003	.9412	.06254	-1.523	.04387	.000900
.9248	.0752	.9043	.06267	-1.767	.06436	.000997
.9373	.0627	.8831	.06788	-1.281	.04483	.000884
.9499	.0501	.8638	.06782	-.626	.06947	.000875
.9599	.0401	.8337	.07178			
.9699	.0301	.8068	.07837			
.9799	.0201	.7677	.08083			
.9850	.0150	.7394	.08199			
.9900	.0100	.7038	.08077			
.9950	.0050	.6676	.08211			

TABLE A-IIa. (Continued) Mean and Turbulent Velocity Around the Duct. Trip Wires on Inlet; Dense Screen at Exit.

x = -2.54
Re= 215,000
U_m= 2.819m/sec
T = 9.4°C
$\nu = 1.329 \times 10^{-6} m^2/sec$

Y/H	yc/H	U/Um	$\sqrt{\overline{u^2}}/U_m$	Angle (deg)	$\sqrt{\overline{v^2}}/U_m$	$\overline{uv}/U_m^2$
.0050	.9950	.9225	.06002			
.0075	.9925	.9511	.06565			
.0100	.9900	.9556	.05983			
.0175	.9825	1.0218	.05171			
.0226	.9774	1.0350	.05906			
.0276	.9724	1.0450	.05721			
.0301	.9699	1.0514	.05976			
.0326	.9674	1.0521	.05676			
.0401	.9599	1.0764	.05618			
.0501	.9499	1.0907	.05535	-.104	.03432	-.001133
.0602	.9398	1.1002	.05259	-1.084	.03104	-.001201
.0652	.9348	1.1102	.05228	-1.357	.05315	-.001021
.0752	.9248	1.1154	.05049	-1.520	.03733	-.000740
.0877	.9123	1.1289	.05062	-2.063	.04424	-.000636
.1003	.8997	1.1345	.04978	-2.712	.03372	-.000594
.1504	.8496	1.1624	.04141	-3.259	.02922	-.000527
.2005	.7995	1.1686	.04018	-4.309	.02217	-.000392
.2506	.7494	1.1736	.03277	-5.170	.02134	-.000230
.3008	.6992	1.1650	.02803	-5.337	.01868	-.000219
.3509	.6491	1.1541	.02240	-5.850	.01479	-.000124
.4010	.5990	1.1395	.01964	-6.070	.01372	-.000074
.4511	.5489	1.1289	.01241	-6.889	.01755	-.000019
.5013	.4987	1.1124	.01401	-6.447	.01909	.000120
.5489	.4511	1.1003	.01350	-6.298	.01867	.000060
.5990	.4010	1.0757	.01990	-6.327	.01440	.000064
.6491	.3509	1.0614	.02694	-5.933	.02084	.000259
.6992	.3008	1.0384	.03365	-5.312	.01849	.000111
.7494	.2506	.9977	.04761	-5.033	.01804	.000435
.7995	.2005	.9546	.05804	-4.740	.01324	.000543
.8496	.1504	.9034	.06515	-4.167	.02965	.000825
.8997	.1003	.8394	.07275	-2.887	.03661	.000746
.9248	.0752	.8027	.07604	-3.325	.05213	.001093
.9373	.0627	.7730	.07956	-1.664	.07016	.001113
.9499	.0501	.7442	.08668			
.9599	.0401	.7196	.08905			
.9699	.0301	.6815	.08985			
.9799	.0201	.6288	.09225			
.9850	.0150	.5998	.09656			
.9900	.0100	.5471	.09181			
.9950	.0050	.4868	.09482			

TABLE A-IIa. (Continued) Mean and Turbulent Velocity Around the Duct. Trip Wires on Inlet; Dense Screen at Exit.

x = -0.76cm
Re= 216,000
U_m= 2.819m/sec
T = 9.6°C
ν = $1.320 \times 10^{-6} m^2/sec$

y/H	yc/H	U/Um	$\sqrt{\overline{u^2}}/U_m$	Angle (deg)	$\sqrt{\overline{v^2}}/U_m$	$\overline{uv}/U_m^2$
.0050	.9950	1.1531	.05599			
.0101	.9899	1.1631	.05439			
.0151	.9849	1.1791	.05177			
.0302	.9698	1.2132	.05222			
.0402	.9598	1.2218	.05272			
.0503	.9497	1.2349	.05062	-3.003	.04758	-.000328
.0603	.9397	1.2431	.04978	-3.523	.03462	-.000536
.0754	.9246	1.2435	.04965	-4.811	.03299	-.000604
.1005	.8995	1.2427	.04665	-5.724	.02217	-.000422
.1508	.8492	1.2442	.04147	-6.972	.02399	-.000411
.2010	.7990	1.2308	.03411	-8.083	.02510	-.000360
.2513	.7487	1.2097	.02738	-9.257	.02129	-.000111
.3015	.6985	1.1914	.01945	-9.492	.02298	-.000162
.3518	.6482	1.1671	.01830	-9.638	.01861	-.000108
.3518	.6482	1.1587	.01899			
.3518	.6482	1.1645	.01622			
.4020	.5980	1.1419	.01561	-9.920	.01320	.000001
.4523	.5477	1.1165	.01778	-9.931	.01136	.000042
.5000	.5000	1.0959	.01888	-9.976	.01442	.000062
.5477	.4523	1.0835	.01894	-9.985	.00941	.000022
.5980	.4020	1.0539	.03161	-9.708	.01050	.000133
.6482	.3518	1.0357	.02880	-9.157	.02258	.000278
.6985	.3015	.9990	.03987	-8.135	.02349	.000270
.7487	.2513	.9548	.05151	-7.772	.01715	.000482
.7990	.2010	.9123	.05656	-6.669	.03187	.000477
.8492	.1508	.8537	.06551	-5.685	.03784	.000760
.8995	.1005	.7816	.07866	-4.435	.06352	.001173
.9246	.0754	.7269	.08806	-3.879	.06828	.001421
.9397	.0603	.6891	.09084	-2.182	.05213	.001186
.9397	.0603	.6844	.09305	-1.075	.06021	.000997
.9497	.0503	.6657	.09228		.10520	.001227
.9598	.0402	.6349	.10017			
.9698	.0302	.6049	.09926			
.9799	.0201	.5356	.10530			
.9849	.0151	.4959	.11062			
.9899	.0101	.4347	.10682			
.9950	.0050	.3879	.11351			

TABLE A-IIa. (Continued) Mean and Turbulent Velocity Around the Duct. Trip Wires on Inlet; Dense Screen at Exit.

5deg Around the Turn
Re= 216,000
U_m= 2.819m/sec
T = 9.5°C
ν = $1.324 \times 10^{-6} m^2/sec$

y/H	yc/H	U/Um	$\sqrt{\overline{u^2}}/U_m$	Angle (deg)	$\sqrt{\overline{v^2}}/U_m$	$\overline{uv}/U_m^2$
.0075	.9900	1.3810	.05132			
.0100	.9875	1.3750	.04934			
.0150	.9825	1.3917	.05209			
.0200	.9775	1.4019	.04991			
.0300	.9675	1.4051	.05068			
.0400	.9575	1.4131	.04786	-2.760	.07436	-.000532
.0500	.9475	1.3998	.04716	-3.941	.05608	-.000525
.0600	.9375	1.4016	.04505	-4.088	.03012	-.000607
.0750	.9225	1.3965	.04377	-5.154	.04004	-.000443
.1000	.8975	1.3708	.04358	-5.970	.01997	-.000431
.1500	.8475	1.3360	.03821	-7.639	.02279	-.000219
.2000	.7975	1.2974	.03501	-8.182	.01871	-.000248
.2500	.7475	1.2543	.02566	-8.979	.01779	-.000091
.3000	.6975	1.2139	.02515	-9.202	.01403	-.000125
.3500	.6475	1.1811	.01491	-9.100	.01603	.000000
.4000	.5975	1.1470	.01594	-9.344	.01830	.000076
.4500	.5475	1.1111	.02246	-9.326	.00366	.000089
.5000	.4975	1.0791	.02227	-9.300	.01471	.000112
.5500	.4475	1.0548	.02738	-9.432	.00726	.000144
.6000	.3975	1.0245	.03142	-8.704	.01898	.000169
.6500	.3475	.9839	.04185	-8.259	.02009	.000393
.7000	.2975	.9415	.05209	-7.420	.01974	.000730
.7500	.2475	.8838	.06252	-6.306	.02158	.000713
.8000	.1975	.8295	.07111	-5.518	.02886	.001222
.8500	.1475	.7523	.08595	-3.289	.03189	.001272
.9000	.0975	.6533	.10299	-1.835	.04510	.002344
.9250	.0725	.5790	.11037	-2.300	.07461	.002700
.9400	.0575	.5469	.13095	-3.485	.05252	.003263
.9500	.0475	.4812	.13120			
.9600	.0375	.4549	.13737			
.9700	.0275	.3928	.14458			
.9800	.0175	.3017	.13086			
.9850	.0125	.2749	.11066			

TABLE A-IIa. (Continued) Mean and Turbulent Velocity Around the Duct. Trip Wires on Inlet; Dense Screen at Exit.

15deg Around the Turn
Re= 218,000
U_m= 2.819m/sec
T = 9.7°C
ν = $1.320 \times 10^{-6} m^2/sec$

y/H	yc/H	U/Um	$\sqrt{\overline{u^2}}/U_m$	Angle (deg)	$\sqrt{\overline{v^2}}/U_m$	$\overline{uv}/U_m^2$
.0050	.9950	1.5388	.05063			
.0100	.9900	1.5472	.04689			
.0150	.9850	1.5598	.04689			
.0200	.9800	1.5556	.04869			
.0300	.9700	1.5636	.04985			
.0400	.9600	1.5482	.04702	.359	.07148	-.000580
.0500	.9500	1.5349	.04817	.335	.06266	-.000014
.0600	.9400	1.5326	.04779	-.800	.03173	-.000151
.0750	.9250	1.5125	.04625	-1.566	.03912	-.000231
.1000	.9000	1.4830	.04483	-2.156	.03228	-.000215
.1500	.8500	1.4266	.03685	-3.369	.02748	-.000133
.2000	.8000	1.3642	.03564	-3.918	.01320	-.000171
.2500	.7500	1.3181	.02655	-4.483	.01624	-.000072
.3000	.7000	1.2632	.02681	-4.980	.00832	-.000093
.3500	.6500	1.2176	.02098	-5.139	.01076	.000019
.4000	.6000	1.1685	.01778	-5.569	.01254	.000007
.4500	.5500	1.1331	.01907	-5.064	.01877	.000021
.5088	.4913	1.0768	.02885	-5.650	.02622	.000369
.5500	.4500	1.0402	.03679	-5.502	.00889	.000404
.6000	.4000	.9920	.04312	-4.870	.02077	.000617
.6500	.3500	.9477	.05202	-4.552	.03218	.001067
.7000	.3000	.8959	.05842	-3.799	.03648	.001189
.7500	.2500	.8245	.07399	-2.413	.04316	.001863
.8000	.2000	.7298	.08835	-2.333	.04782	.002971
.8500	.1500	.6557	.10583	-1.731	.07512	.005013
.9000	.1000	.5277	.14720	-.086	.05868	.003907
.9250	.0750	.4762	.14735		.15001	.004529
.9400	.0600	.4202	.13098			
.9500	.0500	.3662	.14499			
.9600	.0400	.3514	.11250			
.9700	.0300	.2922	.09323			

TABLE A-IIa. (Continued) Mean and Turbulent Velocity Around the Duct. Trip Wires on Inlet; Dense Screen at Exit.

30deg Around the Turn
Re= 218,000
U_m= 2.819m/sec
T = 9.7°C
ν = $1.316 \times 10^{-6} m^2/sec$

Y/H	yc/H	U/Um	$\sqrt{\overline{u^2}}/U_m$	Angle (deg)	$\sqrt{\overline{v^2}}/U_m$	$\overline{uv}/U_m^2$
.0050	.9950	1.6922	.04754			
.0100	.9900	1.7027	.04715			
.0150	.9850	1.7134	.04586			
.0200	.9800	1.7023	.04843			
.0300	.9700	1.6987	.04625			
.0400	.9600	1.6772	.04625	-.417	.03939	.000271
.0525	.9475	1.6597	.04341	-.710	.05071	.000062
.0600	.9400	1.6384	.04921	-.441	.04190	.000124
.0750	.9250	1.6170	.04444	-1.094	.02886	.000118
.1025	.8975	1.5677	.04225	-1.046	.02769	.000020
.1500	.8500	1.4872	.03916	-1.767	.02084	.000136
.1875	.8125	1.4411	.03504	-1.931	.01103	.000090
.2125	.7875	1.3863	.02975	-2.230	.01641	-.000011
.2500	.7500	1.3413	.02240	-2.420	.02430	.000162
.3000	.7000	1.2724	.02490	-2.413	.01184	.000088
.3000	.7000	1.2703	.01634			
.3000	.7000	1.2702	.02120			
.3500	.6500	1.2111	.02464	-2.447	.00648	.000067
.3750	.6250	1.1756	.01545			
.4000	.6000	1.1558	.02745	-2.271	.00692	.000116
.4000	.6000	1.1458	.02097			
.4250	.5750	1.1197	.01877			
.4250	.5750	1.1199	.01989			
.4500	.5500	1.1065	.02598	-2.480	.01907	.000228
.4500	.5500	1.1065	.02598	-2.665	.02876	.000459
.5000	.5000	1.0566	.03174	-2.255	.03199	.000629
.5500	.4500	1.0040	.04479	-2.196	.02459	.000832
.6000	.4000	.9437	.05285	-1.839	.04116	.001397
.6500	.3500	.8961	.05829	-1.127	.04828	.001817
.7000	.3000	.8161	.07946	-.445	.05489	.003001
.7500	.2500	.7410	.10041	-.226	.08775	.005826
.8000	.2000	.6415	.13426	-.631	.08912	.008324
.8000	.2000	.6385	.13625			
.8500	.1500	.5492	.16703	.865	.09376	.010292
.9000	.1000	.4749	.16078	2.335	.11481	.010537
.9250	.0750	.4289	.13942	3.256	.14787	.005335
.9400	.0600	.3948	.12590			
.9500	.0500	.3795	.15352			
.9600	.0400	.3806	.11624			

TABLE A-IIa. (Continued) Mean and Turbulent Velocity Around the Duct. Trip Wires on Inlet; Dense Screen at Exit.

45deg Around the Turn
Re= 218,000
U_m= 2.819m/sec
T = 9.7°C
ν = $1.316 \times 10^{-6} m^2/sec$

y/H	yc/H	U/Um	$\sqrt{\overline{u^2}}/U_m$	Angle (deg)	$\sqrt{\overline{v^2}}/U_m$	$\overline{uv}/U_m^2$
.0075	.9925	1.7712	.04702			
.0100	.9900	1.7725	.04650			
.0200	.9800	1.7661	.05139			
.0300	.9700	1.7554	.04560			
.0350	.9650	1.7439	.05114			
.0350	.9650	1.7445	.05165			
.0400	.9600	1.7326	.04830	.370	.06499	.000524
.0500	.9500	1.7183	.04830	.530	.03262	.000428
.0600	.9400	1.6994	.04754	.269	.03989	.000265
.0750	.9250	1.6681	.04972	.006	.02176	.000394
.1000	.9000	1.6221	.04392	.249	.02254	.000295
.1500	.8500	1.5301	.04031	.051	.01966	.000273
.2000	.8000	1.4439	.03079	-.040	.02427	.000255
.2500	.7500	1.3587	.02848	-.052	.01437	.000130
.3000	.7000	1.2842	.02425	-.244	.01468	.000105
.3500	.6500	1.2201	.01997	-.361	.02156	.000181
.4000	.6000	1.1539	.02726	-.061	.02619	.000418
.4500	.5500	1.0928	.02701	-.149	.03400	.000505
.5000	.5000	1.0426	.03750	.114	.04479	.001074
.5500	.4500	.9812	.04972	-.161	.04182	.001302
.6000	.4000	.9181	.06258	.628	.05123	.002209
.6500	.3500	.8481	.08410	1.904	.05929	.003787
.7000	.3000	.7801	.10686	1.146	.10768	.008882
.7500	.2500	.6986	.11921	1.261	.12494	.011159
.8000	.2000	.6231	.13221	1.354	.13466	.012587
.8500	.1500	.5679	.13677	1.865	.12858	.011290
.9000	.1000	.4796	.13182	1.477	.10252	.009055
.9250	.0750	.4476	.12681	.954	.07707	.008575
.9400	.0600	.4582	.10680			
.9500	.0500	.4600	.11888			
.9600	.0400	.4378	.11095			

TABLE A-IIa. (Continued) Mean and Turbulent Velocity Around the Duct. Trip Wires on Inlet; Dense Screen at Exit.

60deg Around the Turn
Re= 218,000
U_m=2.819m/sec
T = 9.8°C
$\nu = 1.313 \times 10^{-6} m^2/sec$

y/H	yc/H	U/Um	$\sqrt{\overline{u^2}}/U_m$	Angle (deg)	$\sqrt{\overline{v^2}}/U_m$	$\overline{uv}/U_m^2$
.0050	.9950	1.8058	.04882			
.0100	.9900	1.8043	.04728			
.0150	.9850	1.8009	.04534			
.0200	.9800	1.7898	.04650			
.0200	.9800	1.7848	.04586			
.0300	.9700	1.7795	.04676	.770	.06424	.000479
.0625	.9375	1.7188	.04457	1.343	.04072	.000151
.0750	.9250	1.6836	.04405	.842	.03653	.000275
.0875	.9125	1.6564	.04135	1.754	.02521	.000258
.1375	.8625	1.5569	.03839	1.503	.02186	.000368
.1875	.8125	1.4708	.03452	1.572	.02378	.000324
.2375	.7625	1.3801	.02732	1.506	.02012	.000144
.2875	.7125	1.3038	.02502	1.604	.02069	.000151
.3375	.6625	1.2289	.02342	1.154	.03349	.000486
.3875	.6125	1.1663	.02508	1.422	.02849	.000332
.4000	.6000	1.1505	.02950	1.176	.03813	.000616
.4375	.5625	1.1045	.02905	1.645	.03621	.000451
.4500	.5500	1.0894	.03667	.841	.05352	.001547
.4500	.5500	1.0909	.03695			
.5000	.5000	1.0252	.04882	1.669	.06265	.002082
.5500	.4500	.9714	.05849	1.436	.07250	.003171
.5500	.4500	.9705	.05773			
.6000	.4000	.9104	.08214	2.632	.07365	.004337
.6500	.3500	.8223	.11249	2.795	.09436	.007937
.7000	.3000	.7598	.12156	3.537	.11689	.009843
.7500	.2500	.6794	.13286	2.957	.13181	.012621
.7750	.2250	.6594	.12587	3.222	.16735	.016285
.8000	.2000	.5861	.13093		.15170	.014636
.8000	.2000	.6014	.13277	3.755	.14476	.013080
.8250	.1750	.5786	.14093	3.398	.14735	.014884
.8500	.1500	.5560	.12932	4.340	.13775	.011036
.9000	.1000	.5251	.11256	3.698	.12068	.005950
.9000	.1000	.5315	.11962	4.269	.13796	.003992
.9250	.0750	.5082	.10562			
.9250	.0750	.5152	.11003		.08136	.006566
.9400	.0600	.5259	.10283			
.9400	.0600	.4990	.10356			
.9500	.0500	.5079	.09489			
.9500	.0500	.4930	.11097			
.9600	.0400	.4995	.10614			
.9625	.0375	.5015	.09771			
.9700	.0300	.5069	.09264			

TABLE A-IIa. (Continued) Mean and Turbulent Velocity Around the Duct. Trip Wires on Inlet; Dense Screen at Exit.

90deg Around the Turn
Re= 216,000
U_m= 2.819m/sec
T = 9.5°C
ν = $1.324 \times 10^{-6} m^2/sec$

y/H	yc/H	U/Um	$\sqrt{\overline{u^2}}/U_m$	Angle (deg)	$\sqrt{\overline{v^2}}/U_m$	$\overline{uv}/U_m^2$	y/H	U/Um	$\sqrt{\overline{u^2}}/U_m$
.0050	.9950	1.6941	.06570				.9400	.5923	.08937
.0100	.9900	1.7446	.05063				.9400	.5777	.08937
.0150	.9850	1.7576	.04895				.9500	.5814	.08746
.0200	.9800	1.7566	.04508				.9500	.5845	.08870
.0300	.9700	1.7446	.04779				.9600	.5732	.09161
.0400	.9600	1.7256	.04702				.9600	.5692	.08972
.0500	.9500	1.7062	.04174	1.724	.08117	.001360	.9700	.5704	.09617
.0600	.9400	1.6834	.04199	1.431	.04261	.000702	.9700	.5632	.08937
.0750	.9250	1.6533	.04161	2.053	.04056	.000792			
.1000	.9000	1.6038	.03968	1.351	.03990	.000694			
.1500	.8500	1.5066	.03375	1.617	.03315	.000470			
.1500	.8500	1.5094	.03231						
.1500	.8500	1.5222	.03329						
.1750	.8250	1.4802	.02801						
.2000	.8000	1.4223	.02975	2.239	.03107	.000309			
.2000	.8000	1.4331	.02827						
.2250	.7750	1.3897	.02641						
.2500	.7500	1.3403	.02406	1.941	.03792	.000340			
.2500	.7500	1.3495	.02223						
.2750	.7250	1.3072	.02564						
.3000	.7000	1.2600	.02457	2.050	.03044	.000174			
.3000	.7000	1.2708	.02385						
.3000	.7000	1.2880	.02284						
.3250	.6750	1.2344	.02395						
.3500	.6500	1.1853	.04268	2.313	.01579	.000337			
.3500	.6500	1.1975	.02998						
.3750	.6250	1.1670	.02925						
.4000	.6000	1.1210	.04249	2.300	.02943	.000203			
.4000	.6000	1.1270	.04259						
.4250	.5750	1.1098	.04666						
.4500	.5500	1.0598	.05285	2.924	.05865	.001769			
.4750	.5250	1.0283	.06120						
.5000	.5000	.9958	.07255	2.509	.08368	.003554			
.5000	.5000	1.0014	.08469						
.5250	.4750	.9691	.08519						
.5500	.4500	.9257	.09589	3.757	.10543	.006768			
.6000	.4000	.8658	.10558	4.446	.12694	.010098			
.6500	.3500	.7932	.11288	4.400	.15848	.014394			
.7000	.3000	.7405	.11234	3.756	.17682	.014343			
.7500	.2500	.6965	.11276	4.114	.17197	.012989			
.8000	.2000	.6605	.11258	3.859	.17029	.012117			
.8500	.1500	.6122	.09916	4.946	.16163	.008270			
.9000	.1000	.6061	.09769	2.635	.06507	.004304			
.9250	.0750	.5870	.08784	3.030	.13721	.003999			
.9250	.0750	.5948	.08803	2.284	.12582	.004851			

TABLE A-IIa. (Continued) Meand and Turbulent Velocity Around the Duct. Trip Wires on Inlet; Dense Screen at Exit.

120deg Around the Turn
Re= 217,000
U_m= 2.819m/sec
T = 9.7°C
ν = $1.316 \times 10^{-6} m^2/sec$

y/H	yc/H	U/Um	$\sqrt{\overline{u^2}}/U_m$	Angle (deg)	$\sqrt{\overline{v^2}}/U_m$	$\overline{uv}/U_m^2$
.0050	.9950	1.1390				
.0100	.9900	1.4024	0.18536			
.0150	.9850	1.6106	.06552			
.0200	.9800	1.6476	.05823			
.0300	.9700	1.6590	.05861			
.0400	.9600	1.6486	.04965	1.631	.01613	.000531
.0500	.9500	1.6283	.04728	1.198	.04650	.000625
.0600	.9400	1.6269	.04779	1.584	.03509	.000334
.0750	.9250	1.6006	.04470	1.353	.05290	.000789
.1000	.9000	1.5641	.04715	2.899	.04732	.000747
.1500	.8500	1.4808	.04057	2.691	.04621	.000382
.2000	.8000	1.4016	.03519	3.106	.04893	.000248
.2500	.7500	1.3252	.03667	2.936	.04781	.000326
.3000	.7000	1.2485	.03724	3.358	.05381	.000286
.3500	.6500	1.1894	.04869	3.626	.06565	.001103
.4000	.6000	1.1168	.06725	3.390	.10224	.004096
.4500	.5500	1.0571	.07832	4.204	.10899	.005035
.5000	.5000	.9896	.09142	3.902	.13606	.008845
.5500	.4500	.9176	.10629	4.893	.13369	.009020
.6000	.4000	.8736	.10623	4.586	.16155	.011226
.6500	.3500	.8210	.10361	3.691	.17390	.010499
.7000	.3000	.7794	.10363	2.251	.19725	.012972
.7500	.2500	.7434	.10075	3.869	.18680	.010959
.8000	.2000	.7114	.09282	3.754	.17758	.009470
.8500	.1500	.6824	.09034	2.332	.15194	.006787
.9000	.1000	.6583	.08406	3.924	.15321	.004490
.9125	.0875	.6591	.08576	2.707	.10591	.003102
.9250	.0750	.6438	.08186			
.9400	.0600	.6401	.08103			
.9500	.0500	.6269	.08560			
.9550	.0450	.6352	.08185			

TABLE A-IIa. (Continued) Mean and Turbulent Velocity Around the Duct. Trip Wires on Inlet; Dense Screen at Exit.

180deg Around the Turn
Re= 206,000
U_m= 2.819m/sec
T = 8.4°C
$\nu = 1.368 \times 10^{-6} m^2/sec$

y/H	yc/H	U/Um	$\sqrt{\overline{u^2}}/U_m$	Angle (deg)	$\sqrt{\overline{v^2}}/U_m$	$\overline{uv}/U_m^2$
.0050	.9950	-.1288	.19489			
.0101	.9899	-.1557	.21226			
.0151	.9849	-.1048	.25551			
.0201	.9799	-.1016	.25357			
.0201	.9799	-.1190	.24215			
.0302	.9698	-.0546	.28813			
.0402	.9598	-.0056	.32212			
.0503	.9497	.1277	.36855			
.0628	.9372	.3948	.48370			
.0754	.9246	.4921	.52871			
.0854	.9146	.6032	.48600	7.725	.21089	.057238
.0980	.9020	.8489	.41413	20.964	.17918	.060622
.1005	.8995	.7329	.53461			
.1005	.8995	.8561	.48891			
.1106	.8894	.9982	.37958	19.308	.16345	.052404
.1106	.8894	.9034	.43829	15.665	.18486	.065177
.1231	.8769	1.1214	.32279	19.883	.16228	.027205
.1357	.8643	1.1982	.25423	18.834	.14052	.017085
.1357	.8643	1.1326	.33269	20.984	.16235	.033065
.1482	.8518	1.2319	.23425	21.251	.13016	.007268
.1508	.8492	1.1986	.33440			
.1608	.8392	1.2445	.16721	21.234	.12132	.006954
.1608	.8392	1.2645	.18896	20.400	.14959	.007361
.1734	.8266	1.2766	.13093	20.539	.11889	.003347
.1859	.8141	1.2798	.12691	21.071	.14565	.002842
.2211	.7789	1.2911	.10881	21.408	.10199	-.001308
.2462	.7538	1.2751	.07570	21.489	.09395	-.000078
.2965	.7035	1.2737	.05695	20.082	.10486	.001632
.3467	.6533	1.2661	.05638	18.887	.10815	.001114
.3970	.6030	1.2363	.06361	18.660	.11852	.002216
.4472	.5528	1.2011	.06066	16.650	.16137	.004879
.4975	.5025	1.1628	.06718	16.941	.17155	.001023
.5477	.4523	1.1351	.07018	14.795	.19555	.003876
.5980	.4020	1.0997	.07626	14.472	.20259	.002253
.6482	.3518	1.0695	.08170	13.615	.20410	.003312
.6985	.3015	1.0491	.08192	12.025	.22016	.002927
.7487	.2513	1.0276	.08221	10.291	.21277	.002143
.7990	.2010	1.0051	.08067	8.483	.21206	.003334
.8492	.1508	.9977	.07828	7.050	.18935	.000150
.8995	.1005	.9840	.07729	4.457	.14754	.000541
.9246	.0754	.9775	.07459	3.948	.09970	-.000171
.9372	.0628	.9787	.07214	3.612	.12382	.000691
.9497	.0503	.9735	.07489			
.9573	.0427	.9770	.07409			
.9698	.0302	.9603	.08694			
.9799	.0201	.9237	.10984			
.9849	.0151	.9002	.11310			
.9899	.0101	.8249	.11562			
.9950	.0050	.7579	.13519			

TABLE A-IIa. (Continued) Mean and Turbulent Velocity Around The Duct. Trip Wires on Inlet; Dense Screen at Exit.

Separation Bubble Data
U_m= 2.819m/sec
T = 6.1°C
ν = 1.468x10^{-6}m^2/sec

x = +2.54cm

y/H	yc/H	U/Um	$\sqrt{u^2}/U_m$
.0050	.9950	-.3164	.23710
.0101	.9899	-.3081	.24251
.0151	.9849	-.3114	.23835
.0202	.9798	-.2874	.25875
.0302	.9698	-.2410	.26680
.0403	.9597	-.1852	.28638
.0504	.9496	-.1746	.28769
.0630	.9370	-.0729	.31058
.0756	.9244	-.0109	.37293
.1008	.8992	.2429	.43410
.1511	.8489	.7282	.48162
.2015	.7985	1.1042	.39362
.2519	.7481	1.3285	.22402

x = +5.08cm

y/H	yc/H	U/Um	$\sqrt{u^2}/U_m$
.0051	.9949	-.2425	.24052
.0101	.9899	-.2515	.23982
.0152	.9848	-.2143	.25050
.0202	.9798	-.2157	.25030
.0303	.9697	-.1941	.26444
.0404	.9596	-.1240	.29097
.0505	.9495	-.1109	.28711
.0631	.9369	-.0083	.33226
.0758	.9242	.0286	.34998
.1010	.8990	.1936	.42345
.1515	.8485	.4480	.42418
.2020	.7980	.7811	.44625
.2525	.7475	1.1057	.34604
.3030	.6970	1.2565	.25670

x = +8.46cm

y/H	yc/H	U/Um	$\sqrt{u^2}/U_m$
.0051	.9949	-.0548	.22872
.0101	.9899	-.0464	.21951
.0152	.9848	-.0278	.22389
.0203	.9797	.0039	.20579
.0304	.9696	.0377	.24078
.0405	.9595	.0464	.25862
.0506	.9494	.0946	.25960
.0633	.9367	.1202	.28406
.0759	.9241	.1995	.33791
.1013	.8987	.3032	.37476
.1519	.8481	.5058	.38095
.2025	.7975	.7769	.37595
.2532	.7468	.9699	.35283
.3038	.6962	1.1274	.29272

x = +11.84cm

y/H	yc/H	U/Um	$\sqrt{u^2}/U_m$
.0051	.9949	.1126	.19693
.0101	.9899	.2537	.24958
.0152	.9848	.2796	.25125
.0203	.9797	.2844	.24374
.0304	.9696	.3056	.25311
.0405	.9595	.3172	.26294
.0506	.9494	.3131	.26345
.0633	.9367	.3918	.28772
.0759	.9241	.3798	.27976
.1013	.8987	.4596	.29748
.1519	.8481	.5686	.32310
.2025	.7975	.7289	.33716

TABLE A-IIa. (Continued) Mean and Turbulent Velocity Around the Duct. Trip Wires on Inlet; Dense Screen at Exit.

x = +15.20cm
Re= 192,000
U_m= 2.819m/sec
T = 6.1°C
ν = $1.468 \times 10^{-6} m^2/sec$

y/H	yc/H	U/Um	$\sqrt{\overline{u^2}}/U_m$	Angle (deg)	$\sqrt{\overline{v^2}}/U_m$	$\overline{uv}/U_m^2$	y/H	U/Um	$\sqrt{\overline{u^2}}/U_m$
.0051	.9949	.4217	.22448				.9595	1.1656	.09034
.0101	.9899	.4254	.23866				.9696	1.1574	.10363
.0152	.9848	.4866	.23339				.9797	1.1321	.10821
.0203	.9797	.4888	.22627				.9848	1.1248	.11745
.0304	.9696	.5120	.21869				.9899	1.1035	.12003
.0405	.9595	.5414	.23018				.9949	1.0684	.12928
.0506	.9494	.5691	.23283			-.007189			
.0633	.9367	.5667	.24309						
.0633	.9367	.5784	.23587						
.0759	.9241	.5867	.24194						
.0759	.9241	.5994	.24810						
.1013	.8987	.6185	.25388						
.1013	.8987	.6652	.24252	-5.407	.11506	-.015583			
.1266	.8734	.6621	.27261	-4.353	.15982	-.017320			
.1392	.8608	.6784	.27258	-5.510	.18406	-.019081			
.1519	.8481	.7368	.27398						
.1519	.8481	.7076	.26925	-3.242	.17290	-.020176			
.1646	.8354	.7035	.28361	-3.653	.17716	-.020174			
.1899	.8101	.7895	.28377	-4.322	.15694	-.019389			
.2025	.7975	.7891	.27871	-5.820	.16365	-.018800			
.2278	.7722	.8785	.27442	-4.066	.18317	-.018124			
.2506	.7494	.9377	.25815	-5.258	.16496	-.012365			
.2532	.7468	.9463	.25808						
.3013	.6987	1.0205	.22519	-4.417	.17757	-.010998			
.3038	.6962	.9904	.23062						
.3494	.6506	1.0654	.21665	-3.481	.15728	-.006213			
.3544	.6456	1.0547	.20893						
.4000	.6000	1.1116	.17040	-2.202	.16363	-.003207			
.4051	.5949	1.1183	.15758						
.4506	.5494	1.1454	.13752	-2.548	.15338	.001151			
.4557	.5443	1.1461	.13558						
.4987	.5013	1.1665	.11466	-1.676	.17453	.003133			
.5063	.4937	1.1604	.11959						
.5494	.4506	1.1724	.10690	-1.247	.17189	.003400			
.5570	.4430	1.1868	.10012						
.5823	.4177	1.1757	.10613						
.6000	.4000	1.1714	.10808	-.623	.16056	.003920			
.6076	.3924	1.1801	.10206						
.6481	.3519	1.1769	.09650	-.501	.16984	.004338			
.6987	.3013	1.1724	.09292	-1.027	.18234	.006882			
.7468	.2532	1.1792	.09267	-.918	.17086	.007266			
.7975	.2025	1.1861	.08333	-1.014	.15523	.004767			
.8228	.1772	1.1835	.08601						
.8481	.1519	1.1872	.08132						
.8734	.1266	1.1859	.07917						
.8987	.1013	1.1791	.08061	-.647	.12075	.002384			
.9241	.0759	1.1804	.07987	-.182	.10985	.002139			
.9367	.0633	1.1715	.08678	-1.007	.07830	.002045			
.9494	.0506	1.1750	.08634	-.798	.07419	.001917			

TABLE A-IIa. (Concluded) Mean and Turbulent Velocity Around the Duct. Trip Wires on Inlet. Dense Screen at Exit.

x = +26.70
Re= 192,000
U_m= 2.819m/sec
T = 6.1°C
ν = $1.468 \times 10^{-6} m^2/sec$

y/H	yc/H	U/U_m	$\sqrt{\overline{u^2}}/U_m$	Angle (deg)	$\sqrt{\overline{v^2}}/U_m$	$\overline{uv}/U_m^2$
.0051	.9949	.6272	.14547			
.0101	.9899	.6676	.16547			
.0152	.9848	.6850	.16658			
.0203	.9797	.7001	.16825			
.0304	.9696	.7077	.17463			
.0405	.9595	.7310	.17419			
.0506	.9494	.7426	.18615			.000512
.0633	.9367	.7566	.18902	-2.856	.07768	-.005319
.0759	.9241	.7832	.18952	-.601	.07109	-.003631
.1013	.8987	.8125	.18995	-1.135	.11606	-.006146
.1519	.8481	.8390	.19674	-.864	.13908	-.008422
.2025	.7975	.8904	.20899	-.368	.13996	-.011484
.2532	.7468	.9166	.21332	-.612	.14192	-.010570
.3038	.6962	.9762	.19205	-.920	.16235	-.010051
.3544	.6456	1.0192	.18373	-.984	.16231	-.010818
.4051	.5949	1.0686	.17043	-.785	.17535	-.009253
.4557	.5443	1.0704	.17547	-.338	.15336	-.007496
.4937	.5063	1.0877	.14783	-.323	.16531	-.004940
.5443	.4557	1.1129	.14344	.089	.14368	-.003322
.5949	.4051	1.1331	.13081	-.263	.14941	.000809
.6456	.3544	1.1535	.11422	.442	.15684	-.000032
.6962	.3038	1.1468	.10964	1.132	.14109	-.000158
.7468	.2532	1.1585	.09868	.379	.13430	.002586
.7975	.2025	1.1703	.08751	.889	.12824	.001510
.8481	.1519	1.1739	.08784	.707	.10811	.002482
.8987	.1013	1.1669	.08240	1.204	.11331	.002456
.9241	.0759	1.1674	.08496	-.172	.09784	.001940
.9367	.0633	1.1625	.08818	-.472	.08557	.002043
.9494	.0506	1.1555	.09736	.199		.002715
.9595	.0405	1.1486	.10708			
.9696	.0304	1.1311	.11608			
.9797	.0203	1.0937	.12848			
.9848	.0152	1.0800	.11885			
.9899	.0101	1.0525	.13094			
.9949	.0051	1.0051	.13055			

TABLE A-IIb. Mean and Turbulent Velocity Variations With Exit Screen and Reynolds Number. Trip Wires on Inlet.

x = -24.4cm, No Screen

$\nu = 1.297 \times 10^{-6} m^2/sec$

Re = 300,000 U_m = 3.880m/sec				Re = 431,000 U_m = 5.569m/sec			
y/H	yc/H	U/Um	$\sqrt{\overline{u^2}}/U_m$	y/H	yc/H	U/Um	$\sqrt{\overline{u^2}}/U_m$
.0150	.9850	.8120	.06938	.0150	.9850	.8190	.06972
.0301	.9699	.8485	.06968	.0301	.9699	.8537	.07484
.0752	.9248	.9207	.06006	.0752	.9248	.9219	.05492
.1504	.8496	.9793	.05135	.1504	.8496	.9871	.04631
.2506	.7494	1.0273	.04097	.2506	.7494	1.0310	.03770
.3008	.6992	1.0469	.03288	.3008	.6992	1.0494	.03300
.3759	.6241	1.0603	.02343	.3759	.6241	1.0617	.02759
.4950	.5050	1.0697	.01339	.4950	.5050	1.0722	.01454
.6241	.3759	1.0678	.01837	.6241	.3759	1.0667	.02119
.6992	.3008	1.0573	.02539	.6992	.3008	1.0553	.02935
.7494	.2506	1.0432	.03343	.7494	.2506	1.0375	.03280
.8496	.1504	.9940	.04747	.8496	.1504	.9916	.04183
.9248	.0752	.9046	.06317	.9248	.0752	.9182	.05482
.9699	.0301	.8196	.07193	.9699	.0301	.8317	.06664
.9850	.0150	.7493	.08020	.9850	.0150	.7995	.07636

Table A-IIb. Mean and Turbulent Velocity Variations With Exit Screen and Reynolds Number. Trip Wires on Inlet.

Re = 340,000 — 90 deg. Around the Turn, No Screen
U_m = 4.490m/sec — $\nu = 1.341 \times 10^{-6} m^2/sec$

y/H	yc/H	U/Um	$\sqrt{\overline{u^2}}/U_m$	Angle (deg)	$\sqrt{\overline{v^2}}/U_m$	$\overline{uv}/U_m^2$
.0100	.9900	1.4937	.10665			
.0200	.9800	1.7469	.04754			
.0300	.9700	1.7526	.04549			
.0400	.9600	1.7401	.04417			
.0500	.9500	1.7219	.04392			
.0750	.9250	1.6709	.04303			
.1000	.9000	1.6166	.04037			
.1500	.8500	1.5156	.03616	.523	.03376	.000458
.2000	.8000	1.4280	.02726			
.2500	.7500	1.3434	.02766	.646	.03348	.000318
.3000	.7000	1.2730	.02362	.404	.04280	.000521
.3500	.6500	1.2055	.02661	.776	.04612	.000512
.4000	.6000	1.1286	.04328			
.4500	.5500	1.0648	.05855			
.5000	.5000	.9964	.07506	1.759	.06835	.003457
.5500	.4500	.9352	.08667	2.087	.09804	.006066
.6000	.4000	.8685	.09359	3.480	.10440	.006691
.6500	.3500	.8015	.10313	4.470	.12508	.008654
.7000	.3000	.7450	.09841	3.313	.15342	.011243
.7000	.3000	.7375	.10767	3.765	.13716	.010247
.7500	.2500	.6829	.10475	3.032	.15747	.011932
.8000	.2000	.6627	.10383	2.888	.15850	.011323
.8500	.1500	.6245	.09600	2.643	.14668	.008482
.9000	.1000	.5953	.09176	3.952	.08137	.004544
.9375	.0625	.5764	.09819			

Re =472,000 — 90 deg. Around the Turn, No Screen
U_m = 6.218m/sec — $\nu = 1.341 \times 10^{-6} m^2/sec$

y/H	yc/H	U/Um	$\sqrt{\overline{u^2}}/U_m$	Angle (deg)	$\sqrt{\overline{v^2}}/U_m$	$\overline{uv}/U_m^2$
.0100	.9900	1.5727	.09482			
.0200	.9800	1.7282	.04701			
.0300	.9700	1.7254	.04608			
.0400	.9600	1.7063	.04410			
.0500	.9500	1.6881	.04235			
.0750	.9250	1.6379	.04014			
.1000	.9000	1.5872	.03875			
.1500	.8500	1.4900	.03386	1.719	.03818	.000394
.2000	.8000	1.4012	.02804			
.2500	.7500	1.3222	.02420	1.730	.03514	.000397
.3000	.7000	1.2616	.02576			
.3500	.6500	1.1842	.03633	1.107	.03983	.000628
.4000	.6000	1.1147	.03861			
.4500	.5500	1.0493	.05275			
.5000	.5000	.9816	.06752	2.162	.06165	.002383
.5500	.4500	.9275	.07103	2.861	.08603	.004060
.6000	.4000	.8597	.08279	3.518	.10906	.006208
.6000	.4000	.8619	.08425	3.098	.11455	.007333
.6500	.3500	.7956	.09814	3.672	.12207	.007606
.7000	.3000	.7468	.10170	3.475	.14392	.009583
.7500	.2500	.7087	.10281	4.385	.13826	.009357
.8000	.2000	.6610	.09717		.14413	.007834
.8500	.1500	.6200	.09147	4.249	.13871	.007627
.9000	.1000	.5992	.08335	2.983	.10332	.005763
.9375	.0625	.5923	.08377			

TABLE A-IIb. (Continued) Mean and Turbulent Velocity Variations With Exit Screen and Reynolds Number. Trip Wires on Inlet.

x = -17.27cm, Coarse Screen at Exit
$\nu = 1.395 \times 10^{-6} m^2/sec$

Re= 136,000
U_m= 1.874m/sec

y/H	U/Um	$\sqrt{\overline{u^2}}/U_m$
.0050	.5904	.08824
.0100	.6668	.07330
.0150	.7012	.06924
.0201	.7340	.07025
.0301	.7765	.06867
.0401	.8061	.06877
.0501	.8271	.06390
.0627	.8442	.06641
.0752	.8686	.06688
.1003	.9066	.06240
.1504	.9764	.05626
.2005	1.0164	.03792
.2506	1.0387	.03714
.3008	1.0563	.02892
.3509	1.0677	.03018
.4010	1.0857	.05943
.4511	1.0900	.05793
.5013	1.0944	.09580

Re= 275,000
U_m= 3.780m/sec

y/H	U/Um	$\sqrt{\overline{u^2}}/U_m$
.0050	.6833	.07970
.0100	.7201	.07333
.0150	.7597	.07843
.0201	.7708	.07688
.0301	.8146	.07452
.0401	.8472	.07455
.0501	.8745	.07085
.0627	.8903	.06785
.0752	.9105	.06513
.1003	.9528	.06000
.1504	.9896	.05695
.2005	1.0354	.04290
.2506	1.0587	.04321
.3008	1.0791	.04090
.3509	1.0867	.03797
.4010	1.0928	.04147
.4511	1.0947	.03419
.5013	1.0943	.04099

Re= 363,000
U_m= 4.997m/sec

y/H	U/Um	$\sqrt{\overline{u^2}}/U_m$
.0050	.6833	.08201
.0100	.7396	.08243
.0150	.7652	.08737
.0201	.7983	.08548
.0301	.8320	.08192
.0401	.8671	.08335
.0501	.8811	.07494
.0627	.9107	.07205
.0752	.9277	.07200
.1003	.9669	.06428
.1504	1.0135	.05574
.2005	1.0331	.04708
.2506	1.0606	.04126
.3008	1.0744	.03365
.3509	1.0842	.02311
.4010	1.0892	.02049
.4511	1.0943	.01715
.5013	1.0943	.01643

Re= 446,000
U_m= 6.141m/sec

y/H	U/Um	$\sqrt{\overline{u^2}}/U_m$
.0050	.7101	.10199
.0100	.7332	.09070
.0150	.7900	.08361
.0201	.8121	.08229
.0301	.8575	.07032
.0401	.8655	.07182
.0501	.8998	.06618
.0627	.9168	.07006
.0752	.9263	.05919
.1003	.9567	.05617
.1504	.9987	.05420
.2005	1.0369	.04659
.2506	1.0607	.04051
.3008	1.0748	.03034
.3509	1.0835	.02584
.4010	1.0905	.02123
.4511	1.0929	.01863
.5013	1.0943	.01721

TABLE A-IIb. (Concluded) Mean and Turbulent Velocity Variations With Exit Screens and Reynolds Number. Trip Wires on Inlet.

x = +30.90cm, Coarse Screen at Exit
Re = 430,000
U_m = 6.315 m/sec
ν = 1.468×10^{-6} m^2/sec

y/H	yc/H	U/Um	$\sqrt{\overline{u^2}}/U_m$	Angle (deg)	$\sqrt{\overline{v^2}}/U_m$	$\overline{uv}/U_m^2$
.0101	.9899	.3886	.18983			
.0152	.9848	.4072	.20297			
.0203	.9797	.4082	.19994			
.0253	.9747	.4130	.20969			
.0304	.9696	.4373	.20929			
.0506	.9494	.4656	.20071	-3.638	.43124	-.009853
.0633	.9367	.4956	.20681	-5.668	.25753	-.006154
.0886	.9114	.5146	.21557	-4.704	.15558	-.006215
.1392	.8608	.6316	.24365	-7.378	.12964	-.010795
.1899	.8101	.8081	.26409	-6.799	.13966	-.013143
.2405	.7595	.9110	.24364	-5.045	.15407	-.014200
.2911	.7089	1.0003	.22087	-4.500	.13245	-.006065
.3418	.6582	1.0862	.18824	-3.312	.11882	-.003251
.3924	.6076	1.1372	.14740	-2.759	.12303	.000761
.4430	.5570	1.1496	.12830	-1.880	.12127	.002535
.4937	.5063	1.1817	.12458	-.347	.13714	.001510
.5443	.4557	1.2135	.10498	-.337	.13556	.002451
.5949	.4051	1.1962	.09719	1.105	.13463	.001283
.6456	.3544	1.1967	.09335	.960	.13537	.001450
.6962	.3038	1.2040	.08753	.748	.15352	.003429
.7468	.2532	1.2040	.09076	1.040	.15782	.004930
.7975	.2025	1.1936	.09613	1.021	.14042	.001746
.8481	.1519	1.2134	.08613	1.553	.12337	.002297
.8937	.1063	1.2004	.07361	.237	.11572	.001660
.9241	.0759	1.2004	.07844	.529	.13827	.001599
.9367	.0633	1.2014	.07728	1.385	.12809	.001193
.9494	.0506	1.1944	.08333	1.636	.11894	.002165
.9595	.0405	1.1878	.08619			
.9696	.0304	1.1828	.09558			
.9797	.0203	1.1504	.11455			
.9848	.0152	1.1307	.11958			
.9899	.0101	1.1069	.12458			

x = -25.40cm, Dense Screen
Re = 104,000
U_m = 1.372m/sec
ν = 1.372×10^{-6} m^2/sec

y/H	yc/H	U/Um	$\sqrt{\overline{u^2}}/U_m$
.0050	.9950	.6700	.08082
.0100	.9900	.7224	.07024
.0150	.9850	.7716	.06351
.0201	.9799	.7864	.07071
.0301	.9699	.8191	.07182
.0401	.9599	.8478	.06696
.0501	.9499	.8613	.06231
.0627	.9373	.8840	.06662
.0752	.9248	.9089	.06496
.0877	.9123	.9200	.06364
.1003	.8997	.9304	.05864
.1504	.8496	.9800	.04942
.2005	.7995	1.0153	.04576
.2506	.7494	1.0404	.04344
.3008	.6992	1.0631	.03036
.3509	.6491	1.0753	.02307
.4010	.5990	1.0791	.01756
.4511	.5489	1.0822	.01387
.5013	.4987	1.0840	.01209
.5489	.4511	1.0849	.01229
.5990	.4010	1.0822	.01433
.6491	.3509	1.0756	.02629
.6992	.3008	1.0678	.02733
.7494	.2506	1.0593	.03478
.7995	.2005	1.0236	.04771
.8496	.1504	.9940	.04791
.8997	.1003	.9293	.06149
.9123	.0877	.9164	.06258
.9248	.0752	.9016	.05771
.9373	.0627	.8758	.06200
.9499	.0501	.8478	.06078
.9599	.0401	.8236	.06509
.9699	.0301	.7929	.06731
.9799	.0201	.7676	.06571
.9850	.0150	.7389	.07176
.9900	.0100	.6953	.07282
.9950	.0050	.6502	.08291

TABLE A-III. Surface Shear Stress Evaluation.

1.7H upstream			10 degrees around the turn			50 degrees around the turn		
Re	U_m m/s	U_τ/U_m	Re	U_m m/s	U_τ/U_m	Re	U_m m/s	U_τ/U_m
182,000	2.86	0.0360	338,000	5.31	0.0195	200,000	3.14	0.0216
216,000	3.39	0.0365	364,000	5.71	0.0189	224,000	3.52	0.0216
247,000	3.88	0.0361	392,000	6.17	0.0189	256,000	4.02	0.0206
272,000	4.27	0.0359	392,000	6.17	0.0189	273,000	4.29	0.0215
304,000	4.77	0.0358	418,000	6.56	0.0189	301,000	4.73	0.0215
336,000	5.28	0.0358	441,000	6.92	0.0189	324,000	5.09	0.0218
357,000	5.60	0.0359	457,000	7.17	0.0192	354,000	5.56	0.0229
381,000	5.98	0.0357	413,000	6.48	0.0193	375,000	5.89	0.0231
403,000	6.33	0.0359	389,000	6.11	0.0193	401,000	6.30	0.0238
431,000	6.77	0.0357	369,000	5.79	0.0193	425,000	6.67	0.0234
451,000	7.08	0.0358	342,000	5.37	0.0188	450,000	7.06	0.0235
408,000	6.41	0.0358	313,000	4.91	0.0196	418,000	6.56	0.0225
357,000	5.60	0.0359	293,000	4.58	0.0194	378,000	5.93	0.0224
306,000	4.80	0.0363	248,000	3.89	0.0215	341,000	5.35	0.0222
258,000	4.05	0.0361	235,000	3.69	0.0204	313,000	4.91	0.0216
197,000	3.09	0.0363	214,000	3.36	0.0205	281,000	4.41	0.0218
148,000	2.32	0.0634	188,000	2.95	0.0216	250,000	3.92	0.0216
104,000	1.63	0.0370	166,000	2.61	0.0228	216,000	3.59	0.0221
						197,000	3.09	0.0223
						173,000	2.72	0.0233
						150,000	2.35	0.0246

70 degrees around the turn			90 degrees around the turn			110 degrees around the turn		
Re	U_m m/s	U_τ/U_m	Re	U_m m/s	U_τ/U_m	Re	U_m m/s	U_τ/U_m
216,000	3.39	0.0276	437,000	6.86	0.0288	213,000	3.34	0.0261
247,000	3.88	0.0274	386,000	6.06	0.0281	234,000	3.67	0.0264
274,000	4.30	0.0272	642,000	5.37	0.0276	259,000	4.07	0.0268
307,000	4.82	0.0267	300,000	4.71	0.0281	283,000	4.44	0.0262
324,000	5.09	0.0267	267,000	4.19	0.0278	304,000	4.77	0.0269
356,000	5.59	0.0269	232,000	3.64	0.0275	336,000	5.28	0.0264
374,000	5.87	0.0273	195,000	3.06	0.0275	356,000	5.59	0.0270
405,000	6.36	0.0273	153,000	2.40	0.0274	380,000	5.97	0.0275
424,000	6.66	0.0275				443,000	6.96	0.0291
459,000	7.21	0.0277				433,000	6.80	0.0284
422,000	6.63	0.0276				398,000	6.25	0.0276
377,000	5.92	0.0276				365,000	5.73	0.0274
354,000	5.56	0.0273				343,000	5.39	0.0272
316,000	4.96	0.0275				306,000	4.80	0.0273
276,000	4.33	0.0281				281,000	4.41	0.0275
253,000	3.97	0.0281				256,000	4.02	0.0276
232,000	3.64	0.0275				232,000	3.64	0.0273
205,000	3.22	0.0278				209,000	3.28	0.0272
172,000	2.70	0.0284				184,000	2.89	0.0275
144,000	2.26	0.0302				158,000	2.48	0.0278
122,000	1.92	0.0315				132,000	2.07	0.0294

TABLE A-III. (Concluded). Surface Shear Stress Evaluation.

130 degrees around the turn			170 degrees around the turn		
Re	U_m m/s	U_τ/U_m	Re	U_m m/s	U_τ/U_m
216,000	3.39	0.0350	335,000	5.26	0.0378
244,000	3.83	0.0315	348,000	5.46	0.0408
281,000	4.41	0.0312	373,000	5.86	0.0414
304,000	4.77	0.0312	414,000	6.50	0.0389
323,000	5.07	0.0314	433,000	6.80	0.0407
349,000	5.48	0.0319	387,000	6.08	0.0395
377,000	5.92	0.0319	367,000	5.76	0.0400
400,000	6.28	0.0321	344,000	5.40	0.0397
423,000	6.64	0.0332	306,000	4.80	0.0391
446,000	7.00	0.0333	287,000	4.51	0.0382
405,000	6.36	0.0333	272,000	4.27	0.0367
374,000	5.87	0.0325	239,000	3.75	0.0379
345,000	5.42	0.0326	218,000	3.42	0.0378
305,000	4.79	0.0321	194,000	3.05	0.0366
282,000	4.43	0.0320	173,000	2.72	0.0365
257,000	4.03	0.0323	137,000	2.15	0.0376
228,000	3.58	0.0318	123,000	1.93	0.0380
205,000	3.22	0.0316	97,000	1.52	0.0410
177,000	2.78	0.0316			
156,000	2.45	0.0315			
127,000	1.99	0.0325			
110,000	1.73	0.0346			

TABLE A-IVa Spanwise Turbulent Velocity Component at 90 Degrees Around the Turn. Trip Wires on Inlet; Coarse Screen at Exit. $\nu = 1.42 \times 10^{-6} m^2/sec.$

Re	U_m m/s	$\sqrt{\overline{w^2}}/U_m$
y/H = 0.975		
218,000	3.08	.146
481,000	6.80	.147
425,000	6.00	.146
362,000	5.12	.150
325,000	4.60	.160
263,000	3.72	.171
208,000	2.95	.193
172,000	2.43	.209
136,000	1.92	.167
y/H = 0.949		
136,000	1.92	.152
444,000	6.28	.156
379,000	5.36	.148
345,000	4.88	.155
280,000	3.96	.171
226,000	3.20	.183
172,000	2.43	.187
136,000	1.92	.179
y/H = 0.898		
135,000	1.92	.177
441,000	6.28	.150
376,000	5.36	.162
342,000	4.88	.155
278,000	3.96	.181
224,000	3.20	.193
171,000	2.43	.206
135,000	1.92	.173
y/H = 0.848		
135,000	1.92	.158
445,000	6.34	.136
445,000	6.34	.136
376,000	5.36	.134
342,000	4.88	.139
278,000	3.96	.152
278,000	3.96	.148
278,000	3.96	.148
242,000	3.44	.158
180,000	2.57	.170
y/H = 0.797		
125,000	1.79	.156
458,000	6.52	.127
458,000	6.52	.144
441,000	6.28	.154
396,000	5.64	.154
332,000	4.72	.153
287,000	4.08	.151
225,000	3.20	.167
162,000	2.31	.192
y/H = 0.695		
171,000	2.43	.158
441,000	6.28	.146
368,000	5.24	.132
342,000	4.88	.135
287,000	4.08	.145
242,000	3.44	.161
180,000	2.56	.209
135,000	1.92	.200
y/H = 0.619		
135,000	1.92	.186
441,000	6.28	.175
377,000	5.36	.151
377,000	5.36	.159
377,000	5.36	.198
342,000	4.88	.188
278,000	3.96	.138
233,000	3.32	.135
144,000	2.05	.179
y/H = 0.500		
207,000	2.95	.120
261,000	3.72	.155
315,000	4.48	.157
360,000	5.12	.174
394,000	5.61	.183
441,000	6.28	.160

TABLE A-IVb. Variation of the Spanwise Turbulent Velocity Component with Distance from the Surface for Fixed Reynolds Numbers. 90 Degree Around the Turn; Trip Wires on the Inlet; Coarse Screen at the Exit.

Re = 200,000 U_m = 9.33m/sec		Re = 400,000 U_m = 18.7m/sec	
$\frac{y}{H}$	$\frac{\sqrt{\overline{w^2}}}{U_m}$	$\frac{y}{H}$	$\frac{\sqrt{\overline{w^2}}}{U_m}$
.975	.195	.975	.145
.949	.185	.949	.151
.898	.200	.898	.152
.848	.167	.848	.135
.797	.175	.797	.153
.695	.169	.695	.136
.619	.140	.619	.165
.500	.111	.500	.184
Re = 300,000 U_m = 14.0m/sec		Re = 450,000 U_m = 21.0m/sec	
.975	.161	.975	.145
.949	.164	.949	.158
.898	.174	.898	.150
.848	.144	.848	.136
.797	.153	.797	.154
.695	.144	.695	.148
.619	.143	.619	.177
.500	.16	.500	-

APPENDIX B

TABULATED DATA FOR FLOW WITH ROUGHNESS ON THE LOWER SURFACE OF THE DUCT INLET

A set of mean and turbulent velocity distributions were obtained for a range of Reynolds numbers from approximately 200,000 to 500,000. The lower surface of the duct inlet was roughened with coarse gravel approximately 1cm in height. The gravel was secured to the inlet in a band approximately 5 cm wide with epoxy paint, Figure B-1. The gravel was coated with the epoxy paint and then placed on the inlet.

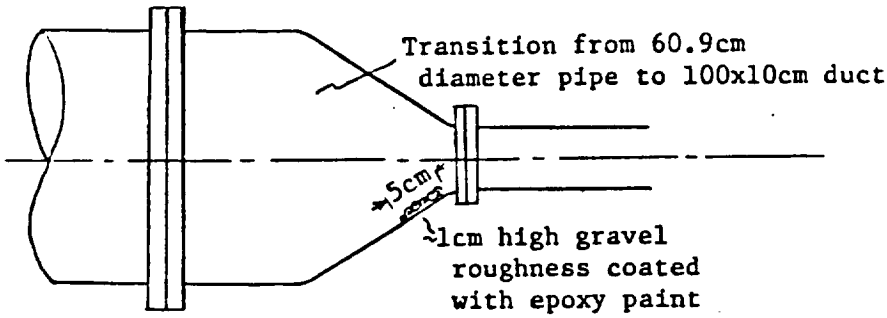

Figure B-1. Rough inlet condition.

The static pressure coefficients on both the inside and outside surfaces of the duct are tabulated in Table B-I. Both oil and water manometers and diaphragm pressure transducers were employed in the measurement of static pressure. In order to determine the Reynolds number effect on the static pressure, the pressure transducer was Connected to measure the difference between the pressure on the top surface at the reference point 109.2 cm upstream of the start of the turn, Figure A-2, and each static tape along the duct wall. For each location the values of Δp was measured as a function of the bulk velocity Reynolds number. Table B-Ia lists the values of c_p for a range of Reynolds numbers obtained at each location. The value of c_p for specific Reynolds numbers, listed in Table B-Ib, were obtained from the faired data given in Table B-Ia. Least square fits of the variation of c_p with the bulk Reynolds number for each location are tabulated in Table B-Ic.

Table B-II lists the mean and turbulent velocity measurements around the duct. The laser velocimeter data was also obtained by setting the measuring volume at a fixed location and varying the flow Reynolds number. Table B-IIa lists the actual data obtained at each location. Table B-IIb lists the mean and turbulent velocity distributions at specific Reynolds numbers obtained from the faired data of Table B-IIa.

Table B-IIc lists a special set of measurements of the mean and turbulent velocities obtained along the inside surface near the turn exit where a separation bubble occurs. Also listed on Table B-IIc is the percent time the flow was reversed (or in the upstream direction) determined from probability distributions of the fluctuating velocities. The data listed in Table B-IIc is viewed as more accurate than the separation data listed in Table B-IIa. The extremely large fluctuations in velocity in the separation region made it difficult to keep the signals within the range of the laser counter and the computer digital systems.

Table B-IId lists mean velocity distributions obtained for the rough inlet condition and different outlet conditions. All the data listed in Table B-IIa through c are for the case of a coarse screen across to duct outlet. In Table B-IId both a "dense" screen and no screen conditions are reported.

TABLE B-Ia. Static Pressure Coefficient Variation with Reynolds Number at Specific Locations Around the Duct.

Location	Re	C_p
10°inside	218,500	-.593
	280,000	-.693
	316,000	-.727
	353,000	-.744
	410,000	-.763
	480,000	-.777
30°inside	302,000	-1.827
	323,000	-1.821
	360,000	-1.800
	421,000	-1.784
50°inside	302,000	-2.180
	302,500	-2.179
	355,000	-2.161
	418,000	-2.167
	490,000	-2.171
70°inside	265,000	-2.246
	290,000	-2.269
	332,000	-2.269
	385,000	-2.272
	433,000	-2.262
	490,000	-2.303
110°inside	277,500	-2.140
	302,500	-2.165
	365,000	-2.169
	441,000	-2.162
	499,000	-2.175
130°inside	229,000	-1.593
	300,000	-1.660
	340,000	-1.696
	393,000	-1.703
	454,000	-1.741
	502,000	-1.752
150°inside	244,000	-1.269
	288,000	-1.285
	325,000	-1.326
	363,000	-1.347
	453,000	-1.402
	507,000	-1.376
170°inside	263,000	-1.166
	294,000	-1.183
	331,000	-1.185
	379,000	-1.215
	460,000	-1.260
	508,000	-1.305

Location	Re	C_p
10°outside	276,000	.186
	300,500	.205
	380,000	.205
	428,000	.171
	474,000	.207
	529,000	.205
30°outside	279,000	.408
	383,000	.412
	538,000	.415
50°outside	275,000	.458
	309,000	.459
	377,000	.458
	426,000	.455
	483,000	.459
	540,000	.463
70°outside	418,000	.450
	531,000	.455
	275,000	.452
90°outside	275,000	.462
	338,000	.453
	397,000	.453
	477,000	.453
	531,000	.453
110°outside	279,000	.459
	306,000	.458
	375,000	.457
	416,000	.455
	481,000	.450
	538,000	.453
130°outside	268,000	.443
	388,000	.427
	533,000	.425
150°outside	270,000	.405
	398,000	.387
	535,000	.382
170°outside	272,000	.319
	311,000	.331
	386,000	.308
	473,000	.303
	544,000	.300

TABLE B-Ia. (Concluded) Static Pressure Coefficient Variation with Reynolds Number at Specific Locations Around the Duct.

Location	Re	C_p
36.8cm upst	273,000	.002
	303,000	-.002
	377,000	-.010
	408,000	-.012
	472,000	-.014
	532,000	-.015
11.4cm upst	273,000	-.088
	397,000	-.106
	541,500	-.119
6.9cm dnst	227,000	-.494
	300,000	-.663
	354,000	-.632
	398,000	-.645
	458,000	-.649
	532,000	-.633
17.5cm dnst	273,000	-.342
	313,000	-.358
	383,000	-.382
	487,000	-.388
	539,000	-.386

TABLE B-Ib. Static Pressure Coefficient Variation Around the Duct at Fixed Reynolds Numbers.

Location (° around turn)	C_p Re= 200,000	C_p Re= 300,000	C_p Re= 400,000	C_p Re= 500,000
10° inside	-.623	-.688	-.753	-.818
30° inside	-1.865	-1.827	-1.790	-1.753
50° inside	-2.180	-2.175	-2.170	-2.166
70° inside	-2.243	-2.259	-2.276	-2.292
110° inside	-2.144	-2.154	-2.165	-2.175
130° inside	-1.596	-1.652	-1.708	-1.764
150° inside	-1.256	-1.304	-1.352	-1.399
170° inside	-1.124	-1.179	-1.234	-1.289
10° outside	.190	.193	.196	.200
30° outside	.406	.409	.412	.414
50° outside	.456	.457	.459	.460
70° outside	.450	.451	.452	.453
90° outside	.460	.458	.455	.452
110° outside	.461	.458	.455	.452
130° outside	.445	.438	.431	.425
150° outside	.409	.400	.391	.383
170° outside	.331	.322	.312	.302
11.4 cm upst	-.081	-.092	-.104	-.115
36.8 cm upst	.004	-.002	-.009	-.016
6.9 cm dnst (inside)	-.559	-.593	-.627	-.660
17.5 cm dnst	-.339	-.355	-.371	-.387

TABLE B-Ic. Least Squares Coefficients for the Static Pressure Coefficient Variation With Reynolds Number

Location	A	B
(inside surface)		
1.14H upst.	$+1.148 \times 10^{-7}$	-.0580
10^{o}	-6.486 "	-.0494
30^{o}	+3.732 "	-1.939
50^{o}	+4.624 "	-2.189
70^{o}	-1.640 "	-2.210
110^{o}	-1.003 "	-2.124
130^{o}	-5.596 "	-1.484
150^{o}	-4.770 "	-1.161
170^{o}	-5.498 "	-1.484
.67H dnst.	-3.369 "	-.4919
(outside surface)		
1.74H upst.	-6.662×10^{-7}	+.0178
10^{o}	-3.229×10^{-8}	+.1835
30^{o}	+2.643 "	+.4011
50^{o}	+1.177 "	+.4539
70^{o}	+1.060 "	+.4480
90^{o}	-2.723 "	+.4658
110^{o}	-2.993 "	+.4673
130^{o}	-6.607 "	+.4673
150^{o}	-8.620 "	+.4259
170^{o}	-9.724 "	+.3508
0.78H dnst.	$+5.993 \times 10^{-7}$	-1.392
1.72H "	-1.610 "	-.3069

Where; $c_p = ARe + B$

TABLE B-IIa. Mean and Turbulent Velocity Variations with Reynolds Number. Roughness on Inlet, Coarse Screen at Exit.

10H Upstream of the Turn
Temp = 7.3°C
$\nu = 1.413 \times 10^{-6} m^2/sec$

y/H	Re	U/Um	$\sqrt{\overline{u^2}}/U_m$
.0076	222,000	.717	.101
	277,500	.752	.105
	332,000	.758	.114
	370,000	.744	.101
	468,000	.749	.097
	530,000	.744	.091
.0126	250,500	.736	.096
	309,000	.755	.102
	383,000	.754	.109
	470,500	.747	.092
	538,000	.746	.097
.0202	242,000	.735	.096
	300,500	.781	.112
	387,000	.783	.105
	463,000	.769	.093
	532,500	.765	.091
.0303	300,000	.790	.107
	382,000	.778	.097
	470,000	.779	.096
	536,500	.777	.093
.0505	261,000	.797	.104
	301,000	.800	.104
	388,000	.798	.100
	471,000	.811	.094
.1010	257,000	.856	.107
	390,500	.859	.109
	522,500	.859	.107
.2020	255,000	.960	.106
	390,500	.974	.089
	532,500	.947	.110
.3030	252,000	1.014	.083
	405,500	1.008	.075
	547,000	1.007	.081
.5050	260,500	1.066	.023
	308,000	1.081	.026
	396,000	1.068	.025
	473,000	1.068	.026
	535,000	1.071	.023
	217,000	1.079	.022
	371,000	1.114	.027
	520,000	1.103	.022
.6944	266,000	1.084	.016
	377,000	1.082	.011
	526,000	1.071	.013
.8586	240,500	1.051	.017
	382,500	1.056	.017
	534,000	1.062	.018
.9343	258,500	1.044	.040
	379,000	1.044	.032
	528,000	1.049	.039
.9596	277,500	1.002	.063
	292,000	1.010	.057
	384,000	1.002	.050
	437,000	.977	.058
	542,500	.996	.063
.9848	259,500	.891	.104
	298,000	.898	.066
	404,000	.897	.064
	480,000	.882	.070
	547,000	.895	.074
.9924	263,000	.852	.074
	304,000	.866	.071
	405,000	.873	.062
	482,500	.855	.072
	547,500	.859	.078

Table B-IIa. (Continued) Mean and Turbulent Velocity Variations with Reynolds Number. Roughness on Inlet, Coarse Screen at Exit.

1.7H Upstream of the Turn
Temp = 3.6°C
$\nu = 1.591 \times 10^{-6} m^2/sec$

y/H	Re	U/Um	$\sqrt{\overline{u^2}}/U_m$	$\sqrt{\overline{v^2}}/U_m$	$\overline{uv}/U_m^2$	Angle (deg)	V/Um
0.005	192,600	.621	.074				
	273,300	.575	.089				
	333,300	.576	.104				
	440,900	.683	.073				
	487,200	.688	.066				
.0125	195,500	.731	.071				
	283,900	.730	.082				
	335,900	.766	.064				
	451,200	.780	.060				
.0300	196,500	.802	.059				
	307,300	.806	.061				
	341,000	.815	.063				
	466,100	.813	.064				
.0500	216,400	.959	.067	.112	-.0177	-1.2	-.0199
	312,900	.904	.067	.094	-.0074	0.3	.0046
	369,700	.899	.066		-.0062	0.4	.0066
	441,200	.869	.059	.118	-.0091	1.2	.0189
.1000	200,400	.879	.055	.044	-.0058	0.3	.0049
	300,400	.873	.062		-.0038	0.6	.0085
	367,200	.896	.054	.082	-.0005	0.3	.0041
	453,600	.865	.053		-.0004	0.3	.0038
.3000	202,800	.937	.043	.022	-.0028	-0.6	-.0101
	301,600	.942	.045	.034	-.0079	-0.3	-.0053
	368,400	.962	.041	.044	-.0097	-1.0	-.0173
	465,300	.935	.048	.027	-.0144	0.2	.0026
.5000	202,600	.975	.029	.028	-.0016	-0.7	-.0121
	302,800	.961	.028	.028	-.0042	0.3	.0054
	367,800	.997	.030	.026	-.0056	2.1	.0373
	463,900	.969	.031	.026	-.0078	-0.3	-.0056
.6850	200,400	.981	.020	.016	-.0003	0.2	.0030
	291,900	.992	.018	.015	-.0007	0.1	.0019
	375,600	1.019	.019	.020	-.0004	-0.5	-.0084
	474,800	.980	.024	.008	-.0006	-0.6	-.0101
.8850	195,200	.876	.048	.041	.0090	-0.1	-.0014
	295,800	.904	.048	.125	-.0416	-0.9	-.0148
	367,200	.918	.044	.042	.0078	0.6	.0009
	468,600	.913	.045	.007	.0153	0.0	.0001

TABLE B-IIa. (Continued) Mean and Turbulent Velocity Variations with Reynolds Number. Roughness on Inlet, Coarse Screen at Exit.

Start of the Turn
Temp = 3.5°C
$\nu = 1.584 \times 10^{-6} m^2/sec$

y/H	Re	U/Um	$\sqrt{\overline{u^2}}/U_m$	$\sqrt{\overline{v^2}}/U_m$	$\overline{uv}/U_m^2$	Angle (deg)	V/Um
.0075	210,200	1.105	.053				
	352,900	1.040	.048				
	462,800	1.130	.043				
.0125	198,600	1.127	.049				
	348,400	1.138	.046				
	477,000	1.126	.043				
.0300	202,300	1.112	.046				
	353,500	1.129	.043				
	477,000	1.125	.041				
.0500	195,900	1.112	.046	.026	-.0046	-6.2	-.121
	361,700	1.130	.042	.069	-.0038	-5.9	-.116
	480,900	1.118	.041	.197	.1284	-5.7	-.111
.1000	197,500	1.087	.042	.039	-.0053	-7.7	-.147
	353,300	1.118	.052	.017	-.0063	-7.8	-.153
	471,200	1.099	.039	.021	-.0112	-8.3	-.161
.3000	197,500	1.011	.036	.029	-.0035	-10.7	-.192
	335,800	1.024	.035	.030	-.0056	-10.1	-.183
	468,800	1.020	.034	.031	-.0088	-10.6	-.190
.5000	200,400	1.084	.028	.023	-.0009	-10.3	-.197
	336,300	1.044	.026	.023	-.0028	-10.0	-.184
	439,500	1.047	.027	.020	-.0034	-10.1	-.170
.6850	196,900	.987	.043	.089	-.0331	11.1	.193
	340,200	.989		.034	.0031	-8.1	
	423,300	.973	.033	.016	.0050	-8.8	-.150
.8850	182,700	.711	.097		.0114	-5.4	-.068
	352,500	.715	.079	.084	.0243	-5.2	-.065
	431,500	.733	.075	.026	.0295	-5.6	-.072
.9550	192,000	.465	.074				
	358,700	.470	.092				
	431,700	.488	.100				

TABLE B-IIa. (Continued) Mean and Turbulent Velocity Variations with Reynolds Number. Roughness on Inlet, Coarse Screen at Exit.

90 deg. Around the Turn
Temp = 3.3°C
$\nu = 1.601 \times 10^{-6} m^2/sec$

y/H	Re	U/Um	$\sqrt{\overline{u^2}}/U_m$	$\sqrt{\overline{v^2}}/U_m$	$\overline{uv}/U_m^2$	Angle (deg)	V/Um
.0125	199,000	1.757	.061				
	278,000	1.717	.075				
	417,000	1.653	.076				
.0500	193,000	1.705	.051				
	309,000	1.700	.045				
	412,000	1.655	.047				
.1000	188,000	1.519	.040				
	304,000	1.501	.042				
	403,000	1.516	.042				
.3000	199,000	1.163	.031				
	298,000	1.176	.030				
	408,000	1.148	.034				
.5000	194,000	.996	.073	.074	.0317	2.0	.0356
	302,000	.999	.053	.076	.0402	1.3	.0222
	418,000	.964	.063	.027	.0056	1.4	.0241
.6850	176,000	.771	.116	.119	.0925	3.9	.0525
	306,000	.763	.094	.122	.1323	3.2	.0424
	420,000	.771	.140	.088	.1377	1.2	.0169
.8850	192,000	.593	.088	.109	.0485	0.9	.0098
	306,000	.596	.081	.123	.0675	0.1	.0009
	403,000	.654	.173		.0512	7.4	.0849
.9550	199,000	.591	.091				
	302,000	.600	.086				
	417,000	.582	.077				
.9800	197,000	.556	.087				
	306,000	.572	.079				
	421,000	.558	.079				
.9995	195,000	.537	.088				
	277,000	.540	.075				
	412,000	.545	.081				

TABLE B-IIa. (Continued) Mean and Turbulent Velocity Variations with Reynolds Number. Roughness on Inlet, Coarse Screen at Exit.

170 deg Around the Turn
Temp = 5.1°C
$\nu = 1.519 \times 10^{-6} m^2/sec$

y/H	Re	U/Um	$\sqrt{\overline{u^2}}/U_m$	$\sqrt{\overline{v^2}}/U_m$	$\overline{uv}/U_m^2$	Angle (deg)	V/Um
.2000	190,000	1.433	.051	.097	.0037	16.6	.4329
	306,000	1.424	.047				
	455,000	1.394	.044	.097	-.0173	16.4	.4104
.3000	186,500	1.219	.047				
	291,500	1.330	.048				
	457,000	1.311	.043				
.5000	184,000	1.028	.071				
	296,000	1.166	.065				
	461,000	1.158	.071				
.6850	185,500	.889	.072				
	300,000	1.001	.070				
	463,000	.977	.073				
.9250	188,000	.781	.068				
	324,000	.924	.069				
	455,000	.912	.068				
.9850	183,000	.729	.066				
	300,000	.822	.069				
	464,000	.811	.056				

TABLE B-IIa. (Continued) Mean and Turbulent Velocity Variations with Reynolds Number. Roughness on Inlet, Coarse Screen at Exit.

Exit of the Turn
Temp = 4.3°C
$\nu = 1.568 \times 10^{-6} m^2/sec$

y/H	Re	U/Um	$\sqrt{\overline{u^2}}/U_m$	$\sqrt{\overline{v^2}}/U_m$	$\overline{uv}/U_m^2$	V/Um
.1000	148,000	1.296	.104	.0856	.000365	.508
	312,000	1.117	.265			.488
	438,000	1.096	.201			.387
.2000	172,000	1.207	.045	.0912	-.000497	.442
	324,000	1.241	.059	.0766	-.000196	.515
	452,000	1.259	.051	.0768	-.000101	.523
.3000	162,000	1.197	.053	.1111	.000748	.403
	335,000	1.238	.050	.0827	-.00838	.463
	461,000	1.209	.044	.0806	-.000391	.457
.5000	156,000	1.013	.067	.1592	-.002140	.290
	333,000	1.116	.052	.1434	-.000614	.327
	457,000	1.089	.049	.1512	.001230	.311
.6850	161,000	.944	.069	.1970	.00394	.149
	328,000	1.030	.058	.1815	.00155	.221
	457,000	1.004	.061	.1702	.000234	.203
.8850	156,000	.920	.064			
	341,000	.975	.053			
	458,000	.962	.062			

TABLE B-IIa. (Continued) Mean and Turbulent Velocity Variations with Reynolds Number. Roughness on Inlet, Coarse Screen at Exit.

0.5H Downstream of the Turn
Temp = 5.7°C
$\nu = 1.512 \times 10^{-6} m^2/sec$

Y/H	Re	U/Um	$\sqrt{\overline{u^2}}/U_m$	$\sqrt{\overline{v^2}}/U_m$	$\overline{uv}/U_m^2$	Angle (deg)	V/Um
.2000	204,000	1.058	.113	.228	-.2214	-22.6	-.4416
	383,000	.989	.133	.171	.0004	0.3	.0057
	546,000	1.032	.181		.0276	0.6	.0103
.3000	209,000	1.122	.071	.085	.0089	6.1	.1205
	397,000	1.088	.082	.087	-.0387	5.6	.1076
	549,000	1.172	.075	.089	-.0129	5.6	.1148
.5000	211,000	1.092	.064	.136	.0100	7.6	.1450
	397,000	1.062	.056	.099	-.0114	7.2	.1349
	549,000	1.164	.059	.115	.0200	6.8	.1398
.6850	207,000	1.151	.070	.188	.0026	5.7	.1141
	403,000	1.055	.058	.139	-.0134	6.3	.1161
	549,000	1.127	.056	.160	.0669	5.1	.1014
.8850	205,000	1.148	.076				
	375,000	1.140	.069				
	547,000	1.125	.065				
.9600	205,000	1.125	.065				
	409,500	1.049	.060				
	553,000	1.121	.063				
.9850	205,000	1.108	.069				
	397,000	1.037	.059				
	549,000						
.9925	205,000	1.041	.093				
	401,000	.959	.073				
	549,000	1.033	.073				

TABLE B-IIa. (Concluded) Mean and Turbulent Velocity Variations with Reynolds Number. Roughness on Inlet, Coarse Screen at Exit.

3.05H Downstream of the Turn
Temp = 8.2°C
$\nu = 1.382 \times 10^{-6} m^2/sec$

y/H	Re	U/Um	$\sqrt{\overline{u^2}}/U_m$	$\sqrt{\overline{v^2}}/U_m$	$\overline{uv}/U_m^2$	V/Um
.0075	208,000	.531	.106			
	274,000	.580	.140			
	391,000	.587	.136			
	470,000	.519	.138			
	556,000	.543	.135			
.0125	216,000	.532	.103			
	314,000	.572	.131			
	384,000	.601	.130			
	483,000	.614	.144			
	560,000	.614	.135			
.0300	212,000	.602	.114			
	288,000	.677	.128			
	375,000	.685	.157			
	483,000	.684	.147			
	546,000	.717	.129			
.1000	210,000	.715	.122	.094	-.0032	-.0009
	285,000	.763	.148	.131	-.0064	-.0036
	377,000	.792	.162	.090	-.0042	-.0135
	448,000	.791	.152	.140	-.0026	-.0252
	533,000	.779	.141		-.0004	-.0109
.3000	196,000	.948	.186	.125	-.0098	-.040
	340,000	.948	.170	.100	-.0050	-.061
	442,500	.930	.146	.147	-.0035	-.058
	521,000	.919	.167	.081	-.0048	-.059
.5000	207,000	1.077	.133	.137	-.0042	.001
	332,000	1.082	.143	.115	-.0030	-.028
	400,000	1.212	.158		-.0011	-.005
	518,000	1.093	.142		-.0009	-.015
.6850	204,000	1.140	.114	.133	-.0008	.015
	345,000	1.148	.158	.158	.0001	.009
	445,000	1.148	.108	.090	-.0011	.017
	514,000	1.163	.100	.111	.0012	.017
.9000	173,000	1.157	.075	.097	.0012	.0090
	276,000	1.120	.075	.089	.0010	-.0070
	364,000	1.122	.069	.092	.0006	-.0093
	460,000	1.120	.078	.065	.0010	-.0072
	540,000	1.142	.074	.086	.0014	-.0033
.9700	174,000	1.137	.097			
	271,000	1.107	.100			
	367,000	1.112	.087			
	452,000	1.123	.090			
	529,000	1.145	.095			
.9875	181,000	1.125	.114			
	298,000	1.085	.107			
	363,000	1.102	.101			
	457,000	1.099	.111			
	527,000	1.104	.113			
.9925	153,000	1.181	.113			
	217,000	1.086	.128			
	295,000	1.059	.131			
	364,000	1.074	.108			
	443,000	1.073	.126			
	485,000	1.071	.126			
	524,000	1.086	.112			

TABLE B-IIb. Mean and Turbulent Velocity Distributions.

Station 10 H ahead of turn

Re=	200,000		300,000		400,000		500,000	
y/H	U/U_m	$\sqrt{u^2}/U_m$	U/U_m	$\sqrt{u^2}/U_m$	U/U_m	$\sqrt{u^2}/U_m$	U/U_m	$\sqrt{u^2}/U_m$
0.0076		0.0990		0.1090	0.7432	0.0980		0.0950
0.0126	0.698	0.0920	0.7569	0.1010	0.7503	0.1065	0.7503	0.0925
0.0202	0.714	0.0830	0.7800	0.1120	0.7676	0.1030	0.7673	0.0920
0.0303	0.749	0.0910	0.7931	0.1070	0.8588	0.1090	0.8584	0.1080
0.0505	0.783	0.1040	0.8039	0.1035	0.7975	0.0995	0.8029	0.0950
0.1010	0.848	0.1070	0.8618	0.1070	0.8588	0.1090	0.8584	0.1080
0.2020	0.936	0.1100	0.9631	0.1020	0.9696	0.0900	0.9514	0.1050
0.3030	1.020	0.0860	1.0080	0.0800	1.0080	0.0750	1.0100	0.0770
0.5050	1.080	0.0210	1.0760	0.0250	1.0660	0.0275	1.0690	0.0245
0.6940	1.090	0.0240	1.0900	0.0140	1.0750	0.0120	1.0690	0.0130
0.8590	1.050	0.0165	1.0560	0.0165	1.0570	0.0170	1.0590	0.0175
0.9340	1.040	0.0460	1.0410	0.0360	1.0440	0.0320	1.0470	0.0365
0.9600	1.020	0.0980	1.0080	0.0550	0.9837	0.0520	0.9818	0.0620
0.9850	0.886		0.8987	0.0655	0.8952	0.0640	0.8841	0.0710
0.9920	0.827	0.0785	0.8669	0.0710	0.8751	0.0630	0.8532	0.0735

1.71 H upstream

Re=	200,000		300,000		400,000		500,000	
y/H	U/U_m	$\sqrt{u^2}/U_m$	U/U_m	$\sqrt{u^2}/U_m$	U/U_m	$\sqrt{u^2}/U_m$	U/U_m	$\sqrt{u^2}/U_m$
0.0050	0.618	0.0748	0.5720	0.0985	0.6430	0.0842	0.6910	0.0692
0.0125	0.731	0.0705	0.7400	0.0762	0.7770	0.0599	0.7810	0.0598
0.0300	0.801	0.0583	0.8050	0.0605	0.8130	0.0640	0.8140	0.0639
0.0500	0.846	0.0552	0.8470	0.0550	0.8470	0.0562	0.8450	0.0577
0.1000	0.897	0.0533	0.8970	0.0525	0.8960	0.0538	0.8960	0.0552
0.3000	0.988	0.0432	1.0040	0.0442	1.0000	0.0479	0.9970	0.0491
0.5000	1.051	0.0352	1.0680	0.0327	1.0640	0.0323	1.0610	0.0340
0.6850	1.105	0.0208	1.1060	0.0222	1.1110	0.0258	1.1100	0.0282
0.8850	1.022	0.0540	1.0290	0.0535	1.0320	0.0525	1.0290	0.0552
0.9550	0.912	0.0599	0.9200	0.0625	0.9190	0.0608	0.9070	0.0635
0.9800	0.800	0.0712	0.8300	0.0758	0.8500	0.0757	0.8450	0.0778

Start of turn

Re=	200,000		300,000		400,000		500,000	
y/H	U/U_m	$\sqrt{u^2}/U_m$	U/U_m	$\sqrt{u^2}/U_m$	U/U_m	$\sqrt{u^2}/U_m$	U/U_m	$\sqrt{u^2}/U_m$
0.0120	1.129	0.0435	1.1390	0.0455	1.1380	0.0460	1.1300	0.0445
0.0300	1.111	0.0465	1.1260	0.0450	1.1270	0.0420	1.1270	0.0410
0.0500	1.115	0.0465	1.1320	0.0445	1.1270	0.0415	1.1210	0.0410
0.1000	1.090	0.0420	1.1200	0.0515	1.1120	0.0495	1.1030	0.0430
0.5000		0.0275	1.0410	0.0260	1.0430	0.0265	1.0470	0.0275
0.6850	0.979	0.0420	0.9760	0.0350	0.9650	0.0330	0.9750	0.0335
0.8850	0.708	0.0935	0.7050	0.0825	0.7230	0.0760	0.7370	0.0745
0.9550	0.452	0.0750	0.4480	0.0855	0.4790	3.0970	0.4940	0.1025

$T = 8.1^{\circ}C$

$\nu = 1.38 \times 10^{-6} m^2/sec$

TABLE B-IIb. (Concluded). Mean and Turbulent Velocity Distributions.

.508 after turn

Re=	200,000		300,000		400,000		500,000	
y/H	U/U_m	$\sqrt{u^2}/U_m$	U/U_m	$\sqrt{u^2}/U_m$	U/U_m	$\sqrt{u^2}/U_m$	U/U_m	$\sqrt{u^2}/U_m$
0.0100	0.0410	0.1260	-0.0840	0.2100	-0.0600	0.1540		0.1540
0.0150	0.0930	0.2200	-0.0820	0.2080	-0.0270	0.1800	-0.0030	0.1560
0.0200	0.1140	0.2140	-0.0730	0.2000	-0.0090	0.1790	0.0120	0.1580
0.0300	0.2140	0.2600	0.0050	0.2440	0.0480	0.2150	0.0430	0.1800
0.0500	0.2480	0.3160	0.0800	0.2740	0.1030	0.2420	0.1090	0.2180
0.0625	0.4540		0.1490	0.2930	0.1440	0.2520	0.1790	0.2300
0.0750	0.4370	0.3560	0.2800	0.3210	0.3050	0.2880	0.3600	0.2630
0.1000	0.7340	0.2810	0.4960	0.2640	0.4900	0.2600	0.4630	0.3020
0.2000	1.0620	0.1130	1.0570	0.1150	1.0600	0.1380	1.0480	0.1830
0.3000	1.1220	0.0700	1.1630	0.0780	1.1710	0.0820	1.1750	0.0760
0.5000	1.0850	0.0640	1.1320	0.0590	1.1520	0.0570	1.1690	0.0620
0.6850	1.1020	0.0720	1.1610	0.0620	1.1520	0.0570	1.1380	0.0550
0.8850	1.1240	0.0760	1.1480	0.0710	1.1430	0.0680	1.1320	0.0640
0.9600	1.1240	0.0660	1.1280	0.0620	1.1360	0.0620	1.1180	0.0630
0.9850	1.0420	0.0940	1.0250	0.0790	1.0430	0.0730	1.0420	0.0730

3.03 H downstream of the turn

Re=	200,000		300,000		400,000		500,000	
y/H	U/U_m	$\sqrt{u^2}/U_m$	U/U_m	$\sqrt{u^2}/U_m$	U/U_m	$\sqrt{u^2}/U_m$	U/U_m	$\sqrt{u^2}/U_m$
0.0076	0.5340	0.0980	0.5490	0.1390	0.5400	0.1370	0.5230	0.1370
0.0126	0.5340	0.0970	0.5530	0.1230	0.6110	0.1330	0.6000	0.1400
0.0303	0.5900	0.1130	0.6740	0.1320	0.6760	0.1550	0.6830	0.1440
0.1010	0.6870	0.1260	0.7720	0.1500	0.7870	0.1590	0.7810	0.1450
0.2020	0.8580		0.8600		0.8580		0.8340	
0.3030	0.9290	0.1860	0.9460	0.1750	0.9380	0.1570	0.9190	0.1610
0.5050	0.9620	0.1330	1.0580	0.1390	1.0760	0.1580	1.0830	0.1600
0.6920	1.0630	0.1320	1.1380	0.1490	1.1440	0.1130	1.1620	0.1060
0.8990	1.1470	0.0760	1.1140	0.0750	1.1200	0.0720	1.1280	0.0750
0.9700	1.1290	0.0980	1.1000	0.0970	1.1140	0.0880	1.1280	0.0950
0.9870	1.1070	0.1330	1.0930	0.1070	1.0960	0.1060	1.1090	0.1120
0.9920	1.1000	0.1260	1.0680	0.1310	1.0710	0.1130	1.0830	0.1240

TABLE B-IIb. (Continued). Mean and Turbulent Velocity Distributions.

90 degrees around turn

Re=	200,000		300,000		400,000		500,000	
y/H	U/U_m	$\sqrt{u^2}/U_m$	U/U_m	$\sqrt{u^2}/U_m$	U/U_m	$\sqrt{u^2}/U_m$	U/U_m	$\sqrt{u^2}/U_m$
0.0120	1.751	0.0610	1.7000	0.0760	1.6520	0.0770	1.6220	0.0775
0.0500	1.702	0.0510	1.6980	0.0460	1.6520	0.0470	1.6300	0.0490
0.1000	1.518	0.0410	1.5230	0.0420	1.5020	0.0420	1.4860	0.0410
0.3000	1.167	0.0315	1.1690	0.0300	1.1430	0.0340	1.1190	0.0370
0.5000	0.994	0.0725	0.9980	0.0535	0.9680	0.0605	0.9470	0.0670
0.6850	0.767	0.1100	0.7610	0.1090	0.7650	0.1080	0.7740	0.1030
0.8850		0.1090		0.0950	0.6520	0.1070	0.6480	0.1050
0.9550	0.589	0.0910	0.5990	0.0860	0.5870	0.0785	0.5720	0.0750
0.9800	0.554	0.0860	0.5700	0.0800	0.5620	0.0800	0.5500	0.0800
0.9950	0.536	0.0875	0.5390	0.0790	0.5430	0.0760	0.5440	0.0740

170 degrees around turn

Re=	200,000		300,000		400,000		500,000	
y/H	U/U_m	$\sqrt{u^2}/U_m$	U/U_m	$\sqrt{u^2}/U_m$	U/U_m	$\sqrt{u^2}/U_m$	U/U_m	$\sqrt{u^2}/U_m$
0.0050	0.1064	0.2400	-0.0480	0.1080	-0.0286	0.0990	-0.0205	0.0730
0.0100	0.1596	0.3200	-0.3470	0.1690	-0.0077	0.1690	-0.0040	0.1570
0.0150	0.3377	0.3080	-0.0120	0.2230	0.0270	0.2190	0.0187	0.1940
0.0200	0.6015	0.3760	0.1024	0.3040	0.0762	0.2360	0.0808	0.2320
0.0300	0.7959	0.3470	0.3712	0.3720	0.2417	0.3680	0.2638	0.3440
0.0500	1.1450	0.2740	0.8224	0.3810	0.6321	0.4150	0.6884	0.4180
0.1000	1.2760	0.0660	1.2760	0.1300	1.2370	0.1370	1.2780	0.1100
0.2000	1.4120	0.0510	1.4360	0.0490	1.3900	0.0468	1.3910	0.0450
0.3000	1.2760	0.0475	1.3180	0.0480	1.2960	0.0471	1.3120	0.0430
0.5000	1.0080	0.0720	1.0760	0.0720	1.0710	0.0715	1.0780	0.0710
0.6850	0.8849	0.0720	0.9856	0.0708	0.9851	0.0700	0.9768	0.0721
0.9250	0.7818	0.0690	0.8896	0.0701	0.9167	0.0698	0.9098	0.0682
0.9750	0.7383	0.0670	0.8200	0.0700	0.7976	0.0668	0.8223	0.0569

Exit around turn

Re=	200,000		300,000		400,000		500,000	
y/H	U/U_m	$\sqrt{u^2}/U_m$	U/U_m	$\sqrt{u^2}/U_m$	U/U_m	$\sqrt{u^2}/U_m$	U/U_m	$\sqrt{u^2}/U_m$
0.0100	-0.0936	0.1580	-0.1060	0.1340	-0.0647	0.1120	-0.0611	0.1040
0.0130	0.0000	0.2090	-0.0985	1.3400	-0.0511	0.1090	-0.0521	0.1040
0.0150	0.0430		-0.1150		-0.0560		0.0544	
0.0200	0.1030	0.2330	-0.0679	0.1590	-0.0320	0.0925	-0.0121	0.0685
0.0250	0.2370		-0.0012		0.0088		0.0263	
0.0300	0.3810	0.3830	0.0580	0.2800	0.0667	0.2320	0.0814	0.2130
0.0400	0.4890	0.3640	0.1890	0.3440	0.1860	0.3320	0.2080	0.3290
0.0500	0.6660	0.3480	0.3020	0.3870	0.2880	0.3850	0.3180	0.3820
0.1000	1.1780	0.2080	1.1230	0.2630	1.0950	0.2140	1.0930	0.1820
0.2000	1.2130	0.0533	1.2400	0.0582	1.2460	0.0545	1.2580	0.0503
0.3000	1.2130	0.0532	1.2400	0.0512	1.2038	0.0468	1.2080	0.0438
0.5000	1.0660	0.0701	1.1120	0.0540	1.0950	0.0505	1.0850	0.0500
0.6850	0.9910	0.0715	1.0318	0.0585	0.9980	0.0595	1.0040	0.0612
0.8850	0.9490	0.0698	0.9790	0.0540	0.9570	0.0578	0.9610	0.0625

TABLE B-IIc. Velocity and Percent Flow Reversal in the Separation Bubble. Roughness on Inlet, Coarse Screen at Exit.

150 deg. Around the Turn
Temp = 8.8°C
$\nu = 1.356 \times 10^{-6} m^2/sec$

y/H	Re	U/Um	$\sqrt{u^2}$/Um	% Rev
.0050	201,400	.561	.602	8.6
	260,500	.460	.349	11.8
	316,900	.472	.320	8.9
	427,200	.446	.325	9.7
	429,200	.447	.317	8.4
	511,000	.431	.460	6.4
.0100	201,100	.579	.621	16.9
	321,500	.715	.352	2.5
	427,200	.654	.820	2.9
	511,600	.579	.300	2.6
.0150	201,000	.999	.324	0.3
	305,900	.641	.394	4.0
	435,200	.607	.365	3.8
	517,600	.647	.500	2.4
.0200	297,500	.862	.385	2.1
	420,500	.823	.369	1.4
	488,100	.799	.497	.0
	201,100	1.166	.296	
.0300	259,100	.850	.380	1.6
	259,400	.818	.379	1.9
	311,200	.833	.375	1.8
	310,000	.837	.379	1.5
	415,500	.795	.341	0.8
	500,500	.743	.414	1.9
	493,200	.748	.426	6.1
.0500	202,700	1.357	.131	
	308,900	1.395	.375	
	421,700	1.376	.119	
	510,300	1.436	.254	
.0750	203,700	1.332	.163	
	323,500	1.406	.130	
	428,800	1.413	.086	
	520,500	1.492	.132	
.1000	211,400	1.282	.063	
	259,100	1.386	.074	
	321,700	1.400	.069	
	431,500	1.406	.068	
	514,600	1.392	.075	

160 deg. Around the Turn
Temp = 8.8°C
$\nu = 1.356 \times 10^{-6} m^2/sec$

y/H	Re	U/Um	$\sqrt{u^2}$/Um	% Rev
.0050	195,700	.648	.521	4.3
	192,200	.456	.370	11.7
	330,800	.252	.295	24.6
	413,500	.257	.294	24.0
	522,800	.263	.303	23.6
.0100	318,700	.315	.336	22.0
	408,700	.268	.300	22.7
	510,000	.228	.279	25.2
	199,500	.509	.388	8.2
.0150	200,000	.546	.399	8.1
	305,000	.265	.327	25.5
	399,500	.258	.301	24.2
	495,700	.231	.289	27.2
	196,800	.577	.393	8.2
.0200	197,500	.750	.409	4.3
	303,000	.417	.388	18.5
	400,900	.413	.359	14.9
	506,400	.351	.301	14.5
.0300	192,700	1.122	.311	0.3
	312,100	.830	.405	3.9
	416,400	.709	.383	3.6
	489,300	.678	.395	4.3
.0500	194,700	1.221	.171	.0
	322,400	1.189	.298	0.2
	394,500	1.180	.299	.0
	504,600	1.085	.331	.0
.0750	193,600	1.298	.093	
	306,200	1.344	.130	
	403,900	1.358	.123	
	500,200	1.348	.129	
.1000	200,900	1.289	.085	
	312,100	1.366	.065	
	404,600	1.371	.061	
	498,400	1.365	.079	

TABLE B-IIc. (Continued) Velocity and Percent Flow Reversal in the Separation Bubble. Roughness on Inlet, Coarse Screen at Exit.

170 deg. Around the Turn
Temp = 8.3°C
$\nu = 1.375 \times 10^{-6} m^2/sec$

y/H	Re	U/Um	$\sqrt{u^2}$/Um	% Rev
.0075	258,000	-.039	.195	77.3
	311,000	-.034	.221	79.8
	406,000	.095	.541	71.1
	509,000	-.030	.230	74.8
.0100	295,000	-.019	.222	67.7
	196,000	.248	.369	32.3
	408,000	-.016	.235	65.6
	477,000	-.026	.232	66.0
.0150	297,000	.045	.270	58.3
	191,000	.372	.409	23.2
	303,000	.025	.258	61.2
	414,000	.050	.271	54.1
	503,000	.023	.254	59.0
.0200	205,000	.277	.412	32.6
	487,000	.104	.309	45.8
	400,000	.090	.293	49.1
	299,000	.098	.305	50.6
				33.7
.0300	299,000	.253	.384	35.2
	421,000	.227	.373	35.9
	479,000	.207	.355	35.4
.0500	191,000	1.095	.337	1.5
	483,000	.628	.556	10.7
	412,000	.662	.450	9.5
	296,500	.664	.461	10.3
.0075	295,000	1.156	.324	0.8
	413,000	1.128	.343	0.9
	505,000	1.066	.347	1.8
	200,000	1.217	.173	0.1
.1000	200,000	1.255	.099	.0
	481,000	1.355	.196	.0
	396,000	1.291	.174	0.1
	302,000	1.271	.171	.0

180 deg. Around the Turn
Temp = 8.4°C
$\nu = 1.374 \times 10^{-6} m^2/sec$

y/H	Re	U/Um	$\sqrt{u^2}$/Um	% Rev
0075	291,800	-.086	.219	74.8
0100	291,800	-.103	.232	74.9
	422,100	-.075	.317	71.4
	511,400	-.082	.187	74.1
0150	510,700	-.071	.225	70.0
	410,800	-.098	.237	69.8
	291,400	-.071	.247	72.7
0200	291,600	-.057	.246	70.4
	423,500	-.040	.247	66.0
	504,300	-.044	.246	66.4
0400	197,000		.468	12.3
	507,400	.229	.386	34.7
	396,900	.221	.396	35.9
	287,200	.224	.419	36.9
0500	506,300	.287	.389	28.9
	402,100	.324	.431	28.3
	289,400	.289	.442	31.9
0750	289,600	.708	.465	9.1
	415,200	.712	.464	8.9
	499,300	.656	.440	9.4
	197,000	1.070	.324	1.2

TABLE B-IIc. (Concluded) Velocity and Percent Reversal in the Separation Bubble. Roughness on Inlet, Coarse Screen at Exit.

.505H Downstream of the Turn
Temp = 8.2°C
$\nu = 1.379 \times 10^{-6} m^2/sec$

y/H	Re	U/Um	$\sqrt{u^2}$/Um	% Rev
.0076	315,500	-.177	.329	80.3
	358,000	-.049		76.1
.0101	313,000	-.212	.264	80.4
	314,000	-.223	.262	81.6
	409,000	-.214	.270	81.0
	502,000	-.218	.263	78.7
.0152	294,000	-.178	.275	77.0
	415,000	-.180	.276	76.8
	507,000	-.166	.257	78.7
.0202	299,000	-.175	.279	74.7
	396,000	-.169	.283	74.9
	507,000	-.155	.256	75.8
.0303	292,000	-.124	.289	67.0
	423,000	-.105	.321	71.9
	502,000	-.092	.275	66.6
	417,000	-.118	.298	68.2
.0505	292,000	-.055	.341	59.2
	407,000	.005	.342	52.2
	502,000	-.011	.317	54.8
.0758	207,000	.292	.410	30.5
	312,000	.145	.407	42.6
	410,000	.162	.378	39.0
	502,000	.118	.378	46.9
.1010	199,500	.460	.427	18.2
	313,000	.276	.432	31.0
	410,000	.331	.419	27.0
	507,500	.272	.392	30.3
.1515	216,000	.671	.421	9.0
	310,000	.682	.434	8.8
	409,000	.663	.423	8.7
	505,000	.641	.407	8.5
.2020	213,000	.901	.375	3.7
	305,500	.956	.377	2.4
	416,000	.920	.389	2.7
	497,000	.914	.377	2.6
.3030	212,000	1.134	.248	0.3
	305,500	1.216	.264	0.4
	411,500	1.205	.262	0.1
	496,000	1.162	.273	0.1

1.0H Downstream of the Turn
Temp = 8.0°C
$\nu = 1.518 \times 10^{-6} m^2/sec$

y/H	Re	U/Um	$\sqrt{u^2}$/Um	% Rev
.0075	245,000	.101	.184	28.9
	312,000	.070	.159	22.8
	418,000	.124	.207	21.1
	508,000	.094	.170	19.3
	545,000	.098	.181	21.9
	208,000	.203	.191	15.1
.0125	205,000	.341	.183	0.6
	323,000	.147	.219	12.4
	423,000	.165	.213	17.1
	530,000	.101	.206	16.9
.0300	208,000	.393	.150	0.2
	357,000	.243	.237	12.1
	542,000	.301	.195	1.7

.758H Downstream of the Turn
Temp = 8.2°C
$\nu = 1.379 \times 10^{-6} m^2/sec$

y/H	Re	U/Um	$\sqrt{u^2}$/Um	% Rev
.0075	210,000	.263	.303	23.2
	310,400	.048	.253	55.2
	410,900	.067	.242	53.3
	515,900	.039	.153	63.8
.0100	206,000	.210	.261	25.6
	309,600	.091	.291	44.7
	402,000	.100	.307	45.0
	508,200	.102	.282	43.2
.0150	212,000	.252	.286	24.7
	313,600	.145	.310	36.9
	402,200	.158	.325	35.9
	516,200	.173	.291	33.6
.0200	204,000	.329	.284	16.2
	314,000	.145	.310	36.4
	406,200	.182	.333	35.1
	511,600	.179	.296	31.2
.0300	203,000	.360	.274	12.5
	308,400	.183	.310	33.9
	404,400	.208	.312	29.0
	517,600	.238	.300	23.6
.0500	198,000	.443	.263	7.3
	310,900	.272	.301	22.8
	416,400	.276	.324	22.7
	511,100	.282	.298	20.0

TABLE B-IId. Mean Velocity Distributions With Different Exit Screens. Roughness on Inlet.

90 Degrees Around the Turn

Dense Screen			
Re=	197,000	292,100	377,200
U_m=	2.58m/s	3.82m/s	4.93m/s
y/H	U/U_m	U/U_m	U/U_m
.008	1.267	1.410	1.387
.010	1.578	1.531	1.515
.020	1.649	1.657	1.608
.050	1.615	1.678	1.610
.102	1.530	1.518	1.486
.203	1.339	1.347	1.328
.305	1.202	1.215	1.191
.500	0.999	1.015	1.001
.699	0.762	0.779	0.773
.899	0.594	0.620	0.608
.950	0.577	0.582	0.587
.975	0.557	0.572	0.576

No Screen				
Re=	199,000	291,500	385,400	463,700
U_m=	2.58m/s	3.79m/s	5.00m/s	6.02m/s
y/ H	U/Um	U/Um	U/Um	U/Um
.008	1.613	1.582	1.621	1.628
.010	1.663	1.654	1.664	1.645
.020	1.653	1.648	1.639	1.632
.030	1.648	1.648	1.638	1.604
.050	1.614	1.601	1.600	1.567
.100	1.496	1.497	1.494	1.465
.200	1.335	1.336	1.327	1.299
.300	1.196	1.195	1.192	1.178
.490	0.976	0.983	0.974	0.971
.688	0.719	0.740	0.752	0.756
.886	0.595	0.617	0.626	0.625
.936	0.578	0.569	0.584	0.595

Exit of the Turn

No Screen				
Re=	199,000	291,500	385,400	463,700
U_m=	2.60m/s	3.81m/s	5.04m/s	6.06m/s
y/H	U/Um	U/Um	U/Um	U/Um
.005		-.028	-.045	-.073
.010	.320	-.013	-.018	-.036
.020	.550	.050	.039	.008
.030	.720	.152	.153	.105
.050	.893	.428	.427	.415
.100	1.174	1.077	1.105	1.067
.150	1.122	1.236	1.248	1.245
.200	1.198	1.224	1.243	1.246
.300	1.155	1.201	1.212	1.206
.500	1.058	1.118	1.136	1.132

APPENDIX C

TABULATED DATA FOR FLOW WITH SMOOTH INLET SURFACES

The initial evaluation of the flow in the turn-around duct was made with smooth inlet surfaces. These preliminary measurements were made using a laser tracker system at nominally low Reynolds numbers. The measurements tabulated in Appendices A and B were made using a laser counter system. While the laser tracker mean velocity measurements agree reasonably well with the laser counter results over much of the flow field, the tracker velocities close to the surface appear to be too high. The data served to identify the major features of the flow in the turn-around duct. However, the data may be too limited to be used as a bases for improvement or computer models.

Table C-I lists the static pressure coefficients obtained for a Reynolds number range from 77,700 to 207,000. The data were obtained by setting the flow Reynolds number and then measuring the pressure difference with a diaphragm pressure transducer at each location around the turn. At the low flows it was more difficult to maintain the constant Reynolds number, thus some scatter in the individual values of c_p occurred.

Table C-IIa lists the mean velocities obtained with the laser tracker system for a nominal Reynolds number of 86,000. Figure C-1 identifies the location of the 11 stations listed on Table C-IIa. U is the tangential component of velocity and V is the radial component of velocity. The angle α correspond to flow toward the inner surface.

The tracker system mean velocity evaluations were found to be too high near the surface when compared to the "Log Law." Tracker measurements become increasingly less reliable in highly turbulent flow and when the scattering particle density decreases. However, comparison of the measured velocities near the surface with the expected log law variation suggested the error was related to the distance from the surface -- and not the turbulence level, Figure C-2. The following relation was developed to correct the measurements.

$$U_{corr} = U_{mes} \left[1 - 0.25\, e^{-7.2y} \right] \qquad \text{(for y in cm)} \qquad \text{(C-1)}$$

Table C-IIa lists the mean velocity values corrected - Corr (Near Wall) using equation (C-1).

The original measurements with the laser tracker system did not employ a frequency shifter (Bragg Cell). Once the separation bubble on the inside surface at the exit of the turn was identified, measurements with the frequency shifter optics were made in the separation region. Table C-IIa lists the velocities obtained in the separation region. These data in the separation region are viewed as preliminary, since the tracker limitations are severely taxed in the highly fluctuating flow.

Table C-IIb lists the mean and turbulent velocities measured for different values of Reynolds number at a large number of locations around the duct. The correction for the mean velocities near the surface obtained from equation (C-1) are listed separately in Table C-IIc. The turbulent velocities, $\sqrt{u^2}$, may also be aliased near the surfaces, but it was not possible to develop a correction. The measurements reported in Appendices A and B suggest the turbulence measurements with the tracker system, Table C-IIb, are possibly too small in magnitude. The low values of the fluctuating velocities may be due to the inability of the tracker to follow large changes in the velocity.

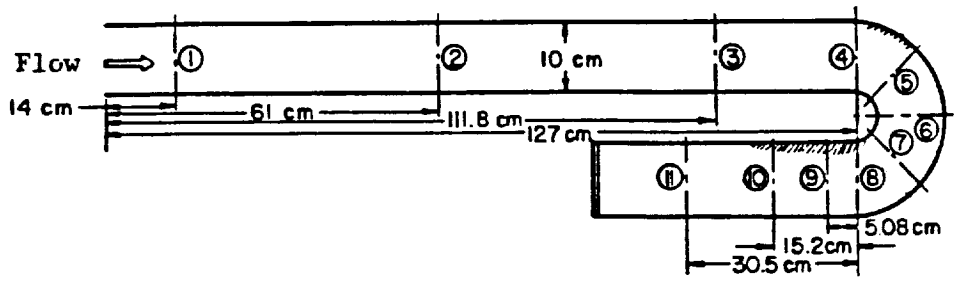

Figure C-1. Station Locations Around the Duct.

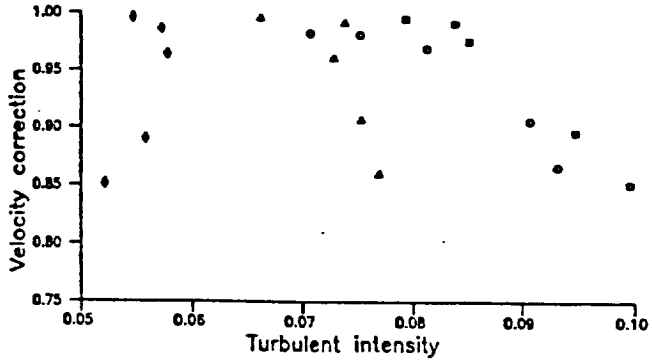

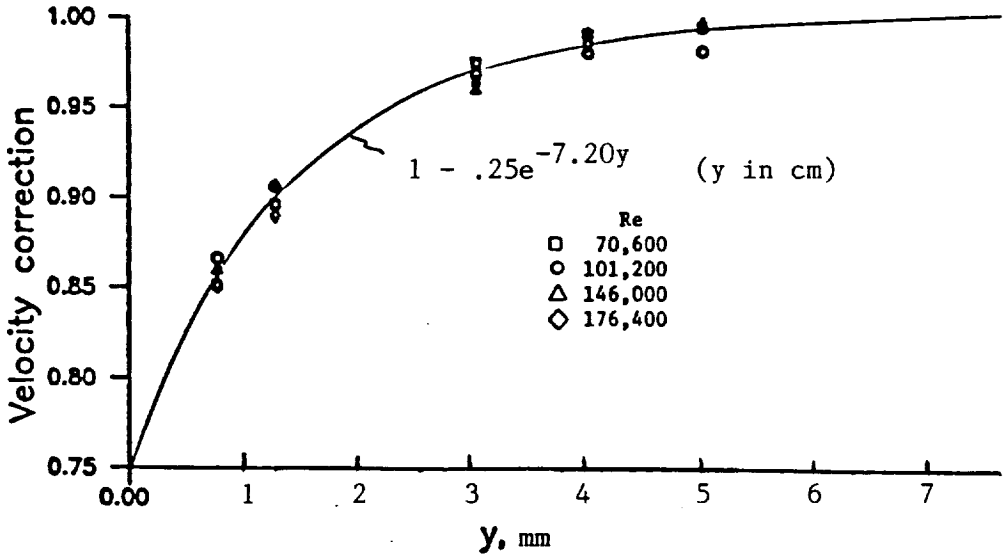

Figure C-2. Laser Velocimeter Correction Near the Surface.

TABLE C-I. Static Pressure Coefficient Distributions.
Smooth Inlet; Dense Screen at Exit.

Re =	77,000	91,700	113,000	126,000	161,000	179,000	189,000	207,000
U_m =	1.17m/s	1.32m/s	1.62m/s	1.82m/s	2.30m/s	2.58m/s	2.85m/s	3.12m/s
T =	5.2 °C	6.8 °C	6.8 °C	6.8 °C	7.1 °C	6.8 °C	5.5 °C	5.2 °C
υ =	1.51-6	1.44-6	1.44-6	1.44-6	1.43-6	1.44-6	1.51-6	1.51-6m^2/s
Location	Cp	Cp	Cp	Cp	Cp	Cp	Cp	Cp
69cm	-0.0653	-0.0604	-0.0694	-0.0578	0.0172	0.1102	-0.0109	0.1278
93	-0.0867	-0.0778	-0.0903	-0.0777	0.0037	0.1177	-0.0158	0.0888
113	-0.1029	-0.0998	-0.1337	-0.1206	-0.0545	0.1152	-0.0656	0.0691
Outside Surface								
10 Degrees								
30	0.1097	0.1580	0.1812	0.2020	0.2250	0.2238	0.1914	0.2783
50	0.3144	0.2360	0.2779	0.3012	0.3363	0.3190	0.2561	
70	0.4135	0.2563	0.3001	0.3321	0.3845	0.3569	0.3851	0.3848
90	0.4166	0.4166	0.4166	0.4166	0.4166	0.4166	0.4166	
110	0.3430	0.3425	0.3876	0.4128	0.4436	0.4188	0.3456	0.4075
130	0.3867	0.3297	0.3986	0.4108	0.4427	0.3923	0.4277	
150	0.4129	0.3597	0.4093	0.4262	0.4448	0.4203	0.4259	0.4017
170	0.2846	0.2998	0.3431	0.3594	0.3951	0.3630	0.3630	
	0.2612	0.2104	0.2650	0.2776	0.2909	0.2568	0.2374	0.2643
Inside Surface								
10 Degrees	-1.8700	-1.8470	-1.8550	-1.8610	-1.5360	-1.7610	-2.0210	-2.0070
30	-2.6090	-2.5500	-2.5630	-2.4770	-2.8470	-2.6120	-2.4970	-2.4160
50	-2.8280	-2.8400	-2.8490	-2.7380	-3.0100	-2.8190	-2.8130	-2.9540
70	-2.8740	-2.8740	-2.8740	-2.8740	-2.8740	-2.8740	-2.8740	-2.8740
90	-3.2470	-2.9650	-3.0030	-2.9160	-3.1020	-3.1040	-3.1270	-3.0520
110	-2.7190	-2.7390	-2.7210	-2.7090	-2.7070	-2.5670	-2.6130	-2.6780
130	-2.5480	-2.5590	-2.5590	-2.5580	-1.9380	-2.3520	-2.2940	-2.3630
150	-1.8650	-2.1160	-2.1590	-2.1310	-1.6930	-1.8080	-1.7380	-1.8740
170	-1.4060	-1.6020	-1.5450	-1.5370	-1.2490	-1.7360	-1.5160	-1.6730
Downstream of Turn								
10cm	-0.6055	-0.6135	-0.5990	-0.6027	-0.4724	-0.7150	-0.8053	-0.8873
20	-0.5358	-0.5367	-0.5361	-0.5403	-0.3885	-0.6131	-0.5853	-0.5675

TABLE C-IIa. Mean Velocity and Angle Measurements.

	Station No. 1 Re = 87,100 U_m = 1.22 m/s $\upsilon = 1.394 \times 10^{-6} m^2/s$			Station No. 2 Re = 85,500 U_m = 1.18 m/s $\upsilon = 1.386 \times 10^{-6} m^2/s$			Station No. 3 Re = 84,400 U_m = 1.17 m/s $\upsilon = 1.386 \times 10^{-6} m^2/s$		
y/H	U/U_m	V/U_m	Angle Deg	U/U_m	V/U_m	Angle Deg	U/U_m	V/U_m	Angle Deg
0.0050	0.7951	-		0.7061	-	-	0.7671	-	
0.0127	0.8396	-		0.7493	-0.1410	-10.60	0.7962	0.0660	4.70
0.0254	0.8991	0.0288	1.84	0.7914	-0.1200	-8.54	0.8238	-0.0369	-2.51
0.0635	0.9556	-0.0009	-0.05	0.8882	0.0034	0.24	0.9126	-0.0145	-0.88
0.1270	1.0130	0.0132	0.76	0.9615	0.0279	1.62	0.9900	0.0283	1.60
0.2540	1.0190	0.0138	0.73	1.0080	0.0322	1.79	1.0600	0.0223	1.19
0.3810	1.0230	0.0101	0.53	1.0340	0.0195	1.04	1.0720	0.0120	0.63
0.5000	1.0250	0.0266	1.40	1.0420	0.0238	1.25	1.0680	0.0198	1.01
0.6350	1.0310	0.0256	1.35	1.0490	0.0119	0.62	1.0640	0.0145	0.78
0.7620	1.0250	0.0299	1.58	1.0480	0.0178	0.90	1.0270	0.0206	1.11
0.8890	1.0130	0.0206	1.14	0.9817	0.0279	1.49	0.9435	0.0249	1.47
0.9530	0.9266	0.0314	1.91	0.9520	0.0161	0.98	0.8604	0.0120	0.76
0.9910	0.8364	0.0288	1.96	0.8727	0.0500	3.22	0.7826	0.0283	2.07
0.9980	0.7996			0.7802			0.6059		
# Corr.	(Near Wall)								
0.0050	0.6575			0.5837			0.6346		
0.0125	0.7562			0.6744			0.7158		
0.0254	0.8627			0.7589			0.7906		
0.0635	0.9529			0.8860			0.9103		
0.9110	0.7264			0.7578			0.6795		
0.9980	0.6332			0.6181			0.4797		

	Station No.4 Re = 87,400 U_m = 1.24m/s $\upsilon = 1.386 \times 10^{-6} m^2/s$			Station No. 5 Re = 89,700 U_m = 1.24m/s $\upsilon = 1.386 \times 10^{-6} m^2/s$		
y/H	U/U_m	V/U_m	Angle Deg	U/U_m	V/U_m	Angle Deg
0.0050	1.2160	-	-	1.6830	0.0285	0.98
0.0127	1.2300	0.0145	0.68	1.6790	0.0269	0.95
0.0254	1.2130	-0.1010	-4.75	1.5710	0.0095	0.34
0.0635	1.2150	-0.1540	-7.15	1.4680	-0.0167	-0.63
0.1270	1.1900	-0.1860	-8.73	1.2610	-0.0071	-0.27
0.2540	1.1150	-0.2250	-11.10	1.1120	0.0079	0.39
0.3810	1.0520	-0.2190	-11.60	0.9919	0.0071	1.38
0.5000	0.9919	-0.2040	-11.40	0.8367	0.0261	1.75
0.6350	0.9154	-0.1670	-10.10	0.7025	0.1180	9.51
0.7620	0.8095	-0.1220	-8.11	0.5113	0.0600	6.16
0.8890	0.6856	-0.0370	-3.15	0.4760	0.0490	5.98
0.9530	0.5214	-0.0510	-5.50	0.4466		
0.9910						
0.9980						
# Corr.	(Near Wall)					
0.0050	1.0060			1.6810		
0.0125	1.2300			1.6120		
0.0254	1.1650			1.5670		
0.0635	1.2120			0.3878		
0.9110						
0.9980						

TABLE C-IIa. (Concluded). Mean Velocity and Angle Measurements.

	Station No. 6 Re = 85,300 U_m = 1.18m/s $\upsilon = 1.386 \times 10^{-6} m^2/s$			Station No. 7 Re = 82,100 U_m = 1.14m/s $\upsilon = 1.380 \times 10^{-6} m^2/s$			Station No. 8 Re = 81,900 U_m = 1.13m/s $\upsilon = 1.380 \times 10^{-6} m^2/s$		
y/H	U/U_m	V/U_m	Angle Deg	U/U_m	V/U_m	Angle Deg	U/U_m	V/U_m	Angle Deg
0.0051				1.1310			0.5739		
0.0127	1.5670			1.4740	0.0820	3.16	0.5986		
0.0254	1.8890	-0.0340	-1.03	0.1540	0.0290	1.07	0.8141	0.113	8.24
0.0635	1.8340	0.0080	0.24	1.5240	0.0274	0.88	1.0090	0.269	13.90
0.1270	1.7260	-0.0140	-0.44	1.4370	0.0550	2.13	1.1700	0.371	17.20
0.2540	1.4790	-0.0120	-0.47	1.2500	0.0820	3.67	1.1420	0.342	16.20
0.3810	1.2850	0.0470	2.07	1.0805	0.0890	4.60	1.0620	0.332	17.10
0.5000	1.1270	0.0540	2.69	0.9561	0.1120	6.47	0.9912	0.277	15.10
0.6350	0.9544	0.1220	6.82	0.8404	0.0760	4.98	0.9450	0.208	12.20
0.7620	0.8435	0.1660	10.70	0.7611	0.0990	7.38	0.9030	0.144	7.36
0.8890	0.7387	0.0520	3.63	0.6479	0.0440	3.66	0.8680	0.048	3.08
0.9530	0.7251	0.3120	21.60	0.0632	0.0110	0.92	0.8534	0.070	4.62
0.9910	.7156			0.6066			0.8222		
# Corr.	(Near Wall)						Separation		
								% Rev.	
0.0050				0.9351			-0.064	78	
0.1270	1.5660			1.3260			-0.075	75	
0.0254	1.8174			1.4790			0.106	19	
0.0635	1.8290			1.5200			0.459	6	
0.1270									
0.9850	0.5128								
0.9910				0.5259					

	Station No. 9 Re = 94,100 U_m = 1.30m/s $\upsilon = 1.382 \times 10^{-6} m^2/s$			Station No. 10 Re = 92,800 U_m = 1.28m/s $\upsilon = 1.380 \times 10^{-6} m^2/s$			Station No. 11 Re = 92,000 U_m = 1.27m/s $\upsilon = 1.380 \times 10^{-6} m^2/s$		
y/H	U/U_m	V/U_m	Angle Deg	U/U_m	V/U_m	Angle Deg	U/U_m	V/U_m	Angle Deg
0.0051	0.4190			0.5203			0.7174		
0.0127	0.3857			0.5108		54.80	0.7145	0.289	21.60
0.0254	0.3755	-0.136	-17.50	0.5457	-0.223	-20.10	0.7460	-0.130	-9.69
0.0635	0.4790	-0.893	-7.92	0.6685	-0.010	-0.77	0.7894	1.090	7.44
0.1270	0.7849	-0.028	-1.93	0.7597	-0.097	-6.43	0.8182	-0.025	-1.69
0.2540	1.0900	0.060	3.06	0.9662	-0.055	-3.19	0.8756	-0.002	-0.10
0.3810	1.1140	0.079	4.02	1.0570	-0.008	-0.44	0.9331	0.012	0.68
0.5000	1.0690	0.078	4.11	1.0860	0.001	0.05	1.0000	-0.013	-0.70
0.6350	1.1090	0.097	4.85	1.0830	-0.004	-0.24	1.0250	0.004	0.23
0.7620	1.0870	0.014	0.70	1.0820	0.004	0.22	1.0340	0.013	0.68
0.8890	1.0920	-0.004	-0.27	1.0850	-0.012	-0.58	1.0390	0.007	0.38
0.9530	1.1130	-0.042	-2.15	1.0600	0.004	0.25	1.0170	0.036	2.02
0.9910	1.0530			*.9779			0.8905		
		% Rev.			% Rev.		(Near Wall)		
0.0050	0.1150	97		-0.0520	85		0.5930		
0.1270	0.1300	88		-0.0240	61		0.6400		
0.0254	0.0840	76		0.0580	9		0.7160		
0.0635	0.0490	65		0.3640	3		0.7870		
0.1270		9		0.4770	2				
0.9850	0.8270								
0.9910									

*y/H = .98

TABLE C-IIb. Mean and Turbulent Velocity Distributions Around the Duct. Smooth Inlet; Dense Screen at Exit.

113 H upstream of the turn

	Re = 74,700 U_∞ = 1.161 m/sec T = 4.4 °C ν = 1.55 x 10-6m^2/sec					Re = 171,000 U_∞ = 2.654 m/sec T = 4.4 °C ν = 1.55 x 10-6m^2/sec				
y/H	U/U_m	Angle Deg	$\sqrt{u^2}/U_m$	$\sqrt{v^2}/U_m$	$\overline{UV}/U_m^2$	U/U_m	Angle Deg	$\sqrt{u^2}/U_m$	$\sqrt{v^2}/U_m$	$\overline{UV}/U_m^2$
0.013	0.8805	-	0.0527	-	-	-	-	-	-	-
0.030	0.9567	-	0.0493	-	-	1.0080	-	0.0161	-	-
0.041	0.9911	-	0.0389	-	-	1.0150	-	0.0182	-	-
0.051	1.0040	-	0.0360	-	-	1.0210	-3.5	0.0168	0.0255	-0.000058
0.076	1.0200	-0.2	0.0297	0.0353	-0.00011	1.0180	-0.6	0.0179	0.0188	-0.000024
0.102	1.0270	-0.3	0.0284	0.0284	-0.00004	1.0160	0.2	0.0173	0.0205	-0.000057
0.152	1.0320	0.4	0.0269	0.0292	-0.00006	1.0210	0.3	0.0158	0.0194	-0.000062
0.203	1.0390	0.1	0.0262	0.0303	-0.00005	1.0230	0.8	0.0155	0.0191	-0.000051
0.305	1.0440	0.1	0.0258	0.0261	-0.00001	1.0270	0.2	0.0137	0.0184	-0.000029
0.381	1.0470	0.8	0.0244	0.0259	-0.00001	1.0290	0.3	0.0132	0.0180	-0.000010
0.500	1.0510	0.1	0.0268	0.0246	-0.00001	1.0300	-0.2	0.0133	0.0171	0.000005
0.500	1.0450	-	0.0234	-	-	1.0250	-	0.0138	-	-
0.619	1.0450	0.7	0.0227	0.0251	0.00003	1.0270	0.6	0.0143	0.0183	0.000015
0.695	1.0400	0.8	0.0237	0.0239	0.00001	1.0220	0.6	0.0147	0.0184	0.000013
0.797	1.0350	0.9	0.0264	0.0273	0.00006	1.0180	0.8	0.0181	0.0209	0.000029
0.848	1.0340	1.0	0.0308	0.0363	0.00012	1.0130	1.2	0.0213	0.0259	0.000094
0.898	1.0100	1.1	0.0423	0.0446	0.00024	-	-	-	-	-
0.924	0.9782	1.4	0.0556	0.0591	0.00048	0.9810	1.3	0.0386	0.0378	0.000500
0.949	0.9530	-	0.0598	-	-	0.9595	-	0.0449	-	-
0.959	0.9144	-	0.0766	-	-	0.9433	-	0.0497	-	-
0.970	0.9005	-	0.0722	-	-	0.9309	-	0.0511	-	-
0.987	0.8411	-	0.0814	-	-	0.8960	-	0.0560	-	-
0.992	0.8285	-	0.0814	-	-	-	-		-	-

1.52 ahead of the turn

	Re = 79,400 U_∞ = 1.261 m/sec T = 3.6 °C ν = 1.59 x 10-6m^2/sec					Re = 147,000 U_∞ = 2.343 m/sec T = 3.3 °C ν = 1.59 x 10-6m^2/sec				
y/H	U/U_m	Angle Deg	$\sqrt{u^2}/U_m$	$\sqrt{v^2}/U_m$	$\overline{UV}/U_m^2$	U/U_m	Angle Deg	$\sqrt{u^2}/U_m$	$\sqrt{v^2}/U_m$	$\overline{UV}/U_m^2$
0.008	0.8187		0.0642							
0.010						0.8433		0.0471		
0.013	0.8487		0.0627			0.8509		0.0503		
0.030	0.8758		0.0635			0.8877		0.0530		
0.041	0.9014		0.0642			0.9014		0.0534		
0.051	0.9207		0.0616			0.9154		0.0531		
0.076	0.9596		0.0572			0.9591		0.0483		
0.102	0.9918	1.3	0.0531	0.0894	-0.000350	0.9827	-0.2	0.0439	0.0407	-0.000267
0.152	1.0250	2.1	0.0443	0.0159	-0.000050	1.0150	2.3	0.0382		
0.203	1.0530	0.1	0.0342	0.0255	-0.000093	1.0320	0.7	0.0241	0.0204	-0.000110
0.305	1.0710	0.4	0.0251	0.0518	0.00103C	1.0420	-0.3	0.0160	0.0165	-0.000032
0.381	1.0760	0.1	0.0203	0.0233	0.000020	1.0450	0.4	0.0150	0.0170	-0.000020
0.500	1.0790	0.3	0.0193	0.0238	-0.000050	1.0410		0.0151		
0.500	1.0830		0.0217			1.0450	2.5	0.0127	0.0147	0.000020
0.619	1.0620		0.0269			1.0330	2.5	0.0145	0.0149	0.000047
0.695	1.0430		0.0368			1.0210	2.1	0.0248	0.0156	0.000225
0.797	0.9973		0.0485			0.9910	2.3	0.0422	0.0163	0.000560
0.846	0.9628		0.0562			0.9625	2.7	0.0494	0.0256	0.000574
0.898	0.9127		0.0631			0.9070	0.9	0.0575	0.0045	0.000464
0.924	0.8685		0.0664			0.8782		0.0571		
0.949	0.8257		0.0708			0.8475		0.0582		
0.956	0.8073		0.0687			0.8233		0.0597		
0.970	0.7824		0.0699			0.7964		0.0611		
0.987	0.6848		0.0724			0.7214		0.0578		
0.992	0.6510		0.0758			0.6911		0.0580		

TABLE C-IIb. (Continued.) Mean and Turbulent Velocity Distributions Around the Duct. Smooth Inlet; Dense Screen at Exit.

Start of the turn

	Re = 73,200 U_∞ = 1.163 m/sec T = 3.4 °C ν = 1.59 x $10^{-6}m^2$/sec					Re = 142,000 U_∞ = 2.257 m/sec T = 3.2 °C ν = 1.59 x $10^{-6}m^2$/sec				
y/H	U/U_m	Angle Deg	$\sqrt{u^2}/U_m$	$\sqrt{v^2}/U_m$	$\overline{uv}/U_m^2$	U/U_m	Angle Deg	$\sqrt{u^2}/U_m$	$\sqrt{v^2}/U_m$	$\overline{uv}/U_m^2$
0.008						1.3370		0.0411	-	-
0.013	1.3460		0.0436			1.3340		0.0424		
0.030	1.3500		0.0414			1.3340		0.0425		
0.041	1.3490		0.0402			1.3290		0.0402		
0.051	1.3520		0.0412			1.3280		0.0389		
0.076	1.3380		0.0386			1.3230		0.0339		
0.102	1.3240	-10.1	0.0376	0.0262	-0.000230	1.3070	-10.0	0.0314	0.0307	-0.000219
0.152	1.2960	-10.5	0.0318	0.0261	-0.000210	1.2640	-10.1	0.0186	0.0158	-0.000062
0.203	1.2500	-11.8	0.0256	0.0233	-0.000069	1.2150	-11.0	0.0193	0.0161	-0.000020
0.305	1.1890	-12.2	0.0176	0.0180	-0.000040	1.1470	-12.1	0.0163	0.0172	0.000026
0.381	1.1360	-12.7	0.0178	0.0159	-0.000007	1.0960	-12.3	0.0159	0.0178	0.000036
0.500	1.0590	-12.5	0.0201	0.0190	0.000040	1.0220	-12.0	0.0226	0.0213	0.000095
0.500	1.0580		0.0312			0.9783	-12.0	0.0210	0.0193	0.000053
0.619	0.9767	-9.7	0.0384	0.0294	0.000280	0.9079	-11.6	0.0312	0.0215	0.000093
0.695	0.9232	-8.6	0.0486	0.0317	0.000420	0.8728	-9.0	0.0438	0.0243	0.000170
0.797	0.8449	-6.2	0.0614	0.0341	0.000640	0.8412	-7.3	0.0601	0.0151	0.000476
0.846	0.7679	-3.6	0.0723	0.0413	0.000961	0.7873	-4.6	0.0644	0.0329	0.000467
0.898	0.7029	-3.8	0.0781	0.0573	0.000320	0.7146	-3.5	0.0740	0.0351	0.000591
0.924	0.6471		0.0824			0.6744		0.0790		
0.949	0.5614		0.0908			0.5993		0.0838		
0.956	0.5082		0.0981			0.5702		0.0863		
0.970						0.4754		0.0793		
0.985						0.2726		0.0337		

10 degrees around the turn

	Re = 81,400 U_∞ = 1.293 m/sec T = 3.6 °C ν = 1.59 x $10^{-6}m^2$/sec					Re = 109,000 U_∞ = 1.735 m/sec T = 3.4 °C ν = 1.59 x $10^{-6}m^2$/sec					Re = 134,000 U_∞ = 2.134 m/sec T = 3.3 °C ν = 1.59 x 10-6m^2/sec				
y/H	U/U_m	Angle Deg	$\sqrt{u^2}/U_m$	$\sqrt{v^2}/U_m$	$\overline{uv}/U_m^2$	U/U_m	Angle Deg	$\sqrt{u^2}/U_m$	$\sqrt{v^2}/U_m$	$\overline{uv}/U_m^2$	U/U_m	Angle Deg	$\sqrt{u^2}/U_m$	$\sqrt{v^2}/U_m$	$\overline{uv}/U_m^2$
0.005	1.4670	-	0.0446	-	-	-	-	-	-	-					
0.008	-	-		-	-	-	-	-	-	-	1.4690		0.0311		
0.010	1.4750	-	0.0444	-	-	1.4340	-	0.0359	-	-	-		-		
0.013	1.4760	-	0.0431	-	-	1.4290	-	0.0368	-	-	1.4620		0.0329		
0.030	1.4730	-4.9	0.0435	0.0442	-0.000095	1.4250	-	0.0377	-	-	1.4590		0.0350		
0.041	1.4670	-5.6	0.0410	0.0198	-0.000440	1.4290	-2.2	0.0372	0.0448	0.000020	1.4560	-4.3	0.0343	0.0193	0.000020
0.051	1.4580	-4.8	0.0394	0.0363	-0.000100	1.4200	-3.1	0.0367	0.0324	-0.000100	1.4510	-4.7	0.0336	0.0123	-0.000035
0.076	1.4310	-6.6	0.0376	0.0379	-0.000089	1.4020	-3.8	0.0342	0.0103	0.000030	1.4280	-5.6	0.0311	0.0216	-0.000022
0.102	1.3990	-6.9	0.0351	0.0271	-0.000130	1.3810	-4.4	0.0305	0.0177	-0.000052	1.3950	-5.7	0.0267	0.0224	-0.000020
0.152	1.3370	-7.8	0.0270	0.0265	-0.000083	1.3290	-4.7	0.0244	0.0196	-0.000030	1.3330	-6.6	0.0221	0.0152	-0.000010
0.203	1.2750	-9.1	0.0248	0.0219	-0.000010	1.2700	-5.4	0.0219	0.0177	0.000009	1.2740	-7.7	0.0179	0.0182	0.000006
0.305	1.1730	-8.3	0.0208	0.0240	0.000010	1.1760	-6.4	0.0173	0.0204	0.000034	1.1660	-7.8	0.0168	0.0168	0.000035
0.381	1.1190	-9.6	0.0223	0.0246	0.000072	1.1100	-6.3	0.0183	0.0231	0.000068	1.1060	-7.9	0.0215	0.0125	0.000073
0.500	1.0140	-7.8	0.0306	0.0233	0.000180	1.0220	-6.2	0.0250	0.0298	0.000240	1.0010	-6.1	0.0265	0.0188	0.000200
0.500	1.0270	-8.4	0.0278	0.0284	0.000190	1.0030		0.0261	-						
0.615	0.9205	-6.5	0.0423	0.0336	0.000606	0.9122	-5.8	0.0366	0.0281	0.000404	0.9169	-5.6	0.0396	0.0228	0.000465
0.695	0.8637	-4.6	0.0511	0.0305	0.000617	0.8488	-4.4	0.0498	0.0268	0.000651	0.8629	-4.6	0.0474	0.0303	0.000663
0.797	0.7590	-2.9	0.0723	-	-	0.7599	-2.3	0.0612	0.0348	0.001080	0.7570	-1.7	0.0625	0.0299	0.000952
0.846	0.6784	0.4	0.0811	0.0397	0.001400	0.7140	-0.8	0.0656	0.0435	0.001270	0.7057	0.1	0.0691	0.0831	0.001350
0.898	0.6048		0.0913			0.6396	2.0	0.0757	0.0563	0.001200	0.6230	3.3	0.0807	0.0535	0.000830
0.924	0.5567		0.0996			0.5941	3.9	0.0861	0.0512	0.001190	0.5733		0.0881		
0.949	0.4791		0.1037			0.5117		0.0964			0.4717		0.0891		
0.956	0.4374		0.1043			0.4811		0.1004							
0.970	0.4027		0.1028			0.4611		0.1022							
0.987	0.3233		0.0863			0.3882		0.0986							
0.990	0.3188		0.0778			0.3870		0.0908							

Data in dashed boxes corrected for near wall effect; Table C-IIc.

TABLE C-IIb. (Continued.) Mean and Turbulent Velocity Distributions Around the Duct. Smooth Inlet; Dense Screen at Exit.

45 degrees around the turn

	Re = 87,600 U_∞ = 1.391 m/sec T = 3.3 °C ν = 1.59 x 10^{-6} m^2/sec					Re = 154,000 U_∞ = 2.441 m/sec T = 3.3 °C ν = 1.59 x 10^{-6} m^2/sec				
y/H	U/U_m	Angle Deg	$\sqrt{u^2}/U_m$	$\sqrt{v^2}/U_m$	$\overline{uv}/U_m^2$	U/U_m	Angle Deg	$\sqrt{u^2}/U_m$	$\sqrt{v^2}/U_m$	$\overline{uv}/U_m^2$
0.013	1.6120		0.0371							
0.030	1.6120		0.0356							
0.041	1.6040	-2.3	0.0338	0.0389	0.000020					
0.051	1.5900	-3.3	0.0349	0.0317	0.000091					
0.102	1.5520	-0.9	0.0311	0.0332	0.000120	1.5220	-2.7	0.0278	0.0216	0.000130
0.152	1.4490	-2.7	0.0241	0.0239	0.000030					
0.203	1.3640	-2.6	0.0218	0.0251	0.000072	1.3300	-0.6	0.0172	0.0189	0.000078
0.305	1.2010	-3.4	0.0208	0.0250	0.000062					
0.381	1.0990	-1.9	0.0236	0.0297	0.000180	1.0740	-1.0	0.0184	0.0264	0.000217
0.500	0.9656		0.0352							
0.500	0.9373	1.4	0.0384	0.0324	0.000470	0.9514	0.7	0.0265	0.0327	0.000438
0.615	0.8142	2.9	0.0538	0.0482	0.001280	0.8376	4.0	0.0462	0.0375	0.001120
0.695	0.7791	5.8	0.0527	0.0495	0.001210	0.7992	6.2	0.0243	0.0661	0.001280
0.797	0.6835	8.6	0.0767	0.1038	0.005951	0.7182	8.9	0.0506	0.0566	
0.846	0.6206	8.3	0.0822	0.0650	0.003260	0.6789	8.7	0.0547		
0.898	0.5882	9.4	0.1032	0.0703	0.005446	0.6090	14.1	0.0593		
0.924	0.5534		0.1010			0.5956	15.6	0.0618	0.0880	
0.949	0.5104		0.1014			0.5391	14.5	0.0710	0.0844	0.001250
0.956	0.5032		0.0940			0.5198		0.0797		
0.970	0.4874		0.0920			0.5016		0.0797		
0.987	0.4567		0.0947			0.4762		0.0797		
0.990						0.4687		0.0745		

90 degrees around the turn

	Re = 94,500 U_∞ = 1.501 m/sec T = 3.3 °C ν = 1.59 x 10^{-6} m^2/sec					Re = 138,000 U_∞ = 2.193 m/sec T = 3.3 °C ν = 1.59 x 10^{-6} m^2/sec					Re = 151,000 U_∞ = 2.404 m/sec T = 3.6 °C ν = 1.59 x 10^{-6} m^2/sec				
y/H	U/U_m	Angle Deg	$\sqrt{u^2}/U_m$	$\sqrt{v^2}/U_m$	$\overline{uv}/U_m^2$	U/U_m	Angle Deg	$\sqrt{u^2}/U_m$	$\sqrt{v^2}/U_m$	$\overline{uv}/U_m^2$	U/U_m	Angle Deg	$\sqrt{u^2}/U_m$	$\sqrt{v^2}/U_m$	$\overline{uv}/U_m^2$
0.100						1.6300		0.0304							
0.013	1.6730		0.0453								1.6310		0.0344		
0.030	1.6870		0.0424			1.6580		0.0351			1.6370		0.0364		
0.041	1.6680	-0.2	0.0456		0.000433	1.6480		0.0368			1.6310	-1.5	0.0320	0.0366	0.000178
0.051	1.6490	-1.5	0.0436	0.0221	0.000631	1.6270	0.1	0.0368			1.6290	0.0	0.0265	0.0400	0.000120
0.076						1.5900	-1.0	0.0333	0.0234	0.000241	1.5740	0.1	0.0321	0.0278	0.000196
0.102	1.5610	-0.8	0.0374	0.0279	0.000417	1.5390	-0.7	0.0310	0.0152	0.000309	1.5230	0.0	0.0332	0.0355	0.000439
0.152	1.4600	-1.2	0.0324	0.0320	0.000150	1.4400	-0.4	0.0247	0.0295	0.000255	1.4190	-1.0	0.0287	0.0332	0.000294
0.203	1.3550	-1.3	0.0331	0.0401	0.000160	1.3420	-0.6	0.0223	0.0306	0.000282	1.3210	-1.6	0.0292		
0.305	1.1790	-1.4	0.0462	0.0546	0.000380	1.1780	0.7	0.0281	0.0383	0.000100	1.1590	0.7	0.0282	0.0203	0.000458
0.381	1.0600	0.2	0.0735	0.0822	0.000421	1.0700	-0.1	0.0367	0.0504	-0.000120	1.0510	0.2	0.0458	0.0707	-0.000003
0.500	0.9068		0.0935			0.9388	2.4	0.0413	0.0658	0.000150	0.8848	1.3	0.0815	0.0913	-0.000230
0.500	0.9125	-1.2	0.0857	0.1393	0.003190	0.9242	3.4	0.0634	0.0727	0.000323	0.9237	3.4	0.0650	0.0758	-0.001210
0.615	0.8493	7.5	0.0831	0.1113	0.006690	0.8334	1.3	0.0702	0.1029	0.000435	0.8291	4.4	0.0727	0.1038	-0.000642
0.695	0.8034	2.7	0.0866	0.1391	0.002530	0.7887	2.8	0.0779	0.1029	0.000887	0.7936	3.4	0.0770	0.1073	-0.000490
0.797	0.6962	4.4	0.0849	0.1162	0.003360	0.6970	3.5	0.0863	0.0989	0.000641	0.7185	6.1	0.0805	0.0994	0.000730
0.846	0.6523	3.6	0.0884	0.1162	0.004210	0.6748	4.1	0.0784	0.1144	0.002740	0.6917	5.6	0.0747	0.0704	0.000026
0.898	0.5961	5.9	0.0776	0.1155	0.003950	0.6161	4.7	0.0787	0.0797	0.002420	0.6482	8.1	0.0772	0.0766	0.001800
0.924	0.5867	0.6	0.0748	0.1271	0.001720	0.6078	3.5	0.0804	0.0820	0.001790	0.6316		0.0754		
0.949	0.5625		0.0766			0.5926		0.0792			0.6212	4.0	0.0719	0.0385	0.001860
0.956	0.5652		0.0789			0.5900		0.0723			0.6070	2.7	0.0727	0.0623	0.002090
0.970	0.5520		0.0790			0.5839		0.0760			0.6042		0.0745		
0.987	0.5380		0.0845			0.5654		0.0754			0.5927		0.0737		

TABLE C-IIb. (Continued.) Mean and Turbulent Velocity Distributions Around the Duct. Smooth Inlet; Dense Screen at Exit.

135 degrees around the turn

	Re = 86,500 U_∞ = 1.374 m/sec T = 3.6 °C υ = 1.59 x 10^{-6} m^2/sec					Re = 161,000 U_∞ = 2.561 m/sec T = 3.6 °C υ = 1.59 x 10^{-6} m^2/sec				
y/H	U/U_m	Angle Deg	$\sqrt{u^2}/U_m$	$\sqrt{v^2}/U_m$	$\overline{UV}/U_m^2$	U/U_m	Angle Deg	$\sqrt{u^2}/U_m$	$\sqrt{v^2}/U_m$	$\overline{UV}/U_m^2$
0.015	1.4680		0.0734			1.4080		0.0512		
0.030	1.5690		0.0577			1.4270		0.0513		
0.041	1.5480		0.0561			1.4390	-1.0	0.0452	0.0469	-0.000930
0.051	1.5420	0.7	0.0576		0.000522	1.4460	0.7	0.0432	0.0338	-0.000614
0.076	1.5190	0.4	0.0523	0.0372	0.000556	1.4210	0.8	0.0384	0.0259	-0.000098
0.102	1.4940	0.8	0.0515	0.0547	0.000260	1.3640	5.0	0.0316	0.0510	-0.000085
0.152	1.4100	0.1	0.0503	0.0850	-0.000905	1.3030	3.5	0.0320	0.0551	-0.000047
0.203	1.3420	1.1	0.0648	0.0838	-0.000728	1.1770	3.4	0.0376	0.0743	-0.001010
0.305	1.1420	1.7	0.0858	0.1268	0.001250	1.0870	2.9	0.0410	0.0594	-0.000389
0.381	1.0240	1.8	0.0952	0.1416	0.000630	0.9693		0.0537		
0.500	0.9095	-3.4	1.0420	0.1662	0.003970					
0.500	0.8869	-6.7	0.0964	0.1743	0.006140	0.9534	3.0	0.0637	0.1082	-0.000847
0.615	0.8358	-5.8	1.0330	0.1539	0.004530	0.8469	2.6	0.0773	0.0755	0.000068
0.695	0.8174	-5.6	0.0964	0.1431	0.004420	0.8081	1.8	0.0707	0.0931	0.000769
0.797	0.7331	-3.8	0.0895	0.1297	0.004350	0.7950	1.9	0.0806	0.0995	0.000440
0.846	0.7114	-3.1	0.0793	0.1153	0.002720	0.7189	2.8	0.0730	0.0927	0.000096
0.898	0.6945	-0.2	0.0780	0.1052	0.001910	0.6900	0.2	0.0697	0.0979	0.001560
0.924	0.6655	-0.1	0.0780	0.0908	0.001470	0.6779	2.6	0.0614	0.0718	-0.000154
0.946	0.6504		0.0787			0.6741		0.0694		
0.956	0.6486		0.0719			0.6615		0.0659		
0.970	0.6411		0.0648			0.6686		0.0618		
0.987	0.6178		0.0711			0.6541		0.0465		

180 degrees around the turn

	Re = 83,100 U_∞ = 1.272 m/sec T = 4.7 °C υ = 1.531 x 10^{-6} m^2/sec					Re = 99,700 U_∞ = 1.582 m/sec T = 3.6 °C υ = 1.589 x 10^{-6} m^2/sec					Re = 181,000 U_∞ = 2.871 m/sec T = 3.7 °C υ = 1.589 x 10^{-6} m^2/sec				
y/H	U/U_m	Angle Deg	$\sqrt{u^2}/U_m$	$\sqrt{v^2}/U_m$	$\overline{UV}/U_m^2$	U/U_m	Angle Deg	$\sqrt{u^2}/U_m$	$\sqrt{v^2}/U_m$	$\overline{UV}/U_m^2$	U/U_m	Angle Deg	$\sqrt{u^2}/U_m$	$\sqrt{v^2}/U_m$	$\overline{UV}/U_m^2$
0.005	0.5111		0.0693												
0.013	0.5895		0.0481												
0.030	0.9013		0.1538												
0.041	0.9746	10.8	0.1471	0.1062	-0.003280	0.9694		0.0228			1.1410		0.0471		
0.051	1.0450	12.0	0.1322		0.004500	1.0570		0.0767			1.1770		0.0620		
0.076	1.1820	11.9	0.1010	0.0871	0.001380	1.1150		0.0817			1.1580		0.0554		
0.102	1.2280	16.0	0.0842	0.0562	0.000017	1.1970	14.0	0.0759		0.004480	1.1680		0.0497		
0.152	1.2310	13.4	0.0615	0.1117	0.001090	1.2170	12.2	0.0862	0.0418	0.002130	1.1920	17.3	0.0695	0.0511	-0.000860
0.203	1.1810	10.5	0.0700	0.1360	-0.000540	1.2550	13.7	0.0878	0.0717	0.001570	1.2120	20.3	0.0679	0.0446	0.002510
0.305	1.0960	9.0	0.0840	0.1522	-0.003340	1.1770	11.6	0.0703	0.1221	-0.000650	1.2020	19.5	0.0510	0.0424	0.001460
0.381	1.0460	5.6	0.0880	0.1743	-0.000670	1.1060	7.4	0.0705	0.1333	-0.001420	1.1260	9.6	0.0526	0.0708	0.000180
0.500	0.9902	0.6	0.0923	0.1833	0.001380	1.0630	4.0	0.0628	0.1426	-0.001210	1.0550	5.3	0.0564	0.0727	0.000970
0.500						1.0290	0.6	0.0796	0.1286	0.000670	1.0280	0.9	0.0581	0.0852	0.000690
0.615	0.9578	-2.4	0.0889	0.1647	0.003370	0.9996	0.9	0.0842	0.1605	0.001820					
0.695	0.9418	-3.4	0.0879	0.1470	0.002350	0.9936	-2.6	0.0924	0.1360	0.002720	0.9879	-9.5	0.0339	0.0216	-0.000320
0.797	0.9147	-2.5	0.0806	0.1301	0.002750	0.9672	-4.0	0.0753	0.1316	0.004010	0.9631		0.0610		
0.846	0.8934	-1.9	0.0779	0.1177	0.002520	0.9507	-2.5	0.0729	0.1260	0.002570	0.9297		0.0442		
0.898	0.8754	-1.3	0.0705	0.0916	0.001380	0.9189	-0.5	0.0724	0.1058	0.001170	0.8990		0.0507		
0.924	0.8601	-0.2	0.0676	0.0882	0.001140	0.9012	-1.0	0.0712	0.0978	0.001900	0.8795		0.0288		
0.949	0.8495	-0.9	0.0672	0.0668	0.000830	0.8900	-0.8	0.0605	0.3930	0.000810	0.8500		0.0222		
0.956	0.8435		0.0655			0.8790		0.0519							
0.970	0.8358		0.0674			0.8746		0.0426							
0.987	0.8004		0.0689			0.8618		0.0393							
						0.8447		0.0356							

Data in solid boxes in separation region, questionable measurements.

TABLE C-IIb. (Continued.) Mean and Turbulent Velocity Distributions Around the Duct. Smooth Inlet; Dense Screen at Exit.

0.508 H downstream of the turn

	Re = 79,100 U_∞ = 1.177 m/sec T = 5.8 °C υ = 1.482 x $10^{-6}m^2$/sec					Re = 170,000 U_∞ = 2.534 m/sec T = 5.6 °C υ = 1.482 x $10^{-6}m^2$/sec				
y/H	U/U_m	Angle Deg	$\sqrt{u^2}/U_m$	$\sqrt{v^2}/U_m$	$\overline{uv}/U_m^2$	U/U_m	Angle Deg	$\sqrt{u^2}/U_m$	$\sqrt{v^2}/U_m$	$\overline{uv}/U_m^2$
0.030										
0.041						0.7359		0.0402		
0.051	0.4081	-26.2	0.1569		-0.003130	0.7551		0.0574		
0.076	0.6178	-23.9	0.1761		0.000450	0.7534	-1.7	0.0786		
0.102	0.7771	-4.2	0.1844	0.0386	-0.006380	0.9681	-9.5			0.000240
0.152	0.9972	-2.4	0.1572	0.1183	0.001480	1.0340	-3.5	0.0647	0.0747	0.000610
0.203	1.1370	2.3	0.1186	0.1099	0.000440	1.0660	-2.8	0.0852	0.0688	-0.000530
0.305	1.1460	7.3	0.0909	0.1292	0.001140	1.1390	1.7	0.0845	0.0897	-0.000220
0.381	1.1240	5.2	0.0823	0.1506	0.000350	1.1090	3.0	0.0778	0.0768	-0.000100
0.500	1.0980	4.4	0.0868	0.1828	-0.001170	1.0530	0.8	0.0691	0.0601	-0.000480
						1.0170	0.2	0.0639	0.0795	-0.001090
0.615	1.0810	0.2	0.0809	0.1828	0.000980					
0.695	1.0530	0.5	0.0905	0.1741	0.000800	0.9969	0.1	0.0631	0.0859	-0.001360
0.797	1.0540	1.1	0.0901	0.1564	0.001060	0.9906	-0.1	0.0641	0.0982	-0.000190
0.846	1.0430	-0.1	0.0761	0.1457	0.002090	0.9870	-0.3	0.0754	0.0832	0.000460
0.898	1.0380	8.3	0.0704	0.1129	-0.000150	0.9699	0.0	0.0679	0.0884	0.001120
0.924	1.0410	0.0	0.0696	0.1140	0.001160	0.9719	-0.6	0.0663	0.0824	0.000810
0.949	1.0440	-1.0	0.0725		0.000970	0.9601	-1.1	0.0579	0.0816	0.001010
0.956	1.0530		0.0677			0.9580	2.2	0.0584		0.000700
0.970	1.0710		0.0779			0.9521		0.0500		
0.982	1.0410		0.0749			0.9598		0.0503		
						0.9570		0.0414		

1.52 H downstream of the turn

	Re = 81,100 U_∞ = 1.205 m/sec T = 5.8 °C υ = 1.482 x $10^{-6}m^2$/sec					Re = 163,000 U_∞ = T = 5.8 °C υ = 1.482 x $10^{-6}m^2$/sec				
y/H	U/U_m	Angle Deg	$\sqrt{u^2}/U_m$	$\sqrt{v^2}/U_m$	$\overline{uv}/U_m^2$	U/U_m	Angle Deg	$\sqrt{u^2}/U_m$	$\sqrt{v^2}/U_m$	$\overline{uv}/U_m^2$
0.005	*0.4631		0.0750			0.8249		0.0306		
0.013	0.5701		0.1526			0.8243		0.0630		
0.030	0.6477		0.1609			0.7913		0.0794		
0.041	0.6373		0.1661			0.8415		0.0827		
0.051	0.6578	-15.2	0.1662	0.1968	-0.001960	0.8374	-2.4	0.0926	0.0509	-0.000370
0.076	0.8121	-8.2	0.1572		0.003190	0.8994	-4.4	0.0792		0.001640
0.102	0.8890	-7.8	0.1500	0.1643	-0.001230	0.9516	-5.2	0.0905	0.0946	0.001140
0.152	0.9031	-4.7	0.1572	0.0994	-0.002550	0.9775	-2.5	0.0885	0.0823	-0.000180
0.203	0.9813	-3.2	0.1448	0.1108	-0.001540	1.0070	-3.5	0.0881	0.0890	0.000350
0.305	1.0580	-0.9	0.1144	0.1238	-0.000250	1.0240	-0.9	0.0900	0.0942	-0.000400
0.381	1.0510	-0.7	0.1093	0.1309	-0.000410	1.0250	-1.4	0.0857	0.1006	-0.000320
0.500	1.0610	0.6	0.1051	0.1375	-0.000090	1.0420	-1.3	0.0850	0.0960	-0.000840
0.500	1.0760	0.6	0.0990	0.1418	-0.001920					
0.615	1.0730	1.0	0.0914	0.1471	-0.000840	1.0400	-2.5	0.0876	0.0953	0.000570
0.695	1.0750	0.7	0.0841	0.1301	-0.000430	1.0350	-0.3	0.0811	0.1094	-0.000010
0.797	1.0760	1.4	0.0762	0.1197	0.000480	1.0540	-0.8	0.0651	0.1044	0.000300
0.846	1.0710	1.0	0.0785	0.1088	0.000360	1.0400	-0.3	0.0665	0.0951	0.001090
0.898	1.0600	1.8	0.0739	0.0968	0.000350	1.0250	0.9	0.0657	0.0851	0.000160
0.924	1.0580	3.4	0.0758		0.000910	1.0170	1.9	0.0657	0.0246	0.001780
0.949	1.0520		0.0794			1.0100	-0.1	0.0661	0.0830	-0.000890
0.956	1.0450		0.0813			1.0080		0.0694		
0.970	1.0060		0.0995			1.0040		0.0695		
0.987						0.9847		0.0662		

*y/H = .008

TABLE C-IIb. (Concluded.) Mean and Turbulent Velocity Distributions Around the Duct. Smooth Inlet; Dense Screen at Exit.

3.05 H downstream of the turn

	Re = 82,200 U_m = 1.235 m/sec T = 6.7 °C υ = 1.454 x 10^{-6} m^2/sec						Re = 169,000 U_m = 2.590 m/sec T = 6.0 °C υ = 1.477 x 10^{-6} m^2/sec				
y/H	U/U_m	Angle Deg	$\sqrt{u^2}/U_m$	$\sqrt{v^2}/U_m$	$\overline{uv}/U_m^2$		y/H	U/U_m	Angle Deg	$\sqrt{u^2}/U_m$	$\sqrt{v^2}/U_m$	$\overline{uv}/U_m^2$
0.008	0.5970		0.1319				0.027	0.8391				
0.015	0.7029		0.1435				0.053	0.9190				
0.025	0.7480		0.1492				0.078	0.9375	-1.7	0.0781		
0.051	0.8196	-3.1	0.1447				0.129	0.9929	-0.9	0.0575	0.0559	-0.000100
0.076	0.8611	-0.3	0.1437	0.0920	-0.001000		0.180	0.9863	-1.5	0.0783	0.0482	-0.000860
0.127	0.8907	-0.1	0.1454	0.1006	-0.001920		0.282	1.0090	-2.2	0.0736	0.0926	0.000010
0.178	0.9186	-0.3	0.1444	0.0875	-0.000800		0.358	1.0170	-2.4	0.0808	0.0572	-0.000660
0.279	0.9926	0.5	0.1386	0.1185	-0.001890		0.472	1.0050	-1.4	0.0739	0.0524	-0.000260
0.355	1.0070	2.1	0.1354	0.1272	-0.002420							
0.472	1.0030	3.3	0.1217	0.1149	-0.001550							
0.615	1.0650	3.6	0.1062	0.1289	-0.000210		0.615	1.0140	-0.7	0.0748	0.0663	-0.000050
0.695	1.0810	3.9	0.0958	0.1168	-0.001980		0.695	1.0260	-0.3	0.0813	0.0819	0.000370
0.797	1.0850	2.5	0.0872	0.1085	-0.000290		0.797	1.0150	1.3	0.0570	0.0663	0.000610
0.846	1.0910	3.4	0.0870	0.0990	0.000410		0.846	1.0160	1.0	0.0622	0.0688	-0.000120
0.898	1.1000	2.1	0.0818	0.0938	-0.000020		0.898	1.0160	1.3	0.0603	0.0636	-0.000150
0.924	1.1100	2.6	0.0830	0.0805	-0.000010		0.924	1.0210	2.0	0.0567	0.0361	-0.001410
0.949	1.0930		0.0858				0.949	1.0160	2.7	0.0602	0.0069	-0.000150
0.956	1.0980		0.0833				0.956	0.9951	2.4	0.0634	0.0474	0.000630
0.970	1.0850		0.0884				0.970	0.9967		0.0598		
0.987	1.0590		0.0905				0.987	0.9914		0.0638		
0.992	1.0090		0.1004				0.992	0.9741		0.0272		

TABLE C-IIc. Near Wall Velocity Corrections for the Measurements Reported in TABLE C-IIb.

	11.3 H up		1.52 H up		0 Degrees		10 Degrees		
Re =	74,000	171,000	79,400	147,000	73,200	142,000	81,400	109,000	134,000
y/H	U/U_m	U/U_m	U/U_m	U/U_m	U/U_m	U/U_m	U/U_m	U/U_m	U/U_m
0.005							1.212		
0.008			0.701			1.144			1.257
0.010				0.742			1.297	1.261	
0.013	0.793		0.764	0.766	1.210	1.201	1.328	1.286	1.315
0.030	0.930	0.976	0.851	0.863	1.312	1.297	1.431	1.386	1.419
0.041	0.977	1.001	0.890	0.890	1.331	1.312	1.448	1.411	1.442
0.051	0.998	1.014	0.914	0.909	1.344	1.320	1.418	1.411	1.442
0.992	0.709		0.556	0.592					
0.990	0.756	0.806					0.281	0.341	
0.987	0.874	0.905	0.616	0.649		0.250	0.290	0.350	
0.970	0.903	0.930	0.761	0.774		0.462	0.391	0.448	
0.959	0.948	0.953	0.798	0.812	0.500	0.563	0.432	0.474	
0.949			0.819	0.842	0.558	0.609	0.476	0.508	0.468

	45 Degrees		90 degrees			135 degrees		180 degrees		
Re =	87,600	145,000	94,500	138,000	151,000	86,500	161,000	83,100	99,700	181,000
y/H	U/U_m	U/U_m	U/U_m	U/U_m	U/U_m	U/U_m	U/U_m	U/U_m	U/U_m	U/U_m
0.010				1.432						
0.013	1.451		1.505		1.471	*1.346				
0.030	1.567		1.641	1.459	1.598					
0.041	1.582		1.647	1.626	1.610	1.548	1.392	Separation		
0.051	1.580		1.639	1.612	1.623	1.537	1.416			
0.990		0.412								
0.987	0.412	0.428	0.483	0.509	0.534	0.557	0.589	0.721	0.761	
0.970	0.473	0.488	0.536	0.567	0.587	0.623	0.650	0.812	0.838	
0.959	0.497	0.513	0.558	0.582	0.599	0.639	0.652	0.831	0.863	
0.949	0.506	0.536	0.558	0.589	0.618	0.646	0.670	0.844	0.873	

	.508 H dw		1.52 H dw		3.05 H dw	
Re =	79,100	170,000	81,000	163,000	82,200	169,000
y/H	U/U_m	U/U_m	U/U_m	U/U_m	U/U_m	U/U_m
0.008					0.511	
0.015					0.644	
0.025					0.718	
0.051					0.814	
0.028						0.718
0.053						0.843
0.079						0.900
0.130						0.986
0.992					0.864	0.833
0.987	0.968+	0.891+		0.886	0.953	0.892
0.970	1.041	0.933	0.979	0.976	1.054	0.968
0.959	1.038	0.939	1.032	0.995	1.083	0.981
0.949	1.038	0.951	1.045	1.004	1.086	1.010

* See Table C-IIb for specific y-values.

\+ y/H = .982

APPENDIX D

SPANWISE FLOW EVALUATION

The spanwise variation of the flow was investigated for a range of flow conditions. As noted, Figure 8, the flow was nearly two dimensional over the center region of the duct. Only near the side walls were major deviations measured. The spanwise measurements were made by varying the cross beam focusing lens. The lens actuator could be moved 20 cm, and either the lens was shifted to a new position of a shorter focal length lens was employed.

Figure D-1 shows the spanwise mean and tangential turbulent velocity variations near the inner wall. The measurement at 160 degrees around the turn show the largest deviations. The excursions at the 160 degree location correlate with the onset of the inner surface separation bubble. The major effect of the separation is noted in the excursions of the tangential turbulent component.

Figure D-2 shows measurements made 3H dowmstream of the turn exit, which is beyond the extent of the inner separation bubble. The large excursions of the tangential turbulent component did not occur beyond the region of separation.

Figure D-3 shows the spanwise variation with Reynolds number of the flow near the inner surface for 160 degrees around the turn. The mean velocity variations are nearly independent of the Reynolds number even near the onset of separation. The tangential turbulent velocities, Figure D-3b, are found to be sensitive to the three-dimensional effects.

Figure D-4 shows spanwise measurements made in the separation region (0.508H downstream of the turn exit). As noted above the three dimensional effects are magnified in the separation region. However, outside the separation bubble (y = 3.81 cm) the flow remains reasonably two dimensional. No pronounced effects of the non-uniformity were found in the tangential turbulent velocity, Figure D-4b. Deviations of the mean velocity profiles in the separation region at different spanwise locations are shoh@ on Figure D-4c. While a moderate deviation in the profiles occur, the extent of the reversed flow region is not greatly altered.

The spanwise velocity variations at 90 degrees around the turn are showm on Figure D-5. The location was investigated for possible indications of the Taylor-Gortler vortex effects. The mean velocity measurements, Figure D-5a and b, do not suggest a pronounced periodic spanwise variation that would be expected if stationary vortex structures were present. Flow visualization suggested that a highly time dependent array of vorticies may be present. The time dependent movement of the vorticies would appear to smooth out the spanwise variations. Only the radial turbulent velocity spanwise variations, Figure D-5d, appears to suggest a

periodic deviation. The original flow measurements indicated the extremely large radial turbulent velocities, which were thought to be caused by a vortex motion.

The present results from the spanwise surveys would appear to justify the use of the two-dimensional assumptions in computing the bulk of the flow field. Only in the separation region are the three-dimensional variations of importance.

Figure D-6 shows the spanwise variation at the turn exit for the case of no exit screen. The measurements were made at the channel centerline. The flow in this no exit screen case made it very close to two-dimensional.

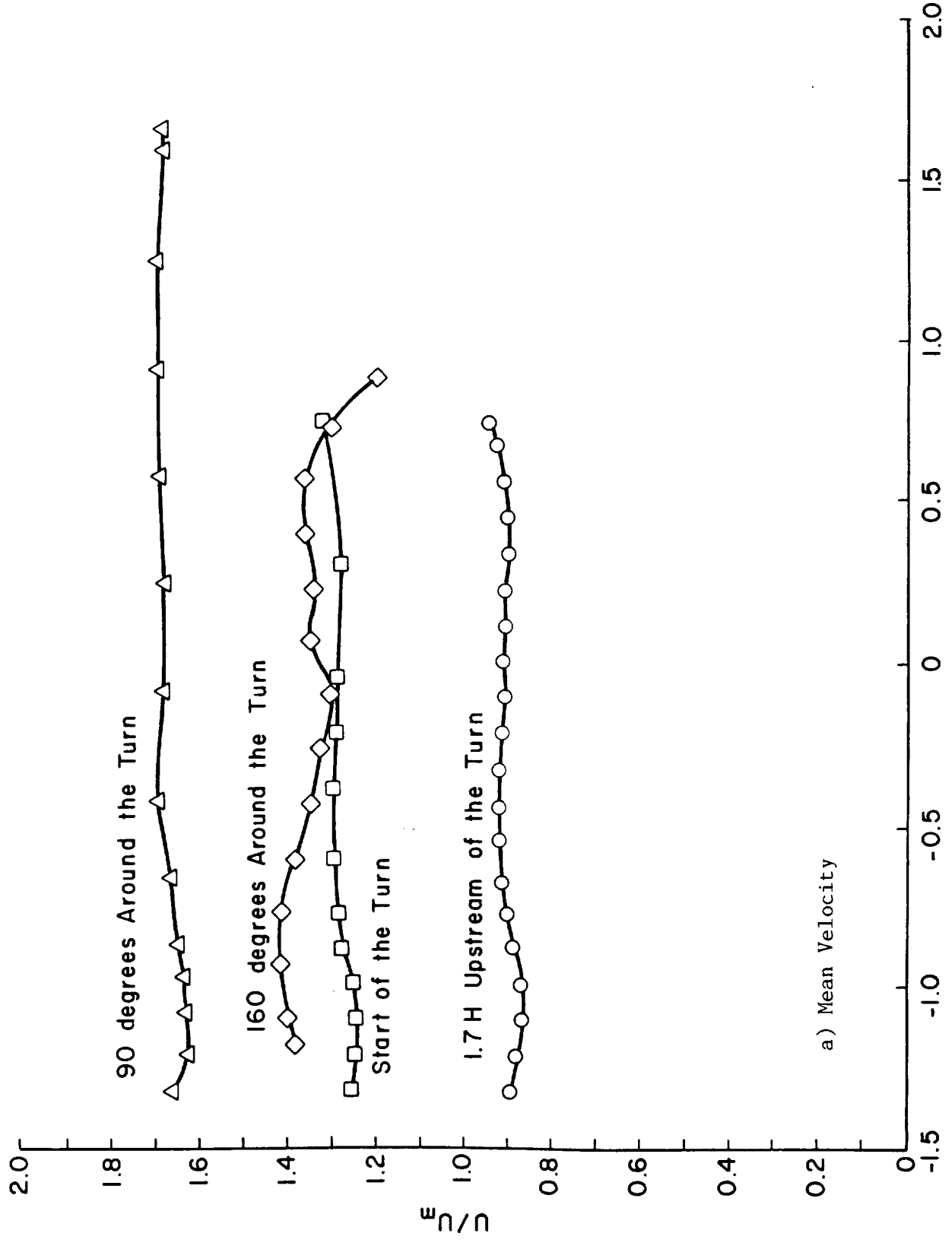

Figure D-1. Spanwise Velocity Variation Near the Inner Surface. y = 0.5 to 0.8cm, Roughness on the Inlet, Coarse Exit Screen.

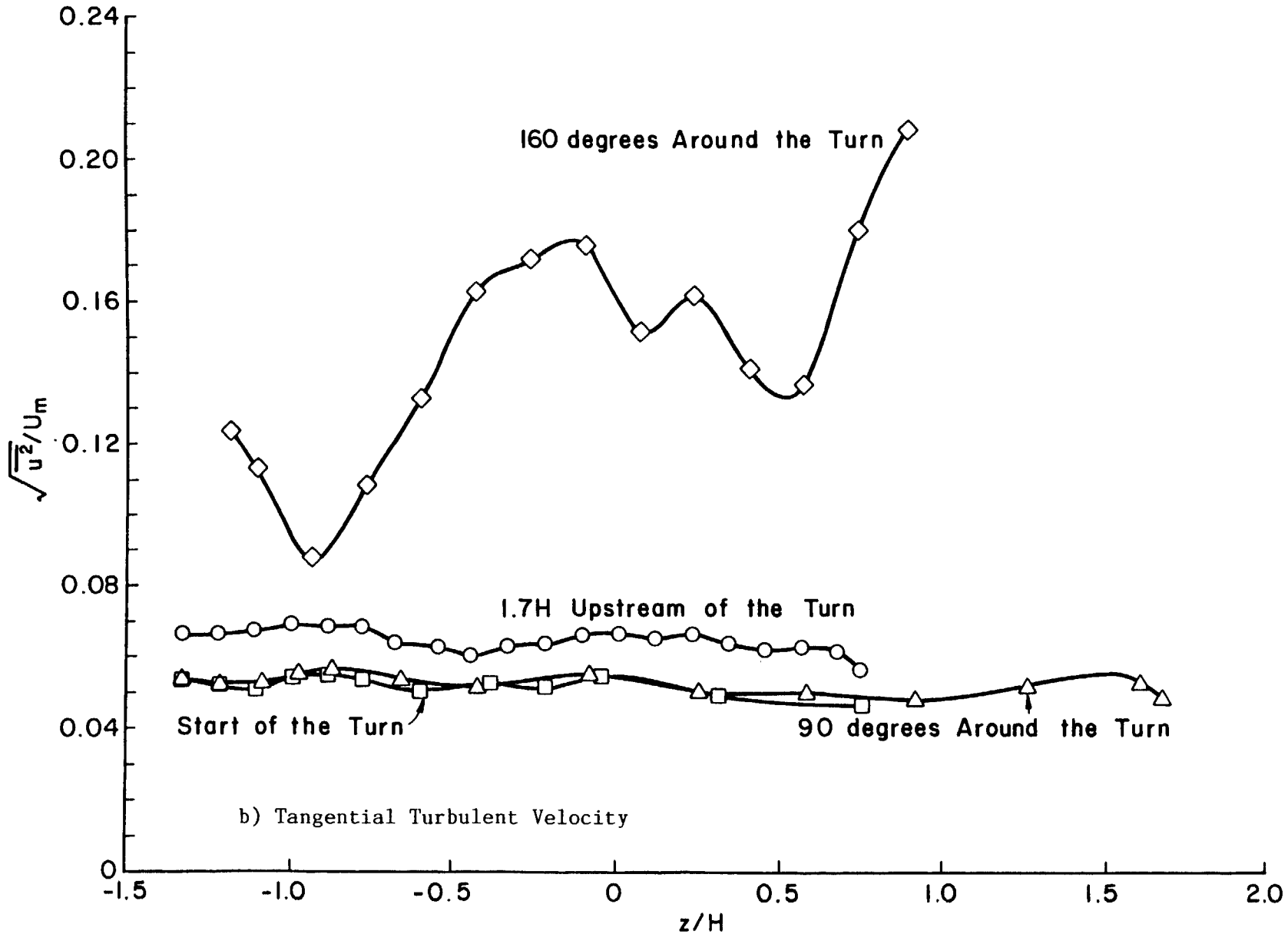

Figure D-1. (Concluded) Spanwise Velocity Variation Near the Inner Surface. y = 0.5 to 0.8cm, Roughness on the Inlet, Coarse Exit Screen.

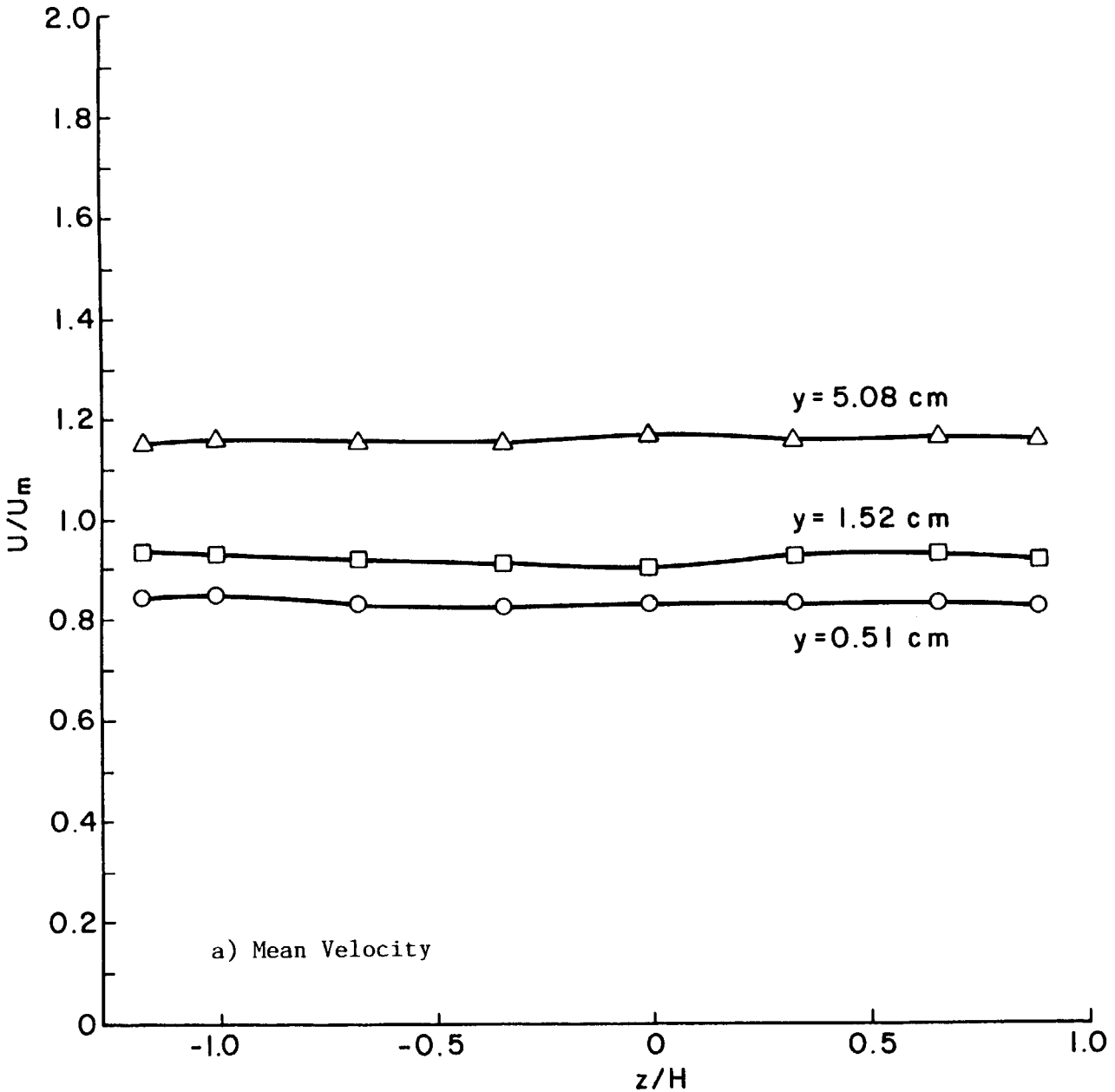

Figure D-2. Station 3H Downstream of Turn Exit, Re=370,000, Roughness on the Inlet

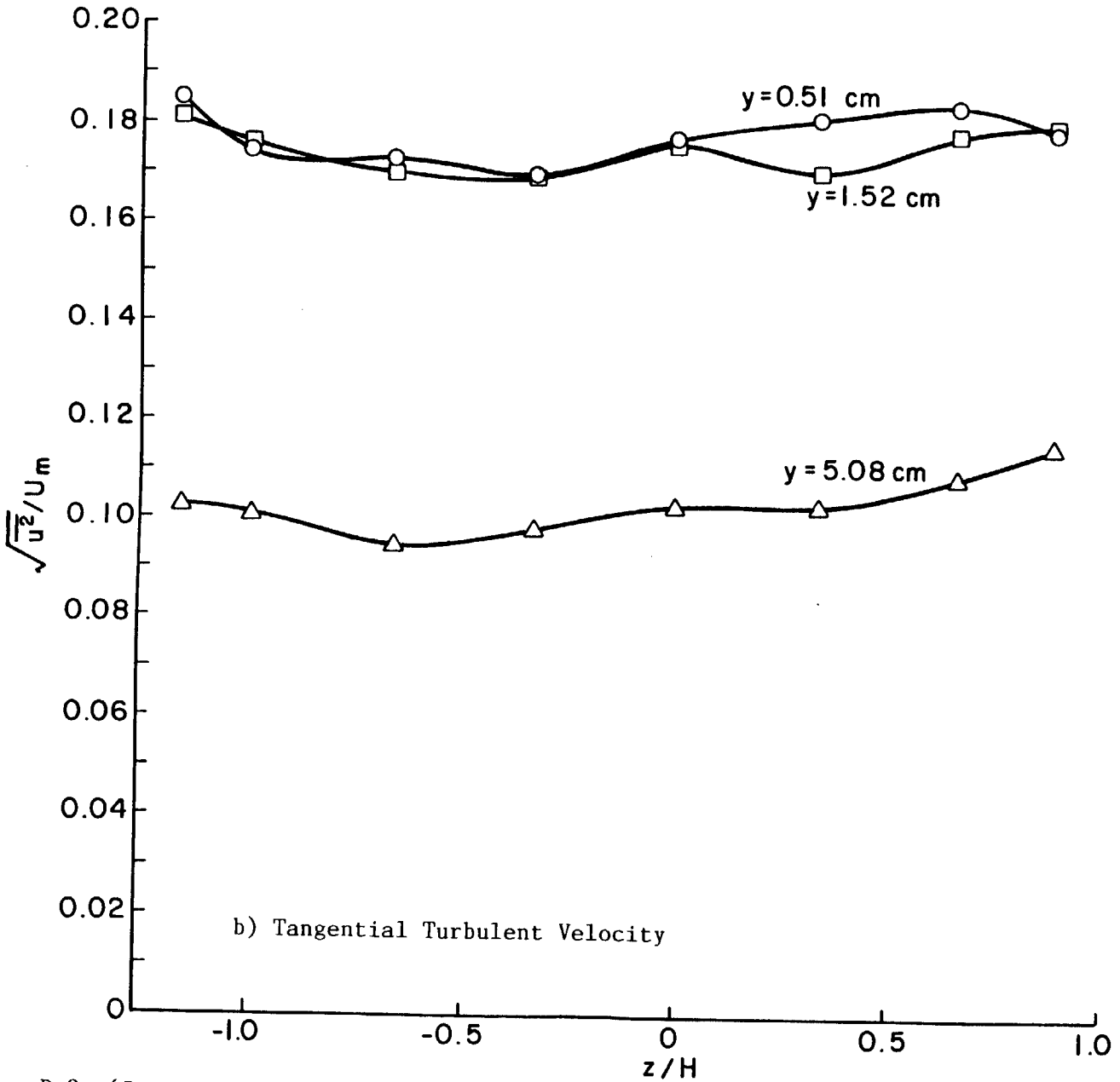

Figure D-2. (Concluded) Station 3H Downstream of Turn Exit, Re=370,000, Roughness on the Inlet.

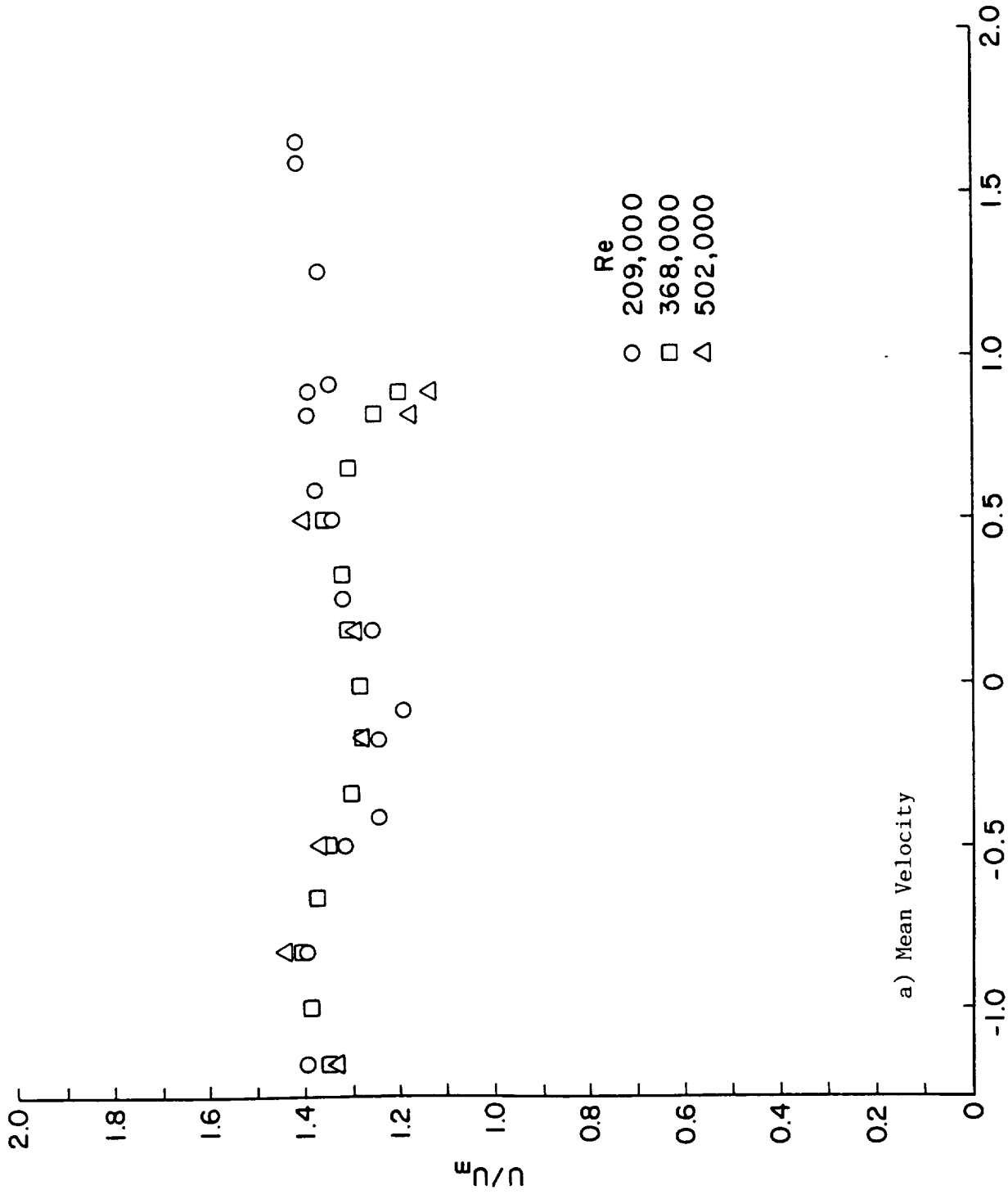

Figure D-3. 160 Degrees Around the Turn, y= 0.5cm, Effect of Reynolds Number, Roughness on the Inlet.

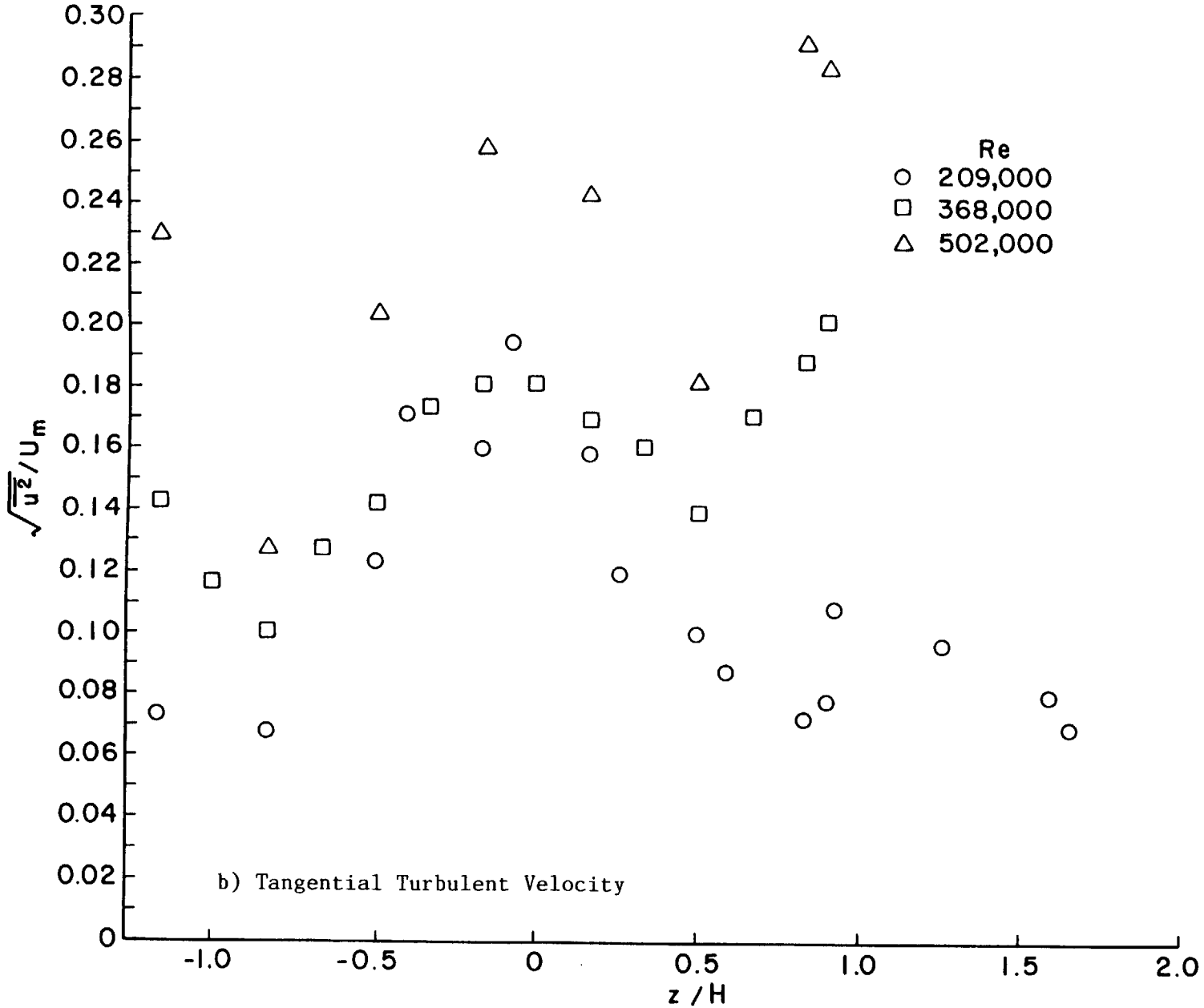

Figure D-3. (Concluded) 160 Degrees Around the Turn, y= 0.5cm, Effect of Reynolds Number, Roughness on the Inlet.

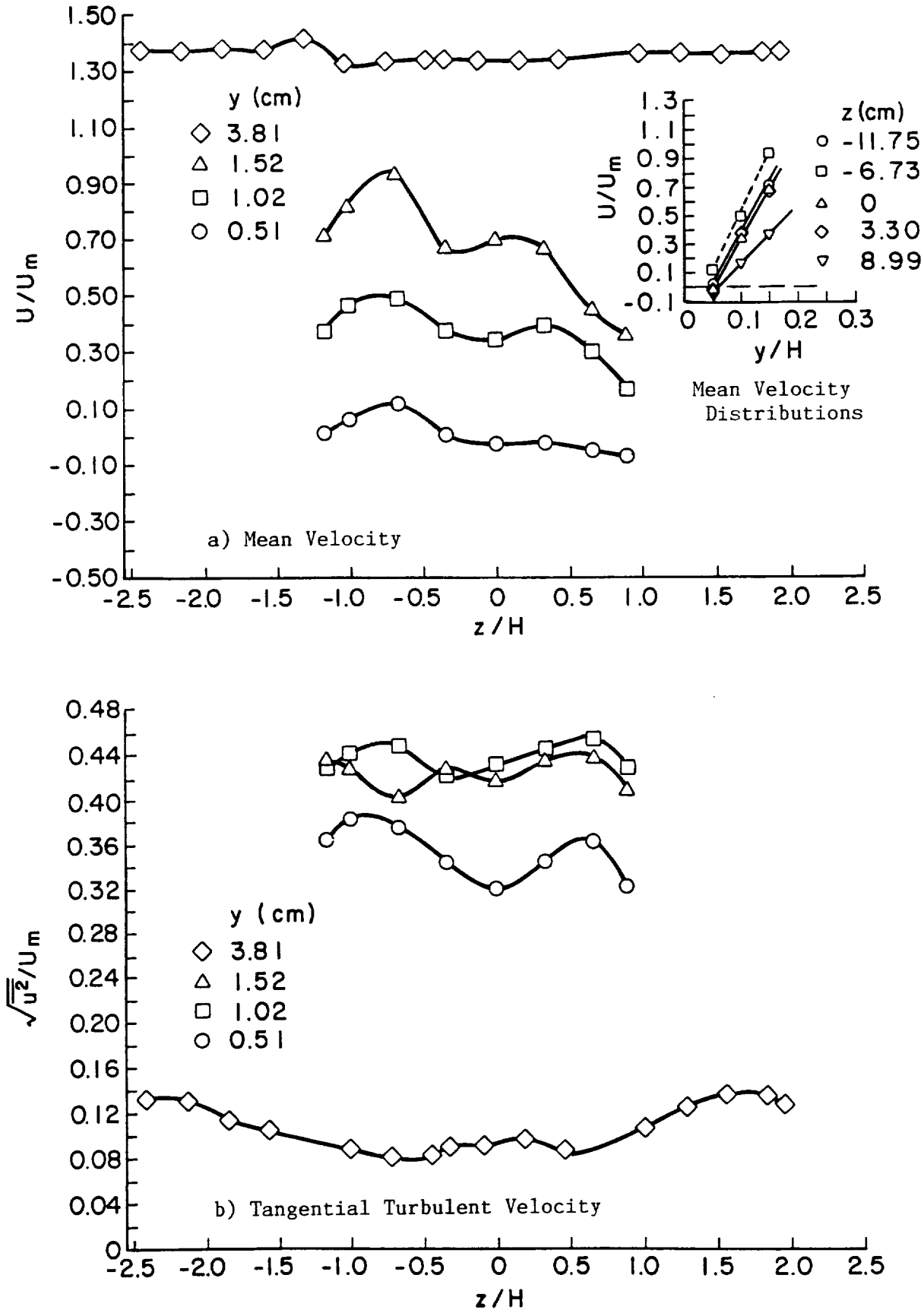

Figure D-4. Spanwise Velocity Variation in the Separation Bubble, 0.508H Downstream of the Turn. Roughness on the Inlet, Coarse Screen at the Exit.

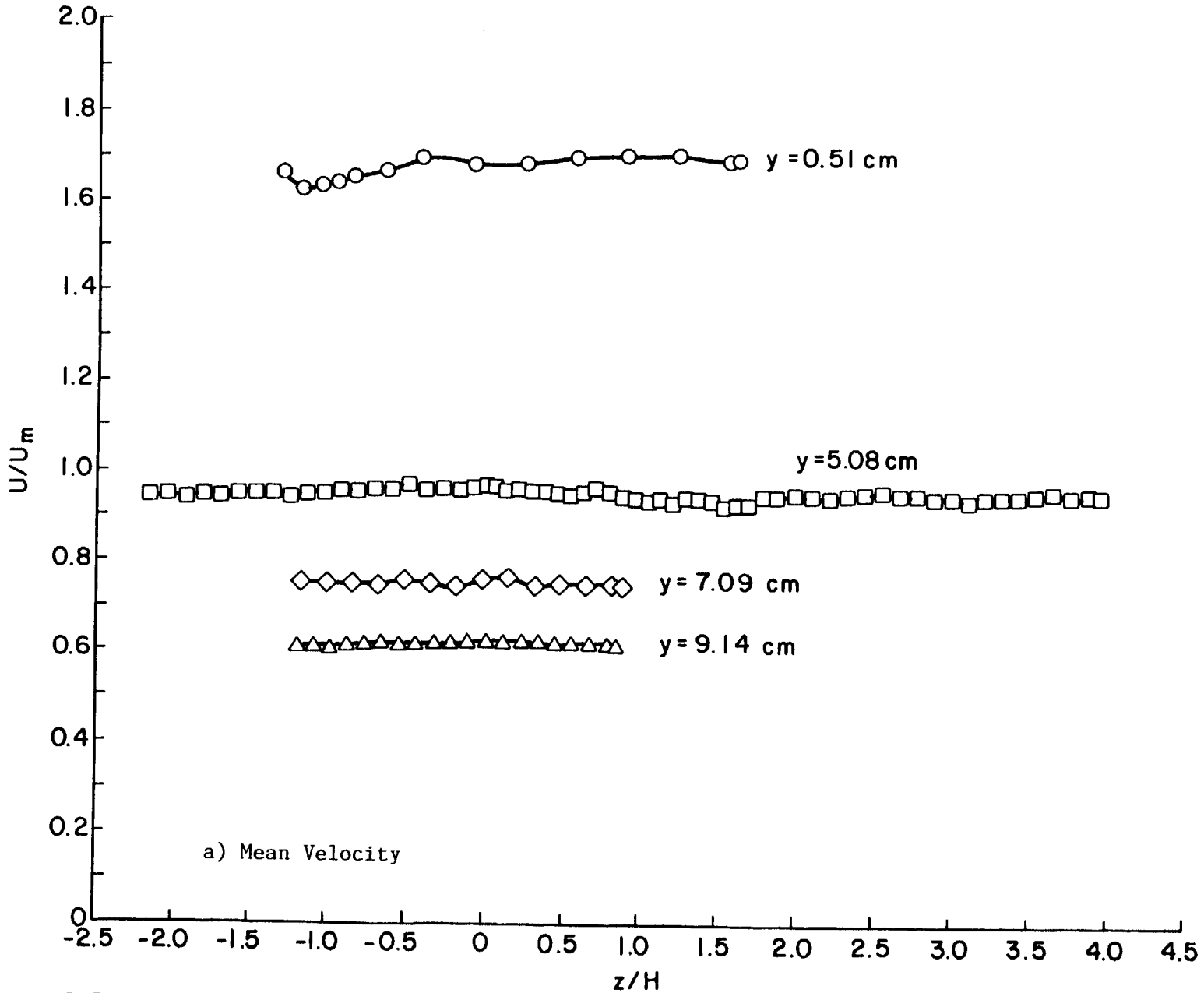

Figure D-5. 90 Degrees Around the Turn, Variation Across the Channel, Re=370,000, Roughness on the Inlet.

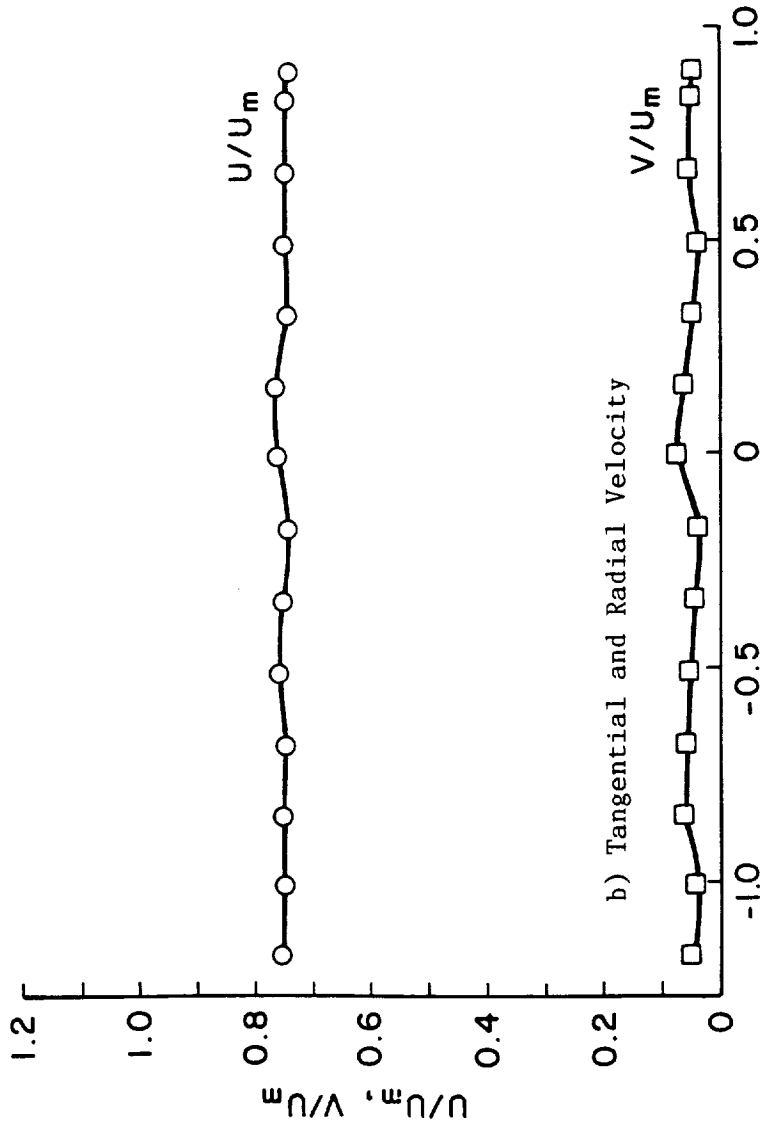

Figure D-5. (Continued)

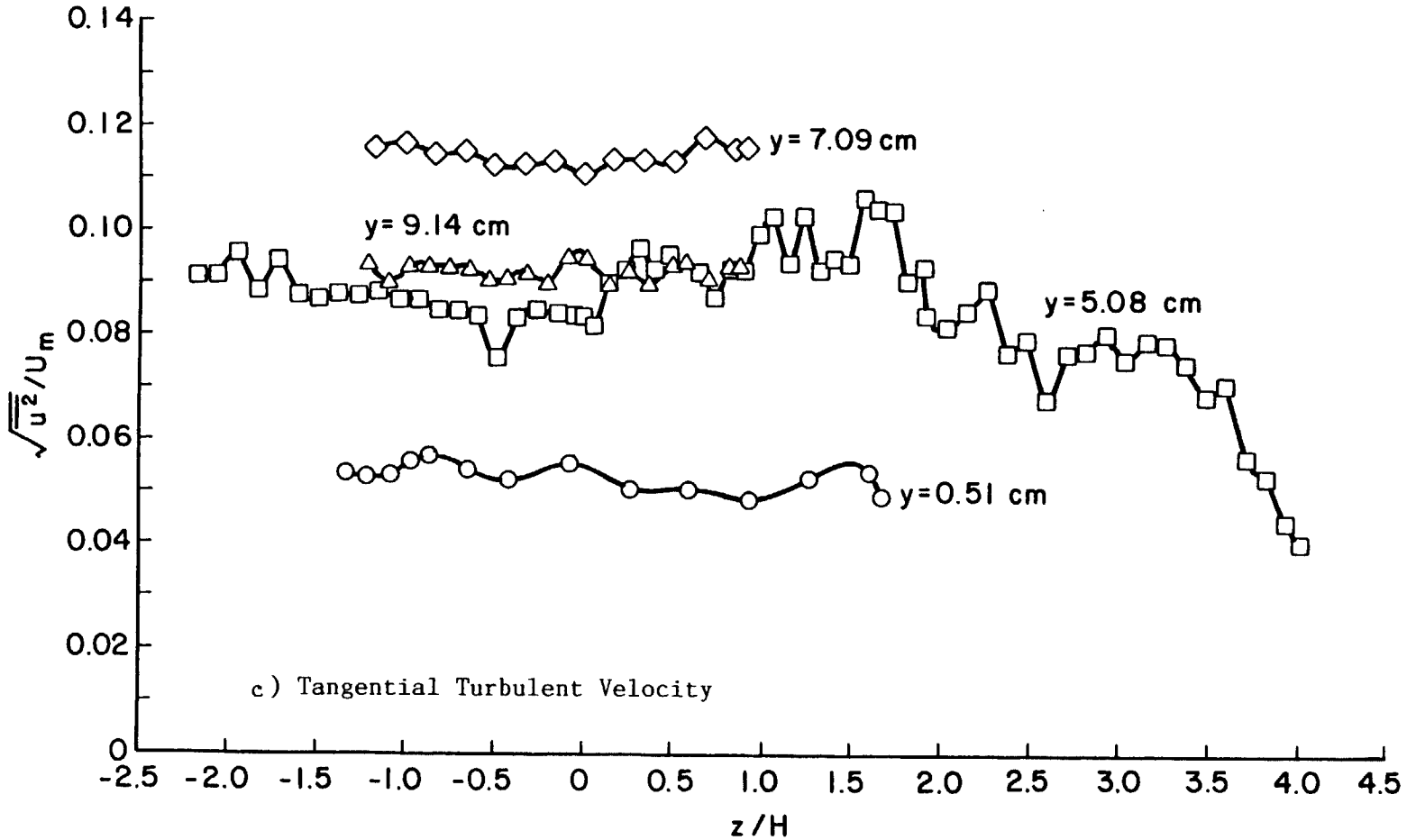

Figure D-5. (Continued)

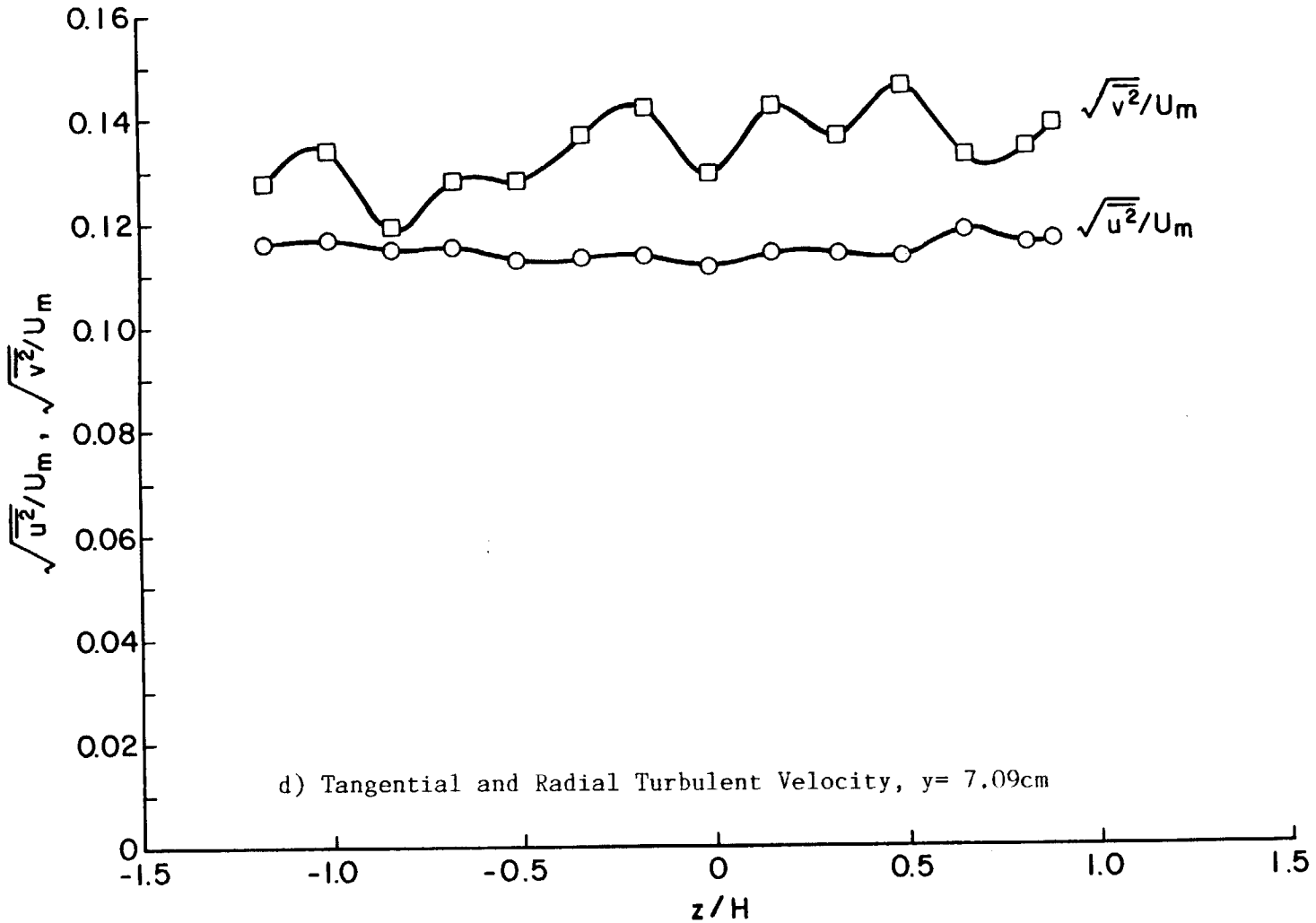

Figure D-5. (Concluded) 90 Degrees Around the Turn, Variation Across the Channel, Re=370,000, Roughness on the Inlet.

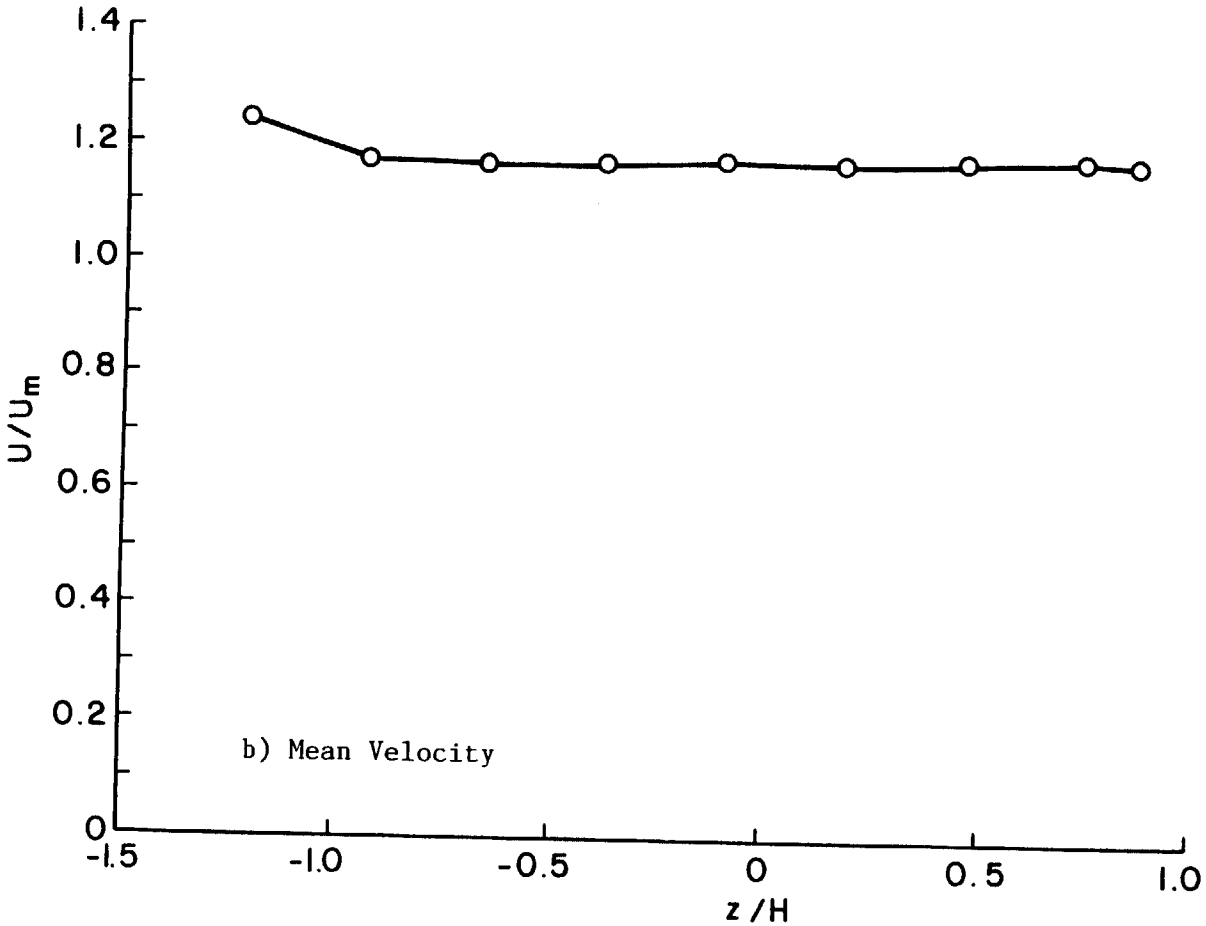

Figure D-6. Spanwise Velocity Variation at the Centerline of the Turn Exit, Roughness on the Inlet, No Exit Screen, Re=376,000.

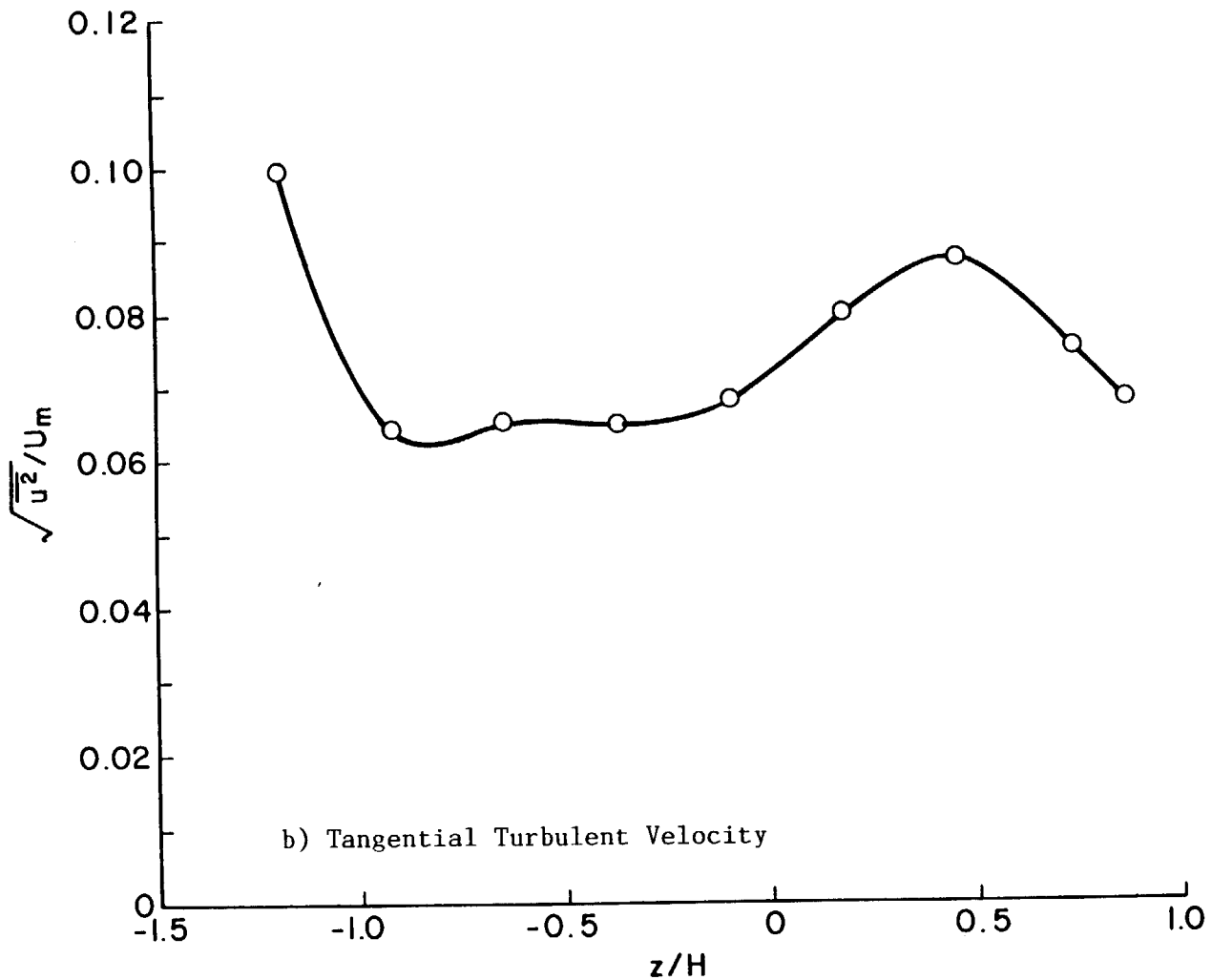

Figure D-6. (Concluded) Spanwise Velocity Variation at the Centerline of the Turn Exit, Roughness on the Inlet, No Exit Screen, Re=376,000.